

Ideal Knots and Other Packing Problems of Tubes

THÈSE N° 4601 (2010)

PRÉSENTÉE LE 22 FÉVRIER 2010

À LA FACULTÉ SCIENCES DE BASE

CHAIRE D'ANALYSE APPLIQUÉE

PROGRAMME DOCTORAL EN MATHÉMATIQUES

ÉCOLE POLYTECHNIQUE FÉDÉRALE DE LAUSANNE

POUR L'OBTENTION DU GRADE DE DOCTEUR ÈS SCIENCES

PAR

Henryk GERLACH

acceptée sur proposition du jury:

Prof. M. Troyanov, président du jury
Prof. J. Maddocks, Prof. J. P. Buser, directeurs de thèse
Prof. S. Hildebrandt, rapporteur
Prof. R. Langevin, rapporteur
Prof. N. Monod, rapporteur



ÉCOLE POLYTECHNIQUE
FÉDÉRALE DE LAUSANNE

Suisse
2010

Abstract

This thesis concerns optimal packing problems of tubes, or thick curves, where thickness is defined as follows. Three points on a closed space curve define a circle. Taking the infimum over all radii of pairwise-distinct point triples defines the *thickness* Δ . A closed curve with positive thickness has a self-avoiding neighbourhood that consists of a disjoint union of normal disks with radius Δ , which is a tube.

The thesis has three main parts. In the first, we study the problem of finding the longest closed tube with prescribed thickness on the unit two-sphere, and show that solutions exist. Furthermore, we give explicit solutions for an infinite sequence of prescribed thicknesses $\Theta_n = \sin \frac{\pi}{2n}$. Using essentially basic geometric arguments, we show that these are the only solutions for prescribed thickness Θ_n , and count their multiplicity using algebraic arguments involving Euler's totient function.

In the second part we consider tubes on the three-sphere \mathbb{S}^3 . We show that thickness defined by global radius of curvature coincides with the notion of thickness based on normal injectivity radius in \mathbb{S}^3 . Then three natural, but distinct, optimisation problems for knotted, thick curves in \mathbb{S}^3 are identified, namely, to fix the length of the curve and maximise thickness, to fix a minimum thickness and minimise length, or simply to maximise thickness with length left free. We demonstrate that optimisers, or ideal shapes, within a given knot type exist for each of these three problems. Finally, we propose a simple analytic form of a strong candidate for a thickness maximising trefoil in \mathbb{S}^3 and describe its interesting properties.

The third and final part discusses numerical computations and their implications for ideal knot shapes in both \mathbb{R}^3 and \mathbb{S}^3 . We model a knot in \mathbb{R}^3 as a finite sequence of coefficients in a Fourier representation of the centreline. We show how certain presumed symmetries pose restrictions on the Fourier coefficients, and thus significantly reduce the number of degrees of freedom. As a consequence our numerical technique of simulated annealing can be made much faster. We then present our numeric results. First, computations approach an approximation of an ideal trefoil in \mathbb{S}^3 close to the analytic candidate mentioned above, but, supporting its ideality, are still less thick. Second, for the ideal trefoil in \mathbb{R}^3 , numerics suggest the existence of a certain closed cycle of contact chords, that allows us to decompose the trefoil knot into two base curves, which once determined, and taken together with the symmetry, constitute the ideal trefoil.

Keywords: Ideal knots, tube packings, thick curves, simulated annealing, Fourier knots, curve symmetries.

Zusammenfassung

Diese Arbeit behandelt optimale Packungsprobleme von Tuben, die wir als dicke Kurven modellieren. Dabei definieren wir Dicke auf Basis des *globalen Krümmungsradius* wie folgt: Drei Punkte auf einer geschlossenen Raumkurve definieren einen Kreis. Die Dicke Δ ist das Infimum aller Radien solcher Kreise durch paarweise verschiedene Tripel. Eine geschlossene Kurve positiver Dicke hat eine selbstschnittfreie tubulare Umgebung, die aus der disjunkten Vereinigung zur Kurve normaler Kreisscheiben mit Radius Δ besteht und die Tube darstellt.

Die vorliegende Arbeit besteht aus drei Hauptteilen. Im ersten Teil untersuchen wir das Problem, die längste geschlossene Kurve vorgeschriebener Dicke auf der zweidimensionalen Einheitskugel zu finden. Wir zeigen, dass Lösungen existieren und geben explizite Lösungen für eine unendliche Folge vorgeschriebener Dicken $\Theta_n = \sin \frac{\pi}{2n}$ an. Mit elementaren, geometrischen Mitteln zeigen wir, dass keine weiteren Lösungen für die vorgeschriebenen Dicken Θ_n existieren und bestimmen ihre Anzahl in Abhängigkeit von n mit Hilfe der Eulerschen φ -Funktion und weiterer algebraischer Argumente.

Im zweiten Teil betrachten wir dicke Kurven auf der 3-Sphäre \mathbb{S}^3 . Wir zeigen, dass Dicke, definiert über den globalen Krümmungsradius, und der normale Injektivitätsradius in \mathbb{S}^3 äquivalent sind. Wir identifizieren drei natürliche, aber unterschiedliche Packungsprobleme verknoteter dicker Kurven in \mathbb{S}^3 : (a) Fixiere die Länge und maximiere die Dicke. (b) Fixiere eine minimale Dicke und minimiere die Länge. Und schließlich (c) maximiere die Dicke ohne Einschränkung der Länge. Wir zeigen, dass zu einer gegebenen zahmen Knotenklasse für jedes der Probleme Optimierer existieren, die ideale Kurven genannt werden. Abschließend stellen wir eine einfache explizite Kurve als Kandidaten für die dickemaximierende Kleeblattschlinge in \mathbb{S}^3 vor und beschreiben seine interessanten Eigenschaften.

Der dritte und letzte Teil behandelt numerische Berechnungen und sich daraus ergebende Folgerungen für ideale Kurven sowohl in \mathbb{R}^3 als auch in \mathbb{S}^3 . Wir modellieren einen Knoten in \mathbb{R}^3 als endliche Folge von Koeffizienten einer Fourier-Darstellung der Mittellinie und zeigen, dass wir ideale Knoten damit approximieren können. Weiter zeigen wir, wie bestimmte, vermutete Symmetrien die Koeffizienten einschränken und so die Anzahl der Freiheitsgrade reduzieren. Dadurch beschleunigen wir den verwendeten Algorithmus (*simulierte Abkühlung*) deutlich.

Danach präsentieren wir unsere numerischen Ergebnisse: Erstens liegt die numerisch gefundene dickemaximierende Kleeblattschlinge sehr nahe bei dem oben erwähnten expliziten Kandidaten, erreicht aber nicht seine Dicke, was die Qualität des Kandidaten bestätigt. Zweitens suggeriert die numerische Simulation der idealen Kleeblattschlinge in \mathbb{R}^3 , dass ein bestimmter, geschlossener Zykel von Kontaktstäben existiert, der die Kleeblattschlinge in zwei zu bestimmende Grundkurven zerlegt. Diese stehen wechselseitig

im Kontakt und mit Hilfe der Symmetrien lässt sich aus ihnen die ganze Kurve erzeugen.

Schlagnorte: Ideale Knoten, Tubenpackung, Dicke Kurven, Simulierte Abkühlung, Fourier-Knoten, Kurvensymmetrien.

Acknowledgements

I would like to thank my supervisors Prof. John H. Maddocks and Prof. Peter Buser who proposed this interesting thesis topic, and were always willing to discuss mathematical issues. I am thankful to the other members of thesis committee, Profs. Stefan Hildebrandt, Rémi Langevin, Nicolas Monod and Marc Troyanov.

I am pleased to thank my collaborators Mathias Carlen, Prof. Heiko von der Mosel and Dr. Philipp Reiter (who also proof read this thesis) for fruitful research, moral support in times of need, and their general attitude to get things done. I am grateful for inspiring discussions with all people who shared their insights, in particular Prof. Oscar Gonzalez, Ben Laurie, Prof. Eric Rawdon, Dr. Torsten Schöneborn and Dr. Eugene Starostin. A hearty thanks to Carine Tschanz, secretary of the Maddocks group, for taking care of all bureaucratic obstacles, and all other group members for their support.

The DFG Research Center MATHEON ‘Mathematics for key technologies’ in Berlin in 2005 supported early research related to this thesis. From 2006-2009 I was supported by the Swiss National Science Foundation (project no. 107878 and 117898). I want to express my gratitude to both of them.

Contents

| | | |
|----------|--|-----------|
| 1 | Introduction | 1 |
| 2 | Thick Curves in \mathbb{R}^N and \mathbb{S}^N | 5 |
| 2.1 | Thickness in \mathbb{R}^N | 5 |
| 2.2 | Thickness in \mathbb{S}^N | 10 |
| 2.3 | Knotted Curves | 15 |
| 2.4 | Convergence Analysis of Curves in \mathbb{R}^N | 16 |
| 2.5 | Examples on Higher Order Information | 21 |
| 3 | Packing Tubes on \mathbb{S}^2 | 25 |
| 3.1 | Explicit solutions | 28 |
| 3.2 | Existence and Properties of General Solutions | 34 |
| 3.3 | Uniqueness | 48 |
| 3.4 | Open Curves | 57 |
| 4 | Ideal Knots in \mathbb{S}^3 | 63 |
| 4.1 | Analysis of Necessary Conditions | 67 |
| 4.2 | From \mathbb{S}^3 to \mathbb{R}^3 | 67 |
| 4.3 | A Competitor for the Ideal Trefoil | 69 |
| 4.4 | Is the Competitor \mathfrak{g} at Least a Local Maximum? | 73 |
| 5 | Computations and Deductions | 77 |
| 5.1 | Biarc Curves | 77 |
| 5.2 | Fourier Representation of Knots | 78 |
| 5.3 | Symmetry of Curves | 80 |
| 5.4 | Symmetry of Fourier Knots in \mathbb{R}^3 | 81 |
| 5.5 | Knot Computations | 85 |
| 5.5.1 | Reading the Plots | 87 |
| 5.5.2 | 3_1 in \mathbb{R}^3 | 88 |
| 5.5.3 | 3_1 in \mathbb{S}^3 | 89 |
| 5.5.4 | 4_1 in \mathbb{S}^3 | 92 |
| 5.5.5 | 5_1 in \mathbb{S}^3 | 93 |
| 5.5.6 | $3_1 p 3_1$ in \mathbb{S}^3 | 94 |
| 5.5.7 | Competitor β_τ with $\alpha = 0.8$ on \mathbb{S}^2 | 96 |
| 5.6 | Ambient Isotopy of the Ideal Trefoil and Contact Curve | 97 |
| 5.7 | Closed Cycles | 102 |

CONTENTS

| | |
|------------------------------------|------------|
| 6 Conclusion and Discussion | 111 |
| Index | 115 |
| Bibliography | 117 |

Chapter 1

Introduction

This thesis concerns the mathematical analysis of optimal packing problems for tubes, including the particular problem of ideal knot shapes, both in \mathbb{R}^3 and \mathbb{S}^3 . Tube packings arise in a variety of real world contexts. How are long strands of viral DNA packed into the tiny volume of the phage head of a bacteriophage [KAB06]? How much hose-pipe can be stored in a given box? While we believe that a physical understanding of optimal tube packings is important in these and other applications, we here focus on rigorous mathematical results available for some rather idealised and specific problems.

Due to the absence of any externally imposed conditions or domains, one of the mathematically most elegant tube packing problems is to consider the shortest length of tube of given diameter that can be tied in a given knot type, where it is understood that the tube must be sealed on itself to form a closed loop, and the tube is self-avoiding. Such questions concern geometric knot theory and ideal knot shapes [SKK98]. Apparently [LSDR99] the first question of this type was posed by L. Siebenmann in 1985: *Can you tie a knot in a one-foot length of one-inch rope?* It is now known that the answer is no [Di03], but it is not known precisely what the shortest possible length is, although computations have revealed that 16.4 times the diameter is sufficient to tie a trefoil knot, and presumably this is close to optimal.

In \mathbb{R}^3 a curve minimizing the quotient of arc-length and thickness in a given knot class is called an *ideal knot* [SKK98]. The existence of ideal knots in the class of $C^{1,1}$ curves has been proven by [GMSvdM02, GdlL03] and [CKS02]. Around the same time Kusner considered thickness maximising knots in the three-sphere [K02].

Only a few optimal shapes are known. So far, no explicit solution of an ideal knot is known, except that the ideal unknot is the circle. Cantarella, Kusner, and Sullivan were able to construct explicit ideal links [CKS02] from circular arcs and straight lines. For example the ideal Hopf-link is two circles of the same radius in orthogonal planes, one running through the centre of the other. They also constructed a chain consisting of a stadium curve and two circles perpendicular to the stadium curve. This example demonstrates that ideal links do not need to have either unique or isolated solutions. Starostin [Sta03] and Cantarella et al. [CFKSW04] studied the shape of the tight clasp and the ideal Borromean rings and derived various semi-explicit shapes. Note however that all of these examples are component-wise planar.

Of course there exist various numerical codes to approximate ideal shapes: For piecewise linear polygonal $C^{0,1}$ knots there are Pieranski's Shrink On No Overlap (SONO)

algorithm [P98], and the RidgeRunner algorithm of Cantarella, Piatek and Rawdon [CPR05, ACPR05]. An estimate of how to inscribe small circular arcs into a polygon to get a thick $C^{1,1}$ curve [BPR05] gives rigorous bounds from such computations. In contrast Carlen et al. used simulated annealing [KGV83] directly on a $C^{1,1}$ numerical discretisation called biarcs [S04, CLMS05] which revealed previously unobserved features, such as local curvature being extremely close to achieve thickness. All of these simulations concerned ideal shapes in \mathbb{R}^3 . To our knowledge no ideal knots in \mathbb{S}^3 have previously been computed analytically or numerically, except for the ideal unknot which is again a circle.

We remark that ideality based on thickness is only one special case of many possible knot energies leading to optimal shapes as discussed for example by O'Hara [O'H03]. Other examples are the *Möbius energy*, an 'electrostatic energy' defined by O'Hara [O'H91], and studied by Freedman, He and Wang [FHW94] with recent results by Reiter [Rt09]. Langevin and Moniot studied integral energies of links in \mathbb{S}^3 [M04, LM05].

Different and surprisingly complex, but equivalent, mathematical definitions of thickness of a tube have emerged [LSDR99]. This thesis is based on that of global radius of curvature, which was introduced for \mathbb{R}^3 in [GM99] and generalised to \mathbb{R}^N in [Ge04]: Through three points in general position in \mathbb{R}^N there is a unique circle. The thickness Δ of a curve is the infimal radius of all circles through distinct point-triples on the curve. A curve with positive thickness is the centreline of a non self intersecting tubular neighbourhood of the same thickness. We show in this thesis that this notion also carries over naturally to \mathbb{S}^3 .

The structure of this thesis is as follows. In Chapter 2 we first collect known facts about thick curves. For example that thick curves have a $C^{1,1}$ arc-length parametrisation. We present different equivalent notions of thickness in \mathbb{R}^N . In Section 2.2 we find that thickness in \mathbb{S}^N can be expressed as thickness in \mathbb{R}^N , and that this notion of thickness coincides with the normal injectivity radius of a curve in \mathbb{S}^N . In Section 2.3 we briefly describe what we mean by a knot, and when two knots are equivalent. In Section 2.4 we present known results of how sequences of thick curves behave, and adapt them to our needs. We conclude this chapter in Section 2.5 with two cautionary examples of sequences of curves converging to their limits both in C^1 and in thickness, but not in $C^{1,1}$. As a consequence it is possible that the curvature of the sequence members may be very different from the curvature of the limit curve.

Chapter 3 is joint work with H. von der Mosel [GevdM09]. We consider the following optimal packing problem:

Problem (P). *Find the longest closed curves of prescribed minimal thickness which fit onto the 2-sphere $\mathbb{S}^2 := \{x \in \mathbb{R}^3 : |x| = 1\}$.*

It is trivial to see that the maximal thickness of a curve on \mathbb{S}^2 is only attained by great circles which have thickness one in \mathbb{R}^3 (see Example 2.17). We show that Problem (P) has a solution for all positive thicknesses Θ smaller than the thickness of a great circle (Theorem 3.1). For certain thicknesses $\Theta_n := \sin(\frac{\pi}{2n})$ we then construct explicit solutions from stacked semicircles (see Figure 3.1 on page 26 and Figure 3.3 on page 29) and count them by an algebraic argument. Then we show that they are the unique solutions for the respective thickness in the sense that there are no others. As a byproduct we find that thick curves can be approximated by C^∞ curves (Corollary 3.12). Finally we sketch the construction of similar solutions for open curves, and how to show their uniqueness.

In Chapter 4 we study different optimisations problems of thick curves in \mathbb{S}^3 . Namely one can

- (a) maximise thickness, with length left free,
- (b) fix length and maximise thickness,
- (c) fix thickness and minimise length, and
- (d) fix thickness and maximise length.

For all four notions we show that solutions exist. As in the \mathbb{R}^N case their arc-length parametrisation is $C^{1,1}$. We consider (a) to be the most natural question (as did [K02]) and call its solutions *ideal knots* in \mathbb{S}^3 . We show that we can dilate curves by conformal dilations if they are contained in a small part of the sphere. Consequently we conjecture that ideal knot shapes can not be contained in a hemisphere of \mathbb{S}^3 . We link ideal shapes in \mathbb{S}^3 and \mathbb{R}^3 by the following observation: If we consider a sequence of solutions of (b) i.e. fix the length and maximise thickness – with the prescribed length going to zero, then as the solutions approach the tangent space \mathbb{R}^3 of \mathbb{S}^3 , some subsequence of \mathbb{S}^3 ideal shapes converges to an ideal shape in \mathbb{R}^3 . In Section 4.3 we give a specific trefoil knot located on a flat Clifford torus that is a strong candidate for the thickness maximising trefoil in the three-sphere, and we study its interesting geometric properties.

Chapter 5 is joint work with M. Carlen (see also [C10]). We briefly introduce the biarc discretisation following [S04] that was used as a basis of our computations. We then reintroduce Fourier knots [T98, K98]

$$\gamma(t) := \sum_{i=1}^k (a_i \cos(2\pi it) + b_i \sin(2\pi it)), \quad t \in \mathbb{S} := \mathbb{R}/\mathbb{Z},$$

for some coefficients $a_i, b_i \in \mathbb{R}^3$, and show that ideal knots can be approximated by them. We briefly study symmetries of curves from an abstract viewpoint, and apply this to find what dependencies symmetry groups impose on the Fourier coefficients.

Section 5.5 presents our numeric results. Notably in \mathbb{S}^3 , and starting from initial trefoils far away from the competitor mentioned previously, our numerical algorithm maximising thickness yielded a shape close to it, but did not achieve its thickness.

It has been observed that the tubular neighbourhood of maximal thickness of ‘the ideal trefoil’ in \mathbb{R}^3 touches itself along a contact curve [PP02, CLMS05]. In Section 5.6 we give a precise description of this conjecture, and with hypotheses inspired from numerical experiments, prove that the contact curve is itself a trefoil.

Finally in Section 5.7 we describe a closed contact cycle on the \mathbb{R}^3 trefoil: A curve is in contact with itself at the points p, q if the distance between p and q is precisely two times the thickness of the curve and the line segment between them is orthogonal to the curve at both ends. Numerics suggest that each point on the ideal trefoil in \mathbb{R}^3 is in contact with two other points. Starting from a point p_1 , it is in contact with a point p_2 that itself is again in contact with a point $p_3 \neq p_1$ and so on. Does this sequence close to a cycle? Our numeric results suggest that there is indeed a closed 9-cycle on the trefoil. The existence of this cycle is significant because it partitions the trefoil in such a way that, using the symmetries, it can be re-constructed from two unknown small pieces of curves mutually in contact.

Chapter 2

Thick Curves in \mathbb{R}^N and \mathbb{S}^N

2.1 Thickness in \mathbb{R}^N

Throughout this thesis we consider closed curves that are at least continuous, i.e. $\gamma \in C^0(I, M)$. The parameter interval I is typically $\mathbb{S} := [0, 1]/(0 \sim 1) \cong \mathbb{R}/\mathbb{Z}$, the unit interval with the endpoints identified. In some cases I is the unit circle \mathbb{S}^1 or the interval $[0, L]$ with the endpoints identified, where L is the arc-length of the curve. The set M is either \mathbb{R}^N or $\mathbb{S}^N \subset \mathbb{R}^{N+1}$ for some $N \in \mathbb{N}$. Here $\mathbb{S}^N := \{x \in \mathbb{R}^{N+1} : |x| = 1\}$ is the N -dimensional unit sphere, and $|\cdot|$ is the Euclidean norm.

There exist several ways to assign a thickness to a curve, namely reach, normal injectivity radius and variants of global radius of curvature [GM99]. We base our work on the latter and generalise it to curves in \mathbb{R}^N (see also [Ge04]):

Definition 2.1 (Global radius of curvature). *For a C^0 -curve $\gamma : I \rightarrow \mathbb{R}^N$ the global radius of curvature at $s \in I$ is*

$$\rho_G[\gamma](s) := \inf_{\sigma, \tau \in I, \sigma \neq \tau, \sigma \neq s, \tau \neq s} R(\gamma(s), \gamma(\sigma), \gamma(\tau)). \quad (2.1)$$

Here $R(x, y, z) \geq 0$ is the radius of the smallest circle through the points $x, y, z \in \mathbb{R}^N$, i.e.

$$R(x, y, z) := \begin{cases} \frac{|x-z|}{2 \sin \angle(x-y, y-z)} & x, y, z \text{ not collinear,} \\ \infty & x, y, z \text{ collinear, pairwise distinct,} \\ \frac{\text{diam}(\{x, y, z\})}{2} & \text{otherwise.} \end{cases}$$

where $\angle(x-y, y-z) \in [0, \pi/2]$ is the smaller angle between the vectors $(x-y)$ and $(y-z) \in \mathbb{R}^N$, and

$$\text{diam}(M) := \sup_{x, y \in M} |x - y| \text{ for } M \subset \mathbb{R}^N$$

is the diameter of the set M . The thickness of γ denoted as

$$\Delta[\gamma] := \inf_{s \in I} \rho_G[\gamma](s) = \inf_{s, \sigma, \tau \in I, \sigma \neq \tau, \sigma \neq s, \tau \neq s} R(\gamma(s), \gamma(\sigma), \gamma(\tau)), \quad (2.2)$$

is defined as the infimum of ρ_G .

A curve γ is called *thick* if $\Delta[\gamma] > 0$. Note that for a homeomorphism $h : I \rightarrow I$ we have $\Delta[\gamma] = \Delta[\gamma \circ h]$ and Δ is positive homogeneous degree one: $\Delta[\lambda\gamma] = |\lambda|\Delta[\gamma]$ for $\lambda \in \mathbb{R}$.

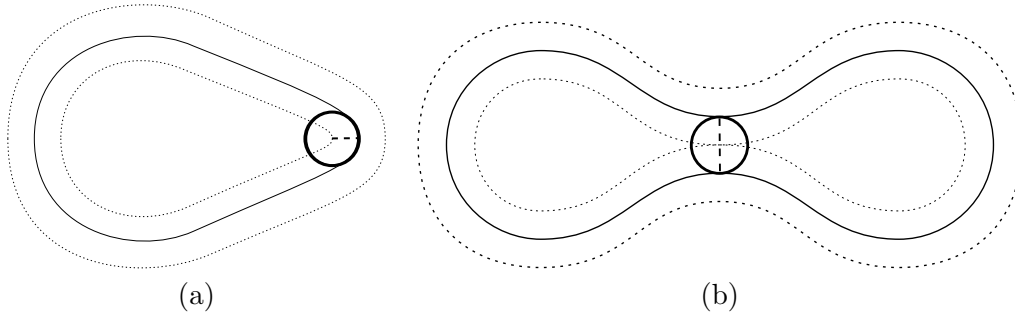


Figure 2.1: The thickness Δ of a curve is bounded by the local radius of curvature (a) and the global self distance (b). The circle is the limit circle approached by the circles through the triples of a minimal sequence of (2.2).

The thickness of a curve is bounded by two typical cases (see Figure 2.1): The local radius of curvature that is approached by $R(x, y, z)$ as x, y and z converge to a single point and the global self distance $2R(x, y, z)$ as two points – say x, y – converge such that $x - z$ is orthogonal to the curve in x and z . In fact, it can be shown that a minimal sequence of (2.2) can always be chosen such that at least two arguments converge [GM99, SvdM04].

If a curve γ is rectifiable it can be parametrised by arc-length, if γ is also thick then it is $C^{1,1}$ -smooth:

Lemma 2.2. [GMSvdM02, Lemma 2], [SvdM03a, Theorem 1 (iii)]

Let $\gamma \in C^0(I, \mathbb{R}^N)$ be rectifiable and parametrised by arc-length, then the following is equivalent:

(i) $\Delta[\gamma] > 0$

(ii) $\gamma \in C^{1,1}(I, \mathbb{R}^N)$ and γ injective. □

Here $C^{1,1}(I, \mathbb{R}^N)$ is the space of C^1 -functions γ whose derivative γ' is Lipschitz continuous, i.e. the norm

$$\|\gamma\|_{C^{1,1}(I, \mathbb{R}^N)} := \sup_{s \in I} |\gamma(s)| + \sup_{s \in I} |\gamma'(s)| + \sup_{s, t \in I, s \neq t} \frac{|\gamma'(s) - \gamma'(t)|}{|s - t|}$$

is finite [E98].

Consequently the curves we consider are usually regular, i.e. $|\gamma'(t)| > 0$ for all t , and parametrised by arc-length or equivalently by constant speed.

Carefully studying the limit of $R(\gamma(s), \gamma(\sigma), \gamma(\tau))$ as τ and σ converge to some $t \in I$ revealed [GM99, GMS02, SvdM04] that instead of the circle through three points one can also consider the circle going through $\gamma(s)$ and $\gamma(t)$ while being tangent to $\gamma'(t)$ in $\gamma(t)$. Because the radius of this circle depends on a point and a tangent in a point we call it pt (we could call R the point-point-point function ppp accordingly):

Definition 2.3 (pt-function). [GMS02] Let $\gamma \in C^1(I, \mathbb{R}^N)$ be a closed and regular curve, i.e. $|\gamma'(t)| > 0$ for all t . For $s, t \in I$ let $\text{pt}[\gamma](s, t)$ be the radius of the smallest

circle going through $\gamma(s)$ and $\gamma(t)$, tangent to $\gamma'(t)$ in $\gamma(t)$, i.e.

$$\text{pt}[\gamma](s, t) := \begin{cases} \infty & \text{if } \gamma(s) - \gamma(t) \text{ parallel to } \gamma'(t), \gamma(s) \neq \gamma(t), \\ 0 & \text{if } \gamma(s) = \gamma(t), \\ \frac{|\gamma(s) - \gamma(t)|}{2 \sin \angle(\gamma(s) - \gamma(t), \gamma'(t))} & \text{otherwise.} \end{cases}$$

If γ is clear from the context we may drop it as an explicit argument to pt .

Remark 2.4. If Γ is parametrised by arc-length, the formula in the general case can be written as

$$\text{pt}[\Gamma](s, t) = \frac{|\Gamma(s) - \Gamma(t)|^2}{2|(\Gamma(s) - \Gamma(t)) \wedge \Gamma'(t)|}$$

with $|u \wedge v|$ the area of the parallelogram spanned by u and v , since we have

$$|u \wedge v| = |u||v| \sin \angle(u, v)$$

and $|\Gamma'| = 1$.

We will see later in this chapter that taking the infimum over pt for regular curves yields the same thickness as taking the infimum over ρ_G .

Next we may consider two point-tangent pairs on the curve. They define a minimal sphere passing through the points and tangent to the curve at those points:

Definition 2.5 (tt-function). [GMS02] Let $\gamma \in C^1(I, \mathbb{R}^N)$ be a closed and regular curve. For $s, t \in I$ let $\text{tt}[\gamma](s, t)$ be the radius of the smallest sphere through $\gamma(s)$ and $\gamma(t)$, tangent to $\gamma'(s)$ in $\gamma(s)$ and tangent to $\gamma'(t)$ in $\gamma(t)$. If $N > 3$ then the involved vectors $(\gamma(s) - \gamma(t))$, $\gamma'(s)$ and $\gamma'(t)$ span a 3-dimensional subspace and we take the radius of the smallest sphere in this subspace. For explicit formulae see [GMS02, C10].

Before we continue we fix some notation:

Definition 2.6 (Distances). Let

$$\text{dist}_{\mathbb{R}^N}(X, Y) := \inf_{x \in X, y \in Y} |x - y| \text{ for } X, Y \subset \mathbb{R}^N,$$

denote the Euclidean distance in \mathbb{R}^N between two sets X and Y . We denote the analogous distance in \mathbb{S}^N by

$$\text{dist}_{\mathbb{S}^N}(X, Y) := \inf_{x \in X, y \in Y} \left\{ \inf_{\substack{\gamma \in C^1([0, 1], \mathbb{S}^N) \\ \gamma(0) = x, \gamma(1) = y}} \int_0^1 |\gamma'(s)| ds \right\},$$

where X and Y may be single points.

Definition 2.7 (Balls). For $r > 0, x \in \mathbb{R}^N$ we define the ball in \mathbb{R}^N as

$$B_r(x) := \{y \in \mathbb{R}^N : \text{dist}_{\mathbb{R}^N}(x, y) < r\} \subset \mathbb{R}^N.$$

For $r > 0, x \in \mathbb{S}^N$ we define the spherical ball in \mathbb{S}^N as

$$\mathcal{B}_r(x) := \{y \in \mathbb{S}^N : \text{dist}_{\mathbb{S}^N}(x, y) < r\} \subset \mathbb{S}^N.$$

The dimension N is usually implied by the centre x .

A useful characterisation of thick curves is that around every point on the curve there exists an open horn torus – an open full torus with both radii equal leaving only a single point as ‘hole’ through which the curve passes – that does not intersect the curve. [Ge04] is based on this idea, but the fact shows up earlier [GMSvdM02, GdlL03].

Definition 2.8 (Torus Property). *Consider a regular curve $\gamma \in C^1(I, \mathbb{R}^N)$. For $\Theta > 0, s \in I$ define*

$$M(s, \Theta) := \bigcup_{z \in C(s, \Theta)} B_{\Theta}(z) \subset \mathbb{R}^N,$$

where

$$C(s, \Theta) := \{\Theta v + \gamma(s) : v \in \mathbb{S}^{N-1} \text{ and } v \perp \gamma'(s)\} \cong \mathbb{S}^{N-2}$$

is the centre-set. We say γ has the torus property with respect to Θ iff $\gamma(I) \cap M(s, \Theta) = \emptyset$ for all $s \in I$.

For completeness we also define the classic notion of normal injectivity radius (according to [LSDR99]):

Definition 2.9 (Normal injectivity radius). *Let $\gamma \in C^1(I, M)$ be a regular curve and $M \subset \mathbb{R}^N$ an embedded manifold. Define the normal bundle of γ by*

$$E := \{(\gamma(s), v) \in TM : s \in I, v \in T_{\gamma(s)}M, \langle v, \gamma'(s) \rangle = 0\},$$

where TM is the tangent bundle of M and $\langle \cdot, \cdot \rangle$ is the scalar product in \mathbb{R}^N . For $r > 0$ we define

$$E_r := \{(x, v) \in E : |v| \leq r\}.$$

Let $\exp : TM \rightarrow M$ be the exponential map (as defined for example in [dC92, pp. 64]). We then define the normal injectivity radius of γ by

$$\text{NIR}[\gamma] := \begin{cases} \sup(\{r > 0 : \exp \text{ is injective on } E_r\} \cup \{0\}) & \text{if } \gamma \text{ is injective,} \\ 0 & \text{otherwise.} \end{cases} \quad (2.3)$$

If the manifold M is not clear from the context, we write NIR_M to emphasize it.

Remark 2.10. (i) *The normal injectivity radius is invariant under monotonic reparametrizations of the curve.*

(ii) *Since E is defined on the image of γ , whenever the mapping γ is not injective, for example double coverings, the normal injectivity radius $\text{NIR}[\gamma]$ is explicitly defined to vanish.*

Definition 2.11 (Tubular neighbourhood in \mathbb{R}^N). *Let $\gamma \in C^1(I, \mathbb{R}^N)$ be a closed, regular curve. Then we define the tubular neighbourhood of γ with radius Θ as*

$$T_{\Theta}(\gamma) := \{x \in \mathbb{R}^3 : \text{dist}_{\mathbb{R}^N}(x, \gamma(I)) < \Theta\} \quad (2.4)$$

$$= \bigcup_{s \in I} D_{\Theta}(\gamma(s), \gamma'(s)), \quad (2.5)$$

where

$$D_{\Theta}(\gamma(s), \gamma'(s)) := \{x \in \mathbb{R}^N : |\gamma(s) - x| < \Theta \text{ and } \langle \gamma(s) - x, \gamma'(s) \rangle = 0\}$$

is the normal disk in $\gamma(s)$.

The equivalence between (2.4) and (2.5) is easy to see by using closest point projection.

All of the above notions lead to the same notion of thickness in \mathbb{R}^N :

Theorem 2.12 (Big equivalence). *Let $\gamma \in C^1(I, \mathbb{R}^N)$ be a closed, regular curve and $\Theta > 0$ some constant. Then the following statements are equivalent:*

- (i) $\Delta[\gamma] > \Theta$.
- (ii) γ is injective and has the torus property with constant Θ .
- (iii) $\Delta_{\text{pt}}[\gamma] := \inf_{s,t \in I, s \neq t} \text{pt}[\gamma](s, t) > \Theta$.
- (iv) $\Delta_{\text{tt}}[\gamma] := \inf_{s,t \in I, s \neq t} \text{tt}[\gamma](s, t) > \Theta$.
- (v) $\text{NIR}_{\mathbb{R}^N}[\gamma] > \Theta$.
- (vi) The tubular neighbourhood $T_\Theta(\gamma)$ is the disjoint union $\dot{\bigcup}_{s \in I} D_\Theta(\gamma(s), \gamma'(s))$ of normal disks.
- (vii) For each x in the tubular neighbourhood $T_\Theta(\gamma)$ there exists a unique closest point $y \in \gamma(I)$ and γ is injective.

Proof. (i),(ii),(iii): These equivalences are proved in [Ge04, Satz 3.25] but have been known before (see e.g. [GdlL03, S04, SvdM04]).

(iii) \Leftrightarrow (iv): This was shown in [GMS02].

(v) \Leftrightarrow (i): This is proven by combining facts from [LSDR99] and [GM99] and generalising to \mathbb{R}^N (cf. proof of Theorem 2.19 for an idea).

(vi),(vii) \Leftrightarrow (i): Statement (vi) is proved in [GMSvdM02, Lemma 3] and (vii) is a direct consequence of this. \square

As a direct consequence of the above and the torus property we have:

Lemma 2.13. [GdlL03, Lemma 2] *Let $\gamma \in C^1(I, \mathbb{R}^N)$ be a closed, regular curve with $\Delta[\gamma] > 0$. Then $\text{diam}(\gamma(I)) \geq 2\Delta[\gamma]$.* \square

One of the ingredients in the proof of Theorem 2.12 is the following lemma which we will use on other occasions too.

Lemma 2.14 (Lipschitz constant for γ'). *Consider a curve $\gamma \in C^1(\mathbb{S}, \mathbb{R}^N)$ with constant speed $L := |\gamma'(s)|$ for all $s \in \mathbb{S}$, and suppose $\Delta[\gamma] \geq \Theta > 0$. Then*

- (i) *the curve γ has a Lipschitz continuous tangent γ' with Lipschitz constant $L\Theta^{-1}$. That is $\gamma \in C^{1,1}(\mathbb{S}, \mathbb{R}^3)$ and*

$$|\gamma'(s) - \gamma'(\sigma)| \leq L\Theta^{-1}|s - \sigma|, \quad \forall s, \sigma \in \mathbb{S}; \quad (2.6)$$

- (ii) *there exists a constant $C \in (0, 1)$ dependent only on Θ , such that*

$$C|s - \sigma| \leq |\gamma(s) - \gamma(\sigma)|/L \leq |s - \sigma|, \quad (2.7)$$

for all $s, \sigma \in \mathbb{S}$ with $|s - \sigma| \leq \Theta/(2L)$.

Proof. For the proof of part (i) see [GMSvdM02, Lemma 2], [GdlL03, Lemma 3] or [Ge04, Satz 2.13]. Part (ii) is a rescaling to non-unit speed of [GdlL03, Lemma 4]. \square

If a curve touches itself globally, as in Figure 2.1(b), we may consider the points of closest approach, i.e. the antipodal points where the circle touches. The dashed line connecting the two points is called a contact chord.

Definition 2.15 (Contact Chord). *Let $\gamma \in C^1(\mathbb{S}, \mathbb{R}^N)$ be a regular curve with $\Delta[\gamma] > 0$ and let $s, t \in \mathbb{S}$ be such that $c(s, t) := \gamma(t) - \gamma(s)$ has length*

$$|c(s, t)| = 2\Delta[\gamma],$$

and $\gamma(s) - \gamma(t)$ is orthogonal to γ , i.e.

$$\langle \gamma'(s), \gamma(s) - \gamma(t) \rangle = 0 \quad \text{and} \quad \langle \gamma'(t), \gamma(s) - \gamma(t) \rangle = 0,$$

then we call $c(s, t)$ a contact chord. If such s and t exist, we say γ has a contact chord connecting $\gamma(s)$ and $\gamma(t)$ or the parameters s and t are globally in contact. The set

$$\{\gamma(s) + hc(s, t) : h \in [0, 1]\} \subset \mathbb{R}^N$$

will also be called a contact chord.

Obviously being in contact is a symmetric relation.

2.2 Thickness in \mathbb{S}^N

In Chapters 3 and 4 we want to consider thick curves on the unit sphere $\mathbb{S}^N \subset \mathbb{R}^{N+1}$. Since \mathbb{S}^N is a subset of \mathbb{R}^{N+1} we can use the same Definition 2.1 of Δ with some remarks:

Remark 2.16.

- (i) *The collinear case $R(x, y, z) = \infty$ cannot arise for $x, y, z \in \mathbb{S}^N$. In fact $\rho_G[\gamma] \in [0, 1]$ for all curves $\gamma : I \rightarrow \mathbb{S}^N$ (see Example 2.17 and [Ge04, Lemma 3.4]).*
- (ii) *Because three distinct points define a two-dimensional plane in \mathbb{R}^{N+1} , and because any non-trivial intersection of a 2-plane with \mathbb{S}^N is a circle we note that for curves on \mathbb{S}^N all circles arising in Definition 2.1 lie completely in \mathbb{S}^N , so the surrounding space \mathbb{R}^{N+1} is not needed to define the global radius of curvature ρ_G . Instead of using the radius of the circle in \mathbb{R}^{N+1} , we could use the spherical radius $\tilde{R}(x, y, z)$ in \mathbb{S}^N which equals $\arcsin R(x, y, z)$ (see Figure 2.2(a)), and define $\tilde{\Delta}[\cdot] \in [0, \pi/2]$ accordingly.*

The following example is well known [K02]:

Example 2.17 (Great circles on spheres). *Let $\partial B_r(0) := \{x \in \mathbb{R}^N : |x| = r\}$ be a sphere of radius $r > 0$. Then the thickest curves on the sphere $\partial B_r(0)$ are great circles with radius r .*

Obviously great circles have thickness r . Now let $\gamma \in C^1(\mathbb{S}, \partial B_r(0))$ be some thick curve on $\partial B_r(0)$ and let x and y be distinct points in the image $\gamma(\mathbb{S})$. The points x, y and 0 span a plane $E \subset \mathbb{R}^N$ which intersects the sphere in a great circle with radius r .

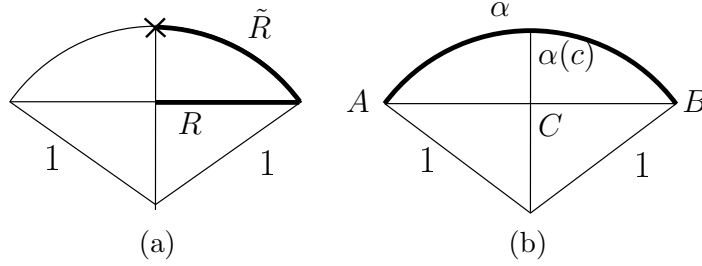


Figure 2.2: (a) The relation of the radius R of a circle in \mathbb{R}^N and the spherical radius $\tilde{R} = \arcsin R$ in \mathbb{S}^N . (b) For any secant \overline{AB} of length shorter than 2 there is a unique geodesic α on the unit sphere.

If there is a point z in the image of γ , but not in the plane E , then $R(x, y, z) < r$ so a curve with thickness $\Delta[\gamma] \geq r$ must be contained in the plane E . Since $\Delta[\gamma] > 0$ implies injectivity, great circles are the only curves in the one-dimensional set $E \cap \partial B_r(0)$ and have maximal thickness r .

In fact the distance in \mathbb{S}^N is related to the distance in the surrounding \mathbb{R}^{N+1} by the arcsin (see Figure 2.2(b)).

Lemma 2.18 (Great arcs and secants). (i) Let $A, B \in \mathbb{S}^N$, with $|A - B| < 2$. Then the secant \overline{AB} joining A and B is associated with a unique unit-speed great arc $\alpha : [a, b] \rightarrow \mathbb{S}^N$ with endpoints A and B and length $2 \arcsin(\overline{AB}/2) < \pi$.

(ii) Define $C := (A + B)/2 \in \mathbb{R}^{N+1}$ and $c := (a + b)/2$. Then $\alpha|_{[a, c]}$ has length $\arcsin(\overline{AC})$. \square

Finally, we prove the equivalence of NIR and Δ in \mathbb{S}^3 similar to the \mathbb{R}^N case in Theorem 2.12 (v).

Theorem 2.19 (NIR and Δ). Let $\gamma \in C^1(I, \mathbb{S}^N)$ be a regular curve. Then

$$\Delta[\gamma] = \sin(\text{NIR}_{\mathbb{S}^3}[\gamma]).$$

Remark 2.20. (i) Note that if we had decided to use $\tilde{R}(\cdot, \cdot, \cdot)$ as proposed in remark 2.16 the conclusion in the above theorem would be $\text{NIR}[\gamma] = \tilde{\Delta}[\gamma]$. But we prefer Δ to keep the notation simpler.

(ii) Theorem 2.19 implies that C^1 -curves that are nicely parametrised (e.g. constant speed) and have a positive normal injectivity radius, also have positive thickness, and so are in fact $C^{1,1}$ -curves by Lemma 2.2.

Proof of Theorem 2.19. We prove that positive $\Delta[\gamma]$ implies $\text{NIR}[\gamma] \geq \arcsin \Delta[\gamma]$, and positive $\text{NIR}[\gamma]$ implies $\Delta[\gamma] \geq \sin \text{NIR}[\gamma]$.

(i) Let $\Delta[\gamma] =: \Theta > 0$ and assume $\text{NIR}[\gamma] < \vartheta := \arcsin \Theta$. Note that $\Theta > 0$ implies injectivity of γ . Then there exist two distinct points $x_0, x_1 \in \gamma(I)$ such that

$$(x_0, v_0), (x_1, v_1) \in E,$$

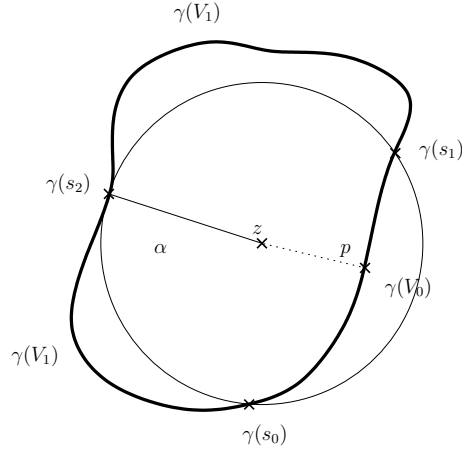


Figure 2.3: Schematic picture of the construction in part (ii) of the proof of Theorem 2.19.

$$0 < |v_1|, |v_0| \leq |v_1| < \vartheta, \quad (2.8)$$

and $\exp(x_0, v_0) = \exp(x_1, v_1) =: y \in \mathbb{S}^N$. Define $z := \exp(x_1, \vartheta \frac{v_1}{|v_1|})$, which corresponds to

$$Z := \frac{y + \exp(x_1, 2\vartheta \frac{v_1}{|v_1|})}{2} \in \mathbb{R}^{N+1},$$

as in Lemma 2.18. The point Z is the centre of a ball of radius Θ tangent to γ at x_1 .

We claim

$$\text{dist}_{\mathbb{S}^N}(x_0, z) < \vartheta. \quad (2.9)$$

First, if x_1, y, z and x_0 are all on the same geodesic arc, the claim holds since x_0 lying inside the short arc connecting x_1 and y implies $|v_0| < |v_1|$, which leads to $\text{dist}_{\mathbb{S}^N}(x_0, z) \leq \text{dist}_{\mathbb{S}^N}(x_0, y) + \text{dist}_{\mathbb{S}^N}(y, z) < \text{dist}_{\mathbb{S}^N}(x_1, y) + \text{dist}_{\mathbb{S}^N}(y, z) = \vartheta$. If x_0 does not lie inside the short arc connecting x_1 and y , we have $\text{dist}_{\mathbb{S}^N}(x_0, z) = |\text{dist}_{\mathbb{S}^N}(x_0, y) - \text{dist}_{\mathbb{S}^N}(y, z)| < \vartheta$.

Suppose now x_0, x_1 and y are not on a geodesic arc. From (2.8) we get

$$\underbrace{\text{dist}_{\mathbb{S}^N}(x_0, y)}_{=|v_0|} + \text{dist}_{\mathbb{S}^N}(y, z) \leq \underbrace{\text{dist}_{\mathbb{S}^N}(x_1, y)}_{=|v_1|} + \text{dist}_{\mathbb{S}^N}(y, z) = \text{dist}_{\mathbb{S}^N}(x_1, z) = \vartheta,$$

and together with the strict triangle inequality we find

$$\text{dist}_{\mathbb{S}^N}(x_0, z) < \text{dist}_{\mathbb{S}^N}(x_0, y) + \text{dist}_{\mathbb{S}^N}(y, z) \leq \vartheta.$$

But this implies $\text{dist}_{\mathbb{R}^{N+1}}(x_0, Z) = |x_0 - Z| < \Theta$, which is a contradiction to the torus property in Theorem 2.12 (ii). Therefore $\text{NIR}[\gamma] \geq \vartheta$ as claimed.

- (ii) To prove the converse, we adapt the proof of [GMSvdM02, Lemma 3]. Let $\text{NIR}[\gamma] =: \vartheta > 0$ and assume $\Delta[\gamma] < \bar{\Theta} := \sin \vartheta$ which implies there exist parameters $s_0, s_1, s_2 \in I$ such that $R(\gamma(s_0), \gamma(s_1), \gamma(s_2)) =: \bar{\delta} < \bar{\Theta}$. Let $Z \in \mathbb{R}^{N+1}$ be the

centre of the circle through the points $\gamma(s_0), \gamma(s_1), \gamma(s_2)$, and let $z \in \mathbb{S}^N$ be the corresponding point on the sphere, which satisfies

$$\text{dist}_{\mathbb{S}^N}(z, \gamma(s_i)) = \tilde{\delta} := \arcsin \bar{\delta} \text{ for } i = 1, 2, 3. \quad (2.10)$$

Because of (2.10), and since \arcsin is strictly monotonic on the interval under consideration, we find $\text{dist}_{\mathbb{S}^N}(z, \gamma(I)) \leq \tilde{\delta} = \arcsin \bar{\delta} < \vartheta$. Since $\gamma(I)$ is compact, we find a point $p \in \gamma(I)$ such that $\text{dist}_{\mathbb{S}^N}(z, \gamma(I)) = \text{dist}_{\mathbb{S}^N}(z, p)$, and since $\gamma \in C^1(I, \mathbb{S}^N)$, we find $\gamma'(\gamma^{-1}(p)) \perp (p - z)$, which implies that $z \in \text{im exp}(E_\delta)$. By assumption the pre-image of z under $\text{exp} : E_\delta \rightarrow \mathbb{S}^N$ contains the single point p .

We have $\text{dist}_{\mathbb{S}^N}(z, p) < \text{dist}_{\mathbb{S}^N}(z, \gamma(s_i)) = \tilde{\delta}, i = 1, 2, 3$, since $(z - \gamma(s_i)) \not\perp \gamma'(s_i)$ implies the existence of some $p' \in \mathbb{S}^N$ with $\text{dist}_{\mathbb{S}^N}(z, p') < \text{dist}_{\mathbb{S}^N}(z, \gamma(s_i))$, and $(z - \gamma(s_i)) \perp \gamma'(s_i)$ for $i = 0, 1, 2$ implies the $\gamma(s_i)$ are all in the pre-image of $\text{exp} : E_\delta \rightarrow \mathbb{S}^N$ which is a contradiction. Without loss of generality, the parameters s_i , partition $I \cong \mathbb{S}$ in three disjoint open sub-arcs, defined by $V_0 := (s_0, s_1), W_1 := (s_1, s_2)$ and $W_2 := (s_2, s_0)$ and we may assume $p \in \gamma(V_0)$.

Next consider the sub-arc $V_1 := W_1 \cup \{s_2\} \cup W_2$, and the shortest great arc $\alpha : [0, 1] \rightarrow \mathbb{S}^N$ joining z and $\gamma(s_2)$. This great arc has the following properties:

$$\begin{aligned} \alpha(0) &= z, \quad \alpha(1) = \gamma(s_2), \\ \text{dist}_{\mathbb{S}^N}(\alpha(s), \gamma(s_2)) &< \text{dist}_{\mathbb{S}^N}(\alpha(s), \gamma(s_i)), \quad 0 < s \leq 1 \quad (i = 0, 1), \end{aligned} \quad (2.11)$$

and $\alpha(s)$ is in the image of $\text{exp} : E_\delta \rightarrow \mathbb{S}^N$. Since $\text{exp} : E_\delta \rightarrow \mathbb{S}^N$ is an injective continuous function on a compact set, it is in fact a homeomorphism. From (2.11) we deduce that neither $\gamma(s_0)$ nor $\gamma(s_1)$ are in the pre-image $\text{exp}^{-1} \circ \alpha([0, 1])$. This means that the pre-image of $\alpha([0, 1])$ is not connected, which is a contradiction to the continuity of exp^{-1} and α . Therefore we have $\Delta[\gamma] \geq \bar{\Theta}$. □

The spaces \mathbb{R}^N and \mathbb{S}^N are related by stereographic projection.

Definition 2.21 (Stereographic projection). *Let $N^\infty \in \mathbb{S}^N$ be some distinguished point, that we call the north pole of \mathbb{S}^N , and let $E \subset \mathbb{R}^{N+1}$ be the N -dimensional tangent plane to \mathbb{S}^N at $S^0 := -N^\infty$, i.e. south pole. We define the stereographic projection $P : \mathbb{S}^N \setminus \{N^\infty\} \rightarrow \mathbb{R}^N$ by the following rule: Every point $x \in \mathbb{S}^N \setminus \{N^\infty\}$ is mapped to x' , the unique intersection point of the plane $E \cong \mathbb{R}^N$ and the ray from N^∞ passing through x (see Figure 2.4 for the $N = 1$ case). If $N^\infty = (1, 0, \dots, 0)$ then for $x = (x_1, \dots, x_{N+1}) \in \mathbb{S}^N \subset \mathbb{R}^{N+1}$ the stereographic projection is*

$$P(x) := \left(\frac{2x_2}{1-x_1}, \dots, \frac{2x_{N+1}}{1-x_1} \right) \in \mathbb{R}^N.$$

Lemma 2.22 (Estimates on stereographic projection from \mathbb{S}^N to \mathbb{R}^N). *Let $P : \mathbb{S}^N \setminus \{N^\infty\} \rightarrow \mathbb{R}^N$ be the stereographic projection of Definition 2.21. Then*

$$R(x, y, z) \leq R(P(x), P(y), P(z))$$

for $x, y, z \in \mathbb{S}^N \setminus \{N^\infty\}$, and

$$\Delta[\gamma] \leq \Delta[P(\gamma)].$$

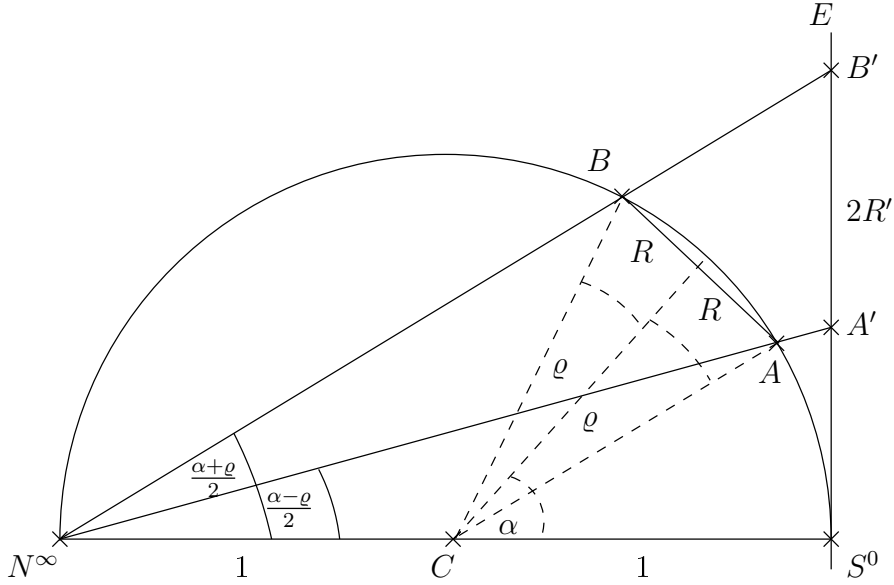


Figure 2.4: The stereographic projection P of Definition 2.21 increases the radius of every circle on \mathbb{S}^3 .

Proof. Fix $x, y, z \in \mathbb{S}^N \setminus \{N^\infty\}$. Let

$$\varrho := \arcsin R(x, y, z) \quad (2.12)$$

be the angular radius of the circle C through x, y, z (see Figure 2.4). The stereographic projection maps circles C to circles C' (see [CG67]). If the circle through x, y, z passes through the north pole N^∞ , $R(P(x), P(y), P(z)) = \infty$ follows and we are finished. More generally, if we want to calculate the radius of the projected circle C' , we may not do so using the projection of the centre of the original circle C , since centres of circles are not mapped to centres of the projected circles. Instead we consider the longitude through the circle centre which is mapped to (the extension of) the diameter of the image circle. Thus the distance between the images A', B' of the two points A, B where the circle C intersects this longitude, immediately provide the new radius. Specifically¹

$$\begin{aligned} R(P(x), P(y), P(z)) &= \left| \frac{\overline{S^0 B'} - \overline{S^0 A'}}{2} \right| \\ &= \left| \tan\left(\frac{\alpha + \varrho}{2}\right) - \tan\left(\frac{\alpha - \varrho}{2}\right) \right| \\ &= \left| \frac{\sin \varrho}{\cos\left(\frac{\alpha + \varrho}{2}\right) \cos\left(\frac{\alpha - \varrho}{2}\right)} \right| \\ &= \left| \frac{2 \sin \varrho}{\cos \alpha + \cos \varrho} \right| \\ &= \left| \frac{2}{\cos \alpha + \cos \varrho} \right| R(x, y, z), \end{aligned} \quad (2.13)$$

¹Aide m emoire: $\tan x + \tan y = \sin(x + y)/(\cos x \cos y)$, and $\cos x \cos y = [\cos(x + y) + \cos(x - y)]/2$.

where $\alpha \in [0, \pi]$ is the angle between the south-pole $S^0 = -N^\infty$, and the centre of the circle through x, y, z . Finally

$$R(P(x), P(y), P(z)) = \left| \frac{2 \sin \varrho}{\cos \alpha + \cos \varrho} \right| \geq \sin \varrho = R(x, y, z).$$

□

Lemma 2.23 (Free spot). *Let $\gamma : \mathbb{S} \rightarrow \mathbb{S}^N, N \geq 2$, be a curve with $\Delta[\gamma] \geq \Theta > 0$. Then there exists a point $N^\infty \in \mathbb{S}^N$ such that*

$$\text{dist}_{\mathbb{R}^N}(\{N^\infty\}, \gamma(\mathbb{S})) \geq \Theta.$$

Proof. Let $s \in \mathbb{S}$ be arbitrary and let $C(s, \Delta[\gamma])$ be the centre-set of the torus around $\gamma(s)$, as defined in Definition 2.8. Then $N^\infty \in C \cap \mathbb{S}^N \neq \emptyset$ does not lie on the curve, and we have $d_{\mathbb{R}^N}(\{N^\infty\}, \gamma(\mathbb{S})) = \Theta$. □

2.3 Knotted Curves

Thick curves can be knotted. Traditionally, few authors in the field of ideal knots cared about topological subtleties of knot theory and we will not break with this tradition. We follow the proceeding of [S04]:

Definition 2.24 (Knots). *Let $M = \mathbb{R}^3$ or $M = \mathbb{S}^3$.*

- (i) *A knot or knot shape $K \subset M$ is the image of a closed, injective, continuous curve $\gamma \in C^0(I, M)$.*
- (ii) *An ambient isotopy is a continuous map $h : M \times [0, 1] \rightarrow M$ with $h(\cdot, 0) = \text{id}_M$ and $h(\cdot, t)$ a homeomorphism for all $t \in [0, 1]$.*
- (iii) *Two knots K_1 and K_2 are ambient isotopic (notation: $K_1 \simeq_M K_2$) if an ambient isotopy $h : M \times [0, 1] \rightarrow \mathbb{R}^3$ exists with $h(K_1, 1) = K_2$.*

Usually we also call γ a knot, not just the set $\gamma(I)$. The subtleties are discussed for example in [BZ03]. We drop the M from \simeq_M if it is clear from the context.

Remark 2.25. *Note that all thick knots are tame in the sense of [BZ03, p. 3]. This was proved in [LSDR99, Theorem 2] for the \mathbb{R}^3 -case. By using the stereographic projection the result lifts to \mathbb{S}^3 . Accordingly we hereafter consider only tame knots.*

Apart from N^∞ the spaces \mathbb{S}^N and \mathbb{R}^N are topologically the same. By Lemma 2.23 we may always assume that the thick knot does not pass through N^∞ and we can lift certain topological properties to \mathbb{S}^N :

Lemma 2.26 (Ambient isotopies under stereographic projection). *Let $P : \mathbb{S}^3 \setminus \{N^\infty\} \rightarrow \mathbb{R}^3$ be the stereographic projection of Definition 2.21 and let γ_0 and $\gamma_1 \in C^0(I, \mathbb{R}^3)$ be two injective curves such that*

$$\gamma_0(I) \simeq_{\mathbb{R}^3} \gamma_1(I).$$

Then

$$P^{-1} \circ \gamma_0(I) \simeq_{\mathbb{S}^3} P^{-1} \circ \gamma_1(I).$$

Proof. Since $\gamma_0(I) \simeq_{\mathbb{R}^3} \gamma_1(I)$ there exists an ambient isotopy $h : \mathbb{R}^3 \times [0, 1] \rightarrow \mathbb{R}^3$ with $\gamma_1(I) = h(\gamma_0, 1)$. Define $\tilde{h} : \mathbb{S}^3 \times [0, 1] \rightarrow \mathbb{S}^3$ by

$$\begin{aligned}\tilde{h}(x, t) &:= P^{-1} \circ h(P(x), t), \\ \tilde{h}(N^\infty, t) &:= N^\infty \quad \text{for all } t \in [0, 1].\end{aligned}$$

Note that $\tilde{h}(\cdot, t)$ is one-to-one and maps compact sets to compact sets and therefore neighbourhoods of N^∞ to neighbourhoods of N^∞ , so the extended map is in fact a homeomorphism for each t . Hence we showed $P^{-1} \circ \gamma_0(I) \simeq_{\mathbb{S}^3} P^{-1} \circ \gamma_1(I)$ by the ambient isotopy \tilde{h} . \square

The following lemma will be useful to prove that the limit of a sequence is in the same knot class.

Lemma 2.27. [Rt05] *Let $\eta \in C^1(\mathbb{S}^1, \mathbb{R}^3)$ be a regular, injective, closed curve. Then there exists a constant $\varepsilon^* > 0$ depending on η such that all $\zeta \in C^1(\mathbb{S}^1, \mathbb{R}^3)$ with $\|\zeta' - \eta'\|_{C^0(\mathbb{S}^1, \mathbb{R}^3)} \leq \varepsilon^*$ are ambient isotopic to η .* \square

We have now approached a convenient function space² for problems concerning thick curves

$$\mathcal{K} := \{\gamma \in C^1(I, M) : \Delta[\gamma] > 0, |\gamma'(t)| \equiv \text{const } \forall t \in I\}, \quad (2.14)$$

and are able to define ideal knots:

Definition 2.28 (Ideal Knot in \mathbb{R}^3). *Let $k \in C^1(\mathbb{S}, \mathbb{R}^3)$ be regular curve representing a knot class. We call $\gamma^* \in C^1(I, \mathbb{R}^3)$ ideal iff*

$$\frac{\mathcal{L}[\gamma^*]}{\Delta[\gamma^*]} = \inf_{\gamma \in C^1(\mathbb{S}, \mathbb{R}^3), \gamma \simeq k} \frac{\mathcal{L}[\gamma]}{\Delta[\gamma]},$$

where $\mathcal{L}[\gamma] := \int_I |\gamma'|$ is the arc-length of γ . The functional

$$\mathcal{R}[\cdot] := \frac{\mathcal{L}[\cdot]}{\Delta[\cdot]}$$

is called ropelength [CKS02].

2.4 Convergence Analysis of Curves in \mathbb{R}^N

So far we only considered a fixed curve and its thickness. This section deals with sequences of thick curves and their limits. Many results in this section have been proved before for \mathbb{R}^3 and most of the time the generalisation to \mathbb{R}^N is straight forward.

To prove the existence of solutions to optimisation problems, one needs first to identify a good solution space \mathcal{K} which we have done in equation (2.14) above. Next, one typically picks an extremal sequence $\{\gamma_n\}$ and finds a convergent subsequence which is done in the next two lemmata.

² By Lemma 2.2 we know $\mathcal{K} \subset C^{1,1}$. Considering only constant speed curves reflects the fact that we are more interested in shapes, than in parametrisations. For some arguments constant speed is technically difficult to achieve, but we can later reparametrise the curve.

Lemma 2.29 (Speed limit I). *Let $\{\gamma_n\}_n \subset C^1(\mathbb{S}, \mathbb{R}^N)$ be a sequence of curves with constant speed $|\gamma'_n(s)| = L_n$, $\Delta[\gamma_n] \geq \Theta > 0$, and $\gamma_n(\mathbb{S}) \subset B_r(0)$ for some constant $r > 0$ for all $n \in \mathbb{N}$. Then there exist two constants $c_1, c_2 > 0$ which bound the speed*

$$0 < c_1 \leq |\gamma'_n(s)| \leq c_2 < \infty, \quad \forall n \in \mathbb{N}, \text{ and } \forall s \in \mathbb{S}.$$

Proof. By Lemma 2.13 there is a lower bound $c_1 > 0$. The upper bound $c_2 < \infty$ is proven in [StvdM04, proof of theorem 6.4, Step 2]. \square

We will quantify the constants later in Lemma 3.13. The next lemma distills methods from [GdlL03].

Lemma 2.30 (Adapted Ascoli). *Let $\{\gamma_i\}_i \subset C^1(\mathbb{S}, \mathbb{R}^N)$ be a sequence of curves with the following properties:*

- (i) *Each γ_i has constant speed $|\gamma'_i(s)| \equiv L_i > 0$ for all $s \in \mathbb{S}$,*
- (ii) *There exists a constant $\Theta > 0$ such that $\Delta[\gamma_i] \geq \Theta$ for all $i \in \mathbb{N}$,*
- (iii) *There exists a constant $r > 0$ such that $\gamma_i(\mathbb{S}) \subset B_r(0)$ for all $i \in \mathbb{N}$.*

Then there exists a subsequence $\{\gamma_{i_j}\}_j \subset \{\gamma_i\}_i$, and a limit $\gamma \in C^1(\mathbb{S}, \mathbb{R}^N)$ such that $\gamma_{i_j} \rightarrow \gamma$ in $C^1(\mathbb{S}, \mathbb{R}^N)$, i.e.

$$\gamma_{i_j} \rightarrow \gamma \text{ in } C^0(\mathbb{S}, \mathbb{R}^N),$$

and

$$\gamma'_{i_j} \rightarrow \gamma' \text{ in } C^0(\mathbb{S}, \mathbb{R}^N).$$

Furthermore $|\gamma'_{i_j}| \rightarrow |\gamma'| = \text{const} > 0$.

Proof. By Lemma 2.29 there exist positive constants c_1 , and c_2 such that $c_1 \leq |\gamma'_i(t)| = L_i \leq c_2$ for all $i \in \mathbb{N}, t \in \mathbb{S}$. This bound implies equicontinuity:

$$\begin{aligned} \gamma_i(s) - \gamma_i(\sigma) &= \int_{\sigma}^s \gamma'_i(\tau) d\tau, \\ |\gamma_i(s) - \gamma_i(\sigma)| &\leq \int_{\sigma}^s \underbrace{|\gamma'_i(\tau)|}_{\leq c_2} d\tau \leq c_2 |s - \sigma|, \\ |\gamma_i(s) - \gamma_i(\sigma)|/c_2 &\leq |s - \sigma|, \end{aligned} \tag{2.15}$$

for all $s, \sigma \in \mathbb{S}$. Since, by (iii), the sequence $\{\gamma_i\}_i$ is also bounded, Ascoli's theorem implies existence of a C^0 -convergent subsequence $\{\gamma_{i_k}\}$ and a limit γ .

Define

$$f_{i_k} := \gamma'_{i_k} \in C^0(\mathbb{S}, \mathbb{R}^N).$$

The sequence $\{f_k\}_k$ is equicontinuous by (2.6), and uniformly bounded so, again by Ascoli's theorem, there exists a subsequence f_{i_j} that converges to some limit $f \in C^0(\mathbb{S}, \mathbb{R}^N)$. By uniqueness of limits we still have $\gamma_{i_j} \rightarrow \gamma$. It remains to show that $\gamma' = f$. Consider

$$\gamma_{i_j}(t) = \gamma_{i_j}(1) + \int_1^t f_{i_j}(\tau) d\tau, \tag{2.16}$$

which implies

$$\gamma(t) = \gamma(1) + \int_1^t f(\tau) d\tau \quad (2.17)$$

since we can exchange the limit and integration by equicontinuity. Thus $f = \gamma'$, $\gamma_{i_j} \rightarrow \gamma$ in $C^1(\mathbb{S}, \mathbb{R}^N)$, and since $|\gamma'_{i_j}(s)| = L_{i_j} \geq c_1$ for all $s \in \mathbb{S}$, we also have for the limit $|\gamma'(s)| = \text{const} \geq c_1 > 0$. \square

Now that we found an accumulation point γ we need to verify that it is itself in the class \mathcal{K} ;

Lemma 2.31 (Upper semicontinuity of Δ). *[GdlL03, Lemma 5] Let $\{\gamma_n\}_n \subset C^1(\mathbb{S}, \mathbb{R}^N)$ be a sequence of curves such that*

- (i) $\Delta[\gamma_n] \geq \Theta > 0$ for all $n \in \mathbb{N}$,
- (ii) $|\gamma'_n(s)| \equiv L_n$ for all $n \in \mathbb{N}, s \in \mathbb{S}$,
- (iii) $\gamma_n \rightarrow \gamma$ in $C^0(\mathbb{S}, \mathbb{R}^N)$.

Then the limit γ is a simple curve in $C^1(\mathbb{S}, \mathbb{R}^N)$ and $\Delta[\gamma] \geq \Theta$. Consequently, if $\Delta[\gamma_n] \rightarrow \eta$, then $\Delta[\gamma] \geq \eta$.

Proof. We know that $\gamma(\mathbb{S}) \subset B_r(0)$ for $r \in \mathbb{R}$ sufficiently large because the curve is compact. We conclude $\gamma_n(\mathbb{S}) \subset B_{2r}(0)$ for n sufficiently large by C^0 -convergence. From Lemma 2.30 we deduce that a subsequence converges $\gamma_{n_i} \rightarrow \gamma$ in $C^1(\mathbb{S}, \mathbb{R}^N)$. The rest of the proof then follows that of [GdlL03, Lemma 5] (see also [GMSvdM02, Lemma 4], [SvdM03a, Lemma 4]). \square

The above lemma also shows for example that an accumulation point γ of a thickness maximising sequence has maximal thickness. Since we deal with knots we also want to make sure that γ is still in the same knot class as the extremal sequence.

Lemma 2.32 (Knot invariance in \mathbb{R}^3). *[GMSvdM02, Lemma 5], [GdlL03, Lemma 6] Let $\{\gamma_n\}_n \subset C^1(\mathbb{S}, \mathbb{R}^3)$ be a sequence of curves such that*

- (i) $|\gamma'_n(s)| \equiv L_n, \forall s \in \mathbb{S}$,
- (ii) $\Delta[\gamma_n] \geq \Theta > 0, \forall n \in \mathbb{N}$,
- (iii) $\gamma_n \rightarrow \gamma$ in $C^0(\mathbb{S}, \mathbb{R}^3)$ as $n \rightarrow \infty$.

Then $\gamma \simeq_{\mathbb{R}^3} \gamma_n$ for all n sufficiently large.

Proof. By Lemma 2.31 the curve γ is embedded, and by Lemma 2.30 and the subsequence principle we have in fact C^1 -convergence. By Lemma 2.27 all curves in a C^1 -neighbourhood of γ are ambient isotopic, so we have $\gamma \simeq_{\mathbb{R}^3} \gamma_n$ for n sufficiently large. \square

The following lemma looks similar to Lemma 2.31 but with reversed roles. This time we know that the limit curve γ is thick and approximate it with a $C^{1,1}$ sequence

$\{\gamma_j\}_j$. If the curvature of each γ_j is bounded³ with respect to the thickness of γ then the thickness of γ_j at least approaches the thickness of γ for $j \rightarrow \infty$. We will use this to show that small variations of a curve, at worst, only slightly reduce its thickness.

Lemma 2.33 (Smooth approximation with positive thickness I). *Let $\gamma \in C^1(\mathbb{S}, \mathbb{R}^N)$ be a closed and regular curve with positive thickness $\Delta[\gamma] > 0$. Then for any sequence $\{\gamma_j\} \subset C^{1,1}(\mathbb{S}, \mathbb{R}^N)$ satisfying*

(i) $\gamma_j \rightarrow \gamma$ in $C^1(\mathbb{S}, \mathbb{R}^N)$ as $j \rightarrow \infty$,

(ii) $\limsup_{j \rightarrow \infty} \|\kappa_j\|_{L^\infty(\mathbb{S})} \leq \frac{1}{\Delta[\gamma]}$, where κ_j denotes the local curvature⁴ of γ_j for $j \in \mathbb{N}$,

one has

$$\liminf_{j \rightarrow \infty} \Delta[\gamma_j] \geq \Delta[\gamma]. \quad (2.18)$$

Proof. Notice that the C^1 -convergence we assume in (i) implies

$$L_j := \mathcal{L}[\gamma_j] \longrightarrow \mathcal{L}[\gamma] = L \quad \text{and} \quad (2.19)$$

$$|\gamma'_j| \longrightarrow |\gamma'| > 0 \quad \text{on } \mathbb{S} \quad \text{as } j \rightarrow \infty,$$

and the arc-length parametrisations $\Gamma_j : [0, L_j] \rightarrow \mathbb{R}^N$ satisfy by assumption (ii)

$$\limsup_{j \rightarrow \infty} \|\Gamma_j''\|_{L^\infty((0, L_j), \mathbb{R}^N)} = \limsup_{j \rightarrow \infty} \|\kappa_j\|_{L^\infty(\mathbb{S})} \leq \frac{1}{\Delta[\gamma]}. \quad (2.20)$$

In order to establish (2.18) it suffices to show that for any given $\varepsilon > 0$ there is some $j_0 = j_0(\varepsilon) \in \mathbb{N}$ such that

$$\Delta[\gamma_j] = \Delta[\Gamma_j] \geq (1 - \varepsilon)\Delta[\gamma], \quad \text{for all } j \geq j_0.$$

We argue by contradiction. If we assume on the contrary that there exists an $\varepsilon_0 > 0$ such that

$$\Delta[\Gamma_j] < (1 - \varepsilon_0)\Delta[\gamma] \quad \text{for a subsequence } j \rightarrow \infty,$$

then for each member j of this subsequence we can find an arc-length parameter $s_j \in [0, L_j]$ such that by definition of thickness (see (2.2))

$$\rho_G[\gamma_j](s_j) < \left(1 - \frac{\varepsilon_0}{2}\right) \Delta[\gamma]. \quad (2.21)$$

It was shown in [StvdM07, Lemma 5] that

$$\rho_G[\gamma_j](s_j) = \rho_{\text{pt}}[\gamma_j](s_j) := \inf_{\tau \in [0, L_j] \setminus \{s_j\}} \text{pt}[\gamma_j](s_j, \tau),$$

with pt as in Definition 2.3. Therefore we can find for each j some arc-length parameter $\sigma_j \in [0, L_j] \setminus \{s_j\}$ such that by (2.21)

$$\text{pt}[\gamma_j](s_j, \sigma_j) < \left(1 - \frac{\varepsilon_0}{4}\right) \Delta[\gamma]. \quad (2.22)$$

³ In Examples 2.34 and 2.35 below we will see that the actual curvature of κ_j does not have to converge to the curvature of γ .

⁴By assumption (i) we can assume that all γ_j are regular curves, and recall that $C^{1,1}((0, 1), \mathbb{R}^N) \cong W^{2,\infty}((0, 1), \mathbb{R}^N)$ so that κ_j exists and is bounded a.e. on $(0, 1)$ for each $j \in \mathbb{N}$. [E98, p. 279]

Going back to the original parametrisation $\gamma_j : \mathbb{S} \rightarrow \mathbb{R}^N$ we find parameters $t_j, \tau_j \in \mathbb{S}^1$ given by

$$\int_0^{t_j} |\gamma_j'(z)| dz = s_j \neq \sigma_j = \int_0^{\tau_j} |\gamma_j'(z)| dz,$$

and by choice of an appropriate subsequence we may assume that

$$(t_j, \tau_j) \rightarrow (t, \tau) \in \mathbb{S} \times \mathbb{S} \quad \text{as } j \rightarrow \infty.$$

Two cases may occur: either these limit parameters t and τ are distinct or they coincide.

Case I. If $t \neq \tau$ then $\gamma(t) \neq \gamma(\tau)$ since γ is simple, and therefore also $\Gamma(s) \neq \Gamma(\sigma)$ for $s := \int_0^t |\gamma'(z)| dz$ and $\sigma := \int_0^\tau |\gamma'(z)| dz$. (Notice that we assumed that γ is a regular curve, i.e., $|\gamma'| > 0$ so that a double point $\gamma(t) = \gamma(\tau)$ for $t \neq \tau$ would imply a double point for the arc-length parametrisation $\Gamma(s) = \Gamma(\sigma)$ which is impossible because $\Delta[\gamma]$ is positive.) We arrive at

$$\Gamma_j(s_j) = \gamma(t_j) \longrightarrow \gamma(t) = \Gamma(s) \quad \text{and} \tag{2.23}$$

$$\Gamma_j(\sigma_j) = \gamma(\tau_j) \longrightarrow \gamma(\tau) = \Gamma(\sigma) \quad \text{as } j \rightarrow \infty.$$

In addition, one has for the derivatives by the C^1 -convergence and in particular by (2.19)

$$\Gamma_j'(\sigma_j) = \frac{\gamma_j'(\tau_j)}{|\gamma_j'(\tau_j)|} \longrightarrow \frac{\gamma'(\tau)}{|\gamma'(\tau)|} = \Gamma'(\sigma) \quad \text{as } j \rightarrow \infty, \tag{2.24}$$

so that we can use an explicit formula for the pt-radius and Theorem 2.12 to obtain from (2.22)

$$\begin{aligned} \left(1 - \frac{\varepsilon_0}{4}\right) \Delta[\gamma] &\stackrel{(2.22)}{>} \text{pt}[\gamma_j](s_j, \sigma_j) = \frac{|\Gamma_j(s_j) - \Gamma_j(\sigma_j)|}{2 \sin \angle(\Gamma_j(s_j) - \Gamma_j(\sigma_j), \Gamma_j'(s_j))} \\ &\xrightarrow{j \rightarrow \infty} \frac{|\Gamma(s) - \Gamma(\sigma)|}{2 \sin \angle(\Gamma(s) - \Gamma(\sigma), \Gamma'(s))} = \text{pt}[\gamma](s, \sigma) \\ &\geq \rho_{\text{pt}}[\gamma](s) \underset{\text{Theorem 2.12}}{\geq} \Delta[\gamma], \end{aligned}$$

which is a contradiction.

Case II. If $t = \tau$ we find $|t_j - \tau_j| \rightarrow 0$ as $j \rightarrow \infty$, so that by (2.19) for $j \gg 1$

$$|s_j - \sigma_j| = \left| \int_{\tau_j}^{t_j} |\gamma_j'(z)| dz \right| \leq 2 \|\gamma'\|_{C^0(\mathbb{S}, \mathbb{R}^3)} |t_j - \tau_j| \rightarrow 0 \quad \text{as } j \rightarrow \infty. \tag{2.25}$$

We apply (2.20) to the Taylor expansion (cf. [StvdM07, (2.20)])

$$\text{pt}[\gamma_j](s_j, \sigma_j) = \frac{\left| \Gamma_j'(\sigma_j) + f_{[\sigma_j, s_j]} \int_{\sigma_j}^{s_j} \Gamma_j''(z) dz du \right|^2}{2 \left| \Gamma_j'(\sigma_j) \wedge \frac{1}{\sigma_j - s_j} \int_0^1 \int_{\sigma_j - u(\sigma_j - s_j)}^{\sigma_j} \Gamma_j''(z) dz du \right|} \tag{2.26}$$

to find for given $\delta > 0$ some $j_1 = j_1(\delta)$ such that for all $j \geq j_1$

$$\left| \int_{\sigma_j}^{s_j} \Gamma_j''(z) dz \right| \leq \int_{[\sigma_j, s_j]} |\Gamma_j''(z)| dz \stackrel{(2.20)}{\leq} (1 + \delta) |s_j - \sigma_j| \frac{1}{\Delta[\gamma]} \quad \text{for all } u \in [\sigma_j, s_j],$$

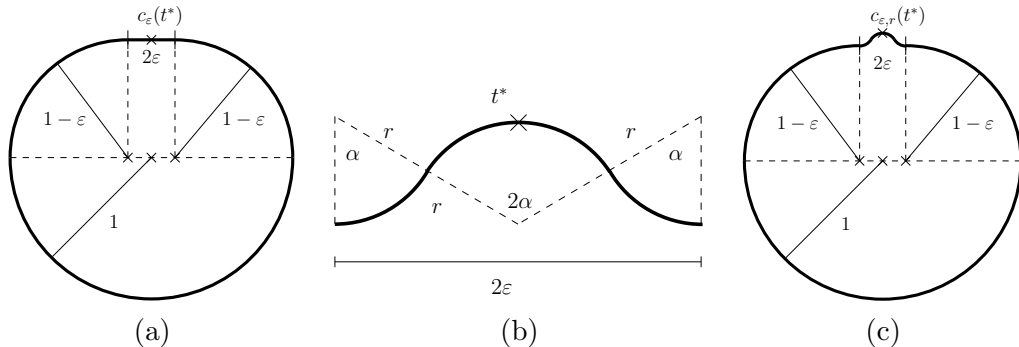


Figure 2.5: The curve shown in (a) approximates the ropelength of a circle for $\varepsilon \rightarrow 0$ but always contains a straight segment. By replacing the straight part with the curve displayed in (b), the curve in (c) approximates the ropelength of a circle for $r \geq 1$ but the curvature at parameter t^* is $1/r$. Note that the radius r depicted in (b) is too small but allows a better visualisation.

and

$$\left| \int_{\sigma_j - u(\sigma_j - s_j)}^{\sigma_j} \Gamma_j''(z) dz \right| \stackrel{(2.20)}{\leq} (1 + \delta) |u| |s_j - \sigma_j| \frac{1}{\Delta[\gamma]} \quad \text{for all } u \in [0, 1].$$

This together with (2.24) and (2.25) allows us to estimate the numerator in (2.26) by $1 - \delta$ from below, and the denominator by $(1 + \delta)/\Delta[\gamma]$ from above for all $j \geq j_2$ for some $j_2 = j_2(\delta) \geq j_1$. We infer from (2.22)

$$\left(1 - \frac{\varepsilon_0}{4}\right) \Delta[\gamma] > \text{pt}[\gamma_j](s_j, \sigma_j) \geq \frac{1 - \delta}{1 + \delta} \Delta[\gamma] \quad \text{for all } j \geq j_2,$$

which is absurd for any $\delta \leq \varepsilon_0/(8 - \varepsilon_0)$. \square

2.5 Examples on Higher Order Information

We expect ideal shapes to be piecewise C^∞ and all known shapes are of this class. Hence it is reasonable to look at higher order information such as curvature or torsion, as has been done for example in [S04]. As recently stated: ‘The differences in the ropelength are very small, but numerical simulations indicate that essential details of the curvature and torsion profiles appear only at the final stage of the tightening process.’ [BPP08] This section gives two examples demonstrating that in fact we can be arbitrarily close to the optimal thickness without seeing a reliable curvature plot.

Example 2.34 (Approximation of circle). *A circle of radius 1 can be approximated by the following construction: Start with a semicircle of radius 1 and attach a quarter circle of radius $1 - \varepsilon$ for some small $\varepsilon > 0$ at each end of the half-circle such that the ends face each other. Finally close the curve with a straight line (see Figure 2.5a). The resulting curve c_ε has the following properties:*

$$\begin{aligned} \mathcal{L}[c_\varepsilon] &= 2\pi - (\pi - 2)\varepsilon, \\ \Delta[c_\varepsilon] &= 1 - \varepsilon, \\ \frac{\mathcal{L}[c_\varepsilon]}{\Delta[c_\varepsilon]} &\rightarrow 2\pi \quad \text{for } \varepsilon \rightarrow 0. \end{aligned}$$

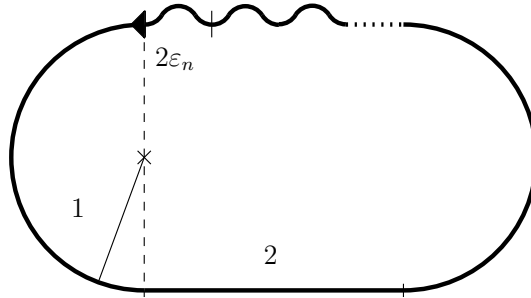


Figure 2.6: This curve converges to a stadium curve in C^1 and its thickness also converges to the thickness of the stadium curve. But it does not converge in $C^{1,1}$ and its curvature does not converge to the curvature of the stadium curve.

Let $\varepsilon < \bar{\varepsilon} < 1$ for some $\bar{\varepsilon} > 0$. For $r \in (\bar{\varepsilon}, \infty)$ the straight 2ε part of c_ε can be replaced by three arcs of radius r of length αr , $2\alpha r$ and αr with angle $\alpha := \arcsin \frac{\varepsilon}{2r}$ (see Figure 2.5 b and c). The resulting curve $c_{\varepsilon,r}$ has the following properties:

$$\begin{aligned} \alpha &:= \arcsin \frac{\varepsilon}{2r} \approx \frac{\varepsilon}{2r} \quad \text{for } \varepsilon \ll 1, \\ \mathcal{L}[c_{\varepsilon,r}] &= 2\pi - \pi\varepsilon + 4\alpha r, \\ \Delta[c_{\varepsilon,r}] &= \min(1 - \varepsilon, r), \\ \frac{\mathcal{L}[c_{\varepsilon,r}]}{\Delta[c_{\varepsilon,r}]} &\rightarrow \frac{2\pi}{\min(1, r)} \quad \text{for } \varepsilon \rightarrow 0. \end{aligned}$$

Consider the curvature at the parameter t^* in the middle of the gap between the two quarter circles (see Figure 2.5). Depending on $r \in [1, \infty]$ any value between 0 and 1 can be achieved, no matter how close to the optimal ropelength the curve $c_{\varepsilon,r}$ is. Note that $c_{\varepsilon,r}$ only converges to a circle in C^1 and not in $C^{1,1}$.

Even ‘worse’ is the next example:

Example 2.35 (Approximation of stadium curve). We can approximate the stadium curve by the curve in Figure 2.6. Let $\varepsilon_n := 1/n$ for $n \in \mathbb{N}$ and fix $r \in (1, \infty)$. We describe the curve in Figure 2.6 clockwise: Start with a half-circle of radius 1 then attach a straight segment of length 2 and again a half circle of radius 1. Then close the curve with n copies of Figure 2.5 (b). The curve $S_{n,r}$ constructed this way has the following properties:

$$\begin{aligned} \alpha_n &:= \arcsin \frac{\varepsilon_n}{2r} \approx \frac{\varepsilon_n}{2r} \quad \text{for } \varepsilon_n \ll 1, \\ \mathcal{L}[S_{n,r}] &= 2\pi + 2 + 4n\alpha_n r \rightarrow 2\pi + 4 \quad \text{for } n \rightarrow \infty, \\ \Delta[S_{n,r}] &= 1. \end{aligned}$$

Although the length and the thickness of $S_{n,r}$ converges to the length and thickness of the stadium curve, the curvature is $1/r$ on a whole interval.

Remark 2.36. Examples 2.34 and 2.35 are cautionary examples, when considering curvature plots of approximations. Even though both curves converge in C^1 to their limit

and the thickness converges to the thickness of the limit they do not converge in $C^{1,1}$. In other words we can not expect to have an estimation of $C^{1,1}$ -closeness in terms of thickness. It is quite possible that the ropelength of an ideal shape γ may be approximated by some γ_ϵ with arbitrary curvature between 0 and $\Delta[\gamma]$. On the other hand, we do not expect an actual ropelength minimiser to show such an oscillating curvature since it would increase its length.

Chapter 3

Packing Tubes on \mathbb{S}^2

This chapter is joint work with Heiko von der Mosel and has been published as a preprint [GevdM09]. At an early stage of this thesis, we wanted to check how well our numerics work in \mathbb{S}^3 . The code inherited from [CLMS05] was not yet ready to compute in \mathbb{R}^4 so we looked for a problem in the two-sphere \mathbb{S}^2 . In \mathbb{S}^2 there is no knot and only a unique maximiser of thickness – great circles as seen in Example 2.17. Instead we considered the following problem:

Problem (P). *Find the longest closed curves of prescribed minimal thickness which fit onto the 2-sphere $\mathbb{S}^2 := \{x \in \mathbb{R}^3 : |x| = 1\}$.*

In the event we found an analytic solution for *some* cases of this problem.

For a precise mathematical formulation of this maximisation problem we recall first that the length functional \mathcal{L} defined on rectifiable continuous closed curves $\gamma : \mathbb{S}^1 \rightarrow \mathbb{R}^3$ is given by

$$\mathcal{L}[\gamma] := \int_{\mathbb{S}^1} |\gamma'(t)| dt,$$

where \mathbb{S}^1 denotes the unit circle $\mathbb{S}^1 \cong \mathbb{R}/2\pi\mathbb{Z}$.

With the notation of Chapter 2 we state problem (P) precisely as:

Problem (P). *Given a constant $\Theta \in (0, 1]$ find a closed curve γ_Θ in the class*

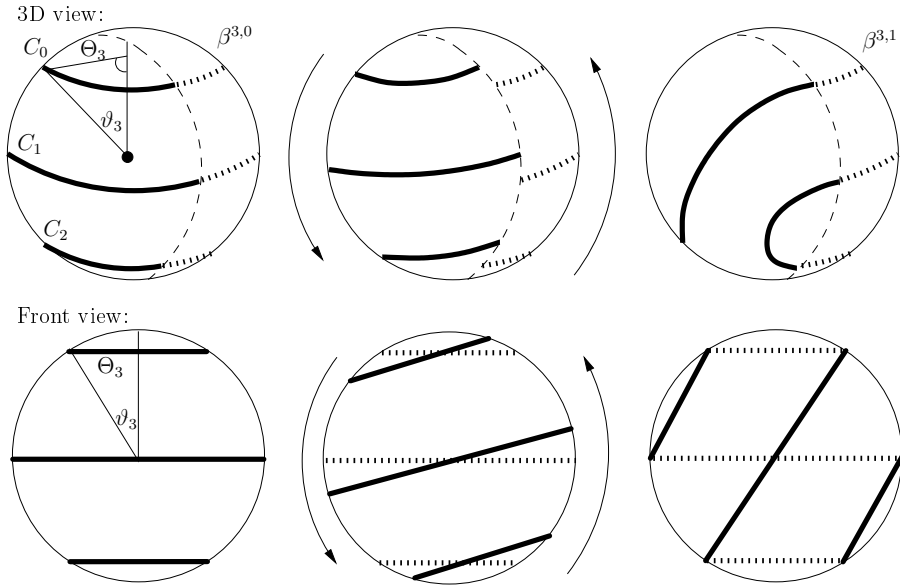
$$\mathcal{C}_\Theta := \{\gamma \in C^{1,1}(\mathbb{S}^1, \mathbb{R}^3) : |\gamma| = 1 \text{ and } |\gamma'| > 0 \text{ on } \mathbb{S}^1, \Delta[\gamma] \geq \Theta\}$$

such that $\mathcal{L}[\gamma_\Theta] = \sup_{\mathcal{C}_\Theta} \mathcal{L}$.

We will show existence of solutions for any Θ and make an extra effort to show that the minimal prescribed thickness is in fact attained by any solution.

Theorem 3.1 (Existence of solutions of (P)). *For each prescribed minimal thickness $\Theta \in (0, 1]$ Problem (P) possesses (at least) one solution $\gamma_\Theta \in \mathcal{C}_\Theta$. In addition, every such solution has minimal thickness, i.e., $\Delta[\gamma_\Theta] = \Theta$.*

The focus of the present chapter is to construct explicit and unique solutions of (P) taking advantage of the symmetry of the target manifold \mathbb{S}^2 . We have seen in Example 2.17 that for given minimal thickness $\Theta = 1$ any great circle on \mathbb{S}^2 provides the unique length maximising closed curve (up to congruence). Any closed curve γ in


 Figure 3.1: Construction of $\beta^{3,1}$ starting from $\beta^{3,0}$.

\mathbb{S}^2 different from a great circle has thickness $\Delta[\gamma]$ less than 1. The great circle happens to be the first (and “simplest”) member of an infinite family of solutions corresponding to the decreasing sequence of prescribed values of thickness

$$\Theta_n := \sin \vartheta_n \quad \text{for } \vartheta_n := \frac{\pi}{2n}, n \in \mathbb{N}. \quad (3.1)$$

The building blocks of these explicit solutions will be semicircles of the n latitudes

$$C_i : \mathbb{S}^1 \rightarrow \mathbb{S}^2, \quad i = 0, \dots, n-1.$$

Here, C_0 is a circle of spherical radius ϑ_n around the north pole, and all latitudinal circles C_i have spherical distance

$$\text{dist}_{\mathbb{S}^2}(C_i, C_{i-1}) = 2\vartheta_n \quad \text{for } i = 1, \dots, n-1,$$

such that the last latitude C_{n-1} is a circle of spherical radius ϑ_n around the south pole; see Figure 3.1.

We may view the union $C_0 \cup \dots \cup C_{n-1}$ as one (discontinuous) curve $\beta^{n,0} : \mathbb{S}^1 \rightarrow \mathbb{S}^2$, where the n connected components C_i of $\beta^{n,0}$ possess mutually disjoint tubular neighbourhoods of uniform radius Θ_n in \mathbb{R}^3 so that $\beta^{n,0}$ has thickness $\Delta[\beta^{n,0}] = \Theta_n$. In order to construct from $\beta^{n,0}$ continuous closed curves $\beta^{n,k}$ consisting of only one component for suitable $k \in \{1, \dots, n-1\}$, we cut the 2-sphere \mathbb{S}^2 into two hemispheres along a longitude such that $\beta^{n,0}$ is cut orthogonally into a collection of $2n$ semicircles.

Now, we keep one hemisphere fixed while turning the other by an angle of $2k\vartheta_n$ (see Figure 3.1) such that the n semicircles of the original curve $\beta^{n,0}$ on the fixed hemisphere together with the now turned semicircles form a closed continuous curve

$$\beta^{n,k} : \mathbb{S}^1 \rightarrow \mathbb{S}^2. \quad (3.2)$$

That this is indeed possible under the additional algebraic condition¹ that the greatest common divisor $\gcd(k, n)$ of k and n equals 1, and that this construction leads to distinct solutions of (P) is the content of

Theorem 3.2 (Explicit solutions of (P)). *For each $n \in \mathbb{N}$ and $k \in \{1, \dots, n-1\}$ with $\gcd(k, n) = 1$ the curves $\beta^{n,k}$ are (up to rigid motions and re-parametrisations) mutually distinct members of the class \mathcal{C}_Θ . They provide explicit piecewise circular solutions of the variational problem (P) for prescribed minimal thickness $\Theta := \Theta_n \in (0, 1]$. In addition, $\Delta[\beta^{n,k}] = \Theta_n$. For $n = 1$ the equator $\beta^{1,0}$ provides the only solution with thickness $\Theta_1 = 1$.*

Interestingly, the solution curves $\beta^{n,k}$, of which some are depicted in Figure 3.3 (a), (b) on page 29, resemble to a striking extent certain so-called *Turing patterns* which arise in chemistry and biology as characteristic concentration distributions of different substances as a result of a diffusion-driven instability; see e.g. [VAB99].

For our variational problem (P) we can prove that the explicit solutions for given thickness $\Theta := \Theta_n$, $n \in \mathbb{N}$, are in fact unique.

Theorem 3.3 (Uniqueness of solutions of (P) for $\Theta = \Theta_n$). *Any closed curve $\gamma_\Theta \in \mathcal{C}_\Theta$ which is a solution of (P) for given minimal thickness $\Theta = \Theta_n$, $n \in \mathbb{N}$, coincides (up to congruence and re-parametrisations) with one of the curves $\beta^{n,k}$ for $k \in \{1, \dots, n-1\}$ with $\gcd(k, n) = 1$. For $n = 1$, i.e. $\Theta_1 = 1$ the equator $\beta^{1,0}$ is the unique solution. In particular, for $\Theta = \Theta_n$ we have exactly $\varphi(n)$ solutions for Problem (P) where φ denotes Euler's totient function [BaSh96] (cf. Table 3.1).*

This uniqueness theorem is a consequence of the following stronger result which employs the two-dimensional volume $\mathcal{V}(\mathcal{T}_\vartheta(\gamma)) := \mathcal{H}^2(\mathcal{T}_\vartheta(\gamma))$ of the tubular neighbourhood

$$\mathcal{T}_\vartheta(\gamma) := \{\xi \in \mathbb{S}^2 : \text{dist}_{\mathbb{S}^2}(\xi, \gamma(\mathbb{S}^1)) < \vartheta\}$$

on \mathbb{S}^2 , to identify *sphere filling curves* as precisely those explicit solutions $\beta^{n,k}$ for $\Theta = \Theta_n$.

Remark 3.4 (Sphere filling curves). *Note that the tubular neighbourhood in \mathbb{R}^3 of a thick curve on \mathbb{S}^2 cannot cover the whole sphere since it touches in the interior (see Figure 3.2). Instead, consider a pointlike light source being placed in the origin 0, then for any closed curve $\gamma \subset \mathbb{S}^2$ its spherical tubular neighbourhood $\mathcal{T}_\vartheta(\gamma)$ may be seen on \mathbb{S}^2 as the shadow of the spatial tubular neighbourhood $B_\Theta(\gamma) \subset \mathbb{R}^3$ for $\Theta = \sin \vartheta$. In that sense the spatial thickness $\Delta[\gamma] = \Theta$ corresponds to a spherical thickness $\vartheta = \arcsin \Theta$ (see Lemma 2.18 and Lemma 3.10). Even the equator $\beta^{1,0}$ together with its spherical tubular neighbourhood $\mathcal{T}_{\pi/2}(\beta^{1,0})$ is sphere filling although the spatial tubular neighbourhood $B_\Theta(\beta^{1,0})$ covers only the considerably smaller equatorial collar $\mathcal{T}_{\pi/3}(\beta^{1,0})$.*

Theorem 3.5 (Sphere filling thick curves). *If $\mathcal{V}(\mathcal{T}_\vartheta(\gamma)) = 4\pi$ for $\vartheta \in (0, \pi/2]$ and some closed curve $\gamma \in \mathcal{C}_\Theta$ with $\Theta = \sin \vartheta \in (0, 1]$, then there is some $n \in \mathbb{N}$ and $k \in \{1, \dots, n-1\}$ with $\gcd(k, n) = 1$, or $n = 1$ and $k = 0$, such that*

$$(i) \quad \vartheta = \vartheta_n,$$

¹ Such a construction was used for a bead puzzle called *the orb* or *orb it* [WT83] in the 1980s and the involved algebra was presumably known to its inventors.

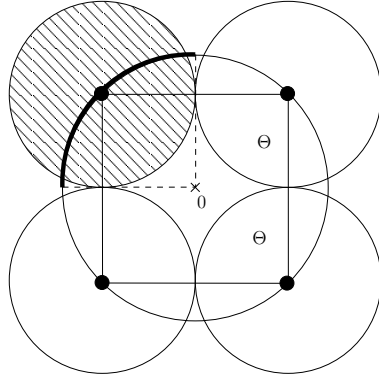


Figure 3.2: A cut through $\beta^{2,1}$ reveals that the tubular neighbourhood in \mathbb{R}^3 of a curve on the two-sphere cannot cover the sphere. It touches itself in the interior and a small part of \mathbb{S}^2 remains uncovered. The spherical tubular neighbourhood can be seen as the shadow of the spatial tubular neighbourhood. Here, the origin casts the shadow of the hatched circle with radius $\Theta = 1/\sqrt{2}$ onto the thick black line on the sphere. This line is the spherical tubular neighbourhood with radius $\vartheta = \arcsin \Theta = \pi/4$ around the black dot. The spherical tubular neighbourhood may cover the sphere in this sense.

(ii) $\Delta[\gamma] = \Theta_n$, where $\Theta_n = \sin \vartheta_n$,

(iii) $\gamma = \beta^{n,k}$.

Notice that this theorem also provides insights about intermediate values $\Theta \in (0, 1]$ of prescribed minimal thickness for arbitrary competitors $\gamma \in \mathcal{C}_\Theta$: Either γ is not a sphere filling curve, i.e.

$$\mathcal{V}(\mathcal{I}_\vartheta(\gamma)) < 4\pi \quad \text{for } \vartheta = \arcsin \Theta,$$

or $\vartheta = \vartheta_n$, $\Delta[\gamma] = \Theta_n$, and $\gamma = \beta^{n,k}$. In particular, neither the maximiser γ_Θ nor *any* competing closed curve $\gamma \in \mathcal{C}_\Theta$ is a sphere filling curve if $\Theta \neq \Theta_n$.

Our additional analysis of the relation between length, volume, and thickness reveals among other things an oscillatory behaviour of the volume $V(\Theta) := \mathcal{V}(\mathcal{I}_\vartheta(\gamma_\Theta))$ as a function of the given minimal thickness Θ . In Figure 3.6 on page 46 the black zig-zag curve serves as a lower bound for $V(\Theta)$ which is attained precisely at each Θ_n , $n \in \mathbb{N}$; see Lemma 3.18 for the details.

Similar results as described above are available for the problem corresponding to (P) on open curves $\gamma : [0, 1] \rightarrow \mathbb{S}^2$. For the details we ask the reader to consult Section 3.4, we refer in particular to Figure 3.7 on page 60 for a first impression of the shapes of length maximising open curves on the 2-sphere.

3.1 Explicit solutions

We recall from the previous section that we obtain the curves $\beta^{n,k}$ for $n \in \mathbb{N}$ and $k \in \{0, \dots, n-1\}$ by cutting the 2-sphere \mathbb{S}^2 into two hemispheres from now on referred to as the *western hemisphere* \mathbb{S}^w and the *eastern hemisphere* \mathbb{S}^e such that the latitudes $C_i : \mathbb{S}^1 \rightarrow \mathbb{S}^2$ for $i = 0, \dots, n-1$, perpendicular to the longitudinal cutting plane satisfy

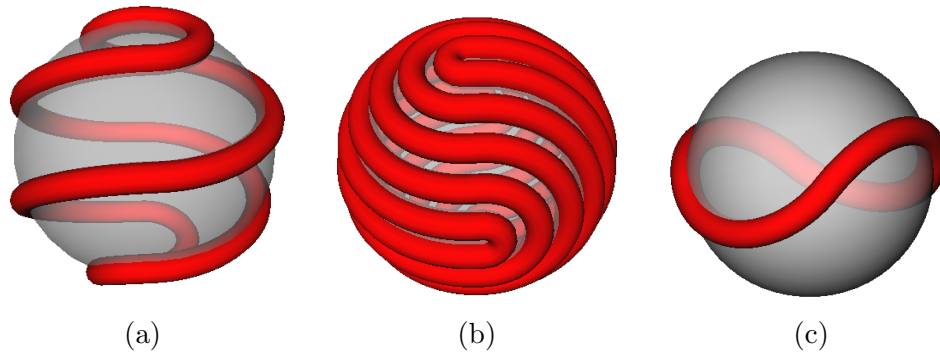


Figure 3.3: (a),(b) Solutions that maximise length for prescribed thickness. (a) $\beta^{4,1}$ has thickness $\Theta_4 = \sin \frac{\pi}{2 \cdot 4}$ with one hemisphere turned by $1 \cdot \Theta_4$. (b) $\beta^{12,5}$ has thickness $\Theta_{12} = \sin \frac{\pi}{2 \cdot 12}$ with one hemisphere turned by $5 \cdot \Theta_{12}$. (c) β_Θ is a good competitor for a thickness $\Theta \in (\Theta_2, \Theta_1)$. None of the curves is depicted with its full spatial thickness.

- (i) C_0 is a circle of spherical radius $\vartheta_n = \pi/(2n)$ about the north pole,
- (ii) $\text{dist}_{\mathbb{S}^2}(C_i, C_{i-1}) = 2\vartheta_n$ for $i = 1, \dots, n-1$,

which implies that C_{n-1} is a circle of spherical radius ϑ_n about the south pole, see Figure 3.1. Keeping the western hemisphere \mathbb{S}^w fixed and turning \mathbb{S}^e by an angle of $2k\vartheta_n$ leads to a collection of $2n$ semicircles whose (generally disconnected) union we may parametrise with constant speed to obtain our candidates

$$\beta^{n,k} : \mathbb{S}^1 \rightarrow \mathbb{S}^2 \quad \text{for } k = 1, \dots, n-1.$$

Lemma 3.6. *For every $n \in \mathbb{N}$ and $k \in \{1, \dots, n-1\}$ with $\gcd(k, n) = 1$ the appropriately re-parametrised curve $\beta^{n,k} : \mathbb{S}^1 \rightarrow \mathbb{S}^2$ is a closed piecewise circular curve whose constant speed parametrisation is of class $C^{1,1}(\mathbb{S}^1, \mathbb{R}^3)$ satisfying*

$$\Delta[\beta^{n,k}] = \Theta_n = \sin \vartheta_n = \sin \frac{\pi}{2n}.$$

Moreover, for distinct $k_1, k_2 \in \{0, \dots, n-1\}$ the curves β^{n,k_1} and β^{n,k_2} are not equivalent, i.e., there is no rigid motion M with $M(\beta^{n,k_1}) = \beta^{n,k_2}$.

Proof. The main issue will be to check, whether or not the resulting curve forms a single closed embedded loop, and we postpone this task and instead analyse its consequences.

Notice that by our choice of the turning angle $2k\vartheta_n$ every endpoint of a semicircle on \mathbb{S}^w meets exactly one endpoint of a semicircle on \mathbb{S}^e , so $\partial\beta^{n,k} = \emptyset$, which means that all connected components of $\beta^{n,k}$ are embedded closed loops. Moreover, our construction connects semicircles in a C^1 -fashion, that is, the tangent lines of the respective semicircles coincide at the common endpoints. Once we are certain that we have obtained one single closed simple curve we can rearrange the sub-arcs of the domain \mathbb{S}^1 corresponding to the various semicircles in the right order to obtain the desired constant speed parametrisation $\beta^{n,k} : \mathbb{S}^1 \rightarrow \mathbb{S}^2$.

To show then, in addition, that $\Delta[\beta^{n,k}] = \Theta_n$, we recall that the original curve $\beta^{n,0}$ consisting of the stack of n disjoint latitudinal circles with mutual spherical distance

$2\vartheta_n$ satisfies $\Delta[\beta^{n,0}] = \Theta_n$. According to Theorem 2.12 this implies that the tubular neighbourhood $B_{\Theta_n}(\beta^{n,0})$ in \mathbb{R}^3 can be expressed as the *disjoint* union of normal disks, i.e.,

$$B_{\Theta_n}(\beta^{n,0}) = \dot{\bigcup}_{s \in \mathbb{S}^1} D_{\Theta_n}(\beta^{n,0}(s), (\beta^{n,0})'(s)),$$

where $D_\theta(\xi, \eta)$ denotes the two-dimensional disk of radius θ centred at $\xi \in \mathbb{R}^3$ and perpendicular to $\eta \in \mathbb{R}^3 \setminus \{0\}$. Moreover, after cutting the \mathbb{S}^2 along a longitudinal plane into the hemispheres \mathbb{S}^w and \mathbb{S}^e one observes that these normal disks centred in \mathbb{S}^w do not intersect \mathbb{S}^e , and vice versa. Therefore also

$$B_{\Theta_n}(\beta^{n,k}) = \dot{\bigcup}_{s \in \mathbb{S}^1} D_{\Theta_n}(\beta^{n,k}(s), (\beta^{n,k})'(s)) \quad \text{for all } k = 0, \dots, n-1, \quad (3.3)$$

since the $\beta^{n,k}$ are obtained by simply turning \mathbb{S}^e against \mathbb{S}^w leading to a piecewise circular closed $C^{1,1}$ -curve.

We claim that for each $x \in B_{\Theta_n}(\beta^{n,k})$ there is exactly one point $p \in \beta^{n,k}(\mathbb{S}^1)$ such that

$$\text{dist}_{\mathbb{R}^3}(x, \beta^{n,k}) = |x - p|, \quad (3.4)$$

which again by Theorem 2.12 implies $\Delta[\beta^{n,k}] \geq \Theta_n$, and since the local radius of curvature of the semicircles $C_0 \cap \beta^{n,k}$ equals Θ_n we arrive at $\Delta[\beta^{n,k}] = \Theta_n$.

In order to prove the claim we use (3.3) to find a unique parameter $s = s(x) \in \mathbb{S}^1$ such that $x \in D_{\Theta_n}(\beta^{n,k}(s), (\beta^{n,k})'(s))$. Since $\beta^{n,k}$ is of class C^1 we know that the segment $x - p$ is perpendicular to the curve $\beta^{n,k}$ at all points $p \in \beta^{n,k}$ satisfying (3.4). If there were one point $p := \beta^{n,k}(t)$ satisfying (3.4) for $t \neq s$, then we would have $x \in D_{\Theta_n}(\beta^{n,k}(t), (\beta^{n,k})'(t))$, hence

$$x \in D_{\Theta_n}(\beta^{n,k}(s), (\beta^{n,k})'(s)) \cap D_{\Theta_n}(\beta^{n,k}(t), (\beta^{n,k})'(t)) \neq \emptyset$$

contradicting the fact that the sets on the right-hand side of (3.3) are disjoint. So the only point satisfying (3.4) is the point $p := \beta^{n,k}(s)$, which proves the claim.

It remains to be shown that each of the $\beta^{n,k}$ with $\text{gcd}(k, n) = 1$ forms one single closed loop. For that purpose we introduce certain checkpoints and study if and how the curve $\beta^{n,k}$ passes through these points. We consider the fixed western hemisphere \mathbb{S}^w and label the $2n$ endpoints of the semicircles counter-clockwise from 0 to $2n - 1$, such that checkpoints number i and $2n - 1 - i$ correspond to the i -th semicircle on \mathbb{S}^w for $i = 0, \dots, n - 1$; see Figure 3.4. The n semicircles on \mathbb{S}^w connect the checkpoints to n pairs which may be viewed as a permutation

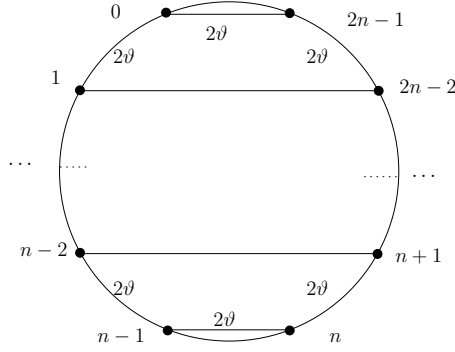
$$c := (0 \ 2n - 1)(1 \ 2n - 2) \cdots (n - 1 \ n)$$

consisting of n cycles of length 2, or alternatively,

$$c(i) \equiv -1 - i \pmod{2n}, \quad i = 0, \dots, 2n - 1.$$

So if we pass through checkpoint i along the corresponding semicircle contained in $\beta^{n,k} \cap \mathbb{S}^w$ we will next pass through checkpoint $c(i)$ as the endpoint of this semicircle upon entering the eastern hemisphere \mathbb{S}^e . To model the turn of the other hemisphere \mathbb{S}^e by an angle of $2\vartheta_n$ against \mathbb{S}^w we use the permutation

$$t := (0 \ 1 \ \cdots \ 2n - 2 \ 2n - 1)$$


 Figure 3.4: Labelling $2n$ checkpoint on a hemisphere for Lemma 3.6

consisting of 1 cycle of length $2n$, so that the turning angle of $2k\vartheta_n$ corresponds to

$$t^k(i) \equiv i + k \pmod{2n} \quad \text{for } k = 1, \dots, n-1.$$

As we proceed along the curve $\beta^{n,k}$ we pass alternately through the semicircles on \mathbb{S}^w and the semicircles on the rotated hemisphere \mathbb{S}^e , respectively. It can easily be checked that if we enter \mathbb{S}^w through checkpoint i then we enter \mathbb{S}^w the next time at checkpoint

$$q(i) := t^{-k} \circ c \circ t^k \circ c(i) \pmod{2n}, \quad i = 0, \dots, 2n-1.$$

We enter through n distinct checkpoints and therefore pass through all semicircles on \mathbb{S}^w and \mathbb{S}^e , respectively, if and only if the permutation $q = t^{-k} \circ c \circ t^k \circ c$ consists of exactly two cycles of common length n . In order to determine under which condition this happens we calculate

$$\begin{aligned} q(i) &\equiv t^{-k} \circ c \circ t^k \circ c(i) \pmod{2n} \\ &\equiv t^{-k} \circ c \circ t^k(-1-i) \pmod{2n} \\ &\equiv t^{-k} \circ c(-1-i+k) \pmod{2n} \\ &\equiv t^{-k}(-1-[-1-i+k]) \pmod{2n} \\ &\equiv t^{-k}(i-k) \pmod{2n} \\ &\equiv i-2k \pmod{2n}, \end{aligned}$$

hence

$$q^l(i) \equiv i - 2kl \pmod{2n}.$$

This relation shows in particular that the reentry after an even checkpoint is again an even checkpoint ensuring that no semicircle on \mathbb{S}^w and for symmetry reasons also on \mathbb{S}^e is left out in the process.

By Lemma 3.7 below, that will also be applied in the construction of open curve solutions in Section 3.4, we conclude that q consists of two cycles of common length n if and only if $(2n)/\gcd(2k, 2n) = n$ which is equivalent to $\gcd(k, n) = 1$, otherwise it consists of $2\gcd(k, n)$ cycles of length $n/\gcd(k, n)$. To see the latter we note that the cyclic group $\langle q \rangle := \{\text{id}, q, q^2, q^3, \dots\}$ operates freely on the set of checkpoints. The

number of algebraically disjoint orbits, i.e. cycles in our situation, is given by the well-known orbit formula [A91]

$$\#\{\text{orbits of } \langle q \rangle\} = \frac{\#\{\text{checkpoints}\}}{|\langle q \rangle|} = \frac{2n}{n/\gcd(k, n)} = 2\gcd(k, n).$$

Switching the roles of the entry and exit checkpoints on the western hemisphere S^w will produce the opposite orientation of the constructed curves. Since each algebraic orbit corresponds to one of the two opposite orientations we end up with $\gcd(k, n)$ closed loops, in particular with one closed curve if $\gcd(k, n) = 1$.

To see that for $k_1 \neq k_2$ the curve β^{n, k_1} cannot be mapped by a rigid motion to β^{n, k_2} we consider the oriented angle between the polar axes connecting the respective north and south poles on \mathbb{S}^w and the tilted \mathbb{S}^e measured counterclockwise in the cutting plane as seen from \mathbb{S}^w . This invariant under rigid motions is in fact different for $k_1 \neq k_2$. This finishes the proof of Lemma 3.6. \square

Lemma 3.7. *For given $r, v \in \mathbb{N}$ let the permutation $q : \{0, \dots, r-1\} \rightarrow \{0, \dots, r-1\}$ be defined as $q(i) := i - v \pmod r$. Then the orbit length of i under the cyclic group $\langle q \rangle$ is $\#\{q^0(i), \dots, q^r(i)\} = r/\gcd(v, r)$.*

Proof. For $l = r/\gcd(v, r)$ we find

$$q^l(i) \equiv i - v \frac{r}{\gcd(v, r)} \equiv i - r \frac{v}{\gcd(v, r)} \equiv i \pmod r \quad \text{for all } i = 0, \dots, r-1,$$

which proves that no cycle in q is longer than $r/\gcd(v, r)$. Now let $m > 0$ be the smallest integer such that

$$q^m(i) \equiv i - vm \equiv i \pmod r \tag{3.5}$$

for some $i \in \{0, \dots, r-1\}$. By (3.5) vm is a multiple of r , i.e. there exists $j \in \mathbb{N}$ such that

$$vm = j \operatorname{lcm}(v, r) = j \frac{vr}{\gcd(v, r)},$$

where $\operatorname{lcm}(v, r)$ denotes the least common multiple of v and r . Cancelling v yields

$$m = j \frac{r}{\gcd(v, r)},$$

which implies $m \geq r/\gcd(r, v)$ and consequently, for $r/\gcd(v, r)$ is the upper bound on the length of any cycle as shown above,

$$m = \frac{r}{\gcd(v, r)}.$$

\square

Remark 3.8. (i) *Since we are only interested in different shapes we do not have to take into account any integer $k \geq n$ since the corresponding arcs $\beta^{n, k} \cap \mathbb{S}^e$ are equivalent with $\beta^{n, k-n} \cap \mathbb{S}^e$ for² $k \geq n$. Therefore the number of distinct closed curves $\beta^{n, k}$ for given $n \in \mathbb{N}$ is identical with the cardinality of the set*

$$A_n := \{k \in \{1, \dots, n\} : \gcd(k, n) = 1\}, \quad n \in \mathbb{N},$$

²For algebraic reasons we do count the case $k = n$ instead of $k = 0$.

| n | $\#A_n$ | n | $\#A_n$ | n | $\#A_n$ | n | $\#A_n$ | n | $\#A_n$ | n | $\#A_n$ |
|-----|---------|-----|---------|-----|---------|-----|---------|-----|---------|-----|---------|
| 1 | 1 | 8 | 4 | 15 | 8 | 22 | 10 | 29 | 28 | 36 | 12 |
| 2 | 1 | 9 | 6 | 16 | 8 | 23 | 22 | 30 | 8 | 37 | 36 |
| 3 | 2 | 10 | 4 | 17 | 16 | 24 | 8 | 31 | 30 | 38 | 18 |
| 4 | 2 | 11 | 10 | 18 | 6 | 25 | 20 | 32 | 16 | 39 | 24 |
| 5 | 4 | 12 | 4 | 19 | 18 | 26 | 12 | 33 | 20 | 40 | 16 |
| 6 | 2 | 13 | 12 | 20 | 8 | 27 | 18 | 34 | 16 | 41 | 40 |
| 7 | 6 | 14 | 6 | 21 | 12 | 28 | 12 | 35 | 24 | 42 | 12 |

Table 3.1: The set $A_n := \{k \in \{1, \dots, n\} : \gcd(k, n) = 1\}$ for $n \in \mathbb{N}$, consists of the values k , such that $\beta^{n,k}$ is a closed curve. By the uniqueness result, Theorem 3.3, $\#A_n = \varphi(n)$ is the number of distinct solutions of Problem (P) for the thickness values $\Theta_n = \sin \frac{\pi}{2n}$. Moreover, $\varphi(n)$ counts all sphere filling curves according to Theorem 3.5.

which equals Euler's totient function $\varphi(n)$ (see e.g. [BaSh96, p. 21]). In Table 3.1 we have listed the number of distinct closed curves of type $\beta^{n,k}$ for $n \leq 42$.

- (ii) If we turn the hemisphere \mathbb{S}^e in Lemma 3.6 by the angle $k \cdot 2\vartheta_n$ for some k with $\gcd(k, n) > 1$ the curve splits into $\gcd(k, n)$ connected components. This configuration is a solution to an optimisation problem similar to (P), namely maximising the length of collections of precisely $\gcd(n, k)$ closed curves on \mathbb{S}^2 subject to the prescribed minimal thickness Θ_n .
- (iii) Recall from Lemma 2.13 the torus property (T): Let $\Delta[\gamma] \geq \Theta > 0$. Then the union of all open balls B_Θ of radius Θ which are tangent to the curve γ at any fixed point $p \in \gamma$ has no point in common with γ . This readily implies the

Spherical torus property (ST): Any closed spherical curve $\gamma : \mathbb{S}^1 \rightarrow \mathbb{S}^2$ with spatial thickness $\Delta[\gamma] = \Theta$ satisfies

$$\gamma(\mathbb{S}^1) \cap \mathcal{B}_\vartheta(\xi) = \emptyset \quad \text{for } \vartheta = \arcsin \Theta$$

for any geodesic open ball

$$\mathcal{B}_\vartheta(\xi) := \{\eta \in \mathbb{S}^2 : \text{dist}_{\mathbb{S}^2}(\eta, \xi) < \vartheta\},$$

whose boundary $\partial\mathcal{B}_\vartheta(\xi)$ is tangent to γ in at least one point of γ .

Definition 3.9 (Tubes without self-overlap). Let $\gamma : \mathbb{S}^1 \rightarrow \mathbb{S}^2$ be a spherical closed curve which possesses a tangent at every point. The spherical tubular neighbourhood

$$\mathcal{T}_\phi(\gamma) = \{x \in \mathbb{S}^2 : \text{dist}_{\mathbb{S}^2}(x, \gamma) < \phi\}$$

is said to be non-self-overlapping if two geodesic arcs of length ϕ emanating from two distinct curve points in a direction perpendicular to γ have at most common endpoints, but otherwise do not intersect.

As a direct consequence of Theorem 2.19 we have

Lemma 3.10 (Thick curves and non-self-overlapping tubes). *All spherical tubular neighbourhoods*

$$\mathcal{T}_\phi(\gamma) = \{x \in \mathbb{S}^2 : \text{dist}_{\mathbb{S}^2}(x, \gamma) < \phi\}, \quad \phi \in (0, \vartheta],$$

of a spherical closed curve $\gamma : \mathbb{S}^1 \rightarrow \mathbb{S}^2$ with spatial thickness $\Delta[\gamma] \geq \Theta = \sin \vartheta$ for $\vartheta \in (0, \pi/2]$ are non-self-overlapping. \square

Proof of Theorem 3.2. According to Lemma 3.6 and Remark 3.8 (i) we find for each $n \in \mathbb{N}$ exactly $\varphi(n)$ distinct closed curves $\beta^{n,k} \in \mathcal{C}_{\Theta_n}$ with $\Delta[\beta^{n,k}] = \Theta_n$. By construction the spherical tubular neighbourhood $\mathcal{T}_{\vartheta_n}(\beta^{n,k})$ covers the 2-sphere except for a set of two-dimensional measure zero:

$$\mathcal{V}(\mathcal{T}_{\vartheta_n}(\beta^{n,k})) = \mathcal{H}^2(\mathcal{T}_{\vartheta_n}(\beta^{n,k})) = 4\pi = \mathcal{H}^2(\mathbb{S}^2). \quad (3.6)$$

Moreover, $\mathcal{T}_{\vartheta_n}(\beta^{n,k})$ is non-self-overlapping in the sense of Definition 3.9. Hence by virtue of the well-known theorem of Hotelling [H39] (see also [W39], [Gr90]), which we are going to adapt to the present context of thick loops in Proposition 3.11, one has

$$\mathcal{L}[\gamma] = \frac{\mathcal{V}(\mathcal{T}_{\vartheta_n}(\beta^{n,k}))}{2 \sin \vartheta_n} \leq \frac{4\pi}{2\Theta_n} = \frac{2\pi}{\Theta_n} \quad \text{for all } \gamma \in \mathcal{C}_{\Theta_n}.$$

This estimate produces a sharp uniform upper bound on the length functional on the class \mathcal{C}_{Θ_n} . Regarding (3.6) this bound is attained by the curves $\beta^{n,k}$, which means that they are length maximising in the class \mathcal{C}_{Θ_n} , i.e. their smooth and regular parametrisations are solutions of Problem (P). \square

3.2 Existence, and Properties of Thickness, Length and Volume of General Solutions

For the volume $\mathcal{V}(\mathcal{T}_\vartheta(\gamma))$ of the tube

$$\mathcal{T}_\vartheta(\gamma) = \{x \in \mathbb{S}^2 : \text{dist}_{\mathbb{S}^2}(x, \gamma) < \vartheta\}$$

on the sphere \mathbb{S}^2 we are going to prove the following version of the theorem of Hotelling [H39] for continuous thick curves:

Proposition 3.11 (Hotelling). *Let $\gamma : \mathbb{S}^1 \rightarrow \mathbb{S}^2$ be a closed rectifiable continuous curve with thickness $\Delta[\gamma] > 0$ and length $\mathcal{L}[\gamma]$. Then for all $\vartheta \in [0, \arcsin(\Delta[\gamma])]$ one has*

$$\mathcal{V}(\mathcal{T}_\vartheta(\gamma)) = 2 \sin(\vartheta) \mathcal{L}[\gamma]. \quad (3.7)$$

In particular, the tubular neighbourhood $\mathcal{T}_{\arcsin \Theta}(\gamma_\Theta)$ of any solution $\gamma_\Theta \in \mathcal{C}_\Theta$ of Problem (P) for given thickness $\Theta \in (0, 1]$ covers the same amount of area on \mathbb{S}^2 .

The obvious idea to prove this result is to approximate such thick curves by smooth ones with controlled minimal thickness for which the classic result of Hotelling is applicable and then go to the limit. That this is indeed possible is guaranteed by Lemma 2.33, which we will also use for a variational argument later on in this section to show that length maximisers attain the prescribed minimal thickness; see Theorem 3.14.

3.2. EXISTENCE AND PROPERTIES OF GENERAL SOLUTIONS

Proof. The length $L := \mathcal{L}[\gamma]$ is positive since $\Delta[\gamma] > 0$. Recall from Lemma 2.2 that the arc-length parametrisation $\Gamma : [0, L] \rightarrow \mathbb{S}^2$ is injective and of class $C^{1,1}([0, L], \mathbb{R}^3)$ satisfying the local curvature bound (deduced from Lemma 2.14(i))

$$\|\Gamma''\|_{L^\infty([0, L], \mathbb{R}^3)} \leq \frac{1}{\Delta[\gamma]}. \quad (3.8)$$

We extend the components Γ^i , $i = 1, 2, 3$, as L -periodic functions onto all of \mathbb{R} . Then we choose a sequence $\epsilon_j \rightarrow 0$ as $j \rightarrow \infty$, a standard nonnegative mollifier $\phi \in C_0^\infty((-1, 1))$, $\phi_\epsilon(s) := \epsilon^{-1}\phi(s/\epsilon)$, and define the smooth L -periodic convolutions

$$\eta_j^i := \phi_{\epsilon_j} * \Gamma^i \in C^\infty(\mathbb{R}) \subset C^\infty([0, L]) \quad \text{for } i = 1, 2, 3,$$

so that $\eta_j := (\eta_j^1, \eta_j^2, \eta_j^3)$ are smooth closed curves in \mathbb{R}^3 approximating Γ in $C^1([0, L], \mathbb{R}^3)$, such that

$$|\eta_j'| \longrightarrow 1 \quad \text{uniformly on } [0, L], \quad \text{and also} \quad (3.9)$$

$$\|\eta_j''\|_{L^\infty([0, L], \mathbb{R}^3)} \leq \|\Gamma''\|_{L^\infty([0, L], \mathbb{R}^3)} \leq \frac{1}{\Delta[\gamma]} \quad \text{for all } j \in \mathbb{N}.$$

Furthermore, we can assume that $|\eta_j| > 0$ for all j , such that the projected curves

$$\gamma_j := \frac{\eta_j}{|\eta_j|} : [0, L] \rightarrow \mathbb{S}^2$$

are well-defined and of class $C^\infty([0, L], \mathbb{R}^3)$ for all $j \in \mathbb{N}$. For all $j \gg 1$ these curves satisfy

$$\begin{aligned} |\gamma_j(t) - \Gamma(t)| &\leq \left| \frac{\eta_j}{|\eta_j|} - \frac{\Gamma(t)}{|\Gamma(t)|} \right| + \left(\frac{|1 - |\eta_j||}{|\eta_j|} |\Gamma(t)| \right) \\ &\leq 2\|\eta_j - \Gamma\|_{C^0([0, L], \mathbb{R}^3)} + 2\|1 - |\eta_j|\|_{C^0([0, L], \mathbb{R}^3)}, \end{aligned}$$

and

$$\begin{aligned} |\gamma_j'(t) - \Gamma'(t)| &= \left| \frac{\eta_j'(t)}{|\eta_j|} - \frac{\eta_j(t) \cdot \eta_j'(t)}{|\eta_j(t)|^3} \eta_j(t) + \underbrace{\frac{\Gamma(t) \cdot \Gamma'(t)}{|\eta_j(t)|^3} \eta_j(t)}_{=0} - \Gamma'(t) \right| \\ &\leq 2\|\eta_j' - \Gamma'\|_{C^0([0, L], \mathbb{R}^3)} + 2|\eta_j(t) \cdot \eta_j'(t) - \Gamma(t) \cdot \Gamma'(t)| \\ &\leq 2\|\eta_j' - \Gamma'\|_{C^0([0, L], \mathbb{R}^3)} + 4\|\eta_j' - \Gamma'\|_{C^0([0, L], \mathbb{R}^3)} + 4\|\eta_j - \Gamma\|_{C^0([0, L], \mathbb{R}^3)}; \end{aligned}$$

hence

$$\gamma_j \longrightarrow \Gamma \quad \text{in } C^1([0, L], \mathbb{R}^3) \quad \text{as } j \rightarrow \infty. \quad (3.10)$$

In addition we compute

$$\begin{aligned} \gamma_j'' &= \left[\frac{\eta_j'}{|\eta_j|} - \frac{\eta_j \cdot \eta_j'}{|\eta_j|^3} \eta_j \right]' \\ &= \frac{\eta_j''}{|\eta_j|} - \frac{\eta_j \cdot \eta_j'}{|\eta_j|^3} \eta_j' - \frac{[|\eta_j'|^2 + \eta_j \cdot \eta_j'']}{|\eta_j|^3} \eta_j - \frac{3(\eta_j \cdot \eta_j')^2}{|\eta_j|^5} \eta_j - \frac{\eta_j \cdot \eta_j''}{|\eta_j|^3} \eta_j'. \end{aligned} \quad (3.11)$$

Since $\eta_j \rightarrow \Gamma$ in $C^1([0, L], \mathbb{R}^3)$ and $\Gamma \cdot \Gamma' \equiv 0$ we find

$$-\frac{\eta_j \cdot \eta_j'}{|\eta_j|^3} \eta_j' - \frac{3(\eta_j \cdot \eta_j')^2}{|\eta_j|^5} \eta_j - \frac{\eta_j \cdot \eta_j'}{|\eta_j|^3} \eta_j' \longrightarrow 0 \text{ in } C^0([0, L], \mathbb{R}^3) \text{ as } j \rightarrow \infty. \quad (3.12)$$

Moreover, one has for any common Lebesgue point $s \in [0, L]$ of Γ'' and γ_j'' for all $j \in \mathbb{N}$ (i.e. for a.e. $s \in [0, L]$):

$$\begin{aligned} & |\eta_j(s) \cdot \eta_j''(s) - \Gamma(s) \cdot \Gamma''(s)| \\ &= \left| \int_{\mathbb{R}} \phi_{\varepsilon_j}(s-t) \Gamma(t) dt \cdot \int_{\mathbb{R}} \phi_{\varepsilon_j}''(s-t) \Gamma(t) dt - \Gamma(s) \cdot \Gamma''(s) \right| \\ &= \left| \int_{\mathbb{R}} \phi_{\varepsilon_j}(s-t) \Gamma(t) dt \cdot \int_{\mathbb{R}} \phi_{\varepsilon_j}(s-t) \Gamma''(t) dt - \Gamma(s) \cdot \Gamma''(s) \right| \\ &= \left| \int_{\mathbb{R}} \phi_{\varepsilon_j}(z) \Gamma(s-z) dz \cdot \int_{\mathbb{R}} \phi_{\varepsilon_j}(z) \Gamma''(s-z) dz - \Gamma(s) \cdot \Gamma''(s) \right| \\ &\leq \left| \int_{\mathbb{R}} \phi_{\varepsilon_j}(z) [\Gamma(s-z) - \Gamma(s)] dz \cdot \int_{\mathbb{R}} \phi_{\varepsilon_j}(z) \Gamma''(s-z) dz \right| \\ &\quad + \left| \int_{\mathbb{R}} \phi_{\varepsilon_j}(z) \Gamma(s) dz \cdot \int_{\mathbb{R}} \phi_{\varepsilon_j}(z) \Gamma''(s-z) dz - \Gamma(s) \cdot \Gamma''(s) \right| \\ &\stackrel{(3.8)}{\leq} \|\Gamma(s-\cdot) - \Gamma(s)\|_{C^0(\overline{B_{\varepsilon_j}(0)}, \mathbb{R}^3)} \frac{1}{\Delta[\gamma]} \\ &\quad + \left| \int_{\mathbb{R}} \phi_{\varepsilon_j}(z) dz \int_{\mathbb{R}} \phi_{\varepsilon_j}(z) [\Gamma(s) - \Gamma(s-z)] \cdot \Gamma''(s-z) dz \right| \\ &\quad + \left| \int_{\mathbb{R}} \phi_{\varepsilon_j}(z) dz \int_{\mathbb{R}} \phi_{\varepsilon_j}(z) \Gamma(s-z) \cdot \Gamma''(s-z) dz - \Gamma(s) \cdot \Gamma''(s) \right| \\ &\leq 2\|\Gamma(s-\cdot) - \Gamma(s)\|_{C^0(\overline{B_{\varepsilon_j}(0)}, \mathbb{R}^3)} \frac{1}{\Delta[\gamma]} \longrightarrow 0 \text{ as } j \rightarrow \infty, \end{aligned}$$

using for the last inequality that the normal curvature of $\Gamma : [0, L] \rightarrow \mathbb{S}^2$ equals -1 a.e. on $[0, L]$ (see e.g. [doC76, Chapter 3.2]), so that in particular

$$\begin{aligned} \Gamma''(s) \cdot \Gamma(s) &= -1 \quad \text{and} \\ \Gamma''(s-z) \cdot \Gamma(s-z) &= -1 \quad \text{for a.e. } z \in \mathbb{R}. \end{aligned}$$

Hence we obtain

$$\|\eta_j \cdot \eta_j'' - \Gamma \cdot \Gamma''\|_{L^\infty((0, L))} \longrightarrow 0 \text{ as } j \rightarrow \infty, \quad (3.13)$$

which we combine with (3.12) and the fact that $\eta_j \rightarrow \Gamma$ in $C^1([0, L], \mathbb{R}^3)$ in (3.11) to obtain by (3.9)

$$\limsup_{j \rightarrow \infty} \|\gamma_j''\|_{L^\infty((0, L), \mathbb{R}^3)} = \limsup_{j \rightarrow \infty} \|\eta_j''\|_{L^\infty((0, L), \mathbb{R}^3)} \stackrel{(3.9)}{\leq} \frac{1}{\Delta[\gamma]}.$$

This together with (3.10) implies for the arc-length parametrisations $\Gamma_j : [0, \mathcal{L}[\gamma_j]] \rightarrow \mathbb{S}^2$ the estimate

$$\limsup_{j \rightarrow \infty} \|\Gamma_j''\|_{L^\infty((0, L), \mathbb{R}^3)} = \limsup_{j \rightarrow \infty} \left\| \frac{|\gamma_j'' \wedge \gamma_j'|}{|\gamma_j'|^3} \right\|_{L^\infty((0, L), \mathbb{R}^3)} \leq \frac{1}{\Delta[\gamma]}.$$

3.2. EXISTENCE AND PROPERTIES OF GENERAL SOLUTIONS

With this inequality and with (3.10) we have verified assumptions (i) and (ii) of Lemma 2.33 for the curve $\Gamma \in C^{1,1}([0, L], \mathbb{R}^3)$ and the approximating curves $\gamma_j : [0, L] \rightarrow \mathbb{S}^2$ each of class $C^\infty([0, L], \mathbb{R}^3)$, so that by (2.18)

$$\liminf_{j \rightarrow \infty} \Delta[\gamma_j] \geq \Delta[\Gamma] = \Delta[\gamma].$$

If we take an appropriate subsequence and relabel we obtain a sequence $\{\gamma_j\} \subset C^\infty([0, L], \mathbb{R}^3)$, $\gamma_j : [0, L] \rightarrow \mathbb{S}^2$ for all $j \in \mathbb{N}$ such that

$$\|\gamma_j - \Gamma\|_{C^1([0, L], \mathbb{R}^3)} < \frac{1}{j} \quad \text{and} \quad \Delta[\gamma_j] > \Delta[\gamma] - \frac{1}{j}. \quad (3.14)$$

In particular, we find for arbitrary given $\vartheta \in (0, \arcsin(\Delta[\gamma]))$ and $\varepsilon > 0$ some $J_0 = J_0(\varepsilon, \vartheta)$ such that

$$\mathcal{T}_{\vartheta - \varepsilon - (2/j)}(\gamma_j) \subset \mathcal{T}_{\vartheta - \varepsilon - (1/j)}(\gamma) \subset \mathcal{T}_{\vartheta - \varepsilon}(\gamma_j) \quad \text{for all } j \geq J_0, \quad (3.15)$$

and according to Lemma 3.10 these nested spherical tubular neighbourhoods are non-self-overlapping in the sense of Definition 3.9. Since the γ_j are smooth with image on \mathbb{S}^2 for all j we may apply the theorem of Hotelling [H39] twice for $j \geq J_1$ for some $J_1 = J_1(\varepsilon, \vartheta) \geq J_0$ with

$$\Delta[\gamma_j] \underset{(3.14)}{>} \Delta[\gamma] - \frac{1}{j} \geq \sin(\vartheta - \varepsilon),$$

to obtain

$$\begin{aligned} 2 \sin(\vartheta - \varepsilon - (2/j)) \mathcal{L}[\gamma_j] &\underset{[\text{H39}]}{=} \mathcal{V}(\mathcal{T}_{\vartheta - \varepsilon - (2/j)}(\gamma_j)) \\ &\underset{(3.15)}{\leq} \mathcal{V}(\mathcal{T}_{\vartheta - \varepsilon - (1/j)}(\gamma)) \\ &\underset{(3.15)}{\leq} \mathcal{V}(\mathcal{T}_{\vartheta - \varepsilon}(\gamma_j)) \\ &\underset{[\text{H39}]}{=} 2 \sin(\vartheta - \varepsilon) \mathcal{L}[\gamma_j] \quad \text{for all } j \geq J_1. \end{aligned}$$

Since (3.14) implies $\mathcal{L}[\gamma_j] \rightarrow \mathcal{L}[\gamma]$ as $j \rightarrow \infty$ we arrive at

$$2 \sin(\vartheta - \varepsilon) \mathcal{L}[\gamma] = \mathcal{V}(\mathcal{T}_{\vartheta - \varepsilon}(\gamma))$$

for the arbitrarily chosen $\varepsilon > 0$, which implies (3.7). □

We actually established within the previous proof the following approximation result which is of independent interest.

Corollary 3.12 (Smooth approximation with positive thickness II). *For any closed continuous, rectifiable, and regular curve $\gamma : \mathbb{S}^1 \rightarrow \mathbb{R}^N$ with positive thickness $\Delta[\gamma] > 0$ and length $L := \mathcal{L}[\gamma]$ there is a sequence of regular closed curves $\eta_j \in C^\infty([0, L], \mathbb{R}^N)$ such that*

$$\eta_j \rightarrow \Gamma \quad \text{in } C^1 \quad \text{as } j \rightarrow \infty \quad \text{and} \quad \liminf_{j \rightarrow \infty} \Delta[\eta_j] \geq \Delta[\gamma], \quad (3.16)$$

where $\Gamma : [0, L] \rightarrow \mathbb{R}^N$ denotes the arc-length parametrisation of γ . If, in addition, $\gamma(\mathbb{S}^1) \subset \mathbb{S}^{N-1}$, then there is a sequence of regular closed curves $\gamma_j \in C^\infty([0, L], \mathbb{R}^N)$ with $\gamma_j([0, L]) \subset \mathbb{S}^{N-1}$ such that (3.16) holds for γ_j instead of η_j . □

As a prerequisite for the proof of the existence result, Theorem 3.1, we show that the velocities of constant speed parametrisations of admissible curves $\gamma \in \mathcal{C}_\Theta$ are controlled solely in terms of the given thickness Θ :

Lemma 3.13 (Speed limit II). *(cf. Lemma 2.29) For all $\gamma \in \mathcal{C}_\Theta$ with $|\gamma'| \equiv \text{const.}$ on \mathbb{S}^1 one has*

$$\Theta \leq |\gamma'| \leq \frac{1}{\Theta} \quad \text{on } \mathbb{S}^1. \quad (3.17)$$

Proof. The upper bound in (3.17) follows from (3.7) in Proposition 3.11 for $\vartheta = \arcsin \Theta$:

$$2\pi|\gamma'| = \mathcal{L}[\gamma] \stackrel{(3.7)}{=} \frac{1}{2 \sin \vartheta} \mathcal{V}(\mathcal{T}_\vartheta(\gamma)) \leq \frac{4\pi}{2\Theta},$$

and the lower bound follows from the *torus property* (see Remark 3.8(iii)), which implies that γ as a closed curve of positive length has to be at least as long as a great circle on one of the spheres ∂B_Θ touching γ in, say $\gamma(0)$, so that

$$2\pi|\gamma'| = \mathcal{L}[\gamma] \geq 2\pi\Theta.$$

□

Proof of Theorem 3.1. We consider the case of closed curves³. The class \mathcal{C}_Θ is not empty for any $\Theta \in (0, 1]$, since any great circle c_g smoothly parametrised with constant speed has thickness $\Delta[c_g] = 1 \geq \Theta$. So there is a maximising sequence $\{\eta_j\} \subset \mathcal{C}_\Theta$ such that

$$L_j := \mathcal{L}[\eta_j] \longrightarrow \sup_{\mathcal{C}_\Theta} \mathcal{L}[\cdot] \quad \text{as } j \rightarrow \infty.$$

Let us point out a shortcut here: Assume the η_j to be parametrised with constant speed, so they satisfy Lemma 2.30 and a sub-sequence converges to some closed η_Θ in C^1 . From Lemma 2.31 we infer $\Delta[\eta_\Theta] \geq \Theta$. Thus we have shown that $\eta_\Theta \in \mathcal{C}_\Theta$ is a solution.

But we have to elaborate the previous step, since we want to reuse some of the inequalities later on. The corresponding arc-length parametrisations $\Gamma_j : [0, L_j] \rightarrow \mathbb{S}^2$ satisfy the uniform estimate (cf. [GMSvdM02, Lemma 2])

$$\begin{aligned} \|\Gamma_j\|_{C^{1,1}([0, L_j], \mathbb{R}^3)} &= \|\Gamma_j\|_{C^0([0, L_j], \mathbb{R}^3)} + \|\Gamma_j'\|_{C^0([0, L_j], \mathbb{R}^3)} + \|\Gamma_j''\|_{L^\infty([0, L_j], \mathbb{R}^3)} \\ &\leq 2 + \frac{1}{\Theta} \quad \text{for all } j \in \mathbb{N}, \end{aligned} \quad (3.18)$$

so that the constant speed re-parametrisations $\gamma_j : \mathbb{S}^1 \rightarrow \mathbb{S}^2$ with $v_j := |\gamma_j'| > 0$ still yield a maximising sequence in \mathcal{C}_Θ and satisfy

$$\gamma_j(t) = \Gamma_j(tv_j), \quad \gamma_j'(t) = \Gamma_j'(tv_j)v_j.$$

Therefore by (3.17) in Lemma 3.13

$$\begin{aligned} |\gamma_j'(t) - \gamma_j'(\tau)| &= v_j |\Gamma_j'(tv_j) - \Gamma_j'(\tau v_j)| \\ &\leq \frac{v_j^2}{\Theta} |t - \tau| \stackrel{(3.17)}{\leq} \frac{1}{\Theta^3} |t - \tau| \quad \text{for all } t, \tau \in \mathbb{S}^1. \end{aligned}$$

³For open curves we will indicate the necessary modifications in Section 3.4.

Consequently, we obtain the uniform bound

$$\begin{aligned} \|\gamma_j\|_{C^{1,1}(\mathbb{S}^1, \mathbb{R}^3)} &\leq \|\gamma_j\|_{C^0(\mathbb{S}^1, \mathbb{R}^3)} + v_j \|\Gamma'_j\|_{C^0([0, L_j], \mathbb{R}^3)} + \frac{1}{\Theta^3} \\ &\leq 1 + \frac{1}{\Theta} + \frac{1}{\Theta^3} \quad \text{for all } j \in \mathbb{N}, \end{aligned} \quad (3.19)$$

which implies by the theorem of Arzelà-Ascoli the existence of a closed curve $\gamma_\Theta \in C^{1,1}(\mathbb{S}^1, \mathbb{R}^3)$ and a subsequence $\{\gamma_j\}$ such that

$$\gamma_j \longrightarrow \gamma_\Theta \quad \text{in } C^1(\mathbb{S}^1, \mathbb{R}^3) \quad \text{as } j \rightarrow \infty.$$

Hence γ_Θ maps \mathbb{S}^1 into \mathbb{S}^2 and has constant speed $|\gamma'_\Theta| \geq \Theta$ because⁴ $|\gamma'_j| \geq \Theta$ for all j by Lemma 3.13. In addition, $\Delta[\gamma_\Theta] \geq \Theta$, since it was proved in [SvdM03a, Lemma 4] and [GdlL03, Lemma 5] that the thickness $\Delta[\cdot]$ is upper semicontinuous with respect to convergence in $C^0(\mathbb{S}^1, \mathbb{R}^3)$ subject to a uniform upper bound on length. Thus we have shown that $\gamma_\Theta \in \mathcal{C}_\Theta$.

Since the length functional $\mathcal{L}[\cdot]$ is continuous with respect to C^1 -convergence we conclude

$$\sup_{\mathcal{C}_\Theta} \mathcal{L}[\cdot] \geq \mathcal{L}[\gamma_\Theta] = \lim_{j \rightarrow \infty} \mathcal{L}[\gamma_j] = \sup_{\mathcal{C}_\Theta} \mathcal{L}[\cdot],$$

i.e., γ_Θ is a length maximising curve. That the prescribed thickness is attained by any solution γ_Θ of Problem (P), i.e. $\Delta[\gamma_\Theta] = \Theta$, is the content of the next theorem, which then concludes the proof of Theorem 3.1. \square

Theorem 3.14 (Solutions of (P) attain thickness). *For any solution $\gamma_\Theta \in \mathcal{C}_\Theta$ of Problem (P) for $\Theta \in (0, 1]$ one has $\Delta[\gamma_\Theta] = \Theta$.*

Proof. There is nothing to prove for $\Theta = 1$ since then the great circle with thickness 1 is the unique solution (up to congruence). Assuming $\Delta[\gamma_\Theta] > \Theta$ for some $\Theta \in (0, 1)$ we will first use Lemma 2.33 to show that variations of the type $(\gamma_\Theta + \varepsilon\psi)/|\gamma_\Theta + \varepsilon\psi|$ are admissible for ε sufficiently small, to conclude with a variational argument that γ_Θ must be a great circle. Then we construct a suitable comparison curve β_{Θ^*} with $\mathcal{L}[\beta_{\Theta^*}] > \mathcal{L}[\gamma_\Theta]$, which contradicts the maximality of γ_Θ .

For brevity we set $\gamma := \gamma_\Theta$ for fixed $\Theta \in (0, 1)$ and $L := \mathcal{L}[\gamma]$, and we may assume w.l.o.g. that $|\gamma'| \equiv \text{const} =: v$ on \mathbb{S}^1 ; hence $v = L/(2\pi)$.

We claim that for any $\psi \in C_0^\infty(\mathbb{S}^1, \mathbb{R}^3)$ there is some $\varepsilon_0 = \varepsilon_0(\psi, \Delta[\gamma]) > 0$ such that for the curves

$$\eta_\varepsilon := \frac{\gamma + \varepsilon\psi}{|\gamma + \varepsilon\psi|} \in C^{1,1}(\mathbb{S}^1, \mathbb{R}^3)$$

we have $\Delta[\eta_\varepsilon] > \Theta$ for all $\varepsilon \in [-\varepsilon_0, \varepsilon_0]$.

For the proof of this claim we notice that $|\gamma| = 1$ so that $\gamma \cdot \gamma' = 0$ on \mathbb{S}^1 , which implies

$$\begin{aligned} \eta_\varepsilon &\longrightarrow \gamma \quad \text{in } C^0(\mathbb{S}^1, \mathbb{R}^3) \quad \text{as } \varepsilon \rightarrow 0, \quad \text{and} \\ \eta'_\varepsilon &= \frac{\gamma' + \varepsilon\psi'}{|\gamma + \varepsilon\psi|} - \frac{(\gamma + \varepsilon\psi) \cdot (\gamma' + \varepsilon\psi')}{|\gamma + \varepsilon\psi|^3} (\gamma + \varepsilon\psi) \\ &\longrightarrow \gamma' \quad \text{in } C^0(\mathbb{S}^1, \mathbb{R}^3) \quad \text{as } \varepsilon \rightarrow 0. \end{aligned}$$

⁴It is also possible to prove $|\gamma'_\Theta| \geq 1$ by comparing the length of the maximiser γ_Θ to that of a great circle which has thickness 1 and is henceforth an admissible comparison curve in \mathcal{C}_Θ for any $\Theta \in (0, 1]$.

As in the proof of Proposition 3.11 we use the fact that γ as a spherical curve has normal curvature equal to -1 , in other words, the arc-length parametrisation $\Gamma : [0, L] \rightarrow \mathbb{S}^2$ of γ satisfies

$$\Gamma \cdot \Gamma'' = -1 \quad \text{a.e. on } [0, L]$$

so that we obtain with

$$\Gamma'(s) = \frac{\gamma'}{|\gamma'|}(t(s)) = \frac{\gamma'(t(s))}{v}$$

and

$$\Gamma'' = \frac{\gamma''(t(s))}{v} \frac{dt}{ds}(s) = \frac{\gamma''(t(s))}{v^2}$$

for the arc-length parameters $s := \int_0^{t(s)} |\gamma'(\tau)| d\tau = vt(s)$. It follows that

$$-1 = \Gamma \cdot \Gamma'' = \frac{\gamma \cdot \gamma''}{v^2},$$

or

$$\gamma \cdot \gamma'' = -v^2, \tag{3.20}$$

which can be used to show the boundedness of η_ε'' :

$$\begin{aligned} \eta_\varepsilon'' &= \frac{\gamma'' + \varepsilon\psi''}{|\gamma + \varepsilon\psi|} - \frac{(\gamma' + \varepsilon\psi') \cdot (\gamma + \varepsilon\psi)}{|\gamma + \varepsilon\psi|^3} (\gamma' + \varepsilon\psi') \\ &\quad - \frac{|\gamma' + \varepsilon\psi'|^2 + (\gamma + \varepsilon\psi) \cdot (\gamma'' + \varepsilon\psi'')}{|\gamma + \varepsilon\psi|^3} (\gamma + \varepsilon\psi) \\ &\quad - \frac{3[(\gamma + \varepsilon\psi) \cdot (\gamma' + \varepsilon\psi')]^2}{|\gamma + \varepsilon\psi|^5} (\gamma + \varepsilon\psi) - \frac{(\gamma + \varepsilon\psi) \cdot (\gamma' + \varepsilon\psi')}{|\gamma + \varepsilon\psi|^3} (\gamma' + \varepsilon\psi'). \end{aligned}$$

Since $\|\gamma\|_{C^{1,1}(\mathbb{S}^1, \mathbb{R}^3)}$ is bounded, $\gamma \cdot \gamma' = 0$ and by (3.20) we deduce for the curvature κ_ε of η_ε

$$\begin{aligned} \limsup_{\varepsilon \rightarrow 0} \|\kappa_\varepsilon\|_{L^\infty((0, 2\pi))} &= \limsup_{\varepsilon \rightarrow 0} \left\| \frac{|\eta_\varepsilon'' \wedge \eta_\varepsilon'|}{|\eta_\varepsilon'|^3} \right\|_{L^\infty((0, 2\pi))} \\ &\leq \|\Gamma''\|_{L^\infty((0, 2\pi), \mathbb{R}^3)} \leq \frac{1}{\Delta[\gamma]}. \end{aligned}$$

Lemma 2.33 applied to $\gamma = \gamma_\Theta$ and $\gamma_j := \eta_{\varepsilon_j}$ for any subsequence $\varepsilon_j \rightarrow 0$ gives

$$\liminf_{j \rightarrow \infty} \Delta[\eta_{\varepsilon_j}] \geq \Delta[\gamma] > \Theta,$$

so that we indeed find $\varepsilon_0 = \varepsilon_0(\psi, \Delta[\gamma]) > 0$ such that

$$\Delta[\eta_\varepsilon] > \Theta \quad \text{for all } \varepsilon \in [-\varepsilon_0, \varepsilon_0],$$

which proves the claim.

Therefore we have $\eta_\varepsilon \in \mathcal{C}_\Theta$ for all $\varepsilon \in [-\varepsilon_0, \varepsilon_0]$ and

$$\mathcal{L}[\gamma] \geq \mathcal{L}[\eta_\varepsilon] \quad \text{for all } \varepsilon \in [-\varepsilon_0, \varepsilon_0].$$

3.2. EXISTENCE AND PROPERTIES OF GENERAL SOLUTIONS

Since $|\gamma + \varepsilon\psi| > 0$ for all $|\varepsilon| \ll 1$ and $|\gamma| = 1$ on \mathbb{S}^1 we can calculate the vanishing first variation of \mathcal{L} at γ :

$$\begin{aligned}
0 &= \frac{d}{d\varepsilon} [\mathcal{L}[\eta_\varepsilon]]_{\varepsilon=0} = \int_0^{2\pi} \frac{d}{d\varepsilon} [|\eta'_\varepsilon|]_{\varepsilon=0} dt \\
&= \int_0^{2\pi} \frac{\eta'_\varepsilon}{|\eta'_\varepsilon|} \cdot \left[\frac{d}{d\varepsilon} \eta'_\varepsilon \right]_{\varepsilon=0} dt = \int_0^{2\pi} \frac{\gamma'}{v} \cdot \frac{d}{d\varepsilon} [\eta'_\varepsilon]_{\varepsilon=0} dt \\
&= v^{-1} \int_0^{2\pi} \left[\gamma' \cdot \psi' - |\gamma'|^2 (\gamma \cdot \psi) - (\psi \cdot \gamma' + \gamma \cdot \psi') (\gamma' \cdot \gamma) \right. \\
&\quad \left. - (\gamma' \cdot \psi) (\gamma \cdot \gamma') + 3(\gamma \cdot \gamma')^2 (\gamma \cdot \psi) \right] dt \\
&= v^{-1} \int_0^{2\pi} \left[\gamma' \cdot \psi' - v^2 (\gamma \cdot \psi) \right] dt.
\end{aligned}$$

Integrating by parts and applying the Fundamental Lemma in the calculus of variations we obtain

$$\gamma'' + v^2 \gamma = 0 \quad \text{a.e. on } \mathbb{S}^1.$$

Since $\gamma \in C^{1,1}$ we obtain immediately $\gamma'' \in C^{1,1}$ and by the standard bootstrap argument finally $\gamma \in C^\infty(\mathbb{S}^1, \mathbb{R}^3)$. Transforming the equation into the arc-length formulation we obtain

$$\Gamma'' = -\Gamma \quad \text{on } [0, L],$$

which has the great circles as their only solutions; see e.g. [doC76, p. 246]. Hence we have shown that if $\Delta[\gamma] > \Theta$ for the solution $\gamma = \gamma_\Theta$ then γ_Θ is a great circle.

For each $\tau \in [\Theta_2, 1)$, Θ_2 as in (3.1), we will construct in Lemma 3.15 below a competitor $\beta_\tau \in \mathcal{C}_\tau$ with

$$\mathcal{L}[\beta_\tau] > 2\pi = \mathcal{L}[\gamma_\Theta]$$

so that we obtain for the special choice $\tau = \Theta^* := \max\{\Theta_2, \Theta\}$ a competitor $\beta_\tau \in \mathcal{C}_{\Theta^*} \subset \mathcal{C}_\Theta$, which leads to the desired contradiction against the maximality of $\mathcal{L}[\gamma_\Theta]$ in \mathcal{C}_Θ . \square

Lemma 3.15 (Explicit competitors β_τ for $\tau \in [\Theta_2, \Theta_1]$). *For every $\tau \in [\Theta_2, \Theta_1] = [\sin(\pi/4), 1]$ there is a closed curve $\beta_\tau \in \mathcal{C}_\tau$ with*

$$\begin{aligned}
\Delta[\beta_\tau] &= \tau, \\
\mathcal{L}[\beta_\tau] &= 8\tau \arccos \sqrt{1 - \frac{1}{2\tau^2}}, \\
\mathcal{V}(\beta_\tau) &= 2\tau \mathcal{L}[\beta_\tau] = 16\tau^2 \arccos \sqrt{1 - \frac{1}{2\tau^2}}.
\end{aligned}$$

In particular, $\mathcal{L}[\beta_\tau] \geq 2\pi$ with equality if and only if β_τ is a great circle, i.e. if $\tau = \Theta_1 = 1$.

Remark 3.16. *Our construction will reveal a one-parameter family $\{\beta_\tau\}$ (parametrised by the prescribed thickness τ) continuously joining the unique solutions for $\tau = \Theta_1 = 1$ and $\tau = \Theta_2$ (see Figure 3.6).*

We strongly believe that these β_τ provide the unique (but not sphere-filling) solutions for every $\tau \in (\Theta_2, \Theta_1)$, which would extend our uniqueness result, Theorem 3.3 to this

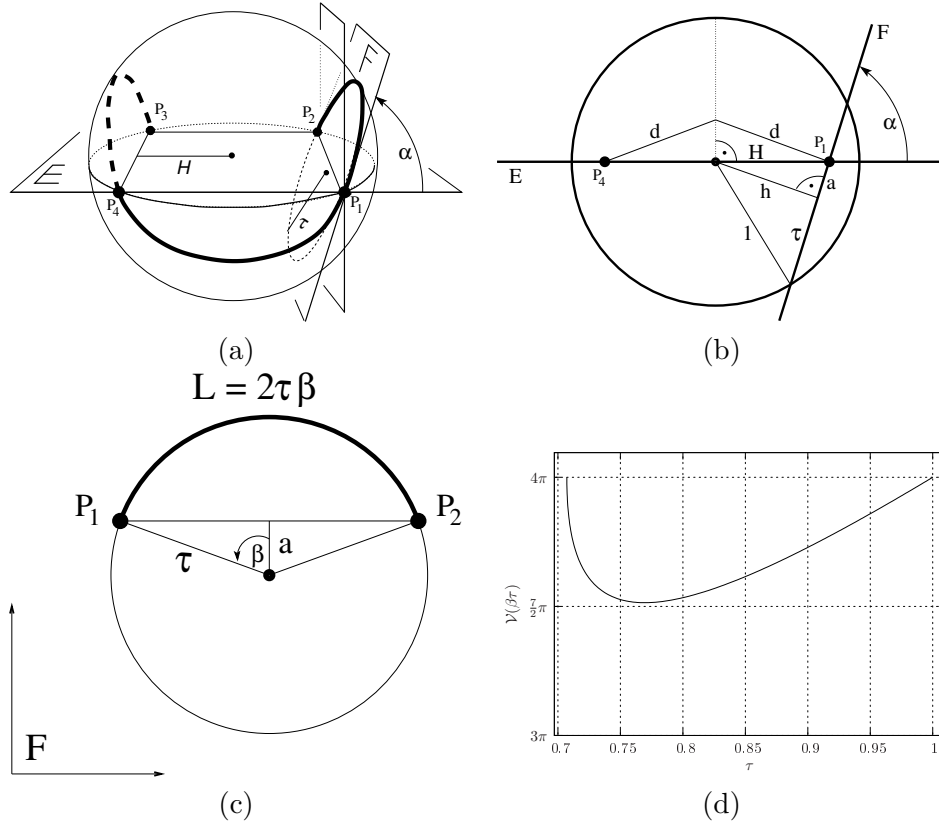


Figure 3.5: (a)–(c) Determining the thickness of β_τ as described in Lemma 3.15. (d) The volume \mathcal{V} of the tubular neighbourhood of β_τ .

continuous range of given thickness values. Up to now, however, we have no proof for this conjecture. We only would like to remark that the curves β_τ are good candidates for the maximisers for $\tau \in (\Theta_2, \Theta_1)$. See also Section 5.5.7.

Proof of Lemma 3.15. To construct β_τ for given $\tau \in [\Theta_2, \Theta_1]$ we equipartition the equator of the \mathbb{S}^2 by four distinct points P_i , $i = 1, 2, 3, 4$, such that these four points are the vertices of a square of edge length $2H := 2 \cdot \frac{1}{\sqrt{2}}$ in the plane E containing the equator. Now we take the plane vertical to E which contains the straight segment P_1P_2 and rotate that plane about the rotation axis through P_1 and P_2 until this rotated plane F intersected with \mathbb{S}^2 is a circle ∂B_τ of radius τ ; see Figure 3.5(a). Let $\alpha = \alpha(\tau)$ be the angle between F and E , and we refer to the side-view in Figure 3.5(b) where E is seen as a horizontal line, to obtain the geometric identities

$$\begin{aligned} a &= H \cos \alpha, & h &= H \sin \alpha, \\ \tau &= \sqrt{1 - h^2} = \sqrt{1 - H^2 \sin^2 \alpha}. \end{aligned}$$

In Figure 3.5(c) the plane F coincides with the drawing plane, and one can read off the relation

$$L = 2\tau\beta = 2\tau \arccos(a/\tau),$$

where L denotes the length of the shorter circular arc on ∂B_τ with endpoints P_1 and P_2 . Repeating this process for the other edges P_2P_3 , P_3P_4 , and P_4P_1 , we obtain four such circular arcs each of length L . Reflecting two opposite of these arcs across the equatorial plane E and taking the union of these reflections with the two remaining arcs we obtain the desired $C^{1,1}$ -curve β_τ which by construction⁵ has length

$$4L = 8\tau \arccos(a/\tau) = 8\tau \arccos \sqrt{1 - \frac{1}{2\tau^2}}.$$

The thickness of β_τ is realized exclusively by the local radius of curvature τ of each circular arc, since neighbouring arcs are separated by the plane S containing the normal disk of radius τ at the common endpoint. All normal disks of radius τ centred on one of these arcs are not only mutually disjoint but also completely contained in the half-space bounded by S that contains the arc itself. (Compare with our argument to prove (3.3) in Section 3.1 in the construction of the explicit solutions $\beta^{n,k}$ whose circular arcs were full semicircles whereas the arcs to build β_τ for $\tau \in (\Theta_2, \Theta_1)$ are strict subsets of semicircles.) And the normal disks of opposite arcs can not intersect if

$$\sqrt{1 - H^2 \sin^2 \alpha} = \tau \leq d := \frac{H}{\sin \alpha};$$

see Figure 3.5(b), which is true since the function

$$f(\alpha) := \frac{1}{2} - \sin^2 \alpha + \frac{1}{2} \sin^4 \alpha$$

satisfies $f(\pi/2) = 0$ and is monotonically decreasing on $[0, \pi/2]$.

Thus we have shown $\Delta[\beta_\tau] = \tau$ and that a smooth and regular parametrisation of β_τ is actually contained in the class \mathcal{C}_τ . The formula for the volume in the statement of the lemma is a direct consequence of Hotelling's theorem, see Proposition 3.11. The four arcs on the great circle each of length $\pi/2$ connecting neighbouring points in $\{P_1, P_2, P_3, P_4\}$ are the shortest possible connections on \mathbb{S}^2 so that $L \geq \frac{\pi}{2}$; hence $\mathcal{L}[\beta_\tau] = 4L \geq 2\pi$ with equality if and only if β_τ is the great circle, i.e. $\tau = \Theta_1 = 1$. \square

We conclude this section by analysing how length and tube volume of solutions depend on the given thickness.

Lemma 3.17 (Length and volume as function of Θ). *For given minimal thickness $\Theta \in (0, 1]$ let γ_Θ be a solution of Problem (P), and define the function $L : (0, 1] \rightarrow [2\pi, \infty)$ by $L(\Theta) := \mathcal{L}[\gamma_\Theta]$ and $V : (0, 1] \rightarrow (0, 4\pi]$ by $V(\Theta) := \mathcal{V}(\mathcal{T}_{\arcsin \Theta}(\gamma_\Theta))$. Then*

- (i) L is a strictly decreasing function on $(0, 1]$.
- (ii) $L(1) = 2\pi$, and $L(\Theta) \rightarrow \infty$ as $\Theta \rightarrow +0$.
- (iii) $\lim_{h \rightarrow +0} L(\Theta - h) = L(\Theta)$ for $\Theta \in (0, 1]$.
- (iv) $L(\Theta) = V(\Theta)/(2\Theta)$ is differentiable at almost every $\Theta \in (0, 1]$.

⁵The circular arcs indeed have common tangent lines at the concatenation points P_i , $i = 1, 2, 3, 4$, since the tangent vectors of the two arcs meeting at, say endpoint P_1 are both contained in the tangent plane $T_{P_1}\mathbb{S}^2$ both enclosing the same angle with $E \cap T_{P_1}\mathbb{S}^2$, such that the reflection across the line $E \cap T_{P_1}\mathbb{S}^2$ produces the common tangent line through P_1 in $T_{P_1}\mathbb{S}^2$.

(v) $2\pi \leq L(\Theta) \leq 2\pi/\Theta$ and $4\pi\Theta \leq V(\Theta) \leq 4\pi$ for all $\Theta \in (0, 1]$.

(vi) The functions L and V are upper semicontinuous on $(0, 1]$.

Proof. (i) For $0 < \Theta < \Theta' \leq 1$ and the corresponding solutions $\gamma_\Theta \in \mathcal{C}_\Theta$ and $\gamma_{\Theta'} \in \mathcal{C}_{\Theta'}$ for Problem (P) we have

$$\Delta[\gamma_{\Theta'}] \geq \Theta' > \Theta \quad (3.21)$$

so that $\gamma_{\Theta'} \in \mathcal{C}_\Theta$ as well. Hence

$$L(\Theta) = \mathcal{L}[\gamma_\Theta] \geq \mathcal{L}[\gamma_{\Theta'}] = L(\Theta'),$$

which proves that L is a decreasing function. If $0 < \Theta < \Theta' < 1$ we know that $\gamma_{\Theta'}$ is not the great circle, and we may assume that $\gamma_{\Theta'}$ has constant speed $v = |\dot{\gamma}_{\Theta'}|$ on \mathbb{S}^1 . Recalling the arguments in the proof of Theorem 3.14, there must be a function $\psi \in C_0^\infty(\mathbb{S}^1, \mathbb{R}^3)$ such that

$$\delta\mathcal{L}[\gamma_{\Theta'}, \psi] := \frac{d}{d\varepsilon} \left[\mathcal{L} \left(\frac{\gamma_{\Theta'} + \varepsilon\psi}{|\gamma_{\Theta'} + \varepsilon\psi|} \right) \right]_{\varepsilon=0} \neq 0,$$

and since the first variation $\delta\mathcal{L}[\gamma_{\Theta'}, \cdot]$ is a linear functional we may assume that

$$\delta\mathcal{L}[\gamma_{\Theta'}, \psi] = 1. \quad (3.22)$$

Notice that (3.21) and the claim established in the proof of Theorem 3.14 imply

$$\Delta \left[\frac{\gamma_{\Theta'} + \varepsilon\psi}{|\gamma_{\Theta'} + \varepsilon\psi|} \right] > \Theta, \quad \text{hence} \quad \frac{\gamma_{\Theta'} + \varepsilon\psi}{|\gamma_{\Theta'} + \varepsilon\psi|} \in \mathcal{C}_\Theta \quad (3.23)$$

for ε sufficiently small. One can check that there is an $\varepsilon_0 = \varepsilon_0(\psi) > 0$ such that

$$\frac{d^2}{d\varepsilon^2} \left[\mathcal{L} \left(\frac{\gamma_{\Theta'} + \varepsilon\psi}{|\gamma_{\Theta'} + \varepsilon\psi|} \right) \right]$$

is bounded uniformly in $\varepsilon \in [-\varepsilon_0, \varepsilon_0]$, so that

$$\mathcal{L} \left(\frac{\gamma_{\Theta'} + \varepsilon\psi}{|\gamma_{\Theta'} + \varepsilon\psi|} \right) = \mathcal{L}[\gamma_{\Theta'}] + \varepsilon\delta\mathcal{L}[\gamma_{\Theta'}, \psi] + O(\varepsilon^2).$$

Hence by virtue of (3.22)

$$\mathcal{L} \left(\frac{\gamma_{\Theta'} + \varepsilon\psi}{|\gamma_{\Theta'} + \varepsilon\psi|} \right) > \mathcal{L}[\gamma_{\Theta'}] \quad \text{for } 0 < \varepsilon \ll 1,$$

which implies by (3.23)

$$L(\Theta) = \mathcal{L}[\gamma_\Theta] \stackrel{(3.23)}{\geq} \mathcal{L} \left[\frac{\gamma_{\Theta'} + \varepsilon\psi}{|\gamma_{\Theta'} + \varepsilon\psi|} \right] > \mathcal{L}[\gamma_{\Theta'}] = L(\Theta')$$

for all $0 < \Theta < \Theta' < 1$. If $\Theta < \Theta' = 1$ we find $\Theta'' \in (\Theta, \Theta')$ so that according to what we have just proved and the monotonicity observed in the beginning

$$L(\Theta) > L(\Theta'') \geq L(\Theta'),$$

3.2. EXISTENCE AND PROPERTIES OF GENERAL SOLUTIONS

which finishes the proof of Part (i).

(ii) For the explicit solutions $\beta^{n,k} \in \mathcal{C}_{\Theta_n}$ constructed in Theorem 3.2 we have $\mathcal{V}(\mathcal{T}_{\arcsin \Theta_n}(\beta^{n,k})) = 4\pi$, and therefore by Proposition 3.11

$$L(\Theta_n) = \mathcal{L}[\beta^{n,k}] = \frac{\mathcal{V}(\mathcal{T}_{\arcsin \Theta_n}(\beta^{n,k}))}{2\Theta_n} = \frac{2\pi}{\Theta_n} = \frac{2\pi}{\sin \frac{\pi}{2n}} \rightarrow \infty \text{ as } n \rightarrow \infty.$$

This together with the strict monotonicity shown in Part (i) establishes $L(\Theta) \rightarrow \infty$ as $\Theta \rightarrow +0$.

(iii) We consider the set of solutions $\{\gamma_{\Theta-h} \in \mathcal{C}_{\Theta-h}\}_h$ for $0 < h < \Theta/2$ and assume that all these curves have constant speed $v_h := |\gamma'_{\Theta-h}| > 0$. Take an arbitrary sequence $h_j \rightarrow 0$. By Lemma 2.30 a subsequence $\gamma_{h_{j_k}}$ converges in C^1 to a curve γ that by Lemma 2.31 has thickness $\Delta[\gamma] \geq \Theta$. We have further $\mathcal{L}[\gamma] = \lim_{k \rightarrow \infty} \mathcal{L}[\gamma_{\Theta-h_{j_k}}]$ by C^1 convergence. The curve γ is a competitor to any optimiser $\gamma_{\Theta} \in \mathcal{C}_{\Theta}$ and consequently

$$\lim_{j \rightarrow \infty} L(\Theta - h_j) \underset{(i)}{\geq} L(\Theta) \geq \mathcal{L}[\gamma] = \lim_{j \rightarrow \infty} L(\Theta - h_j).$$

Since the sequence h_j was arbitrary we finally conclude by the subsequence principle

$$\lim_{h \rightarrow +0} L(\Theta - h) = L(\Theta).$$

(iv) Proposition 3.11 applied to the solution $\gamma_{\Theta} \in \mathcal{C}_{\Theta}$ of Problem (P) gives

$$L(\Theta) = \mathcal{L}[\gamma_{\Theta}] \underset{\text{Prop. 3.11}}{=} \frac{\mathcal{V}(\mathcal{T}_{\arcsin \Theta}(\gamma_{\Theta}))}{2\Theta} = \frac{V(\Theta)}{2\Theta}.$$

Since $L : (0, 1] \rightarrow [2\pi, \infty)$ is (strictly) monotone, it is differentiable a.e. on $(0, 1]$.

(v) By Proposition 3.11 we have

$$\begin{aligned} L(\Theta) = \mathcal{L}[\gamma_{\Theta}] &\underset{\text{Prop. 3.11}}{=} \frac{\mathcal{V}(\mathcal{T}_{\arcsin \Theta}(\gamma_{\Theta}))}{2\Theta} \\ &\leq \frac{4\pi}{2\Theta} = \frac{2\pi}{\Theta} \quad \text{for all } \Theta \in (0, 1]. \end{aligned}$$

On the other hand, the great circle $c_g \in \mathcal{C}_1 \subset \mathcal{C}_{\Theta}$ has length

$$2\pi = \mathcal{L}[c_g] \leq \mathcal{L}[\gamma_{\Theta}] = L(\Theta) \quad \text{for all } \Theta \in (0, 1].$$

The corresponding inequality for the volume $V(\Theta)$ follows now from Part (iv).

(vi) For $\Theta_i \rightarrow \Theta \in (0, 1]$ as $i \rightarrow \infty$ consider a subsequence $\{\Theta_j\} \subset \{\Theta_i\}$ such that

$$L(\Theta_j) \rightarrow \limsup_{i \rightarrow \infty} L(\Theta_i) \quad \text{as } j \rightarrow \infty.$$

If there are infinitely many j such that $\Theta_j \leq \Theta$ then we obtain from Part (iii)

$$\limsup_{i \rightarrow \infty} L(\Theta_i) = \lim_{j \rightarrow \infty} L(\Theta_j) = L(\Theta).$$

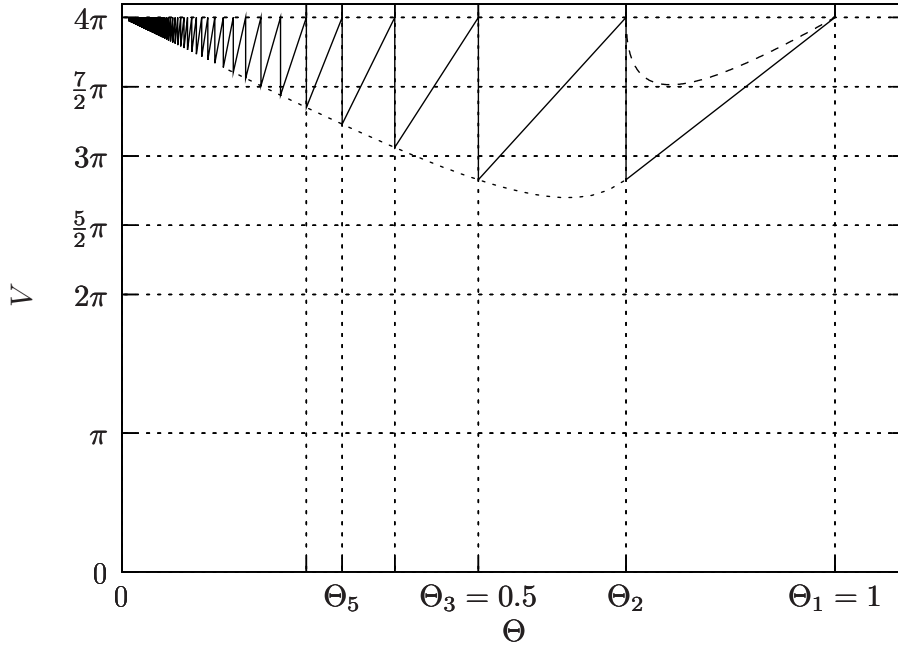


Figure 3.6: A lower bound for $V(\Theta)$ as established by Lemma 3.18. The low peaks are located at $(\Theta_{n+1}, 4\pi\Theta_{n+1}/\Theta_n)$. The dotted hull-curve $h(t) := \left(\sin(\frac{\pi}{2t+2}), 4\pi \sin(\frac{\pi}{2t+2})/\sin(\frac{\pi}{2t})\right)$, $t \in [1, \infty)$ reveals that the spikes are not on a straight line. The values of $V(\Theta_2)$ and $V(\Theta_3)$ happen to be equal. For $\Theta \in (\Theta_2, \Theta_1)$ the volume of $\mathcal{V}(\mathcal{T}_\theta(\beta_\Theta))$ indicates (dashed line) that the curves β_Θ serve as good competitors for Problem (P), see also Figure 3.5(d).

On the other hand, for all j with $\Theta_j > \Theta$ we have by Part (i) $L(\Theta) > L(\Theta_j)$ such that

$$L(\Theta) \geq \lim_{j \rightarrow \infty} L(\Theta_j) = \limsup_{i \rightarrow \infty} L(\Theta_i).$$

Part (iv) implies

$$\limsup_{i \rightarrow \infty} V(\Theta_i) \stackrel{(iv)}{=} \limsup_{i \rightarrow \infty} 2\Theta_i L(\Theta_i) \leq 2\Theta L(\Theta) \stackrel{(iv)}{=} V(\Theta).$$

□

The lower bound for the volume $V(\Theta) = \mathcal{V}(\mathcal{T}_{\arcsin \Theta}(\gamma_\Theta))$ depicted in Figure 3.6 improves the lower estimate in Lemma 3.17 (v) considerably, and is established next.

Lemma 3.18 (Lower volume bound for solutions). *The function $V : (0, 1] \rightarrow (0, 4\pi]$ is differentiable a.e. on $(0, 1]$ and satisfies the estimate*

$$\frac{4\pi}{\Theta_n} \Theta \leq V(\Theta) \leq 4\pi \quad \text{for all } \Theta \leq \Theta_n = \sin \frac{\pi}{2n}, n \in \mathbb{N}.$$

In particular, $4\pi \geq V(\Theta) \geq 4\pi\Theta/\Theta_n$ for $\Theta \in (\Theta_{n+1}, \Theta_n]$, $n \in \mathbb{N}$.

3.2. EXISTENCE AND PROPERTIES OF GENERAL SOLUTIONS

Notice that we can use Proposition 3.11 twice to interpret the lower bound for $V(\Theta)$ as the volume of the tube $\mathcal{T}_{\arcsin \Theta}(\beta^{n,k})$. In fact, for $\vartheta := \arcsin \Theta$ one has

$$\mathcal{V}(\mathcal{T}_{\vartheta}(\beta^{n,k})) \underset{\text{Prop.3.11}}{=} 2\Theta \mathcal{L}[\beta^{n,k}] \underset{\text{Prop.3.11}}{=} 2\Theta \frac{\mathcal{V}(\mathcal{T}_{\vartheta_n}(\beta^{n,k}))}{2\Theta_n} = \frac{4\pi\Theta}{\Theta_n}.$$

Proof. Combining Parts (i) and (iv) of Lemma 3.17 we obtain that V is differentiable a.e. and satisfies

$$0 \geq L'(\Theta) = \left(\frac{V(\Theta)}{2\Theta} \right)' = -\frac{1}{2\Theta^2} V(\Theta) + \frac{1}{2\Theta} V'(\Theta) \quad \text{for a.e. } \Theta \in (0, 1],$$

i.e.,

$$\frac{1}{2\Theta} V'(\Theta) \leq \frac{1}{2\Theta^2} V(\Theta) \quad \text{for a.e. } \Theta \in (0, 1].$$

Since $V(\Theta) \geq 4\pi\Theta > 0$ for all $\Theta \in (0, 1]$ by Lemma 3.17 (v), we conclude

$$(\log V(\Theta))' = \frac{V'(\Theta)}{V(\Theta)} \leq \frac{1}{\Theta} \quad \text{for a.e. } \Theta \in (0, 1].$$

Integrating this inequality on $[\Theta, \Theta_n]$ for $\Theta \in (0, \Theta_n)$, $n \in \mathbb{N}$, we obtain with $V(\Theta_n) = 4\pi$

$$\log 4\pi - \log V(\Theta) = \log V(\Theta_n) - \log V(\Theta) \leq \int_{\Theta}^{\Theta_n} \frac{1}{\Theta} d\Theta = \log \Theta_n - \log \Theta,$$

hence

$$4\pi e^{-\log V(\Theta)} = \frac{4\pi}{V(\Theta)} \leq \Theta_n e^{-\log \Theta} = \frac{\Theta_n}{\Theta},$$

or

$$\frac{4\pi}{\Theta_n} \Theta \leq V(\Theta).$$

□

Corollary 3.19. $V(\Theta) \rightarrow 4\pi$ as $\Theta \rightarrow +0$.

Proof. For $\Theta \in (\Theta_{n+1}, \Theta_n]$ we have

$$V(\Theta) \geq \frac{4\pi\Theta}{\Theta_n} > \frac{4\pi\Theta_{n+1}}{\Theta_n} = 4\pi \frac{\sin \frac{\pi}{2n+2}}{\sin \frac{\pi}{2n}} \xrightarrow{n \rightarrow \infty} 4\pi.$$

□

This asymptotic behaviour of the volume confirms our intuition that it is easier to cover the sphere with thin ropes than with thick ones – there is simply more freedom with long and thin ropes to “fill” the gaps on the surface of the unit sphere.

3.3 Uniqueness

In the following we are going to work with geodesic balls

$$\mathcal{B}_\vartheta(\xi) := \{\eta \in \mathbb{S}^2 : \text{dist}_{\mathbb{S}^2}(\eta, \xi) < \vartheta\}.$$

on the unit sphere. Furthermore, we will use the notation

$$\begin{aligned} \overline{\mathcal{B}_\vartheta(\xi)} &:= \{\eta \in \mathbb{S}^2 : \text{dist}_{\mathbb{S}^2}(\eta, \xi) \leq \vartheta\}, \\ \partial\mathcal{B}_\vartheta(\xi) &:= \{\eta \in \mathbb{S}^2 : \text{dist}_{\mathbb{S}^2}(\eta, \xi) = \vartheta\}. \end{aligned}$$

Proposition 3.20 (Double touching ball). *[Ge04, Satz 3.27] Let $\gamma : \mathbb{S} \rightarrow \mathbb{R}^N$ be a closed, rectifiable and continuous curve with positive thickness $\Theta := \Delta[\gamma] > 0$, and $x \in \mathbb{R}^N$ such that*

$$\gamma(\mathbb{S}) \cap B_\Theta(x) = \emptyset. \quad (3.24)$$

If there are two points $P, Q \in \partial B_\Theta(x) \cap \gamma(\mathbb{S})$ with $0 < \text{dist}_{\mathbb{R}^N}(P, Q) < 2\Theta$, then the shorter circular sub-arc of the geodesic circle connecting P and Q is contained in $\gamma(\mathbb{S})$.

Since we only consider the special case for closed curves we present a new, more intuitive proof than in the diploma thesis [Ge04].

Proof. Recall from Lemma 2.2 that the arc-length parametrisation $\Gamma : [0, L] \rightarrow \mathbb{R}^N$ of γ (with length $L := \mathcal{L}[\gamma] > 0$) is of class $C^{1,1}([0, 1], \mathbb{R}^3)$, which allows us in the following to speak of tangential properties of γ .

We set

$$\begin{aligned} \Theta_0 &:= \Theta, & \Theta_1 &:= \frac{1}{2} \text{dist}_{\mathbb{R}^N}(P, Q) < \Theta_0, \\ x_0 &:= x, & x_1 &:= \frac{P + Q}{2}, \end{aligned}$$

Thus P and Q are antipodal points on the sphere $\partial B_{\Theta_1}(x_1)$. Since by (3.24) γ is tangent to the sphere $\partial B_{\Theta_0}(x_0)$ at P and Q it cannot be tangent to $\partial B_{\Theta_1}(x_1)$ at either P or Q . For if it were $\Delta e\Theta_1 < \Theta_0 = \Delta$ a contradiction. Hence $B_{\Theta_1}(x_1) \cap \gamma(\mathbb{S}) \neq \emptyset$, and we consider the family of balls $B_{\Theta_s}(x_s)$ defined by

$$x_s := x_0 + s(x_1 - x_0) \quad \text{and} \quad \Theta_s := |P - x_s| \quad \text{for } s \in [0, 1],$$

We notice that $\Theta_s < \Theta_0$ for all $s \in (0, 1]$, and claim that

$$\partial B_{\Theta_s}(x_s) \cap \gamma(\mathbb{S}^1) = \{P, Q\} \quad \text{for all } s \in (0, 1]. \quad (3.25)$$

Indeed, otherwise we would have (at least) three points of the curve on a circle on $\partial B_{\Theta_{s^*}}(x_{s^*})$ for some $s^* \in (0, 1]$, with radius less or equal than $\Theta_{s^*} < \Theta_0 = \Theta = \Delta[\gamma]$. This, however, contradicts the definition of $\Delta[\gamma]$ in (2.2).

By (3.24) the curve γ is tangent to $\partial B_{\Theta_0}(x_0)$ at P and Q , and since the $\partial B_{\Theta_s}(x_s)$ sweep out the open region $B_{\Theta_1}(x_1) \setminus \overline{B_{\Theta_0}(x_0)}$, i.e.,

$$B_{\Theta_1}(x_1) \setminus \overline{B_{\Theta_0}(x_0)} \subset \bigcup_{s \in (0, 1]} \partial B_{\Theta_s}(x_s) \setminus \overline{B_{\Theta_0}(x_0)},$$

we conclude from (3.25) that the shorter sub-arc $\gamma_1 \subset \gamma$ connecting P and Q must be on $\partial B_{\Theta_0}(x_0)$. Since every curve but a great circle on a sphere has thickness less than the radius of the sphere, γ_1 is equal to the shorter great arc connecting P and Q . \square

Lemma 3.21 (Characterisation of sphere filling curves). *For a closed rectifiable continuous curve $\gamma : \mathbb{S}^1 \rightarrow \mathbb{S}^2$ with positive thickness $\Theta := \Delta[\gamma] > 0$, $\vartheta := \arcsin \Theta \leq \pi/2$, the following two statements are equivalent:*

(i) $\mathcal{V}(\mathcal{T}_\vartheta(\gamma)) = 4\pi$;

(ii) For any $\xi \in \mathbb{S}^2$ such that $\mathcal{B}_\vartheta(\xi) \cap \gamma(\mathbb{S}^1) = \emptyset$ one of the following is true:

(a) $\partial\mathcal{B}_\vartheta(\xi) \cap \gamma(\mathbb{S}^1) = \{P, Q\}$ with $\text{dist}_{\mathbb{S}^2}(P, Q) = 2\vartheta$ (antipodal points);

(b) $\partial\mathcal{B}_\vartheta(\xi) \cap \gamma(\mathbb{S}^1) = \{\text{semicircle of spherical radius } \vartheta\}$;

(c) $\partial\mathcal{B}_\vartheta(\xi) \cap \gamma(\mathbb{S}^1) = \partial\mathcal{B}_\vartheta(\xi)$.

Proof. (i) \Rightarrow (ii). Let $\xi \in \mathbb{S}^2$ be a point such that the open geodesic ball $\mathcal{B}_\vartheta(\xi)$ has empty intersection with the curve $\gamma(\mathbb{S}^1)$. We claim that

$$\mathcal{S} := \partial\mathcal{B}_\vartheta(\xi) \cap \gamma(\mathbb{S}^1) \neq \emptyset.$$

Indeed, otherwise we could infer $\delta := \text{dist}_{\mathbb{S}^2}(\xi, \gamma(\mathbb{S}^1)) - \vartheta > 0$, so that

$$\mathcal{T}_\vartheta(\gamma) \cap \mathcal{B}_\delta(\xi) = \emptyset,$$

which implies

$$\mathcal{V}(\mathcal{T}_\vartheta(\gamma)) \leq \mathcal{V}(\mathbb{S}^2 \setminus \mathcal{B}_\delta(\xi)) < 4\pi$$

contradicting Assumption (i).

If the closed set \mathcal{S} is contained in an open semicircle on $\partial\mathcal{B}_\vartheta(\xi)$ then we find two points $\eta, \zeta \in \mathcal{S}$ such that⁶

$$0 \leq \text{dist}_{\mathbb{S}^2}(\eta, \zeta) = \max_{\mathcal{S} \times \mathcal{S}} \text{dist}_{\mathbb{S}^2}(\cdot, \cdot) < 2\vartheta. \quad (3.26)$$

Applying Proposition 3.20 we infer that the whole shorter sub-arc of $\partial\mathcal{B}_\vartheta(\xi)$ connecting η and ζ is contained in \mathcal{S} , and is (by (3.26)) consequently equal to \mathcal{S} . On this circular arc we find a point $q \in \mathcal{S}$ with $\text{dist}_{\mathbb{S}^2}(q, \eta) = \text{dist}_{\mathbb{S}^2}(q, \zeta)$, which can be joined with the centre ξ by the unique unit speed geodesic given by the great circle $c_g : [0, 2\pi] \rightarrow \mathbb{S}^2$ with $c_g(0) = q$, $c'_g(0) \perp \mathcal{S}$, and $c_g(\vartheta) = \xi$.

We claim that there is a small number $\varepsilon > 0$, such that

$$\delta := \text{dist}_{\mathbb{S}^2}(c_g(\vartheta + \varepsilon), \gamma(\mathbb{S}^1)) - \vartheta > 0,$$

which would imply that

$$\mathcal{T}_\vartheta(\gamma) \cap \mathcal{B}_\delta(c_g(\vartheta + \varepsilon)) = \emptyset,$$

hence

$$\mathcal{V}(\mathcal{T}_\vartheta(\gamma)) \leq \mathcal{V}(\mathbb{S}^2 \setminus \mathcal{B}_\delta(c_g(\vartheta + \varepsilon))) < 4\pi$$

contradicting Assumption (i) and therefore ruling out the situation that \mathcal{S} is contained in any open semicircle.

To prove the claim we suppose to the contrary that there is a sequence of curve points $p_n \in \gamma(\mathbb{S}^1)$ such that

$$\text{dist}_{\mathbb{S}^2}(c_g(\vartheta + 1/n), \gamma(\mathbb{S}^1)) = \text{dist}_{\mathbb{S}^2}(c_g(\vartheta + 1/n), p_n) \leq \vartheta \quad \forall n \in \mathbb{N}. \quad (3.27)$$

⁶We also allow the coincidence $\eta = \zeta$ (in which case $\mathcal{S} = \{\eta\}$) at this stage.

Since $\gamma(\mathbb{S}^1)$ is compact we may assume that $p_n \rightarrow p \in \gamma(\mathbb{S}^1)$ as $n \rightarrow \infty$. From $\mathcal{B}_\vartheta(\xi) \cap \gamma(\mathbb{S}^1) = \emptyset$ we infer from (3.27) as $n \rightarrow \infty$

$$\vartheta \leq \text{dist}_{\mathbb{S}^2}(\xi, p) = \text{dist}_{\mathbb{S}^2}(c_g(\vartheta), p) = \lim_{n \rightarrow \infty} \text{dist}_{\mathbb{S}^2}(c_g(\vartheta + 1/n), p_n) \leq \vartheta,$$

i.e.,

$$p \in \partial\mathcal{B}_\vartheta(\xi) \cap \gamma(\mathbb{S}^1) = \mathcal{S}. \quad (3.28)$$

On the other hand, one has

$$\text{dist}_{\mathbb{S}^2}(x, \mathcal{S}) \geq \left| \frac{\eta + \zeta}{2} - \xi \right| =: c(\eta, \zeta) > 0$$

for all $x \in \overline{\mathcal{B}_\vartheta(c_g(\vartheta + 1/n))} \setminus \mathcal{B}_\vartheta(\xi)$, since the circular arc \mathcal{S} (with endpoints η and ζ) is strictly shorter than $\pi\vartheta$. Consequently,

$$\text{dist}_{\mathbb{S}^2}(p_n, \mathcal{S}) \geq c(\eta, \zeta) > 0 \quad \text{for all } n \in \mathbb{N},$$

and hence

$$\text{dist}_{\mathbb{S}^2}(p, \mathcal{S}) \geq c(\eta, \zeta) > 0$$

contradicting (3.28), which proves the claim.

Since we now know that \mathcal{S} is not contained in any open semicircle on $\partial\mathcal{B}_\vartheta(\xi)$ we know that $\#\mathcal{S} \geq 3$ unless \mathcal{S} consists precisely of two antipodal points, which is case (a).

If \mathcal{S} is contained in a closed semicircle it must contain the endpoints p_1, p_2 of that semicircle (otherwise it would be contained in a different open semicircle, which was excluded above). Since $\#\mathcal{S} \geq 3$ we find (at least) one point $q \in \mathcal{S} \setminus \{p_1, p_2\}$ so that

$$\text{dist}_{\mathbb{S}^2}(p_1, q) < 2\vartheta \quad \text{and} \quad \text{dist}_{\mathbb{S}^2}(q, p_2) < 2\vartheta.$$

Consequently, we can apply Proposition 3.20 to find that \mathcal{S} equals the closed semicircle with endpoints p_1 and p_2 which is case (b).

Finally we have to deal with the situation that \mathcal{S} is not contained in any closed semicircle. Consider $q \in \mathcal{S}$ and its antipodal point $q' \in \partial\mathcal{B}_\vartheta(\xi)$.

If $q' \in \mathcal{S}$ then we find on each of the two open semicircles $C_1, C_2 \subset \partial\mathcal{B}_\vartheta(\xi)$ bounded by q and q' (at least) one point of \mathcal{S} , say $p_1 \in \mathcal{S} \cap C_1$ and $p_2 \in \mathcal{S} \cap C_2$. Otherwise \mathcal{S} would be contained in one of the two closed semicircles $C_i \cup \{q, q'\}$, $i = 1, 2$.

Since p_1 and p_2 are not antipodal to q or q' we can apply Proposition 3.20 to connect q and q' with p_1 and p_2 by circular arcs contained in \mathcal{S} , which proves $\mathcal{S} = \partial\mathcal{B}_\vartheta(\xi)$, i.e. we are in situation (c).

If, on the other hand, $q' \notin \mathcal{S}$ we have $\text{dist}_{\mathbb{S}^2}(q', \mathcal{S}) > 0$, and we can take the largest open circular arc C on $\partial\mathcal{B}_\vartheta(\xi) \setminus \mathcal{S}$ containing q' . By definition this arc has endpoints $p_1, p_2 \in \mathcal{S}$, and C is strictly shorter than a semicircle, since otherwise \mathcal{S} would be contained in a closed semicircle. Thus we can apply Proposition 3.20 to p_1 and p_2 , to p_1 and q , and to p_2 and q , respectively, to find that the circular arcs on $\partial\mathcal{B}_\vartheta(\xi)$ connecting p_1 and p_2 , p_1 and q , and p_2 and q , are contained in \mathcal{S} , which proves $\mathcal{S} = \partial\mathcal{B}_\vartheta(\xi)$ also in this case. So we are in situation (c) again.

(ii) \Rightarrow (i). For any $\xi \in \mathbb{S}^2$ with $\text{dist}_{\mathbb{S}^2}(\xi, \gamma(\mathbb{S}^1)) \geq \vartheta$ and with (a), or (b), or (c) we infer the existence of a point $p_\xi \in \gamma(\mathbb{S}^1)$ with $\text{dist}_{\mathbb{S}^2}(\xi, p_\xi) = \vartheta$. Hence

$$\mathbb{S}^2 \subset \overline{\mathcal{T}_\vartheta(\gamma)} \subset \mathbb{S}^2,$$

which implies

$$4\pi = \mathcal{V}(\overline{\mathcal{T}_\vartheta(\gamma)}) = \mathcal{V}(\mathcal{T}_\vartheta(\gamma)).$$

□

Lemma 3.22 (Characteristic patterns of sphere filling curves I). *Let $\gamma : \mathbb{S}^1 \rightarrow \mathbb{S}^2$ be a closed rectifiable continuous curve with positive thickness $\Theta := \Delta[\gamma] > 0$, $\vartheta := \arcsin \Theta \leq \pi/2$ such that $\mathcal{V}(\mathcal{T}_\vartheta(\gamma)) = 4\pi$. Suppose that there is a plane $E \subset \mathbb{R}^3$ containing $0 \in \mathbb{R}^3$ such that*

$$k := \sharp(E \cap \gamma(\mathbb{S}^1)) < \infty.$$

Moreover, assume that the intersection

$$\{p_1, \dots, p_k\} := E \cap \gamma(\mathbb{S}^1)$$

satisfies

- (i) $\text{dist}_{\mathbb{S}^2}(p_l, p_{l+1}) = 2\vartheta$ for all $l = 1, \dots, k$, where we set $p_{k+1} := p_1$,
- (ii) γ intersects E orthogonally at each point p_l , $l = 1, \dots, k$.

Then $k = 2n$ for some $n \in \mathbb{N}$, and $\gamma(\mathbb{S}^1)$ contains a semicircle of (Euclidean) radius Θ in each of the two half-spaces bounded by E .

Proof. The positive thickness Θ guarantees that γ is simple, and since γ is also closed, we find that k is even and write $k =: 2n$ for some $n \in \mathbb{N}$.

E cuts the sphere \mathbb{S}^2 into two hemispheres \mathbb{S}^w and \mathbb{S}^e (both taken to be relatively closed in \mathbb{S}^2). It suffices to give the argument for \mathbb{S}^w .

Every intersection point $p_l \in E \cap \gamma(\mathbb{S}^1)$ is connected by the curve γ within \mathbb{S}^w to some other intersection point $p_m \in E \cap \gamma(\mathbb{S}^1)$, $l \neq m$. Since \mathbb{S}^w is homeomorphic to a flat disk and γ is simple, we find two distinct points $p_i, p_j \in E \cap \gamma(\mathbb{S}^1)$ with $\text{dist}_{\mathbb{S}^2}(p_i, p_j) = 2\vartheta$ such that the closed sub-arc $\tilde{\gamma} \subset \mathbb{S}^w \cap \gamma$ connecting p_i and p_j within \mathbb{S}^w satisfies $\tilde{\gamma} \cap E = \{p_i, p_j\}$.

We consider the geodesic ball $\mathcal{B}_\vartheta(\xi)$ that contains p_i and p_j as antipodal points in its boundary $\partial\mathcal{B}_\vartheta(\xi)$. Since γ intersects E orthogonally in p_i and p_j it is tangent to $\partial\mathcal{B}_\vartheta(\xi)$ in p_i and p_j . The spherical torus property (ST) (see Remark 3.8) implies that

$$\gamma(\mathbb{S}^1) \cap \mathcal{B}_\vartheta(\xi) = \emptyset. \tag{3.29}$$

If $\tilde{\gamma} \cap \partial\mathcal{B}_\vartheta(\xi) \setminus \{p_i, p_j\} \neq \emptyset$ then there is (at least) one point $q \in \tilde{\gamma} \cap \partial\mathcal{B}_\vartheta(\xi)$ with

$$0 < \text{dist}_{\mathbb{S}^2}(q, p_i) < 2\vartheta \quad \text{and} \quad 0 < \text{dist}_{\mathbb{S}^2}(q, p_j) < 2\vartheta,$$

so that we can apply Proposition 3.20 to p_i and q , and to p_j and q , to find that $\gamma(\mathbb{S}^1)$ contains the closed semicircle $\partial\mathcal{B}_\vartheta(\xi) \cap \mathbb{S}^w$, which has Euclidean radius $\Theta = \sin \vartheta$, and we are done.

If $\tilde{\gamma} \cap \partial\mathcal{B}_\vartheta(\xi) = \{p_i, p_j\}$ we argue as follows. For an arbitrary $q \in \tilde{\gamma}$ we consider the unit speed geodesic $\eta_q : [0, 2\pi] \rightarrow \mathbb{S}^2$ starting in q perpendicularly to $\tilde{\gamma}$, i.e. with

$$\eta_q(0) = q, \quad \eta'_q(0) \perp \gamma \text{ at } q, \quad |\eta'_q| \equiv 1 \text{ on } [0, 2\pi],$$

so that for $0 < \varepsilon \ll 1$ the point $\eta_q(\varepsilon)$ is contained in the open spherical region $\mathcal{R} \subset \mathbb{S}^2$ bounded by the curve $\tilde{\gamma} \cup (\partial\mathcal{B}_\vartheta(\xi) \cap \mathbb{S}^e)$. Notice first that $\eta_{p_i}(2\vartheta) = p_j$, $\eta_{p_j}(2\vartheta) = p_i$, and also that $\mathcal{R} \cap \gamma(\mathbb{S}^1) = \emptyset$ by our choice of the points p_i, p_j , and by (3.29).

We infer from the spherical torus property (ST) as before that for $q \in \tilde{\gamma}$ we have

$$\gamma(\mathbb{S}^1) \cap \mathcal{B}_\vartheta(\eta_q(\vartheta)) = \emptyset. \quad (3.30)$$

Relation (3.30) readily implies

$$\mathcal{B}_\vartheta(\eta_q(\vartheta)) \subset \mathcal{R} \quad \text{for all } q \in \tilde{\gamma}. \quad (3.31)$$

Since $\mathcal{V}(\mathcal{T}_\vartheta(\gamma)) = 4\pi$, we obtain by Lemma 3.21 either

$$\partial\mathcal{B}_\vartheta(\eta_q(\vartheta)) \cap \gamma(\mathbb{S}^1) = \{q, \eta_q(2\vartheta)\} \quad (\text{antipodal points}), \quad (3.32)$$

a case which will be excluded later, or (in case (b) or (c) of Lemma 3.21) $\gamma(\mathbb{S}^1)$ contains a semicircle

$$S_q := \partial\mathcal{B}_\vartheta(\eta_q(\vartheta)) \cap \gamma(\mathbb{S}^1) \ni q$$

of spherical radius ϑ and therefore of Euclidean radius $\Theta = \sin \vartheta$.

In that case we have

$$S_q \cap \mathbb{S}^w \subset \tilde{\gamma} \quad (3.33)$$

because $\tilde{\gamma}$ is the connected sub-arc of $\gamma \cap \mathbb{S}^w$ containing the point q .

We claim that

$$S_q \cap (\mathbb{S}^e \setminus E) = \emptyset, \quad (3.34)$$

which means $S_q \subset \mathbb{S}^w$, i.e. the conclusion of the proof.

To show (3.34) we assume that there is some point $\tilde{q} \in S_q \cap (\mathbb{S}^e \setminus E)$, which implies that $p_i \in S_q$ or $p_j \in S_q$ by (3.33) and by connectivity of S_q and $\tilde{\gamma}$ whose endpoints are p_i and p_j . Relation (3.29) implies that S_q is tangent to $\partial\mathcal{B}_\vartheta(\xi)$ at p_i or p_j . For S_q is a semicircle of spherical radius ϑ we have either $S_q \subset \partial\mathcal{B}_\vartheta(\xi)$ contradicting the fact that $q \notin \partial\mathcal{B}_\vartheta(\xi)$, or

$$\partial\mathcal{B}_\vartheta(\xi) \cap \partial\mathcal{B}_\vartheta(\eta_q(\vartheta)) = \{p_i\} \quad \text{or} \quad = \{p_j\}.$$

In that case we conclude with (3.30) that $\eta_q(\vartheta) \notin \mathcal{R}$ contradicting (3.31), which proves (3.34).

Finally we need to exclude option (3.32) to finish the whole proof. Since positive thickness $\Theta = \Delta[\gamma]$ implies that the arc-length parametrisation of γ is of class $C^{1,1}$, in particular that the tangent vector is continuous, we infer that the antipodal mapping

$$f : \tilde{\gamma} \longrightarrow \mathbb{S}^2, \quad q \mapsto f(q) := \eta_q(2\vartheta)$$

is continuous. Moreover, $f(q) \in \tilde{\gamma}$ for all $q \in \tilde{\gamma}$, which can be seen as follows. According to (3.32) we have $f(q) \in \gamma(\mathbb{S}^1)$ which yields by (3.29) the relation $f(q) \notin \mathcal{B}_\vartheta(\xi)$. This together with (3.31) implies that

$$f(q) \in \left[\partial\mathcal{B}_\vartheta(\xi) \cap \mathbb{S}^e \right] \cup \left[\mathbb{S}^w \cap \overline{\mathcal{R}} \right],$$

where $\overline{\mathcal{R}}$ denotes the relative closure of \mathcal{R} as a subset of \mathbb{S}^2 . If, however, $f(q)$ were contained in $\partial\mathcal{B}_\vartheta(\xi) \cap \mathbb{S}^e$ then we could conclude by (3.29) that γ is tangent to $\partial\mathcal{B}_\vartheta(\xi)$ in $f(q)$, which implies that q as the antipodal point of $f(q)$ is also contained in $\partial\mathcal{B}_\vartheta(\xi)$, a contradiction.

Therefore $f(q) \in \mathbb{S}^w \cap \overline{\mathcal{R}}$. Since $f(q) \in \gamma(\mathbb{S}^1)$ and since

$$\gamma(\mathbb{S}^1) \cap [\mathbb{S}^w \cap \overline{\mathcal{R}}] = \tilde{\gamma}$$

we have shown that f is a continuous mapping from $\tilde{\gamma}$ to $\tilde{\gamma}$, and we may apply Brouwer's fixed point theorem to infer the existence of a point $q^* \in \tilde{\gamma}$ with

$$\eta_{q^*}(2\vartheta) = f(q^*) = q^* = \eta_{q^*}(0),$$

which would imply

$$2\vartheta = 2\pi \tag{3.35}$$

because η_{q^*} parametrises a great circle on \mathbb{S}^2 with unit speed. But (3.35) is absurd since we assumed $\vartheta \leq \pi/2$. \square

Lemma 3.23 (Characteristic patterns of sphere filling curves II). *Let $\gamma : \mathbb{S}^1 \rightarrow \mathbb{S}^2$ be a closed rectifiable continuous curve with positive thickness $\Theta := \Delta[\gamma] > 0$, $\vartheta := \arcsin \Theta \leq \pi/2$ such that $\mathcal{V}(\mathcal{T}_\vartheta(\gamma)) = 4\pi$. Suppose that there is a point $\xi \in \mathbb{S}^2$ such that the intersection $\partial\mathcal{B}_\vartheta(\xi) \cap \gamma(\mathbb{S}^1)$ contains an open semicircle S , and let $\mathbb{S}^w \subset \mathbb{S}^2$ be the hemisphere containing S such that $\partial\mathbb{S}^w$ intersects $\partial\mathcal{B}_\vartheta(\xi)$ orthogonally. Then there exists an $n \in \mathbb{N}$ such that $\vartheta = \pi/(2n)$, and*

$$\gamma(\mathbb{S}^1) \cap \mathbb{S}^w = \bigcup_{i=1}^n \partial\mathcal{B}_{(2i-1)\vartheta}(\xi) \cap \mathbb{S}^w. \tag{3.36}$$

In other words, if γ contains one semicircle $S = \mathbb{S}^w \cap \partial\mathcal{B}_\vartheta(\xi)$, then $\gamma(\mathbb{S}^1) \cap \mathbb{S}^w$ consists of a whole stack of latitudinal semicircles with mutual spherical distance 2ϑ .

Proof. If $\vartheta = \pi/2$ we find $n = 1$ and $\gamma(\mathbb{S}^1) = \partial\mathcal{B}_\vartheta(\xi)$ is the only admissible curve, and (3.36) follows.

For $\vartheta \in (0, \pi/2)$ there exists $n = n(\vartheta) \in \mathbb{N} \setminus \{1\}$ so that

$$\vartheta \in \left[\frac{\pi}{2n}, \frac{\pi}{2(n-1)} \right).$$

We will show that $\vartheta = \pi/(2n)$ and that (3.36) holds. Notice first that the spherical torus property (ST) (see Remark 3.4) applied to any point $q \in S_1 := S$ implies

$$\gamma(\mathbb{S}^1) \cap \mathcal{B}_\vartheta(\xi) = \emptyset. \tag{3.37}$$

For an arbitrary point $p \in S_1$ consider the unit speed geodesic $\eta_p : [0, 2\pi] \rightarrow \mathbb{S}^2$ starting in p in the direction orthogonal to S_1 , i.e. with

$$\eta_p(0) = p, \quad \eta'_p(0) \perp S_1 \text{ at } p, \quad |\eta'_p| \equiv 1 \text{ on } [0, 2\pi],$$

so that for all $s \in (0, 2\pi - 2\vartheta)$ the point $\eta_p(s)$ is contained in the open region $\mathbb{S}^2 \setminus \overline{\mathcal{B}_\vartheta(\xi)}$. Hence S_1 and therefore γ is tangent to the geodesic circle $\partial\mathcal{B}_\vartheta(\eta_p(\vartheta))$ in the point p . This implies by means of the spherical torus property (ST)

$$\mathcal{B}_\vartheta(\eta_p(\vartheta)) \cap \gamma(\mathbb{S}^1) = \emptyset \quad \text{for all } p \in S_1. \quad (3.38)$$

According to Lemma 3.21 there is at least one point

$$\tilde{p} \in \partial\mathcal{B}_\vartheta(\eta_p(\vartheta)) \cap \gamma(\mathbb{S}^1) \setminus \{p\}.$$

If \tilde{p} is not antipodal to p on $\partial\mathcal{B}_\vartheta(\eta_p(\vartheta))$, i.e. if $\tilde{p} \neq \eta_p(2\vartheta)$, then p and \tilde{p} are contained in a closed semicircle by virtue of options (b) and (c) in Lemma 3.21. Therefore we find a point

$$q \in \partial\mathcal{B}_\vartheta(\eta_p(\vartheta)) \cap \gamma(\mathbb{S}^1) \setminus \{p\}$$

sufficiently close to p such that the unit speed geodesic $\tau_q : [0, 2\pi] \rightarrow \mathbb{S}^2$ with $\tau_q(0) = q$, $\tau_q'(0) \perp \partial\mathcal{B}_\vartheta(\eta_p(\vartheta))$ at q , $\tau_q(s) \in \mathbb{S}^2 \setminus \overline{\mathcal{B}_\vartheta(\eta_p(\vartheta))}$ for all $s \in (0, 2\pi - 2\vartheta)$, intersects S_1 sufficiently early, i.e., such that

$$\tau_q(\sigma) \in S_1 \subset \gamma(\mathbb{S}^1) \quad \text{for some } \sigma \in (0, \vartheta).$$

But this implies

$$\gamma(\mathbb{S}^1) \cap \mathcal{B}_\vartheta(\tau_q(\vartheta)) \neq \emptyset$$

contradicting the spherical torus property (ST) at the point $q \in \gamma(\mathbb{S}^1)$. Hence we have shown that

$$\partial\mathcal{B}_\vartheta(\eta_p(\vartheta)) \cap \gamma(\mathbb{S}^1) = \{p, \eta_p(2\vartheta)\} \quad \text{for all } p \in S_1.$$

Since S_1 is a semicircle contained in $\partial\mathcal{B}_\vartheta(\xi)$ the set

$$S_2 := \bigcup_{p \in S_1} \eta_p(2\vartheta) \subset \gamma(\mathbb{S}^1)$$

is an open semicircle contained in $\partial\mathcal{B}_{3\vartheta}(\xi)$ unless $\vartheta = \pi/3$ (hence $n = 2$) in which case S_2 degenerates to a single point, namely the antipodal point $\bar{\xi}$ of ξ . But this is absurd taking (3.38) into account, since γ is a closed curve with a continuous tangent.

We proceed with this construction by setting

$$S_i := \bigcup_{p \in S_1} \eta_p(2(i-1)\vartheta) \quad \text{for } i = 3, \dots, n,$$

and we have

$$\eta_p'(2(i-2)\vartheta) \perp S_{i-1} \quad \text{at the points } \eta_p(2(i-2)\vartheta) \quad \text{for } i = 3, \dots, n,$$

so that for all $s \in (2(i-2)\vartheta, 2\pi - 2(i-2)\vartheta)$ the point $\eta_p(s)$ is contained in $\mathbb{S}^2 \setminus \overline{\mathcal{B}_{2(i-2)\vartheta}(\xi)}$. Hence S_{i-1} and therefore γ is tangent to each of the geodesic circles $\partial\mathcal{B}_\vartheta(\eta_p((2i-3)\vartheta))$ in the point $\eta_p(2(i-2)\vartheta)$ for $i = 3, \dots, n$, which implies by means of the spherical torus property (ST)

$$\mathcal{B}_\vartheta(\eta_p((2i-3)\vartheta)) \cap \gamma(\mathbb{S}^1) = \emptyset \quad \text{for all } p \in S_1, i = 3, \dots, n. \quad (3.39)$$

Using Lemma 3.21 as before we can prove for each $p \in S_1$ that

$$\partial\mathcal{B}_\vartheta(\eta_p((2i-3)\vartheta)) \cap \gamma(\mathbb{S}^1) = \{\eta_p(2(i-2)\vartheta), \eta_p((2i-2)\vartheta)\} \quad \text{for } i = 3, \dots, n.$$

Each of the sets S_i , is an open semicircle contained in $\partial\mathcal{B}_{(2i-1)\vartheta}(\xi) \cap \mathbb{S}^w$, $i = 1, \dots, n-1$, since

$$\vartheta + (2i-2)\vartheta \leq (2n-3)\vartheta < \frac{2n-3}{2n-2}\pi < \pi \quad \text{for all } i = 1, \dots, n-1.$$

If $\vartheta = \pi/(2n-1)$ then S_n degenerates to a single point (since $\vartheta + (2n-2)\vartheta = \pi$) which contradicts (3.39) for $i = n$ in combination with the fact that γ is closed and has a continuous tangent.

If $\vartheta \in (\pi/(2n-1), \pi/(2n-2))$ then $\vartheta + (2n-2)\vartheta = (2n-1)\vartheta > \pi$, so that $S_n \subset \mathbb{S}^e$ is an open semicircle of spherical radius $(2n-1)\vartheta - \pi < \vartheta$ about the antipodal point $\bar{\xi}$ of ξ , contradicting the definition of thickness $\Theta = \Delta[\gamma] = \sin \vartheta$.

If $\vartheta \in (\pi/(2n), \pi/(2n-1))$ then $\vartheta + (2n-2)\vartheta < \pi$, hence $S_n \subset \mathbb{S}^w$ is an open semicircle of spherical radius $\pi - (2n-1)\vartheta < \vartheta$ about $\bar{\xi}$, again contradicting the definition of thickness.

The only remaining angle is $\vartheta = \pi/(2n)$, so that $S_n \subset \mathbb{S}^w$ is an open semicircle of spherical radius $\pi - (2n-1)\vartheta = \pi/(2n)$ about $\bar{\xi}$, and we have (3.36) in virtue of (3.39), if we add the endpoints of the open semicircles S_i , $i = 1, \dots, n$, using the continuity of γ . \square

Finally we conclude this section with the

Proof of Theorem 3.5. If $\vartheta = \pi/2$ we find $n = 1$, and the only possible solution is the equator $\beta^{1,0}$, and we are done.

For $\vartheta \in (0, \pi/2)$ there is $k = k(\vartheta) \in \mathbb{N} \setminus \{1, 2\}$ such that $2(k-1)\vartheta < 2\pi \leq 2k\vartheta$.

First we are going to prove that there is a closed semicircle S contained in $\gamma(\mathbb{S}^1)$. For this purpose we fix $p \in \gamma(\mathbb{S}^1)$ and define $\eta_p : [0, 2\pi] \rightarrow \mathbb{S}^2$ to be the unit speed geodesic starting in p in a direction orthogonal to γ , i.e. with

$$\eta_p(0) = p, \quad \eta'_p(0) \perp \gamma \text{ at } p, \quad |\eta'_p| \equiv 1 \text{ on } [0, 2\pi].$$

The torus property (T) applied to p implies

$$\gamma(\mathbb{S}^1) \cap \mathcal{B}_\vartheta(\eta_p(\vartheta)) = \emptyset. \quad (3.40)$$

According to Lemma 3.21 either $\eta_p(2\vartheta) \notin \gamma(\mathbb{S}^1)$ in which case p is contained in a closed semicircle $S \subset \mathcal{B}_\vartheta(\eta_p(\vartheta))$ with

$$S \subset \gamma(\mathbb{S}^1), \quad (3.41)$$

or $\eta_p(2\vartheta) \in \gamma(\mathbb{S}^1)$. In the latter case (3.40) implies that γ is tangent to $\partial\mathcal{B}_\vartheta(\eta_p(\vartheta))$, i.e.

$$\eta'_p(2\vartheta) \perp \gamma \text{ at } \eta_p(2\vartheta).$$

In this way we investigate the whole collection of balls

$$\mathcal{B}_\vartheta(\eta_p((2i-1)\vartheta)) \quad \text{for } i = 1, \dots, k,$$

and we claim that *either we find a closed semicircle S on one of the geodesic circles $\partial\mathcal{B}_\vartheta(\eta_p((2i-1)\vartheta))$, $i = 1, \dots, k$, or $\vartheta = \pi/k$, and*

$$\eta_p(2i\vartheta) \in \gamma(\mathbb{S}^1), \quad \eta_p(2k\vartheta) = p, \quad \eta'_p(2i\vartheta) \perp \gamma \text{ at } \eta_p(2i\vartheta) \quad (3.42)$$

for $i = 1, \dots, k$. But (3.42) describes exactly the situation assumed in Lemma 3.22 so that we can conclude the existence of a closed semicircle S of spherical radius ϑ in each of the two hemispheres bounded by $\eta_p([0, 2\pi])$.

To prove the claim we assume that none of the circles $\partial\mathcal{B}_\vartheta(\eta_p((2i-1)\vartheta))$, $i = 1, \dots, k$, contains a closed semicircle $S \subset \gamma(\mathbb{S}^1)$. Then we can apply Lemma 3.25 and the torus property successively – as demonstrated once above for $i = 1$ – to conclude that

$$\gamma(\mathbb{S}^1) \cap \bigcup_{i=1}^k \mathcal{B}_\vartheta(\eta_p((2i-1)\vartheta)) = \emptyset. \quad (3.43)$$

This implies that $2\pi = 2k\vartheta$ since the inequality

$$(2k-2)\vartheta < 2\pi < 2k\vartheta$$

leads to a contradiction: If $(2k-1)\vartheta \geq 2\pi$ then $(2k-1)\vartheta - 2\pi < \vartheta$ which implies

$$p \in \mathcal{B}_\vartheta((2k-1)\vartheta) \quad (3.44)$$

contradicting (3.43). If $(2k-1)\vartheta < 2\pi$ then $2\pi - (2k-1)\vartheta < \vartheta$ which leads to (3.44) as well, again contradicting (3.43). Hence we have shown $\vartheta = \pi/k$ and the properties (3.42) follows from our construction. As in the proof of Lemma 3.22 we find $k = 2n$ for some $n \in \mathbb{N} \setminus \{1\}$ since γ is simple and closed.

Having established the existence of a closed semicircle S contained in the set $\gamma(\mathbb{S}^1) \cap \mathcal{B}_\vartheta(\eta_p((2j-1)\vartheta))$ for (at least) one $j \in \{1, \dots, 2n\}$ we can use Lemma 3.23 to conclude that

$$\gamma(\mathbb{S}^1) \cap \mathbb{S}^w = \bigcup_{i=1}^n \partial\mathcal{B}_{(2i-1)\vartheta}(\eta_p((2j-1)\vartheta)) \cap \mathbb{S}^w,$$

where \mathbb{S}^w denotes the closed hemisphere containing S such that $\partial\mathbb{S}^w$ intersects the circle $\partial\mathcal{B}_\vartheta(\eta_p((2j-1)\vartheta))$ orthogonally.

With that knowledge we observe that the intersection $\gamma(\mathbb{S}^1) \cap \partial\mathbb{S}^w$ consists of $2n$ equidistant points in which γ intersects the plane containing \mathbb{S}^w orthogonally. Therefore Lemma 3.22 is applicable to conclude the existence of an open semicircle S^* of spherical radius ϑ contained in $\gamma(\mathbb{S}^1) \cap \mathbb{S}^e$, where $\mathbb{S}^e := \overline{\mathbb{S}^2} \setminus \mathbb{S}^w$. Again by Lemma 3.23 one finds that also

$$\gamma(\mathbb{S}^1) \cap \mathbb{S}^e = \bigcup_{i=1}^n \partial\mathcal{B}_{(2i-1)\vartheta}(\xi) \cap \mathbb{S}^e \quad \text{for some } \xi \in \mathbb{S}^e.$$

But we have shown in Section 3.1 that the only possible closed and simple curves made of two stacks of equidistant latitudinal semicircles are the curves $\beta^{n,k}$. \square

3.4 Open Curves

We now indicate that a similar construction is also possible for open curves. A tubular neighbourhood of an open curve γ in \mathbb{R}^3 consists of three parts: A half-ball cap at the beginning and end of the curve and a middle part, consisting of the disjoint union of normal discs of given radius centred at the curve.

Problem (P'). *Given a constant $\Omega \in (0, 1]$ find a curve γ_Ω in the class*

$$\mathcal{C}'_\Omega := \{\gamma \in C^{1,1}(I, \mathbb{R}^3) : |\gamma| = 1 \text{ \& } |\gamma'| > 0 \text{ on } I, \Delta[\gamma] \geq \Omega, |\gamma(1) - \gamma(0)| \geq 2\Omega\}$$

with $I = [0, 1]$ such that $\mathcal{L}[\gamma_\Omega] = \sup_{\mathcal{C}'_\Omega} \mathcal{L}$.

With only slight modifications using the additional assumption on the endpoints of the curves in competition, one can prove as in Theorem 3.1 the existence of solutions for Problem (P') for any given $\Omega \in (0, 1]$. Here, the crucial $C^{1,1}$ -estimate from [GMSvdM02, Lemma 2] for closed curves leading to (3.18) in the proof of Theorem 3.1 is replaced by the corresponding $C^{1,1}$ -estimate proved in [Ge04, Satz 2.14] for open curves.

A variant of Proposition 3.11 (Hotelling's theorem) for open curves implies that the volume of the middle part is again proportional to the length of the curve, while the volume of the caps stays fixed for fixed radius.

For certain values $\omega_m = \pi/m$, $2 \leq m \in \mathbb{N}$, of spherical thickness one can perform a similar construction as in the case of closed curves. There are in fact two slightly different situations, depending on whether m is even or odd (see Figure 3.7 on page 60 for examples).

- (i) For m even, consider $m/2$ semicircles with spherical distance $2\omega_m$ stacked up on the western hemisphere as described in the introduction. For the eastern hemisphere we take the north pole as a single point, together with $m/2 - 1$ stacked up semicircles with spherical distance $2\omega_m$, and finally the south pole as a second single point. After turning the eastern hemisphere by the angle ω_m all endpoints of the western semicircles match with the semicircle endpoints and the two single points on the eastern hemisphere. Turning further by the amount of $k \cdot 2\omega_m$, $k \in \{0, \dots, m/2 - 1\}$, one can try to construct a single open connected curve $\alpha^{m,k}$. Note that the first member of this family (for $m = 2, k = 0$) is a semi great circle, which is easily seen to be the unique solution for thickness $\omega_2 = \pi/2$.
- (ii) For m odd, start with a single point C_0 in the north pole, then stack up $(m-1)/2$ circles C_i of spherical radius $2\omega_m$ around the north pole with the last circle C_{m-1} around the south pole of spherical radius ω_m . The discontinuous curve has a tubular neighbourhood of spherical thickness ω_m (note that the neighbourhood about the point C_0 is just a geodesic ball). Next cut the sphere along a longitude (cutting C_0 in two 'half-points') and turn by $k \cdot 2\omega_m$. We denote this possibly discontinuous curve again by $\alpha^{m,k}$.

As in the proof of Lemma 3.6 one can show that the tubular neighbourhood remains a tubular neighbourhood of the same spherical radius after the turning process and the neighbourhoods of the 'half-points' form the spherical caps about the endpoints of the curve. To investigate under which circumstances the resulting curves $\alpha^{m,k}$ constitute one open connected arc we use the same algebraic methods as in Section 3.1.

Lemma 3.24. *For every even $m \in \mathbb{N}$ and $k \in \{0, \dots, m/2 - 1\}$ with $\gcd(2k - 1, m) = 1$ the appropriately re-parametrised curve $\alpha^{m,k} : I \rightarrow \mathbb{S}^2$ is a connected open, piecewise circular curve whose constant speed parametrisation is of class $C^{1,1}(I, \mathbb{R}^3)$ satisfying*

$$\Delta[\alpha^{n,k}] = \Omega_m = \sin \omega_m = \sin \frac{\pi}{m}.$$

Moreover, for distinct $k_1, k_2 \in \{0, \dots, m/2 - 1\}$ the curves α^{m,k_1} and α^{m,k_2} are not congruent. There are $\varphi(m)$ distinct open connected curves for each m .

Proof. As mentioned above only the algebraic arguments need to be adjusted to the present situation of open curves. Set $n := m/2 \in \mathbb{N}$. First consider the western hemisphere \mathbb{S}^w and number the $2n$ endpoints of the (all proper) semicircles counter-clockwise from 0 to $2n - 1$, such that checkpoint number i and $2n - i - 1$ correspond to the i -th semicircle ($i = 0, \dots, n - 1$); see Figure 3.4. For the eastern hemisphere \mathbb{S}^e number the points from 0 to $2n - 1$, where 0 and n correspond to the single points, while i and $2n - i$ correspond to the endpoints of the i -th semicircle ($i = 1, \dots, n - 1$). When turning the hemisphere \mathbb{S}^e by multiples of $2\omega_{2n}$ the curve closes again in a nice C^1 -fashion (note that \mathbb{S}^e was already turned once by ω_{2n} to align the endpoints during construction). Since there are only two endpoints, we will arrive at one open curve and possible several closed curves.

The semicircles on \mathbb{S}^w connect the checkpoints to n pairs, which is a permutation on the checkpoints

$$w(i) \equiv -i - 1 \pmod{2n},$$

so if we pass through checkpoint i along the curve we will next pass through checkpoint $w(i)$. Similarly the eastern hemisphere defines

$$e(i) \equiv -i \pmod{2n}.$$

The twist by $k \cdot 2\omega_n$ is again described by

$$t^k(i) \equiv i + k \pmod{2n}.$$

As we pass along the curve $\alpha^{m,k}$ we run alternately through the semicircles on each hemisphere. If we just entered a hemisphere through checkpoint i we will enter it the next time at the checkpoint $q(i) := t^{-k} \circ e \circ t^k \circ w(i)$. For q we find the formula

$$q(i) \equiv t^{-k} \circ e \circ t^k \circ w(i) \equiv -((-i - 1) + k) - k \equiv i - (2k - 1) \pmod{2n}$$

and after l steps

$$q^l(i) \equiv i - (2k - 1)l \pmod{2n}.$$

In order to see whether $\alpha^{m,k}$ is one connected open curve, we start at checkpoint 0 (which is one end) and note through which checkpoints we pass. The run has to be reflected at the other endpoint, so that we pass through the curve in two directions, passing each checkpoint on the component, not only even or odd ones like in Lemma 3.6. So $\alpha^{m,k}$ is one connected open curve if and only if q consists of one cycle of length $2n$. By Lemma 3.7 this is the case if and only if $\gcd(2k - 1, 2n) = 1$.

To count the solutions, note that $\gcd(2k, 2n) \geq 2$ and therefore

$$\begin{aligned} \#\{k \in \{1, \dots, n\} : \gcd(2k - 1, 2n) = 1\} &= \\ \#\{k \in \{1, \dots, 2n - 1\} : \gcd(k, 2n) = 1\} &= \varphi(m). \end{aligned} \tag{3.45}$$

Each of the $\alpha^{m,k}$ is easily seen to be unique up to rigid motions. \square

Lemma 3.25. *For every odd $m \in \mathbb{N}$ and $k \in \{0, \dots, m-1\}$ with $\gcd(2k, m) = 1$ the appropriately re-parametrised curve $\alpha^{m,k} : I \rightarrow \mathbb{S}^2$ is a connected open, piecewise circular curve whose constant speed parametrisation is of class $C^{1,1}(I, \mathbb{R}^3)$ satisfying*

$$\Delta[\alpha^{n,k}] = \Omega_m = \sin \omega_m = \sin \frac{\pi}{m}.$$

Moreover, for distinct $k_1, k_2 \in \{0, \dots, m-1\}$ the curves α^{m,k_1} and α^{m,k_2} are not congruent. There are $\varphi(m)$ distinct open connected curves for each m .

Proof. Set $n := (m-1)/2 \in \mathbb{N}$. Like in the proof of Lemma 3.24 we check the order in which the curve passes certain checkpoints and if we can reach every checkpoint in one run.

First consider the western hemisphere \mathbb{S}^w and number the $2n+1$ endpoints of the semicircles counter-clockwise from 0 to $2n$, such that the checkpoint numbers i and $2n+1-i$ correspond to the i -th semicircle ($i = 1, \dots, n-1$) and $i = 0$ corresponds to the single point. When turning the hemisphere \mathbb{S}^e by multiples of $2\omega_n$ the curve closes again in a nice C^1 -fashion. Since there are only two endpoints, we will end up with at most one open connected curve and possibly several closed curves. In the extreme case $k = 0$ the open curve degenerates to a point and we have n closed circles.

The semicircles and the single point on the western hemisphere act again as a permutation $c(i) \equiv -i \pmod{2n+1}$ on the checkpoints. The turn by $k \cdot 2\omega_n$ is again described by $t^k(i) \equiv i+k \pmod{2n+1}$. As we pass along the curve $\alpha^{m,k}$ we run alternately through the semicircles on each hemisphere. If we just entered a hemisphere through checkpoint i we will enter it the next time at the checkpoint $q(i) := t^{-k} \circ c \circ t^k \circ c(i)$. For q we find the formula

$$q(i) \equiv t^{-k} \circ c \circ t^k \circ c(i) \equiv -((-i) + k) - k \equiv i - 2k \pmod{2n+1}$$

and after l -steps

$$q^l(i) \equiv i - 2kl \pmod{2n+1}.$$

As in the proof of Lemma 3.24 we find that $\alpha^{m,k}$ is one connected open curve if and only if q consists of one cycle of length $m = 2n+1$. By Lemma 3.7 this is the case if and only if $\gcd(2k, 2n+1) = \gcd(2k, m) = 1$. To count the number of solutions, note that $\gcd(2k, 2n+1) = \gcd(k, 2n+1)$ since $2n+1$ is odd and therefore

$$\begin{aligned} \#\{k \in \{1, \dots, m-1\} : \gcd(2k, m) = 1\} &= \\ \#\{k \in \{1, \dots, m-1\} : \gcd(k, m) = 1\} &= \varphi(m). \end{aligned} \tag{3.46}$$

□

Again we can use the fact, that the tubular neighbourhood of $\alpha^{m,k}$ covers the whole sphere to prove that they are the unique solutions:

Lemma 3.26 (Characterisation of open sphere filling curves). *For an open rectifiable continuous curve $\gamma : I \rightarrow \mathbb{S}^2$ with positive thickness $\Omega := \Delta[\gamma] \in (0, 1)$, $\omega := \arcsin \Omega \in (0, \pi/2)$, and with $|\gamma(0) - \gamma(1)| \geq 2\Omega$ the following two statements are equivalent:*

- (i) $\mathcal{V}(\mathcal{T}_\omega(\gamma)) = 4\pi$;

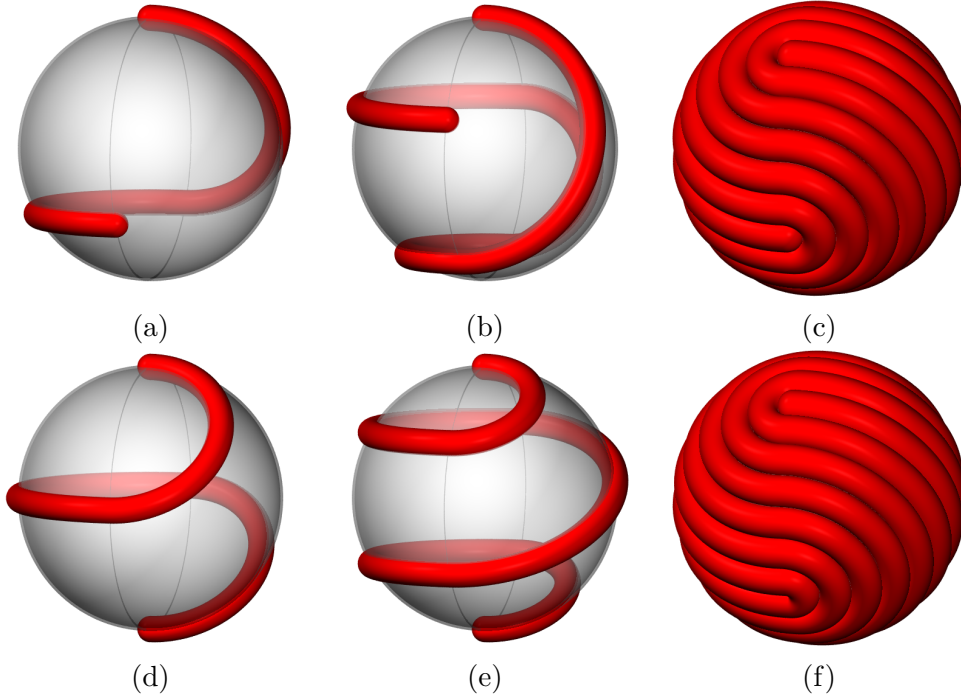


Figure 3.7: Open curves $\alpha^{m,k}$ that maximise length for prescribed thicknesses $\omega_m = \pi/m$: (a) $m = 3, k = 1$; (b) $m = 5, k = 1$; (c) $m = 25, k = 6$; (d) $m = 4, k = 0$; (e) $m = 6, k = 0$; (f) $m = 26, k = 6$. Note that the endpoints of the curve are always antipodal for m even. Only the curves (c) and (f) are depicted with full thickness.

(ii) For any $\xi \in \mathbb{S}^2$ such that $\mathcal{B}_\omega(\xi) \cap \gamma(I) = \emptyset$ one of the following is true:

- (a) $\partial\mathcal{B}_\omega(\xi) \cap \gamma(I) = \{P, Q\}$ with $\text{dist}_{\mathbb{S}^2}(P, Q) = 2\omega$ (antipodal points); γ is tangential to $\partial\mathcal{B}_\omega(\xi)$ in at least one of the points P or Q ;
- (b) $\partial\mathcal{B}_\omega(\xi) \cap \gamma(\mathbb{S}^1) = \{\text{semicircle of spherical radius } \omega\}$.

Proof. The situation for open curves γ differs from that in Proposition 3.20 only in the possibility that apart from γ connecting two points along $\partial\mathcal{B}_\omega(\xi)$ these two points could both be two endpoints of great arcs on γ (cf. [Ge04, Satz 3.27]). However this case can not happen here since we have $|\gamma(1) - \gamma(0)| \geq 2\Omega$.

The cases (ii) \Rightarrow (i) and (i) \Rightarrow (b) and the first part of (a) are proved as in Lemma 3.21. If P or Q is an inner point of γ the tangency is evident. Assume that P and Q are the endpoints of γ both not tangential. Then we could consider the great circle $\eta : (-\pi, \pi) \rightarrow \mathbb{S}^2, \eta(0) = \rho$ intersecting the shorter great arc from P to Q orthogonally in ρ and $\mathcal{B}_{\omega+\epsilon}(\eta(\epsilon))$ would not intersect γ for small $\epsilon > 0$ which would contradict Part (i). \square

Theorem 3.27 (Sphere filling open thick curves). *If $\mathcal{V}(\mathcal{T}_\omega(\gamma)) = 4\pi$ for $\omega \in (0, \pi/2]$ and some open curve $\gamma \in \mathcal{C}'_\Omega$ with $\Omega = \sin \omega \in (0, 1]$, then there is some $m \in \mathbb{N}$ and $k \in \{0, \dots, m/2\}$ with $\text{gcd}(2k-1, m) = 1$ if m is even, or $k \in \{0, \dots, m-1\}$ with $\text{gcd}(2k, m) = 1$ if m is odd, such that*

- (i) $\omega = \omega_m$,
- (ii) $\Delta[\gamma] = \Omega_m$, where $\Omega_m = \sin \omega_m$,
- (iii) $\gamma = \alpha^{m,k}$.

Proof. We will only sketch the proof since for open curves it is slightly easier than for closed curves. Indeed, we have two natural points to start our construction if we equip γ with an orientation, namely the start- and endpoints of the curve. Let $\eta_{p,t}$ be the unit speed great circle going through $\eta_{p,t}(0) = p \in \mathbb{S}^2$ with $\eta'_{p,t} = t \in \mathbb{S}^2$. By Lemma 3.26 we have $\eta_{\gamma(0),t}(2\omega) \in \gamma(I)$ for $t \cdot \gamma'(0) \leq 0$. If $\omega = \pi/2$ then $\eta_{\gamma(0),t}(2\omega) = \gamma(1)$ is the other endpoint, and $\gamma = \alpha^{1,0}$ (otherwise we would have $|\gamma(0) - \gamma(1)| < \Omega$ contradicting the fact that $\gamma \in \mathcal{C}'_\Omega$). If $\omega < \pi/2$ the set $\{\eta_{\gamma(0),t}(2\omega) : t \cdot \gamma'(0) \leq 0, t \in \mathbb{S}^2\}$ will be a semicircle. As in Lemma 3.23 we can continue this process stacking up semicircles until we either arrive at

- (i) a semicircle of spherical radius ω , which implies $\omega = \pi/m$ for some odd $m \in \mathbb{N}$.
- (ii) or a single point, which has to be $\gamma(1)$. This implies $\omega = \pi/m$ for some even $m \in \mathbb{N}$.

In case (i) we can redo the construction with the endpoint and find the two hemispheres each filled with $(m-1)/2$ stacked up semicircles and one single point. Therefore γ must be congruent to $\alpha^{m,k}$ for some odd m and some $k \in \mathbb{N}$. In case (ii) both end caps are contained in one hemisphere, and in the boundary of this hemisphere we find the characteristic pattern, so we can apply Lemma 3.22 and then 3.23 to see that the other hemisphere must consist of stacked up semicircles, so γ is again equivalent to $\alpha^{m,k}$ for an even m and some $k \in \mathbb{N}$. In both cases (i) and (ii) the additional restrictions on k depending on whether m is even or odd are derived in Lemmata 3.24 and 3.25. \square

Chapter 4

Ideal Knots in \mathbb{S}^3

Topological notions concerning knots are largely the same in either \mathbb{R}^3 or \mathbb{S}^3 . However, unlike the \mathbb{R}^3 case, due to its compactness there are multiple natural and different notions of the geometrical idea of ideal knot shape in \mathbb{S}^3 :

- (a) maximise thickness, with length left free,
- (b) fix length and maximise thickness,
- (c) fix thickness and minimise length, and
- (d) fix thickness and maximise length.

In \mathbb{R}^3 due to dilations the notions (a) and (d) are never achieved, and the notions (b) and (c) lead to similar shapes again due to dilations. In \mathbb{S}^3 all notions make sense due to compactness and are (at least in principle) different i.e. can be expected to have different optimal shapes. We did not investigate notion (d) in \mathbb{S}^3 since we dealt extensively with this question in \mathbb{S}^2 in the previous chapter. The most natural notion (a) was considered first in [K02]. We now define the above notions more precisely. Recall from (2.14) on page 16 our choice of admissible curves

$$\mathcal{K} := \{\gamma \in C^1(\mathbb{S}, M) : \Delta[\gamma] > 0, |\gamma'(t)| \equiv \text{const} \forall t \in I\}.$$

Definition 4.1 (Different notions of ideal knots in \mathbb{S}^3). *Let $k \in \mathcal{K}$ be a representative of a tame¹ knot. Define*

$$Q_k := \{\gamma \in C^1(\mathbb{S}, \mathbb{S}^3) : \Delta[\gamma] > 0, |\gamma'(t)| \equiv \text{const} > 0 \forall t \in \mathbb{S}, \gamma \simeq_{\mathbb{S}^3} k\},$$

$$Q_{k,L}^* := \{\gamma \in Q_k : |\gamma'(t)| \equiv L \forall t \in \mathbb{S}\}$$

and

$$Q_{k,\Theta}^+ := \{\gamma \in Q_k : \Delta[\gamma] \geq \Theta\}.$$

(i) We call γ^\dagger ideal if

$$\Delta[\gamma^\dagger] = \sup_{\gamma \in Q_k} \Delta[\gamma].$$

¹In the whole thesis we only consider tame knots. As noted in Remark 2.25 thick knots are necessarily tame.

(ii) Let $L > 0$ be fixed, $|k'(s)| = L$ for all $s \in \mathbb{S}$. We call $\gamma^* \in Q_{k,L}^*$ L -ideal if

$$\Delta[\gamma^*] = \sup_{\gamma \in Q_{k,L}^*} \Delta[\gamma].$$

(iii) Let $\Theta \in (0, 1]$ be fixed, $\Delta[k] \geq \Theta$, and $\mathcal{L}[\gamma] = \int_{\mathbb{S}} |\gamma'(s)| ds$ be the length functional. We call $\gamma^+ \in Q_{k,\Theta}^+$ Θ -ideal if

$$\mathcal{L}[\gamma^+] = \inf_{\gamma \in Q_{k,\Theta}^+} \mathcal{L}[\gamma].$$

In general ideal, L -ideal and Θ -ideal are not the same:

Example 4.2 (L -ideal and Θ -ideal are not the same). In \mathbb{S}^3 great circles maximise thickness $\Delta = 1$. Any three points not on a great circle lie on a circle of radius less than 1. Let k be a parametrisation of a great circle of \mathbb{S}^3 , and let $L > 2\pi$, then the L -ideal knot γ^* in $Q_{k,L}^*$ is not Θ -ideal in $Q_{k,\Theta}^+$, $\Theta := \Delta[\gamma^*]$ because γ^* is longer than the great circle k and strictly thinner.

In \mathbb{S}^3 there are no dilations as in \mathbb{R}^3 . The best we can achieve is a conformal dilation that expands one hemisphere and contracts the other.

Definition 4.3 (Conformal dilation). For $x \in \mathbb{S}^3$ define

$$\text{CD}_r(x) := P^{-1}(rP(x)),$$

where P is the stereographic projection of Definition 2.21.

Lemma 4.4. For an arbitrary knot type, and given length $L > 0$ there exists a representative $k : \mathbb{S} \rightarrow \mathbb{S}^3$ with $\Delta[k] > 0$ and constant speed $|\gamma'| = L$, i.e. Q_k and $Q_{k,L}^*$ are non empty.

Proof. For a given knot type pick a polygonal representative and round off its corners by inscribing small circles without generating self intersections. After constant speed parametrisation it is $C^{1,1}$ and therefore has positive thickness by Lemma 2.2. We call the result k . This shows that Q_k is non-empty.

To construct a representative of a given length L , first construct some thick representative k of the knot type as above. If k is longer than the prescribed L , we project it to \mathbb{R}^3 , scale it down and project it back to \mathbb{S}^3

$$k_\alpha := \text{CD}_\alpha(k).$$

If we take care that k does not pass through the north pole N^∞ , we have the following estimate for the speed (and therefore the length) as $\alpha \rightarrow 0$

$$|k'_\alpha| \leq |\alpha| \underbrace{|DP^{-1}(\alpha P(k))|}_{\rightarrow \text{const}} \underbrace{|DP(k)|}_{\leq \text{const}} \underbrace{|k'|}_{\leq \text{const}} \rightarrow 0,$$

which implies $\mathcal{L}[k_\alpha] \rightarrow 0$ as $\alpha \rightarrow 0$, so k_α attains all lengths between $\mathcal{L}[k]$ and 0. But we can also arbitrarily prolong the curve by gluing in a small patch of a finite step in the generation of the space filling Hilbert curve [Sa94, p. 11] with rounded edges (which become arbitrarily long). By these two steps we find a thick representative k of any length L so $Q_{k,L}^*$ is not empty. \square

Theorem 4.5 (Existence of ideal knots in \mathbb{S}^3). *For any given knot type $k \in \mathcal{K}$:*

(i) *There exists an ideal $\gamma^\dagger \in Q_k$, i.e.*

$$\Delta[\gamma^\dagger] = \sup_{\gamma \in Q_k} \Delta[\gamma].$$

(ii) *For any $L > 0$ there exists an L -ideal $\gamma^* \in Q_{k,L}^*$, i.e.*

$$\Delta[\gamma^*] = \sup_{\gamma \in Q_{k,L}^*} \Delta[\gamma].$$

(iii) *And for any $\Theta \in (0, \Delta[\gamma^\dagger]]$, where γ^\dagger is a solution of (i), there exists a Θ -ideal $\gamma^+ \in Q_{k,\Theta}^+$, i.e.*

$$\mathcal{L}[\gamma^+] = \inf_{\gamma \in Q_{k,\Theta}^+} \mathcal{L}[\gamma].$$

Proof. (i) By Lemma 4.4 the set Q_k is non empty. We define

$$\eta^\dagger := \sup_{\gamma \in Q_k} \Delta[\gamma].$$

By Remark 2.16(i), $1 \geq \eta^\dagger \geq \Delta[k] > 0$. Let $\{\gamma_n\}_n \subset Q_k$ be any maximising sequence such that $\Delta[\gamma_n] \rightarrow \eta^\dagger$. We may assume $\Delta[\gamma_n] \geq \Delta[k] > 0$ for all n . By Lemma 2.30 there exists a subsequence $\{\gamma_{n_i}\}_i$ such that $\gamma_{n_i} \rightarrow \gamma^\dagger$ in $C^1(\mathbb{S}, \mathbb{R}^4)$ for some limit $\gamma^\dagger \in C^1(\mathbb{S}, \mathbb{S}^3)$. Note that the image of γ^\dagger must lie in \mathbb{S}^3 since \mathbb{S}^3 is compact. We have $|\gamma^{\dagger'}(s)| = \text{const} > 0$ for all $s \in \mathbb{S}$ and by Lemma 2.31 $\Delta[\gamma^\dagger] \geq \eta^\dagger$.

It remains to prove that $k \simeq_{\mathbb{S}^3} \gamma^\dagger$. There exists $N^\infty \in \mathbb{S}^3$ with $d_{\mathbb{R}^N}(N^\infty, \gamma^\dagger(\mathbb{S})) = \eta^\dagger$ (see Lemma 2.23). Without loss of generality we may assume N^∞ to be the north-pole of \mathbb{S}^3 . Because of convergence we know that $N^\infty \notin \gamma_{n_i}^\dagger(\mathbb{S})$ for n sufficiently large. Let $P : \mathbb{S}^3 \setminus N^\infty \rightarrow \mathbb{R}^3$ be our stereographic projection. By Lemma 2.22 we have $\Delta[P(\gamma_{n_i})] \geq \Delta[\gamma_{n_i}] \geq \Delta[k] > 0$ and, because P is a diffeomorphism, we have $P(\gamma_{n_i}) \rightarrow P(\gamma^\dagger)$ in $C^1(\mathbb{S}, \mathbb{R}^3)$. After reparametrisation we deduce, by Lemma 2.32, that $P(\gamma_{n_i}) \simeq_{\mathbb{R}^3} P(\gamma^\dagger)$ and therefore, by Lemma 2.26, that $\gamma_{n_i} \simeq_{\mathbb{S}^3} \gamma^\dagger$. Together we have $\gamma^\dagger \in Q_k$. So γ^\dagger is an ideal shape.

(ii) By Lemma 4.4 the set $Q_{k,L}^*$ is non empty. We define

$$\eta^* := \sup_{\gamma \in Q_{k,L}^*} \Delta[\gamma].$$

By Remark 2.16(i) we have $1 \geq \eta^* \geq \Delta[k] > 0$. Let $\{\gamma_n\}_n \subset Q_{k,L}^*$ be any maximising sequence such that $\Delta[\gamma_n] \rightarrow \eta^*$. We may assume $\Delta[\gamma_n] \geq \Delta[k] > 0$ for all n . By Lemma 2.30 we find a subsequence $\{\gamma_{n_i}\}_i$ such that $\gamma_{n_i} \rightarrow \gamma^*$ in $C^1(\mathbb{S}, \mathbb{R}^4)$ for some limit $\gamma^* \in C^1(\mathbb{S}, \mathbb{S}^3)$, and by Lemma 2.31 we have $\Delta[\gamma^*] \geq \eta^*$. To prove that $k \simeq_{\mathbb{S}^3} \gamma^*$ we proceed as in (i). Together we have $\gamma^* \in Q_{k,L}^*$. So γ^* is an L -ideal knot.

(iii) We have $\gamma^\dagger \in Q_{k,\Theta}^+$, so $Q_{k,\Theta}^+$ is non empty. As above we define

$$\eta^+ := \inf_{\gamma \in Q_{k,\Theta}^+} \mathcal{L}[\gamma].$$

By Lemma 2.13 we have $\eta^+ \geq 4\Theta > 0$. We can therefore chose a minimising sequence $\{\gamma_n\}_n \subset Q_{k,\Theta}^+$ such that $\mathcal{L}[\gamma_n] \rightarrow \eta^+$. As above, we find a convergent subsequence $\gamma_{n_i} \rightarrow \gamma^+$ in $C^1(\mathbb{S}, \mathbb{R}^N)$, $\gamma^+ \in Q_{k,\Theta}^+$ and $\mathcal{L}[\gamma^+] = |\gamma^{+'}| = \eta^+$. So γ^+ is Θ -ideal. □

Remark 4.6. (i) The condition $\Theta \in (0, \Delta[\gamma^\dagger]]$ in Theorem 4.5 (iii) is sharp, since any curve in $Q_{k,\Theta}^+$ is a competitor to γ^\dagger .

(ii) Fix some knot type. Define L^\dagger as the supremum of all lengths of ideal shapes. By same methods used in the proof above, we can show that the maximum length is indeed attained. For $L > L^\dagger$ we still find an L -ideal knot γ^* , but it can not be ideal, since it must have $\Delta[\gamma^*] < \Delta[\gamma^\dagger]$ by the definition of L^\dagger .

We can apply the above techniques to compact subsets of \mathbb{R}^3 as well:

Theorem 4.7. Let $C \subset \mathbb{R}^3$ be a compact set and let $k \in C^1(\mathbb{S}, C)$ be a knot in C with $\Delta[k] \geq \Theta > 0$. Then there exists a thickness (length) maximiser $\gamma \in C^1(\mathbb{S}, C)$ (with $\Delta[\gamma] \geq \Delta[k]$), such that $\gamma \simeq_{\mathbb{R}^3} k$.

Proof. Let $\gamma_i \in C^1(\mathbb{S}, C)$ with constant speed $|\gamma_i'| \equiv L_i$, $\Delta[\gamma_i] \geq \Delta[k]$ and $\gamma_i \simeq_{\mathbb{R}^3} k$ be a maximising sequence of Δ (\mathcal{L}). By Lemma 2.30 there exists a convergent subsequence $\{\gamma_{i_j}\}_j$ and a limit γ , such that $\gamma_{i_j} \rightarrow \gamma$ in $C^1(\mathbb{S}, \mathbb{R}^3)$. By compactness of C we have indeed $\gamma \in C^1(\mathbb{S}, C)$. By Lemma 2.31 we have $\Delta[\gamma] \geq \Delta[\gamma_i]$ for all i since it is a thickness maximising sequence. Since the convergence is in C^1 we have

$$\lim_{j \rightarrow \infty} \mathcal{L}[\gamma_{i_j}] = \mathcal{L}[\gamma]$$

and $\mathcal{L}[\gamma] \geq \mathcal{L}[\gamma_i]$ since it is a length maximising sequence. So γ is indeed a maximiser. By Lemma 2.32 we also have $\gamma \simeq_{\mathbb{R}^3} k$ as claimed. □

But for applications open curves are more common, so more work has to be done to treat this case.

Remark 4.8. In \mathbb{R}^3 many authors consider the ropelength $\mathcal{R}[\gamma] = \mathcal{L}[\gamma]/\Delta[\gamma]$, since it reflects the scale-invariance of the shape. We consider it a less natural energy in \mathbb{S}^3 but want to discuss it briefly for completeness.

In \mathbb{S}^3 scaling is more difficult and we expect the family of circles with radius $r \in (0, 1]$, which are the ropelength minimisers of the unknot, to be an exception. Since a lower bound on ropelength does not easily imply a lower bound on thickness, the methods used in this chapter do not carry over.

In fact, it might be possible that while minimising ropelength, the curve contracts to a point and approaches an ideal knot in the tangent space \mathbb{R}^3 . But if such a contraction does not happen, i.e. we are able to show that a ropelength minimiser has at least a certain arc-length, then we get a lower bound on the thickness and we can apply the

methods of this chapter. In this case each ropelength minimiser γ is also L -ideal with $L = \mathcal{L}[\gamma]$ and Θ -ideal with $\Theta = \Delta[\gamma]$. So if we understand the other shapes, we will also understand the shapes of the ropelength minimisers.

4.1 Analysis of Necessary Conditions

Using conformal dilations we derive a necessary condition for ideality of knots in \mathbb{S}^3 .

Theorem 4.9. *Let $\gamma : \mathbb{S} \rightarrow \mathbb{S}^3$ be a thickness-maximising ideal knot. Then γ is not contained in any open geodesic ball $\mathcal{B}_r(x) := \{z \in \mathbb{S}^3 : \text{dist}_{\mathbb{S}^3}(x, z) < r\}$, with $r := \pi/2 - \arcsin \Delta[\gamma]$ and $x \in \mathbb{S}^3$.*

Proof. Assume a ball $\mathcal{B}_r(x)$ exists, such that $\gamma(\mathbb{S}) \subset \mathcal{B}_r(x)$. Without loss of generality $x = S_0$. Set $\varepsilon := \text{dist}_{\mathbb{S}^3}(\gamma(\mathbb{S}), \partial \mathcal{B}_r(x)) > 0$. Then the centres of all circles through three points on $\gamma(\mathbb{S})$ of radius smaller than $(\Delta[\gamma] + \varepsilon/2)$ lie in $\mathcal{B}_{\pi/2}(S_0)$. Therefore, for each such circle C , the image under the conformal dilation (Definition 4.3) $\text{CD}_{1+\delta}(C)$ has a bigger radius for $\delta < \varepsilon/2$, and consequently $\Delta[\text{CD}_{1+\delta}(\gamma)] > \Delta[\gamma]$ for δ sufficiently small, contradicting the maximal thickness of γ . \square

We consider it unlikely that the small circles approaching the thickness of an ideal knot are not completely contained in the spherical ball of above theorem and therefore expect a slightly stronger version to be true:

Conjecture 4.10 (Not contained in hemisphere). *Let $\gamma : \mathbb{S} \rightarrow \mathbb{S}^3$ be a thickness-maximising ideal knot. Then γ is not contained in any ball $\mathcal{B}_{\pi/2}(x)$ with $x \in \mathbb{S}^3$.*

4.2 From \mathbb{S}^3 to \mathbb{R}^3

Consider a series of L -ideal shapes as L goes to 0. The shapes will be contained in a smaller and smaller area of \mathbb{S}^3 that more and more resembles \mathbb{R}^3 . Do the L -ideal shapes approach an ideal shape in the tangent space \mathbb{R}^3 ? The answer is yes as the following theorem shows. Of course we can only expect the convergence of a subsequence since we do not know whether L -ideal shapes are unique.

Theorem 4.11 (Shrinking into the tangent space). *For each $L > 0$, let $\gamma_L : \mathbb{S} \rightarrow \mathbb{S}^3$ be a thickness maximising, constant speed curve with length $|\gamma'_L| = L$ and $\gamma_L(\mathbb{S}) \subset B_L(S_0)$. Define $\bar{\gamma}_L : \mathbb{S} \rightarrow \mathbb{R}^3$ as $P(\gamma_L)/L$ re-parametrised with constant speed, where $P : \mathbb{S}^3 \rightarrow \mathbb{R}^3$ is the stereographic projection from Definition 2.21. Then for any sequence $L_i \searrow 0$ as $i \rightarrow \infty$ a subsequence of $\{\bar{\gamma}_{L_i}\}_i$ converges to an ideal knot (i.e. ropelength-maximiser) $\bar{\gamma} : \mathbb{S} \rightarrow \mathbb{R}^3$ in \mathbb{R}^3 .*

Proof. We first prove

$$L\Delta[\bar{\gamma}_L]/\Delta[\gamma_L] \rightarrow 1 \text{ for } L \rightarrow 0. \quad (4.1)$$

Recall (2.13):

$$R(P(x), P(y), P(z)) = \left| \frac{2}{\cos \alpha + \cos \varrho} \right| R(x, y, z).$$

Since L is an upper bound on the thickness of γ_L we only need to consider small circles close to S_0 and for those the angles α and ϱ go to zero for $L \rightarrow 0$. Therefore the quotient $R/(R \circ P)$ goes to 1, which implies (4.1).

Next, we show

$$L\mathcal{L}[\overline{\gamma}_L]/\mathcal{L}[\gamma_L] \rightarrow 1 \text{ for } L \rightarrow 0. \quad (4.2)$$

$$\begin{aligned} \mathcal{L}[\overline{\gamma}_L] &= \int_{\mathbb{S}} |\overline{\gamma}_L(s)'| ds \\ &= \int_{\mathbb{S}} |(P \circ \gamma_L(s))'|/L ds \\ &= \int_{\mathbb{S}} \underbrace{|DP(\gamma_L(s)) \frac{\gamma_L(s)'}{L}|}_{\approx |\frac{\gamma_L(s)'}{L}|} ds \rightarrow 1 \quad \text{for } L \rightarrow 0, \end{aligned}$$

which proves the above statement. Note that we did not use the optimality of γ_L so far. The above claims rely only on positive thickness and being close enough to S_0 . Combining (4.1) and (4.2) yields

$$\frac{\Delta[\overline{\gamma}_L]}{\mathcal{L}[\overline{\gamma}_L]} / \frac{\Delta[\gamma_L]}{\mathcal{L}[\gamma_L]} \rightarrow 1 \text{ for } L \rightarrow 0. \quad (4.3)$$

Let $\overline{\gamma}^* : \mathbb{S} \rightarrow \mathbb{R}^3$ be an ideal knot in \mathbb{R}^3 with $\mathcal{L}[\overline{\gamma}^*] = 1$. Then for each $L > 0$ small enough there exists a constant $m(L)$ such that the curve $\gamma_L^* : \mathbb{S} \rightarrow \mathbb{S}^3$ defined as $\gamma_L^*(s) := P^{-1}(m(L)\overline{\gamma}^*(s))$ is a competitor to γ_L with length $L = \mathcal{L}[\gamma_L^*]$ and therefore $\Delta[\gamma_L] \geq \Delta[\gamma_L^*]$ by optimality of γ_L . Dividing by $L \frac{\Delta[\gamma_L^*]}{\mathcal{L}[\gamma_L^*]}$ yields

$$\frac{\Delta[\gamma_L]}{L} / \frac{\Delta[\overline{\gamma}_L^*]}{\mathcal{L}[\overline{\gamma}_L^*]} \geq \frac{\Delta[\gamma_L^*]}{L} / \frac{\Delta[\overline{\gamma}_L^*]}{\mathcal{L}[\overline{\gamma}_L^*]} \stackrel{(4.3)}{\rightarrow} 1.$$

Since $\overline{\gamma}_L^*$ is also a ropelength maximiser we have $\frac{\Delta[\overline{\gamma}_L^*]}{\mathcal{L}[\overline{\gamma}_L^*]} = \Delta[\overline{\gamma}^*]$, which implies with the above

$$\liminf_{L \rightarrow 0} \frac{\Delta[\gamma_L]}{L} \geq \Delta[\overline{\gamma}^*].$$

We continue

$$\begin{aligned} \Delta[\overline{\gamma}^*] &\leq \liminf_{L \rightarrow 0} \frac{\Delta[\gamma_L]}{L} \\ &\stackrel{(4.3)}{=} \liminf_{L \rightarrow 0} \Delta[\overline{\gamma}_L] / \underbrace{\mathcal{L}[\overline{\gamma}_L]}_{\rightarrow 1} \\ &= \liminf_{L \rightarrow 0} \Delta[\overline{\gamma}_L] \\ &\leq \limsup_{L \rightarrow 0} \Delta[\overline{\gamma}_L] \\ &\stackrel{\text{optimality}}{\leq} \Delta[\overline{\gamma}^*], \end{aligned}$$

and conclude $\lim_{L \rightarrow 0} \Delta[\overline{\gamma}_L] = \Delta[\overline{\gamma}^*]$.

By Lemma 2.30 a subsequence of γ_L converges in $C^1(\mathbb{S}, \mathbb{R}^3)$ to a limit $\overline{\gamma} : \mathbb{S} \rightarrow \mathbb{R}^3$. The upper semicontinuity of $\Delta[\cdot]$ (Lemma 2.31) guarantees that the limit $\overline{\gamma}$ is indeed a ropelength maximiser. \square

4.3 A Competitor for the Ideal Trefoil

So far very few ideal shapes are known analytically. In \mathbb{R}^3 the circle is known to be the ideal unknot [SDKP98]. In [CKS02] the Hopf-link and other simple links are shown to be ideal. The most complex known shapes are the tight clasp and the Borromean rings [Sta03, CFKSW04] (both based on some natural assumptions). In \mathbb{S}^3 the great circle and the Hopf-Link are known ideal shapes [K02]. All these solutions are component-wise planar.

In this section we want to present a competitor for the ideal trefoil in \mathbb{S}^3 along with its properties. Since the trefoil is a torus knot, it is natural to consider trefoils on tori embedded in the three-sphere ([BPP08] considered trefoils on a torus in \mathbb{R}^3). To define these we use the well-known Hopf coordinates:

Lemma 4.12 (Hopf coordinates). *Consider $\mathbb{S}^3 \subset \mathbb{C}^2$. We can then parametrise $(z_1, z_2) \in \mathbb{S}^3 \subset \mathbb{C}^2$ by*

$$\begin{aligned} z_1 &= e^{i\xi_1} \sin \eta, \\ z_2 &= e^{i\xi_2} \cos \eta, \end{aligned}$$

for $\eta \in [0, \pi/2], \xi_1, \xi_2 \in [0, 2\pi]$.

The metric is given by

$$ds^2 = d\eta^2 + \sin^2 \eta d\xi_1^2 + \cos^2 \eta d\xi_2^2. \quad (4.4)$$

□

For fixed $\eta \in (0, \pi/2)$ we get a torus

$$\mathbb{T}_\eta := \{(e^{i\xi_1} \sin \eta, e^{i\xi_2} \cos \eta) : \xi_1, \xi_2 \in [0, 2\pi]\} \subset \mathbb{S}^3$$

with a flat metric. For $\eta = \pi/4$ this is the famous Clifford torus [Be87] that splits the three-sphere in two equal parts. We will call the whole flat family Clifford tori. The parameter η controls the ‘aspect ratio’ of the torus \mathbb{T}_η . For $\eta = 0$ and $\eta = \pi/2$ the torus collapses to single circles that together form the Hopf-link. The Clifford tori inherit another nice property from the Hopf coordinates: They are a union of unit-circles – the fibres of the Hopf-fibration [Be87].

A straight line $g(t)$ in the parameter set $\mathbb{R}^2/2\pi\mathbb{Z}^2$ with a carefully chosen slope will give an infinite cover of a torus knot. For $g(t) = \frac{3}{2}t$ we get a trefoil (see Figure 4.1) that we lift to \mathbb{T}_η :

$$\begin{aligned} \gamma_\eta(t) &:= \left(e^{it} \sin \eta, e^{ig(t)} \cos \eta \right) \\ &= \left(e^{it} \sin \eta, e^{i3t/2} \cos \eta \right) \\ &= \left[\sin \eta \cos t, \sin \eta \sin t, \cos \eta \cos \frac{3t}{2}, \cos \eta \sin \frac{3t}{2} \right] \in \mathbb{T}_\eta \subset \mathbb{S}^3 \end{aligned} \quad (4.5)$$

for $t \in [0, 4\pi)$. The curves γ_η are smooth and have constant torsion and curvature, so they are helices that close in \mathbb{S}^3 . A similar construction was considered by Banchoff studying self-linking numbers of curves in [B01].

Meanwhile Kusner was ‘tempted to conjecture’:

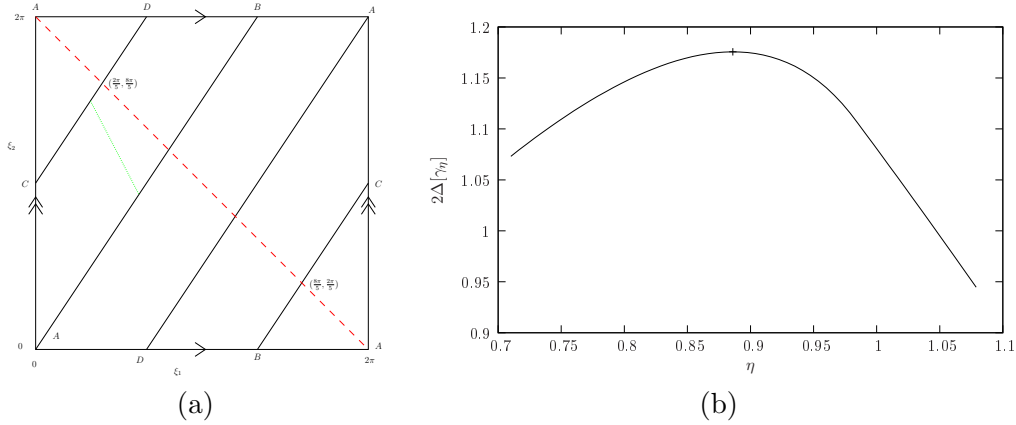


Figure 4.1: (a) The canonical trefoil on a torus in parameter space $\mathbb{R}^2/(2\pi\mathbb{Z})^2$. The short green dotted line shows an example of a self-distance. For some aspect ratio it forms a right angle with the trefoil in the corresponding metric realizing the thickness of the trefoil. The red dashed line and its parallels are always Villarceau-circles on the torus-surface. For the special aspect ratio η^* the red dashed line and the short green dotted line would be parallel. (b) The thickness Δ of the trefoil γ_η . Maximum at $\eta^* = \arctan\left(\frac{\sqrt{3}}{2}\right) \approx 0.886$, $\Delta[\gamma_{\eta^*}] = \sin(\pi/5) \approx 0.588$.

Conjecture 4.13. [K02, p. 177] *Ideal torus knots $T_{2,m}$ in \mathbb{S}^3 are on a flat Clifford torus with optimised aspect ratio.*²

In Remark 4.16 and Section 5.5.5 we will see that the conjecture does not hold for $m = 5$. But the case $m = 3$ is interesting:

Lemma 4.14. *Let γ_η be defined as in (4.5). Then within the family of Clifford trefoils, $\Delta[\gamma_\eta]$ is maximal for*

$$\eta^* = \arctan\left(\sqrt{\frac{3}{2}}\right) \approx 0.886 \quad \text{with} \quad \Delta[\gamma_{\eta^*}] = \sin(\pi/5) \approx 0.588.$$

Proof. We consider the squared distance between $(0, 0) \in \mathbb{R}^2$ and a point on the straight line $(t, g(t) - \pi)$ in the metric defined in (4.4), and denote it by

$$d(t, \eta) := \cos^2(\eta) (3t - \pi)^2 + 4 \sin^2(\eta) t^2.$$

To find the parameter t_{\min} of the closest point we differentiate by t and find

$$d_t(t, \eta) = 6 \cos^2(\eta) (3t - \pi) + 8 \sin^2(\eta) t.$$

Solving $d_t(t_{\min}, \eta) = 0$ yields

$$t_{\min} = \frac{3\pi \cos^2(\eta)}{4 \sin^2(\eta) + 9 \cos^2(\eta)}.$$

² R. Langevin made a similar conjecture in a private communication for the trefoil $T_{2,3}$.

Now calculate the squared distance from the line to the origin as a function of η :

$$\begin{aligned} \text{dmin}(\eta) &:= d(t_{\min}, \eta) \\ &= \cos^2(\eta) \left(\frac{9\pi \cos^2(\eta)}{4 \sin^2(\eta) + 9 \cos^2(\eta)} - \pi \right)^2 + \frac{36\pi^2 \cos^4(\eta) \sin^2(\eta)}{(4 \sin^2(\eta) + 9 \cos^2(\eta))^2} \end{aligned}$$

and maximise it. We compute

$$\begin{aligned} \text{dmin}_\eta(\eta) &= 2 \cos^2(\eta) \left(\frac{9\pi \cos^2(\eta)}{4 \sin^2(\eta) + 9 \cos^2(\eta)} - \pi \right) \\ &\quad \cdot \left(\frac{90\pi \cos^3(\eta) \sin(\eta)}{(4 \sin^2(\eta) + 9 \cos^2(\eta))^2} - \frac{18\pi \cos(\eta) \sin(\eta)}{4 \sin^2(\eta) + 9 \cos^2(\eta)} \right) \\ &\quad - 2 \cos(\eta) \sin(\eta) \left(\frac{9\pi \cos^2(\eta)}{4 \sin^2(\eta) + 9 \cos^2(\eta)} - \pi \right)^2 \\ &\quad - \frac{144\pi^2 \cos^3(\eta) \sin^3(\eta)}{(4 \sin^2(\eta) + 9 \cos^2(\eta))^2} \\ &\quad + \frac{72\pi^2 \cos^5(\eta) \sin(\eta)}{(4 \sin^2(\eta) + 9 \cos^2(\eta))^2} + \frac{720\pi^2 \cos^5(\eta) \sin^3 \eta}{(4 \sin^2(\eta) + 9 \cos^2(\eta))^3}, \end{aligned}$$

and solving $\text{dmin}_\eta(\eta) = 0$ in $[0, \pi/2]$ yields

$$\begin{aligned} \eta_0 &= 0, \\ \eta_1 &= \frac{\pi}{2}, \\ \eta^* &= \arctan \left(\frac{\sqrt{3}}{\sqrt{2}} \right) \approx 0.886, \end{aligned}$$

where $\text{dmin}(\eta^*) = \frac{4\pi^2}{25}$ is the maximum. This is also the squared distance in \mathbb{S}^3 since all points in \mathbb{T}_η have the same η -value and the metric is induced from \mathbb{S}^3 . Calculating the curvature of γ_{η^*} we find $1/\kappa = \sqrt{6/7} \approx 0.926 > \sin(\sqrt{\text{dmin}(\eta^*)}/2) = \sin(\pi/5) \approx 0.588$ so we have indeed $\Delta[\gamma_{\eta^*}] = \sin(\pi/5)$. \square

Definition 4.15 (\mathfrak{g} -Trefoil). *We denote the above curve $\mathfrak{g} : [0, 4\pi] \rightarrow \mathbb{S}^3$ defined as*

$$\mathfrak{g}(t) := \gamma_\eta = \left[\sqrt{\frac{3}{5}} \cos t, \sqrt{\frac{3}{5}} \sin t, \sqrt{\frac{2}{5}} \cos \left(\frac{3}{2}t \right), \sqrt{\frac{2}{5}} \sin \left(\frac{3}{2}t \right) \right].$$

and call it the \mathfrak{g} -trefoil.³ In Hopf coordinates:

$$\mathfrak{g}(t) = \left[\arctan \sqrt{\frac{3}{2}}, t, \frac{3}{2}t \right] \in [0, \pi/2] \times \mathbb{R}/2\pi\mathbb{Z} \times \mathbb{R}/2\pi\mathbb{Z}.$$

³ The name was proposed by J. Maddocks to reflect the conjecture that it maximises global radius of curvature.

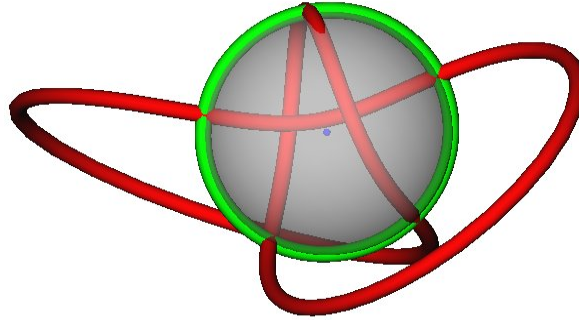


Figure 4.2: The green Villarceau circle intersects the red competitor \mathbf{g} five times in equidistant points. The stereographic projection was chosen such that the green Villarceau circle was not distorted and the distance along it corresponds to distances in \mathbb{S}^3 . Note that the symmetry of \mathbf{g} is lost in this projection. The grey, transparent sphere is a great sphere in \mathbb{S}^3 and separates it in two equal parts: Its inside and its outside.

Remark 4.16. *A similar calculation as in Lemma 4.14 for the $T_{2,5}$ knot with*

$$g(t) := \frac{5}{2}t$$

yields

$$\eta^* = \arctan\left(\sqrt{\frac{5}{2}}\right) \approx 1.007 \quad \text{and} \quad \Delta[\gamma_{\eta^*}] = \sin(\pi/7) \approx 0.434.$$

As we will see in Section 5.5.5 this thickness is bettered by a non-Clifford $T_{2,5}$ knot.

One easily calculates various properties of \mathbf{g} :

Lemma 4.17 (Properties of \mathbf{g}).

| | |
|---|--|
| Thickness $\Delta[\mathbf{g}]$ | $\sin(\pi/5)$ |
| Length $\mathcal{L}[\mathbf{g}]$ | $4\pi\sqrt{\frac{3}{2}}$ |
| Volume of maximal thickness tube $\mathcal{V}[\mathcal{T}_{\pi/5}(\mathbf{g})]$ | $2\sqrt{6}\pi^2\sin^2\left(\frac{\pi}{5}\right)$ |

The trefoil \mathbf{g} has the following geometric properties:

- (i) *For all $t \in [0, 4\pi]$ $\mathbf{g}(t)$ is in self contact with $\mathbf{g}(t + \frac{8\pi}{5})$ and $\mathbf{g}(t + \frac{12\pi}{5})$, these 3 points lie on the same great circle*

$$c_t(s) := \left[\sqrt{\frac{3}{5}} \cos(t+s), \sqrt{\frac{3}{5}} \sin(t+s), \sqrt{\frac{2}{5}} \cos\left(\frac{3}{2}t-s\right), \sqrt{\frac{2}{5}} \sin\left(\frac{3}{2}t-s\right) \right]$$

with $c_t(0) = \mathbf{g}(t)$.

- (ii) *This great circle $c_t(s)$ intersects \mathbf{g} five times (at $\mathbf{g}(\frac{4n\pi}{5})$, $n = 0, 1, 2, 3, 4$), always realizing the self contact. It is a Villarceau circle [Be87] on the Clifford torus \mathbb{T}_{η^*} (depicted as a red dashed line in Figure 4.1(a)).*

- (iii) The vectors $\frac{\partial}{\partial t}\mathbf{g}(t)$, $\frac{\partial^2}{\partial t^2}\mathbf{g}(t)$ and $\frac{\partial}{\partial s}c_t(0)$ are pairwise orthogonal. Thus $\frac{\partial}{\partial s}c_t(0)$ is orthogonal to the tangent and principal normal and so points in the direction of the ‘binormal’ to $\mathbf{g}(t)$ in \mathbb{S}^3 .
- (iv) The curve \mathbf{g} is a helix, i.e. has constant curvature and torsion and has a ‘translational and rotational’ symmetry:

$$h_s \circ \mathbf{g}(t + s) = \mathbf{g}(t) \quad \forall t, s \in \mathbb{R},$$

with the homeomorphism $h_s : \mathbb{S}^3 \rightarrow \mathbb{S}^3$ in Hopf coordinates

$$h_s(\eta, \xi_1, \xi_2) = \left[\eta, \xi_1 - s, \xi_2 - \frac{3}{2}s \right].$$

(See Section 5.3 for a more abstract definition of symmetry.)

□

Assuming that \mathbf{g} is indeed ideal, what can be expected for other thickness maximisers? We make a conjecture with some heuristic justifications. If for each parameter r of γ there are at most two other parameters s, t in contact, i.e.

$$|\gamma(r) - \gamma(t)| = |\gamma(r) - \gamma(s)| = 2\Delta[\gamma]$$

and both $(\gamma(r) - \gamma(t))$ and $(\gamma(r) - \gamma(s))$ are orthogonal to γ (Definition 2.15), we can try to locally improve the thickness as follows:

If $\gamma(r), \gamma(s)$ and $\gamma(t)$ are not on a common great circle we can move $\gamma(r)$ away from $\gamma(s)$ and $\gamma(t)$ so that the self distance of the curve around $\gamma(r)$ increases (linearly). Hence we could expect to find some parameters r^*, s^* and t^* such that $|\gamma(r^*) - \gamma(t^*)| = |\gamma(r^*) - \gamma(s^*)| = 2\Delta[\gamma]$ and $\gamma(r^*), \gamma(t^*)$ and $\gamma(s^*)$ are located on a common great circle. We call such a parameter r^* locked since we can not move it in order to increase thickness quickly (ρ_G could still be increased in second order).

If s^* or t^* are not locked themselves, we could move one of them aside thus unlocking r^* , so we could expect to find a sequence of locked parameters one in contact with the next. All of them are on the same great circle thus partitioning the circle in arcs of length π/n . Therefore we conjecture:

Conjecture 4.18 (Quantised thickness). *Some ideal knots γ in \mathbb{S}^3 have thickness*

$$\Delta[\gamma] \in \{\sin(\pi/n) : n \in \mathbb{N}\}.$$

4.4 Is the Competitor \mathbf{g} at Least a Local Maximum?

We would like to know whether the trefoil has maximal thickness or whether it is at least a local maximiser. In Lemma 4.19 we show that the \mathbf{g} is at least a saddle point in the sense that it satisfies first-order necessary conditions for maximality.

Since thickness is defined as the infimum of pt for pairwise distinct parameters, we have to study the minima of that function. Since the curvature of \mathbf{g} is smaller than $1/\Delta[\mathbf{g}]$ we know that a small neighbourhood of the diagonal is bigger than the minimum.

Furthermore it was shown in [GMS02] that away from the diagonal the local minima of pp and the point point function

$$\text{pp}[\gamma](s, \sigma) := |\gamma(s) - \gamma(\sigma)| \quad (4.6)$$

coincide.

Hence we want to study the minima of the pp -function that for curves γ on \mathbb{S}^3 has the simple form

$$\frac{1}{2}\text{pp}^2[\gamma](s, \sigma) = 1 - \gamma(s) \cdot \gamma(\sigma). \quad (4.7)$$

For a variation $h \in C^\infty(\mathbb{R}/4\pi\mathbb{Z}, \mathbb{R}^4)$ of $\gamma : \mathbb{R}/4\pi\mathbb{Z} \rightarrow \mathbb{S}^3$ with

$$\|h\|_{C^0} < 1, \quad (4.8)$$

$$h(s) \cdot \gamma(s) = 0, \quad \forall s \in \mathbb{R}/4\pi\mathbb{Z}, \quad (4.9)$$

the perturbed curve

$$\gamma_\varepsilon(s) := (1 - \varepsilon^2|h(s)|^2)^{1/2}\gamma(s) + \varepsilon h(s) \in \mathbb{S}^3, \quad (4.10)$$

will be in \mathbb{S}^3 for all sufficiently small ε . Expanding the square root yields

$$\gamma_\varepsilon(s) = \gamma(s) + \varepsilon h(s) - \frac{1}{2}\varepsilon^2|h(s)|^2\gamma(s) + O(\varepsilon^4). \quad (4.11)$$

Substituting (4.11) into (4.7) and expanding gives

$$\begin{aligned} \frac{1}{2}\text{pp}_\varepsilon^2(s, \sigma) &:= \frac{1}{2}\text{pp}^2[\gamma_\varepsilon](s, \sigma) \\ &= (1 - \gamma(s) \cdot \gamma(\sigma)) - \varepsilon(h(s) \cdot \gamma(\sigma) + h(\sigma) \cdot \gamma(s)) \\ &\quad + \frac{1}{2}\varepsilon^2\gamma(s) \cdot \gamma(\sigma)(|h(s)|^2 + |h(\sigma)|^2) - \varepsilon^2 h(s) \cdot h(\sigma) \\ &\quad + O(\varepsilon^3). \end{aligned} \quad (4.12)$$

So far the development has been for a generic curve γ on \mathbb{S}^3 . Now we assume that γ is the \mathfrak{g} -trefoil. In particular we know that each parameter s of the curve \mathfrak{g} is in contact (see Definition 2.15) with $\sigma(s) = s + \frac{8\pi}{5}$, and the parameter set $(s, \sigma(s))$ is a known curve or valley of local minima of pp , i.e. $\mathfrak{g}(s) \cdot \mathfrak{g}(\sigma(s)) = 1 - 2\Delta[\mathfrak{g}]$. Also note that this local minimum is non-degenerate (see Section 5.5.3), in the sense that perpendicular to the valley floor the function increases.

How does the minimum change when perturbing σ ? The perturbed minimum σ_ε will satisfy

$$\left. \frac{\partial}{\partial \sigma} \frac{1}{2}\text{pp}_\varepsilon^2(s, \sigma) \right|_{\sigma=\sigma_\varepsilon(s)} = 0 \quad \text{or} \quad \mathfrak{g}_\varepsilon(s) \cdot \mathfrak{g}'_\varepsilon(\sigma_\varepsilon(s)) = 0, \quad (4.13)$$

otherwise it would not be a local minimum around σ_ε . And we expand the unknown $\sigma_\varepsilon(s)$ to

$$\sigma_\varepsilon(s) = \sigma(s) + \varepsilon\sigma_1(s) + \varepsilon^2\sigma_2(s) + \dots \quad (4.14)$$

Calculating $\frac{\partial}{\partial \sigma}$ of (4.12) yields:

$$\begin{aligned} \frac{\partial}{\partial \sigma} \frac{1}{2}\text{pp}_\varepsilon^2(s, \sigma) &= -\mathfrak{g}(s) \cdot \mathfrak{g}'(\sigma) - \varepsilon [h(s) \cdot \mathfrak{g}'(\sigma) + h'(\sigma) \cdot \mathfrak{g}(s)] \\ &\quad + O(\varepsilon^2). \end{aligned} \quad (4.15)$$

Using this expression in (4.13) and expanding around $\sigma(s)$ yields:

$$\begin{aligned}
0 &= \left. \frac{\partial}{\partial \sigma} \frac{1}{2} \text{pp}_\varepsilon^2(s, \sigma) \right|_{\sigma=\sigma_\varepsilon(s)} & (4.16) \\
&= -\mathbf{g}(s) \cdot \left[\mathbf{g}'(\sigma(s)) + (\varepsilon\sigma_1(s) + \varepsilon^2\sigma_2(s))\mathbf{g}''(\sigma(s)) + \frac{1}{2}\varepsilon^2\sigma_1^2(s)\mathbf{g}'''(\sigma(s)) \right] \\
&\quad + \varepsilon \left[-h(s) \cdot (\mathbf{g}'(\sigma(s)) + \varepsilon\sigma_1(s)\mathbf{g}''(\sigma(s))) - \mathbf{g}(s) \cdot (h'(\sigma(s)) + \varepsilon\sigma_1(s)h''(\sigma(s))) \right] \\
&\quad + O(\varepsilon^2) \\
&= -\mathbf{g}(s) \cdot \mathbf{g}'(\sigma(s)) \\
&\quad + \varepsilon \left[-\mathbf{g}(s) \cdot \sigma_1(s)\mathbf{g}''(\sigma(s)) - h(s) \cdot \mathbf{g}'(\sigma(s)) - \mathbf{g}(s) \cdot h'(\sigma(s)) \right] \\
&\quad + O(\varepsilon^2)
\end{aligned}$$

As this equality should hold for all small ε the coefficient of each power of ε should vanish:

$$\varepsilon^0: -\mathbf{g}(s) \cdot \mathbf{g}'(\sigma(s)) = 0 \text{ which is a property of the } \mathbf{g}\text{-trefoil.}$$

$$\varepsilon^1: -\sigma_1(s)\mathbf{g}(s) \cdot \mathbf{g}''(\sigma(s)) - h(s) \cdot \mathbf{g}'(\sigma(s)) - \mathbf{g}(s) \cdot h'(\sigma(s)) = 0 \text{ which yields}$$

$$\sigma_1(s) = -\frac{h(s) \cdot \mathbf{g}'(\sigma(s)) + \mathbf{g}(s) \cdot h'(\sigma(s))}{\mathbf{g}(s) \cdot \mathbf{g}''(\sigma(s))} \quad (4.17)$$

$$\text{where } \mathbf{g}(s) \cdot \mathbf{g}''(\sigma(s)) = -(3/2) \cos(2\pi/5) \approx 0.46.$$

Now use the expansion of σ_ε in (4.12):

$$\begin{aligned}
\frac{1}{2} \text{pp}_\varepsilon^2(s, \sigma_\varepsilon(s)) &= 1 - \mathbf{g}(s) \cdot \left[\mathbf{g}(\sigma(s)) + (\varepsilon\sigma_1(s) + \varepsilon^2\sigma_2(s) + \varepsilon^3\sigma_3(s)) \underbrace{\mathbf{g}'(\sigma(s))}_{\perp \mathbf{g}(s)} \right] & (4.18) \\
&\quad + \left(\frac{1}{2}\varepsilon^2\sigma_1^2(s) + \varepsilon^3\sigma_1(s)\sigma_2(s) \right) \mathbf{g}''(\sigma(s)) + \frac{1}{6}\varepsilon^3\sigma_1^3(s)\mathbf{g}'''(\sigma(s)) \\
&\quad + \varepsilon \left[-h(s) \cdot (\mathbf{g}(\sigma(s)) + (\varepsilon\sigma_1(s) + \varepsilon^2\sigma_2(s))\mathbf{g}'(\sigma(s)) + \frac{1}{2}\varepsilon^2\sigma_1^2(s)\mathbf{g}''(\sigma(s))) \right. \\
&\quad \quad \left. - \mathbf{g}(s) \cdot (h(\sigma(s)) + (\varepsilon\sigma_1(s) + \varepsilon^2\sigma_2(s))h'(\sigma(s)) + \frac{1}{2}\varepsilon^2\sigma_1^2(s)h''(\sigma(s))) \right] \\
&= 1 - \mathbf{g}(s) \cdot \mathbf{g}(\sigma(s)) \\
&\quad - \varepsilon [h(s) \cdot \mathbf{g}(\sigma(s)) + \mathbf{g}(s) \cdot h(\sigma(s))] \\
&\quad + O(\varepsilon^2)
\end{aligned}$$

Again, consider the coefficients of the ε -powers:

$$\varepsilon^0: 1 - \mathbf{g}(s) \cdot \mathbf{g}(\sigma(s)) = 2\Delta^2[\mathbf{g}]$$

$$\varepsilon^1:$$

$$\begin{aligned}
c_1(s) &:= (h(s) \cdot \mathbf{g}(\sigma(s)) + \mathbf{g}(s) \cdot h(\sigma(s))) & (4.19) \\
&= (h(s) + h(\sigma(s))) \cdot (\mathbf{g}(s) + \mathbf{g}(\sigma(s)))
\end{aligned}$$

Then we have:

Lemma 4.19. *Let \mathfrak{g}_ε be a perturbation of \mathfrak{g} for all sufficiently small ε as defined in (4.10) and let σ_ε be the corresponding perturbation of the contact function satisfying (4.13). Then in the expansion (4.18)*

$$\frac{1}{2}\text{pp}^2[\mathfrak{g}_\varepsilon](s, \sigma_\varepsilon(s)) = 2\Delta^2[\mathfrak{g}] - \varepsilon c_1(s) + O(\varepsilon^2)$$

it is necessary that the function $c_1(s)$ vanishes identically, otherwise the thickness of the perturbation decreases to the first order in ε .

Proof. Since the valley of the pp-function around (s, σ) is non-degenerate, $\sigma_\varepsilon(s)$ defined as the local minima of $f_s(t) := \text{pt}[\mathfrak{g}_\varepsilon](s, t)$ close to $\sigma(s)$, satisfies (4.13). We have

$$\Delta[\mathfrak{g}_\varepsilon] \leq \sqrt{\frac{1}{4}\text{pp}^2[\mathfrak{g}_\varepsilon](s, \sigma_\varepsilon(s))} = \Delta[\mathfrak{g}] - \varepsilon c_1(s)/(4\Delta[\mathfrak{g}]) + O(\varepsilon^2), \quad \forall s \quad (4.20)$$

as an upper bound for the thickness. If c_1 is not sign definite, there exist parameters s^+, s^- such that $c(s^+) > 0$ and $c(s^-) < 0$ and by (4.20) thickness decreases to first order for all sufficiently small ε at one of them. Now assume c_1 is definite, for example

$$c_1(s) \leq 0, \quad \forall s, \quad (4.21)$$

but c_1 does not vanish identically. If the above inequality was valid and strict, then we could have a first order thickness increasing perturbation for $\varepsilon > 0$.

However, we will show that the existence of a perturbation satisfying (4.21) leads to a contradiction.

Let s_0 be a parameter, such that the first order coefficient

$$c_1(s_0) = h(s_0) \cdot \mathfrak{g}(\sigma(s_0)) + \mathfrak{g}(s_0) \cdot h(\sigma(s_0)) < 0 \quad (4.22)$$

is negative. Define $s_i := \sigma(s_{i-1}) = s_0 + \frac{8\pi}{5}i$ for $i = -2, -1, 0, 1, 2$ with $s_{-2} = s_3$. Note that all $\mathfrak{g}(s_i)$ lie on the same great circle and are in contact with each other (see Lemma 4.17(ii)). Now define

$$a_i := h(s_i) \cdot \mathfrak{g}(s_{i+1}), \quad b_i := h(s_{i+1}) \cdot \mathfrak{g}(s_i),$$

and note $c_1(s_i) = a_i + b_i$. Furthermore we have $\alpha \mathfrak{g}(s_{i+1}) = \mathfrak{g}(s_i) + \mathfrak{g}(s_{i+2})$ for some $\alpha \in \mathbb{R}$. Multiplying above by $h(s_{i+1})$ and using (4.9) yields:

$$0 = h(s_{i+1}) \cdot \mathfrak{g}(s_i) + h(s_{i+1}) \cdot \mathfrak{g}(s_{i+2}) = b_i + a_{i+1},$$

i.e. $b_i = -a_{i+1}$. By (4.21) we derive for $i = -2, \dots, 2$

$$c_1(s_i) = a_i - a_{i+1} \leq 0,$$

which implies

$$a_0 \underset{(4.22)}{<} a_1 \leq a_2 \leq \dots \leq a_5 = a_0$$

which is absurd. Therefore c_1 must vanish identically. \square

Remark 4.20. *Lemma 4.19 excludes all perturbation except those for which $c_1(s)$ vanishes identically as possible improvements of \mathfrak{g}_ε . For these variations leading to vanishing $c_1(s)$, further necessary conditions could in principle be derived by computing second and higher variations. Lemma 4.19 is an unusual first order necessary condition because it is non local in character.*

Chapter 5

Computations and Deductions

5.1 Biarc Curves

Since the work of J. Smutny [S04] the Maddocks group has been computing ideal knot shapes using the biarc representation of curves. In this section we will sketch how this is done so the reader may understand what has been computed. For the details we refer to [S04, CLMS05] and [C10].

We can interpolate a curve $\gamma \in C^1(\mathbb{S}, \mathbb{R}^N)$ in C^1 -fashion in some parameters $t_0 < \dots < t_n$. We prescribe the interpolation points $p_i := \gamma(t_i)$ and tangents $t_i := \gamma'(t_i)/|\gamma'(t_i)|$. Conversely starting from a set of *point tangent pairs* $(p_i, t_i) \in \mathbb{R}^N \times \mathbb{S}^N$, under certain conditions, we are able to construct an approximation of γ .

Consider two point-tangent pairs

$$(p_0, t_0), (p_1, t_1) \in \mathbb{R}^N \times \mathbb{S}^N.$$

When t_0, t_1 and $p_1 - p_0$ point approximately in the same direction, more precisely

$$\langle p_1 - p_0, t_0 \rangle > 0 \quad \text{and} \quad \langle p_1 - p_0, t_1 \rangle > 0,$$

we call the point-tangent pairs *proper*. Note that the sequence of the pairs is crucial since the curve goes from p_0 to p_1 .

Now let $(p_0, t_0), (p_1, t_1)$ be proper. The vectors t_0, t_1 and $(p_1 - p_0)$ in general span a three dimensional space in which the following construction will take place, so we can safely assume $N = 3$. The pairs define a sphere $\partial B_r(x) \subset \mathbb{R}^3$ such that p_0 and p_1 lie on $\partial B_r(x)$ and t_0, t_1 are tangent to it at p_0, p_1 respectively. If t_0, t_1 and $(p_1 - p_0)$ are linearly dependent, we set the sphere's radius $r = \infty$, and it degenerates to a plane. T.J. Sharock showed [Sh87] that there exists a family of pairs $(a_\lambda, b_\lambda) \in C^\infty([0, 1], \mathbb{R}^3) \times C^\infty([0, 1], \mathbb{R}^3)$ (with $\lambda \in (0, 1)$) of circular arcs¹ that lie on $\partial B_r(x)$ joining the pair $(p_0, t_0), (p_1, t_1)$ in C^1 -fashion, i.e.

$$\begin{aligned} p_0 &= a_\lambda(0), & t_0 &= a'_\lambda(0)/|a'_\lambda(0)|, \\ a_\lambda(1) &= b_\lambda(0), & a'_\lambda(1)/|a'_\lambda(1)| &= b'_\lambda(0)/|b'_\lambda(0)|, \\ p_1 &= b_\lambda(1) \quad \text{and} \quad t_1 &= b'_\lambda(1)/|b'_\lambda(1)|. \end{aligned}$$

¹ If t_0, t_1 and $(p_1 - p_0)$ are collinear, the arcs degenerate to straight lines.

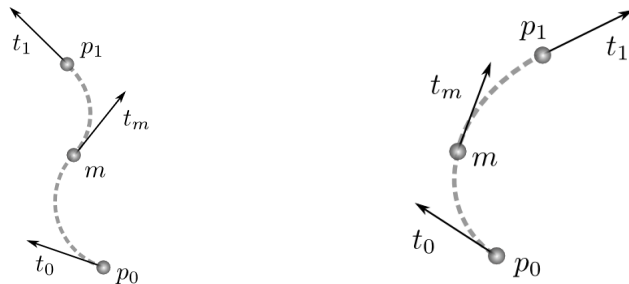


Figure 5.1: Proper point tangent data $(p_0, t_0), (p_1, t_1)$ interpolated by biarcs.

We call such a pair of arcs (a_λ, b_λ) a biarc (see Figure 5.1). The point $m := a_\lambda(1) = b_\lambda(0)$ where both arcs meet is called the *matching point*. The parameter $\lambda \in (0, 1)$ controls the position of the matching point m by the ratio of the distances $|m - p_0|$ and $|m - p_1|$. Therefore we call λ the *matching rule*. For our purpose we chose a matching rule $\lambda = 1/2$ such that $|m - p_0| = |m - p_1|$. For fixed λ a proper point-tangent data pair defines a unique (arc-length parametrised) biarc, hence we call a proper point-tangent data pair also a *proper biarc*. One can prove [S04, Theorem 6.13] that a $C^{1,1}$ curve can be approximated in C^1 by an interpolating biarc curve with enough point-tangent pairs which justifies our use of them.

Instead of interpolating a curve, we can start with a sequence of n point-tangent (p_i, t_i) pairs such that $(p_i, t_i), (p_{i+1}, t_{i+1})$ and $(p_n, t_n), (p_0, t_0)$ are proper and they define an arc-length parametrised biarc curve.

Also note that the three-dimensional affine subspace spanned by t_0, t_1 and $(p_1 - p_0)$ going through p_0 intersects \mathbb{S}^3 in a two-sphere. Since the points p_0, p_1 are on that two-sphere and t_0, t_1 are tangent as well, the above $\partial B_r(x)$ is a subset of \mathbb{S}^3 . Consequently the biarc (a_λ, b_λ) is contained in \mathbb{S}^3 . Thus point-tangent data on \mathbb{S}^3 yields biarc curves on \mathbb{S}^3 , making it easy to model curves on \mathbb{S}^3 .

5.2 Fourier Representation of Knots

In the previous section we saw that we can represent curves with point-tangent data. This has the advantage that an efficient numerical library exists to deal with such curves [C10]. In particular we can easily manipulate such a curve, compute its arc-length and thickness Δ . On the other hand this representation has some drawbacks. It is difficult to take advantage of a presumed symmetry of the curve, and while applying numerical algorithms such as gradient flow or simulated annealing it tended to non-proper point tangent pairs and the computation got stuck. To tackle those issues we reintroduce the Fourier representation of curves into ideal knot shapes (it was first introduced in [K98]; see also [T98]).

Definition 5.1 (Fourier knot). *Let C be a finite sequence of pairs of \mathbb{R}^3 -vectors:*

$$C = \{(a_i, b_i)\}_{i=1, \dots, k} \quad a_i, b_i \in \mathbb{R}^3.$$

We use such a sequence as Fourier coefficients and define

$$\gamma(t) := \sum_{i=1}^k (a_i \cos(f_i t) + b_i \sin(f_i t)), \quad t \in \mathbb{S},$$

as a curve in $C^\infty(\mathbb{S}, \mathbb{R}^3)$ with frequencies $f_i := 2\pi i$. If it is injective, we call γ a Fourier knot.

Remark 5.2. Note that Fourier knots lack a constant term, since we are not interested in translations of the curve.

The use of a Fourier representation in pursuit of ideal knots is justified by the following lemma.

Lemma 5.3 (Approximation with Fourier knots). *Let $\gamma \in C^{1,1}(\mathbb{S})$ be an ideal shape. Then for every $\varepsilon > 0$ there exist a finite set of coefficients $\{(a_i, b_i)\}_i$ such that the Fourier knot*

$$\gamma_\varepsilon(t) := \sum_i (a_i \cos(f_i t) + b_i \sin(f_i t))$$

satisfies

$$\|\gamma - \gamma_\varepsilon\|_{C^1(\mathbb{S})} < \varepsilon \quad \text{and} \quad \Delta[\gamma] - \varepsilon < \Delta[\gamma_\varepsilon].$$

Proof. By Corollary 3.12 there exists a curve $\gamma_{\infty, \varepsilon} \in C^\infty(\mathbb{S}, \mathbb{R}^3)$ such that

$$\|\gamma - \gamma_{\infty, \varepsilon}\|_{C^1(\mathbb{S}, \mathbb{R}^3)} < \varepsilon/2 \quad \text{and} \quad \Delta[\gamma] - \varepsilon/2 < \Delta[\gamma_{\infty, \varepsilon}].$$

By standard Fourier theory there exists a sequence $\{\tilde{\gamma}_i\}_i$ of Fourier curves – each represented by finite coefficients – that approximate $\gamma_{\infty, \varepsilon}$ in a C^2 -fashion. This approximation satisfies Lemma 2.33 and for some large enough index i^* we have

$$\|\gamma_{\infty, \varepsilon} - \tilde{\gamma}_{i^*}\|_{C^{1,1}(\mathbb{S})} < \varepsilon/2, \quad \Delta[\gamma_{\infty, \varepsilon}] - \varepsilon/2 < \Delta[\tilde{\gamma}_{i^*}].$$

Now $\gamma_\varepsilon := \tilde{\gamma}_{i^*}$ is the sought Fourier knot. Ideality of γ and C^1 -convergence imply that indeed $\frac{\mathcal{L}[\gamma_\varepsilon]}{\Delta[\gamma_\varepsilon]} \rightarrow \frac{\mathcal{L}[\gamma]}{\Delta[\gamma]}$ for $\varepsilon \rightarrow 0$. \square

The use of the Fourier representation in simulated annealing to approach ideal shapes has several advantages over the direct use of the biarc point data pairs used previously [S04, CLMS05]:

- (i) They make it easy to inherently model symmetry (see Section 5.4) and by that improve computation speed.
- (ii) Any sequence of coefficients yield a valid Fourier knot while point biarc data needs to be proper which is sometimes difficult to ensure.
- (iii) It is trivial to improve the approximation by adding further coefficient pairs.
- (iv) Fourier knots are C^∞ approximation of the ideal shape, so higher derivatives can be computed (even though the ideal shape might not be as smooth).

The main disadvantage is, that no computer-code exists to evaluate the thickness of Fourier knots. We work around this problem, by interpolating the Fourier knot with a sufficiently fine biarc knot and evaluating thickness on the latter. There is also no easy way to refine a shape locally. If further coefficients are added then usually all coefficients have to change for a better approximation while in the point tangent pair representation only closeby points are involved.

5.3 Symmetry of Curves

This section will give a precise definition for what we mean when we say a curve γ has a certain symmetry.

Definition 5.4 (*G*-Symmetry). *Let $\gamma \in C^0(\mathbb{S}, \mathbb{R}^3)$ be a curve and $G \subset \mathbf{Aut}(C^0(\mathbb{S}, \mathbb{R}^3))$ a group acting on $C^0(\mathbb{S}, \mathbb{R}^3)$.² We call γ *G*-symmetric iff*

$$g \cdot \gamma = \gamma \quad \forall g \in G.$$

*If a curve γ is *G*-symmetric then we call *G* a symmetry-group of γ .*

If *G* is maximal in some respect, we may call it ‘the’ symmetry-group of γ . Just taking the maximal subgroup *G* of $\mathbf{Aut}(C^0(\mathbb{S}, \mathbb{R}^3))$ such that γ is *G* symmetric is not what we want since it is too large. For example it would include all \mathcal{H} defined for each homeomorphism $h : \mathbb{R}^3 \rightarrow \mathbb{R}^3$ with $h \circ \gamma = \gamma$ as $\mathcal{H}[\alpha] := h \circ \alpha$ for $\alpha \in C^0(\mathbb{S}, \mathbb{R}^3)$.

Definition 5.5 (Symmetrised curve). *Let $\gamma \in C^0(\mathbb{S}, \mathbb{R}^3)$ be a curve and $G \subset \mathbf{Aut}(C^0(\mathbb{S}, \mathbb{R}^3))$ a finite group. Then*

$$\gamma_G := \frac{\sum_{g \in G} g \cdot \gamma}{|G|}$$

*is the *G*-symmetrisation of γ .*

Obviously γ_G is *G*-symmetric.

Definition 5.6 (Group of parameter shifts and reflections). *For $x \in \mathbb{R}$ we define the parameter shift $S_x : C^0(\mathbb{S}, \mathbb{R}^3) \rightarrow C^0(\mathbb{S}, \mathbb{R}^3)$ by x of a curve γ as*

$$S_x[\gamma](t) := \gamma(t + x)$$

and the parameter reflection $R_x : C^0(\mathbb{S}, \mathbb{R}^3) \rightarrow C^0(\mathbb{S}, \mathbb{R}^3)$ around x as

$$R_x[\gamma](t) := \gamma(2x - t).$$

Shifts and reflections form a group.

Note that a symmetry-group of a curve is usually not just a subgroup of the orthogonal group $O(3)$, but a subgroup of the product $H \times P$ of a subgroup $H \subset O(3)$ and a subgroup *P* of parameter shifts and reflections.

Example 5.7. *Consider an egg-shaped curve γ as in Figure 5.2. The point-set $\gamma(\mathbb{S})$ is invariant under mirroring along the dashed line m . But the curve is not, because $\gamma(0) \neq m \cdot \gamma(0)$. Chose a t^* such that $\gamma(t^*) = m \cdot \gamma(t^*)$ and define $G := \{\text{id}, m \circ R_{t^*}\}$ then γ will be *G*-symmetric.*

² Here $\mathbf{Aut}(C^0(\mathbb{S}, \mathbb{R}^3))$ is the group of automorphisms of $C^0(\mathbb{S}, \mathbb{R}^3)$, i.e. all functors \mathcal{F} that map $\gamma \in C^0(\mathbb{S}, \mathbb{R}^3)$ one-to-one to $\mathcal{F}[\gamma] \in C^0(\mathbb{S}, \mathbb{R}^3)$. [A91]

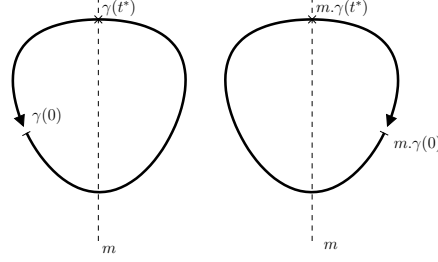


Figure 5.2: The symmetry-group of a curve must take not only the shape into account, but also the parametrisation: The above egg-shaped curve is mirror symmetric to the dashed line as a point-set, but applying the reflection m does not yield the same parametrisation.

5.4 Symmetry of Fourier Knots in \mathbb{R}^3

We will apply the previous section to Fourier knots and determine patterns of the Fourier coefficients representing knots with certain symmetries. We first fix our notation for generators of $O(3)$:

Definition 5.8 (Rotation and Reflection Matrices). *Let $v \in \mathbb{R}^3, \|v\| = 1$. We call $M_v(w) := w - 2\langle v, w \rangle v$ a reflection matrix. M_v mirrors on the hyperplane orthogonal to v . We call*

$$D_{v,\alpha} := \begin{pmatrix} \cos \alpha + v_1^2 (1 - \cos \alpha) & v_1 v_2 (1 - \cos \alpha) - v_3 \sin \alpha & v_1 v_3 (1 - \cos \alpha) + v_2 \sin \alpha \\ v_2 v_1 (1 - \cos \alpha) + v_3 \sin \alpha & \cos \alpha + v_2^2 (1 - \cos \alpha) & v_2 v_3 (1 - \cos \alpha) - v_1 \sin \alpha \\ v_3 v_1 (1 - \cos \alpha) - v_2 \sin \alpha & v_3 v_2 (1 - \cos \alpha) + v_1 \sin \alpha & \cos \alpha + v_3^2 (1 - \cos \alpha) \end{pmatrix}$$

a rotation around v by $\alpha \in \mathbb{R}$.

Next we describe the assumed symmetries of some ideal shapes (which have been conjectured since early numeric simulations).

Conjecture 5.9 (Assumed symmetries of ideal 3_1 , 4_1 and 5_1 knots.). *After a reparametrisation, a translation and a rotation the following symmetry-groups seem plausible from numerical data (see Figure 5.3):*

- *Trefoil³ 3_1 :*

$$\begin{aligned} G_{3_1} &:= \langle D_{(0\ 0\ 1)^t, 2/3\pi} \circ S_{1/3}, D_{(1\ 0\ 0)^t, \pi} \circ R_0 \rangle \\ &= \{ (D_{(0\ 0\ 1)^t, 2/3\pi} \circ S_{1/3})^i \circ (D_{(1\ 0\ 0)^t, \pi} \circ R_0)^j : i = 0, 1, 2, \quad j = 0, 1 \}; \\ |G_{3_1}| &= 6. \end{aligned}$$

- *4_1 -knot:*

$$\begin{aligned} G_{4_1} &:= \langle D_{(0\ 1\ 0)^t, \pi} \circ S_{1/2}, M_{(0\ 1\ 0)^t} \circ D_{(0\ 1\ 0)^t, \pi/2} \circ S_{1/4} \rangle \\ &= \{ (D_{(0\ 1\ 0)^t, \pi} \circ S_{1/2})^i \circ (M_{(0\ 1\ 0)^t} \circ D_{(0\ 1\ 0)^t, \pi/2} \circ S_{1/4})^j : i, j = 0, 1 \}; \\ |G_{4_1}| &= 4. \end{aligned}$$

³The group G_{3_1} is isomorphic to the symmetric group of degree 3. This becomes evident observing the action on the parameter set $\{s_0, s_3, s_3\}$ in Figure 5.12 on page 107.

- 5_1 -knot:

$$\begin{aligned} G_{5_1} &:= \langle D_{(0\ 1\ 0)^t, \pi} \circ R_0 \rangle \\ &= \{(D_{(0\ 1\ 0)^t, \pi} \circ R_0)^j : j = 0, 1\}; \\ |G_{5_1}| &= 2. \end{aligned}$$

Next we need to determine how the group elements described so far act on the Fourier coefficients.

Lemma 5.10 (Actions on Fourier knots). *Let $\gamma(t) = \sum_i^n (a_i \cos(f_i t) + b_i \sin(f_i t))$ be a Fourier knot with $a_i, b_i, \bar{a}_i, \bar{b}_i \in \mathbb{R}^3$ for $i = 1, \dots, n$.*

- Let $M \in O(3)$ be an orthogonal matrix. Then

$$(M.\gamma)(t) = \sum_i (\bar{a}_i \cos(f_i t) + \bar{b}_i \sin(f_i t))$$

with

$$\bar{a}_i := M a_i, \quad \bar{b}_i := M b_i,$$

or

$$\begin{pmatrix} \bar{a}_i \\ \bar{b}_i \end{pmatrix} = \begin{pmatrix} M & 0 \\ 0 & M \end{pmatrix} \begin{pmatrix} a_i \\ b_i \end{pmatrix}$$

- Let S_x be a parameter shift by some $x \in \mathbb{R}$. Then

$$(S_x.\gamma)(t) = \sum_i (\bar{a}_i \cos(f_i t) + \bar{b}_i \sin(f_i t))$$

with

$$\bar{a}_i := \cos(f_i x) a_i + \sin(f_i x) b_i, \quad \bar{b}_i := -\sin(f_i x) a_i + \cos(f_i x) b_i,$$

or

$$\begin{pmatrix} \bar{a}_i \\ \bar{b}_i \end{pmatrix} = \begin{pmatrix} \cos(f_i x) I & \sin(f_i x) I \\ -\sin(f_i x) I & \cos(f_i x) I \end{pmatrix} \begin{pmatrix} a_i \\ b_i \end{pmatrix}$$

- Let R_x be a parameter reflection around $x \in \mathbb{R}$. Then

$$(R_x.\gamma)(t) = \sum_i (\bar{a}_i \cos(f_i t) + \bar{b}_i \sin(f_i t))$$

with

$$\bar{a}_i := \cos(2f_i x) a_i + \sin(2f_i x) b_i, \quad \bar{b}_i := \sin(2f_i x) a_i - \cos(2f_i x) b_i,$$

or

$$\begin{pmatrix} \bar{a}_i \\ \bar{b}_i \end{pmatrix} = \begin{pmatrix} \cos(2f_i x) I & \sin(2f_i x) I \\ \sin(2f_i x) I & -\cos(2f_i x) I \end{pmatrix} \begin{pmatrix} a_i \\ b_i \end{pmatrix}$$

□

Now we can deduce patterns of the Fourier coefficients for curves with these symmetries.

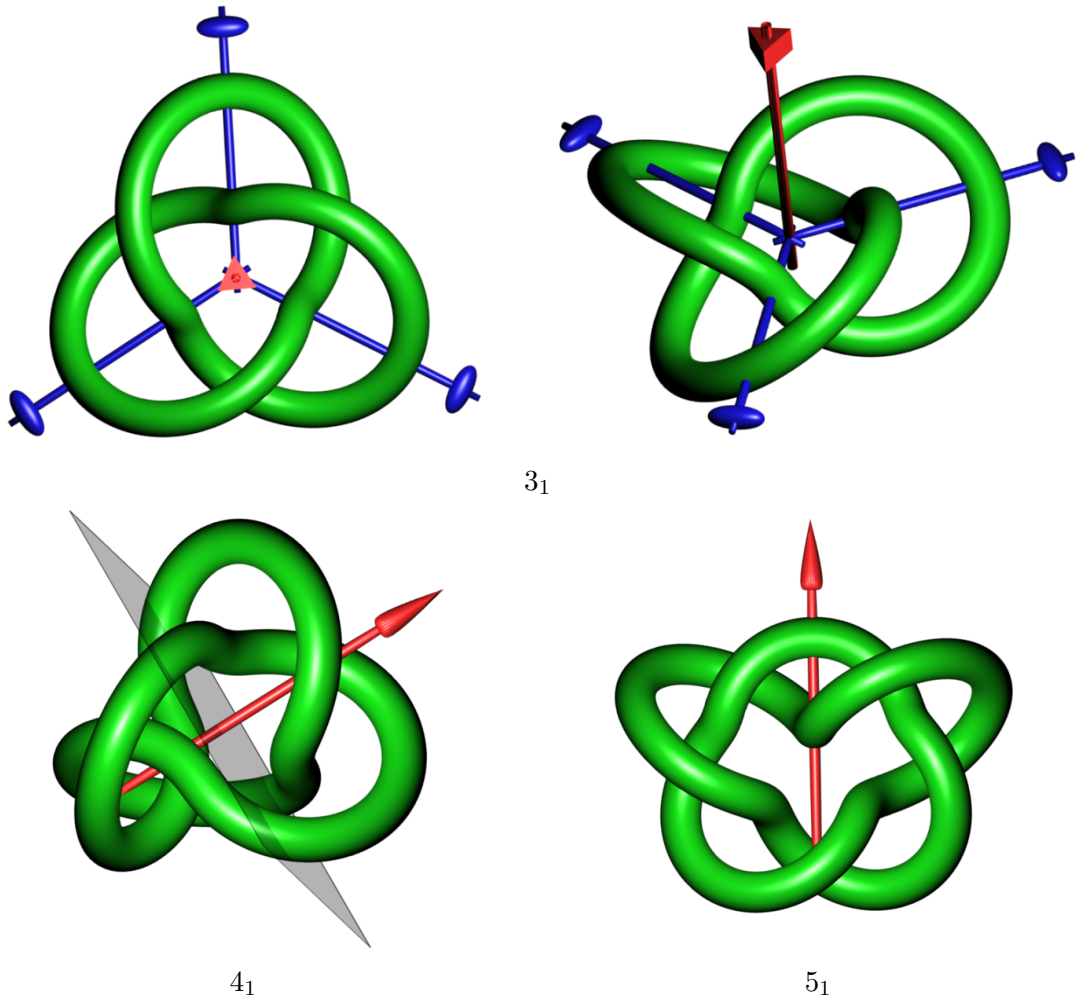


Figure 5.3: Presumed symmetries of the ideal 3_1 , 4_1 and 5_1 knots. The ideal trefoil 3_1 seems to have a 120 degree rotational symmetry around the red axis with the prism and three 180 degree symmetries around the blue axes with the ellipsoids. The ideal 4_1 knot seems to have a 180 degree symmetry around the red axis and a 90 degree rotation around the same axis after a reflection on the grey plane. The ideal 5_1 seems to be symmetric under 180 degree rotations around the red axis. See Conjecture 5.9.

Lemma 5.11 (Fourier coefficients of symmetric 3_1 , 4_1 and 5_1). *Assume that Conjecture 5.9 is true. Then the Fourier-coefficients must fulfil the following identities:*

- *Trefoil: For $i \in \mathbb{N}$:*

$$\begin{aligned} a_{3i+1,1} = -b_{3i+1,2} \in \mathbb{R} \quad , \quad & a_{3i+1,2} = a_{3i+1,3} = b_{3i+1,1} = b_{3i+1,3} = 0 \\ a_{3i+2,1} = b_{3i+2,2} \in \mathbb{R} \quad , \quad & a_{3i+2,2} = a_{3i+2,3} = b_{3i+2,1} = b_{3i+2,3} = 0 \\ & b_{3i+3,3} \in \mathbb{R} \quad , \quad a_{3i+3,1} = a_{3i+3,2} = a_{3i+3,3} = b_{3i+3,1} = b_{3i+3,2} = 0 \end{aligned}$$

- 4_1 : For $i \in \mathbb{N}$:

$$\begin{aligned} a_{4i+1,1} = b_{4i+1,3}, a_{4i+1,3} = -b_{4i+1,1} \in \mathbb{R} \quad , \quad & a_{4i+1,2} = b_{4i+1,2} = 0 \\ & a_{4i+2,2}, b_{4i+2,2} \in \mathbb{R} \quad , \quad a_{4i+2,1} = a_{4i+2,3} = b_{4i+2,1} = b_{4i+2,3} = 0 \\ a_{4i+3,1} = -b_{4i+3,3}, a_{4i+3,3} = b_{4i+3,1} \in \mathbb{R} \quad , \quad & a_{4i+3,2} = b_{4i+3,2} = 0 \\ & a_{4i+4} = b_{4i+4} = 0 \end{aligned}$$

- 5_1 : For $i \in \mathbb{N}$:

$$\begin{aligned} a_{i,1} = a_{i,3} = b_{i,2} = 0 \\ a_{i,2}, b_{i,1}, b_{i,3} \in \mathbb{R} \end{aligned}$$

Conversely if the coefficients fulfil the identities, the curve has the corresponding symmetry.

Proof. Note that two Fourier knots describe the same curve iff all coefficients coincide, since $\sin(f_i t)$ and $\cos(f_i t)$ form an orthogonal basis. Furthermore, a curve γ is G -symmetric iff $\gamma = \gamma_G$.

- **Trefoil:** Let γ be a G_{3_1} -symmetric curve. By Lemma 5.10 there exists for each $g \in G_{3_1}$ and each frequency f_i a 6-dimensional matrix M_g^i that acts on the coefficient vector such that $M_g^i \begin{pmatrix} a_i \\ b_i \end{pmatrix}$ is the i -th coefficient vector of $g \cdot \gamma$.

Computing

$$M_i := \frac{\sum_{g \in G_{3_1}} M_g^i}{|G_{3_1}|}$$

yields:

$$M_{3i+1} = \begin{pmatrix} 1/2 & 0 & 0 & 0 & -1/2 & 0 \\ 0 & 0 & 0 & 0 & 0 & 0 \\ 0 & 0 & 0 & 0 & 0 & 0 \\ 0 & 0 & 0 & 0 & 0 & 0 \\ -1/2 & 0 & 0 & 0 & 1/2 & 0 \\ 0 & 0 & 0 & 0 & 0 & 0 \end{pmatrix}$$

$$M_{3i+2} = \begin{pmatrix} 1/2 & 0 & 0 & 0 & 1/2 & 0 \\ 0 & 0 & 0 & 0 & 0 & 0 \\ 0 & 0 & 0 & 0 & 0 & 0 \\ 0 & 0 & 0 & 0 & 0 & 0 \\ 1/2 & 0 & 0 & 0 & 1/2 & 0 \\ 0 & 0 & 0 & 0 & 0 & 0 \end{pmatrix}$$

$$M_{3i+3} = \begin{pmatrix} 0 & 0 & 0 & 0 & 0 & 0 \\ 0 & 0 & 0 & 0 & 0 & 0 \\ 0 & 0 & 0 & 0 & 0 & 0 \\ 0 & 0 & 0 & 0 & 0 & 0 \\ 0 & 0 & 0 & 0 & 0 & 0 \\ 0 & 0 & 0 & 0 & 0 & 1 \end{pmatrix}$$

Note that $M_i \begin{pmatrix} a_i \\ b_i \end{pmatrix}$ is the i -th coefficient vector of $\gamma_{G_{3_1}}$ and by the above reasoning we have

$$\begin{pmatrix} a_i \\ b_i \end{pmatrix} = M_i \begin{pmatrix} a_i \\ b_i \end{pmatrix}$$

which yields the desired relations.

- 4_1 : For this knot the matrices are

$$M_{4i+1} = \begin{pmatrix} 1/2 & 0 & 0 & 0 & 0 & 1/2 \\ 0 & 0 & 0 & 0 & 0 & 0 \\ 0 & 0 & 1/2 & -1/2 & 0 & 0 \\ 0 & 0 & -1/2 & 1/2 & 0 & 0 \\ 0 & 0 & 0 & 0 & 0 & 0 \\ 1/2 & 0 & 0 & 0 & 0 & 1/2 \end{pmatrix}$$

$$M_{4i+2} = \begin{pmatrix} 0 & 0 & 0 & 0 & 0 & 0 \\ 0 & 1 & 0 & 0 & 0 & 0 \\ 0 & 0 & 0 & 0 & 0 & 0 \\ 0 & 0 & 0 & 0 & 0 & 0 \\ 0 & 0 & 0 & 0 & 1 & 0 \\ 0 & 0 & 0 & 0 & 0 & 0 \end{pmatrix}$$

$$M_{4i+3} = \begin{pmatrix} 1/2 & 0 & 0 & 0 & 0 & -1/2 \\ 0 & 0 & 0 & 0 & 0 & 0 \\ 0 & 0 & 1/2 & 1/2 & 0 & 0 \\ 0 & 0 & 1/2 & 1/2 & 0 & 0 \\ 0 & 0 & 0 & 0 & 0 & 0 \\ -1/2 & 0 & 0 & 0 & 0 & 1/2 \end{pmatrix}$$

$$M_{4i+4} = \begin{pmatrix} 0 & 0 & 0 & 0 & 0 & 0 \\ 0 & 0 & 0 & 0 & 0 & 0 \\ 0 & 0 & 0 & 0 & 0 & 0 \\ 0 & 0 & 0 & 0 & 0 & 0 \\ 0 & 0 & 0 & 0 & 0 & 0 \\ 0 & 0 & 0 & 0 & 0 & 0 \end{pmatrix}$$

and we can deduce the relations.

- 5_1 : Similarly we compute

$$M_i := \frac{\sum_{g \in G_{5_1}} M_g^i}{|G_{5_1}|}$$

and obtain

$$M_i = \begin{pmatrix} 0 & 0 & 0 & 0 & 0 & 0 \\ 0 & 1 & 0 & 0 & 0 & 0 \\ 0 & 0 & 0 & 0 & 0 & 0 \\ 0 & 0 & 0 & 1 & 0 & 0 \\ 0 & 0 & 0 & 0 & 0 & 0 \\ 0 & 0 & 0 & 0 & 0 & 1 \end{pmatrix}$$

which immediately implies the relations.

□

5.5 Knot Computations

In this section, we want to present our numeric results. All numbers have been computed with `libbiarc`⁴. For optimising the trefoil 3_1 in \mathbb{R}^3 we used simulated annealing [KGV83] of Fourier coefficients enforcing the symmetry as in Lemma 5.11. The energy we are minimising in \mathbb{R}^3 is ropelength $\mathcal{R}[\cdot]$ (see Definition 2.28). For evaluating the energy we interpolated the Fourier knot with a biarc curve, resolving the high-curvature regions much more finely than the outer loops of the trefoil. Annealing the Fourier

⁴`libbiarc` version 96c4cef03910, see [C10].

coefficients with symmetry enforced turned out to be much faster than annealing the point-tangent pairs as it was done in [S04, CLMS05] with localized moves. In less than a week of computations starting from an arbitrary trefoil we reached a better thickness than Laurie and Smutny after month long computations. There are two reasons for this performance boost. First and foremost by enforcing the symmetry of the trefoil as in Lemma 5.11 we reduce the degrees of freedom to one sixth of the original number. Second, simulated annealing on Fourier coefficients can be regarded as non-local coordinated moves on biarcs while [S04, CLMS05] only considered local moves. Nevertheless annealing remains a very slow algorithm compared to the piecewise linear simulations of SONO [P98] and RidgeRunner [CPR05] in \mathbb{R}^3 . But adapting these algorithms to find maximisers of thickness in \mathbb{S}^3 would at least require some work.

For shapes in \mathbb{S}^3 we optimise their Fourier coefficients as \mathbb{R}^3 knots then interpolate with biarcs in \mathbb{R}^3 and finally project those point-tangent pairs to \mathbb{S}^3 by the stereographic projection from Definition 2.21 to compute the energy of the biarc-curve in \mathbb{S}^3 . Here the energy is $1/\Delta[\cdot]$, since we want to maximise thickness in \mathbb{S}^3 . The advantage of this approach is that we can use the Fourier representation and thus do not get stuck in non-proper configurations. The price we have to pay is that the sampling of the biarc curve in \mathbb{S}^3 is non-uniform in a way that we do not control.

It is remarkable that SONO, RidgeRunner and our implementation of Fourier knots all ultimately rely on interpolation with arc-curves to get true lower bounds. SONO and RidgeRunner both work on piecewise linear polygonal knots that can be turned into arc-curves by inscribing small circular arcs which yields a lower bound on thickness [BPR05]. Arc curves are a natural choice since they are $C^{1,1}$.

For each biarc curve γ we state the degrees of freedom used for the Fourier coefficients,⁵ the number of point-tangent data pairs used to compute the biarc approximation, and finally the arc-length and thickness of the biarc approximation.⁶

Next we show a picture of each knot in \mathbb{R}^3 with the orientation and $\gamma(0)$ indicated by an arrow. For this purpose we project the \mathbb{S}^3 knots to \mathbb{R}^3 using stereographic projection. Note that the knot gets distorted and distances in \mathbb{S}^3 are difficult to estimate from their \mathbb{R}^3 projections. Also symmetries may get destroyed. As a small visual help to the reader we included a transparent sphere of radius 1 that divides \mathbb{S}^3 in two equal sized balls – the interior and the exterior of the sphere.

We continue with plots of the point to point distance function (already mentioned on page 74)

$$\text{pp}[\gamma](s, t) := |\gamma(s) - \gamma(t)| \tag{5.1}$$

and the Δ/pt and Δ/tt functions from Definition 2.3 and 2.5 respectively. Along the horizontal from left to right we sample $s \in [0, \mathcal{L}[\gamma]]$. Along the vertical we sample from top to bottom $t \in [0, \mathcal{L}[\gamma]]$. The biarc-curve γ is parametrised by arc-length. We use the colour gradient shown in Figure 5.4 from the minimum to the maximum of each function, except that the rainbow part is shrunk to only 1% of the whole scale. We chose such an oscillating colour gradient to make the fine details of the surface plots more visible.

⁵ A Fourier knot has 3 degrees of freedom for each coefficient $a_i, b_i \in \mathbb{R}^3$ of frequency f_i , but this number is reduced when symmetries are enforced.

⁶ We also included MD5-checksums of the used files. The MD5sums enable the reader to uniquely link data files to the plotted graphs and avoid confusion with their previous or future versions. Or even search for the data on the internet.



Figure 5.4: The colour gradient that was used for the plots in this section. The last rainbow part is shrunk to only 1% instead of the displayed 8% of the total scale in order to reveal the fine details.

Further, we plot the curvature of γ as solid line, i.e. Δ/r_i where r_i is the radius of arc i and Δ/ρ_{pt} . In the same graph we also plot Δ/ρ_{pt} as dotted line, usually close to 1. Recall, that ρ_{pt} and r_i are upper bounds for Δ . And finally we zoom in on Δ/ρ_{pt} .

5.5.1 Reading the Plots

While reading this section the reader is advised to consult Section 5.5.2 on page 88 showing the corresponding plots for the trefoil in \mathbb{R}^3 . The pp, pt and tt plots are at first not so easy to understand. First notice that they are invariant under rigid body motions, i.e. for any curve $\gamma : \mathbb{S} \rightarrow \mathbb{R}^N$ and any orthogonal matrix $M \in O(N)$ we have

$$\text{pp}[M.\gamma] = \text{pp}[\gamma], \quad (5.2)$$

$$\text{pt}[M.\gamma] = \text{pt}[\gamma], \quad (5.3)$$

$$\text{tt}[M.\gamma] = \text{tt}[\gamma]. \quad (5.4)$$

Apart from these orthogonal transformations the functions are believed but not known to characterise the curve. Furthermore, pp and tt are symmetric about the diagonal,

$$\text{pp}(s, t) = \text{pp}(t, s), \quad \text{tt}(s, t) = \text{tt}(t, s), \quad \forall s, t \in \mathbb{S},$$

but pt generally is not.

What features can be discovered in those plots? Most beautifully, symmetry groups manifest themselves in all three plots. Recall from Section 5.3 that a symmetry group of a curve can usually be factorised into a subgroup of the orthogonal group $O(N)$ and a group P acting on the parameter. Now let γ be G -symmetric and assume that G can be factorised, i.e. each $g \in G$ can be written as $g = m \circ p$ with $m \in O(N)$ and p acting only on the parameter. This yields for each $g = m \circ p \in G$

$$\text{pp}[\gamma](s, t) = \text{pp}[g.\gamma](s, t) = \text{pp}[m.\gamma](p(s), p(t)) = \text{pp}[\gamma](p(s), p(t)),$$

and similarly

$$\text{pt}[\gamma](s, t) = \text{pt}[\gamma](p(s), p(t)) \quad \text{and} \quad \text{tt}[\gamma](s, t) = \text{tt}[\gamma](p(s), p(t)).$$

The plots of the trefoil in Section 5.5.2 show the (enforced) symmetry shifting one third along the diagonal stemming from the parameter shift $S_{1/3}$ (see Conjecture 5.9) and the point symmetry in the points $(0, 0)$, $(1/3, 1/3)$ and $(2/3, 2/3)$ stemming from the parameter reflection R_0 . The careful reader will notice that there is another point symmetry in $(1/6, 1/6)$, $(1/2, 1/2)$ and $(5/6, 5/6)$. This is due to the fact that the symmetry axis of the 180 degree rotations intersect the knot a second time (see Figure 5.3) so in the generator, we may replace R_0 by $R_{1/2}$.

We are particularly interested in the (absolute) maxima of the $1/pt$ plots (i.e. the minima of the pt -function), as they correspond to parameters where the thickness is attained. The red sinuous line in the $1/pt$ -plot of the trefoil in \mathbb{R}^3 is very close to these local minima. Remember that the rainbow part of the colour-gradient is only 1% of the total scale such that this area is finely resolved.

Another phenomenon is $1/pt$ dropping to 0 at isolated points (i.e. pt becomes infinity). This happens in the blue spots surrounded by green circles e.g. close to the points $(1/6, 1/6)$ and $(1/5, 2/3)$. Such a hole appears, when the line tangent to the knot in t intersects the knot another time in s .

Finally there are the three big green-purple squares along the diagonal, that correspond to the almost circular outer loops of the trefoil. Since pt is constant on circles, circular parts of a curve produce those squares. As a consequence of using biarc-curves, you would see squares close to the diagonal if you would zoom in enough (see Section 5.5.7 for an example).

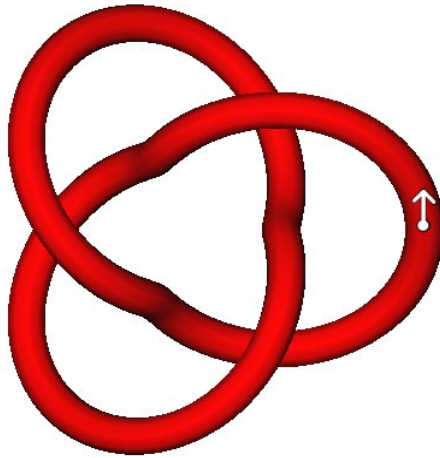
The same phenomenon is visible in the $1/tt$ -plots, but otherwise we use them mainly to see if there is still a lot of noise, since they are most sensitive to that.

5.5.2 3_1 in \mathbb{R}^3

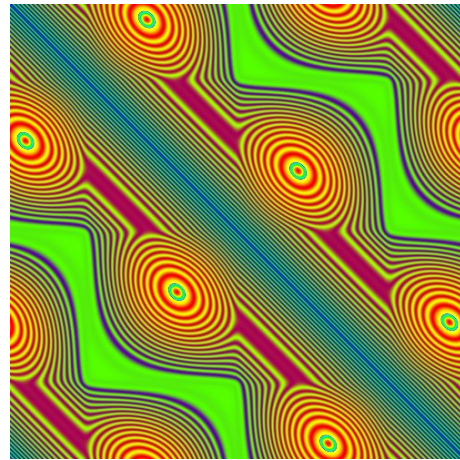
The trefoil in \mathbb{R}^3 was computed using simulated annealing of Fourier coefficients with the conjectured symmetry enforced. The interpolation with biarcs is non-uniform and resolves the highly curved parts more finely (see [C10] for details). It looks well converged, as there is only a little noise in the $1/tt$ -plot. See also Figure 5.6 on page 99 for a 3D-plot of the pp -function.

The ropelength is slightly worse than the 32.74318 reported in [BPP08]. The curvature looks similar to [BPP08] but it does not touch 1 which is possibly difficult to achieve with Fourier knots. Although it is quite different from the curvature found in [S04, CLMS05], which drops to 0 at a few points, and with respect to Example 2.34 we do not feel safe enough to claim what the curvature of the real ideal trefoil would look like. The ρ_{pt} function is very close to constant, which is necessary for an ideal shape without straight segments [GM99].

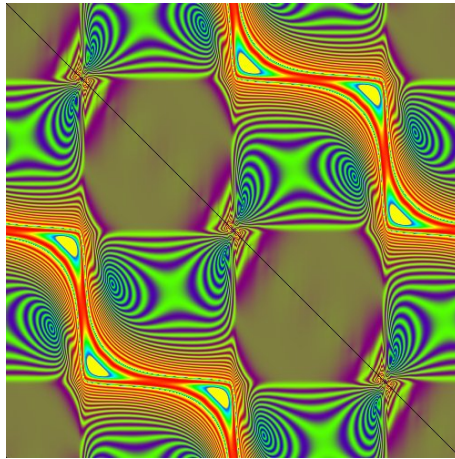
| | | |
|---------------------------------|----------------------------------|----------|
| Name | k3_1 | |
| Degrees of freedom | 165 | |
| Biarc nodes | 333 | |
| Arc-length \mathcal{L} | 1 | |
| Thickness Δ | 0.030539753 | |
| Ropelength \mathcal{L}/Δ | 32.744208 | |
| MD5sums | cf5e2f8550c4c1e91a2fd7f5e9830343 | k3_1.3 |
| | 531492b73b2ec4be2829f6ab2239d4d5 | k3_1.pkf |



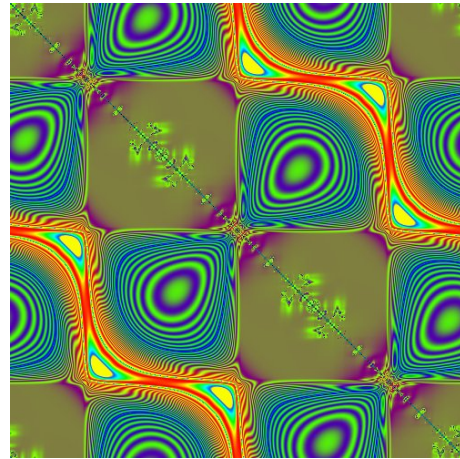
k3_1



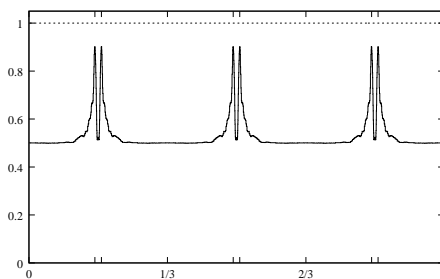
pp



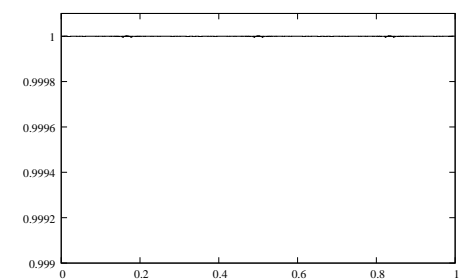
Δ/pt



Δ/tt



$\Delta/(\text{radius of curvature})$



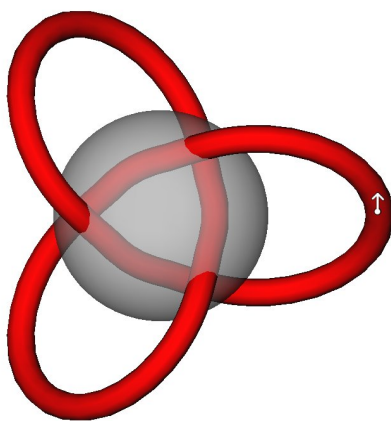
Δ/ρ_{pt}

5.5.3 3_1 in S^3

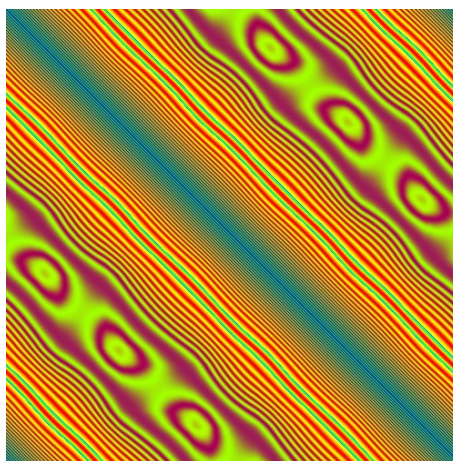
We tried in various ways to find the maximal thickness trefoil in S^3 . Local annealing of point-tangent data pairs of biarcs, annealing Fourier coefficients and annealing Fourier coefficients with symmetry (of the \mathbb{R}^3 trefoil) enforced. Each time we ended up close to the \mathfrak{g} -trefoil described in Section 4.3, but never beat its thickness. Below is the thickest trefoil we found by annealing starting from an arbitrary trefoil.

The $1/pp$ -plot looks well converged, $1/pt$ and $1/tt$ show some noise.

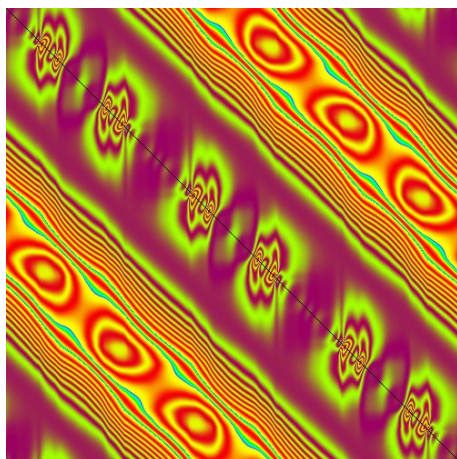
| | | |
|-------------------------|----------------------------------|------------------------|
| Name | k3_1_on_s3_numeric | |
| Degrees of freedom | 45 | |
| Biarc nodes | 300 | |
| Arclength \mathcal{L} | 15.409271 | |
| Thickness Δ | 0.58778345 | |
| MD5sums | 3721b716825117d1f4774c08f4946106 | k3_1_on_s3_numeric.3 |
| | c3df748259b71b19e8e2c49ee955d70a | k3_1_on_s3_numeric.pkf |



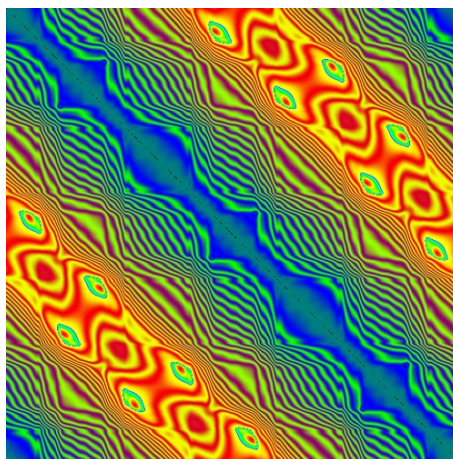
k3_1_on_s3_numeric



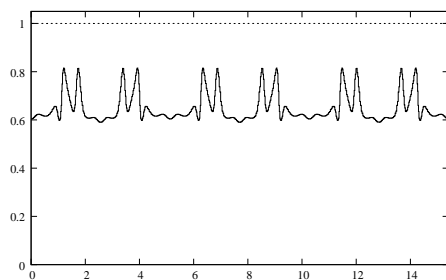
pp



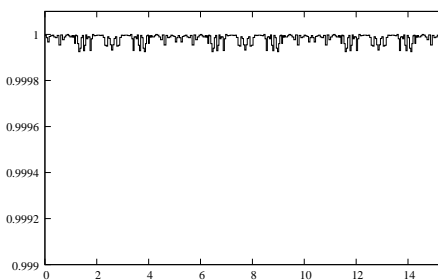
Δ/pt



Δ/tt



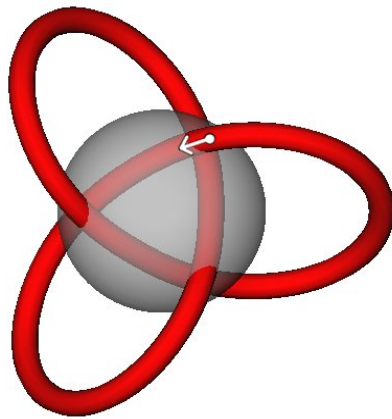
$\Delta/(\text{radius of curvature})$



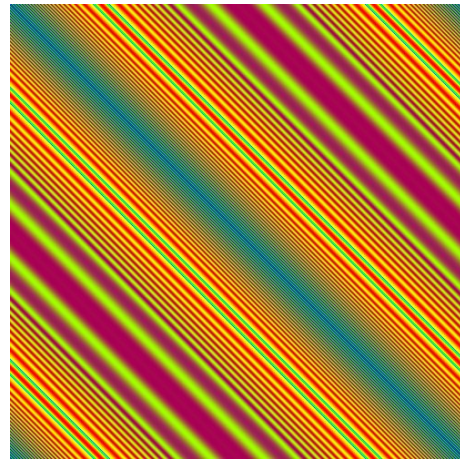
Δ/ρ_{pt}

Compare this to the generated \mathfrak{g} -trefoil below. Since the plots are constant on lines parallel to the diagonal we also look at a vertical cross-section.

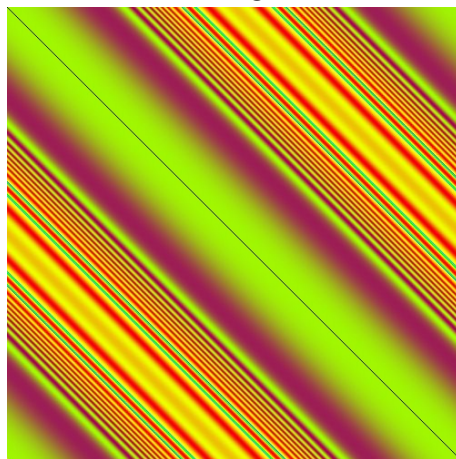
| | | |
|-------------------------|--|--------------------------|
| Name | k3_1_on_s3_generated | |
| Biarc nodes | 200 | |
| Arclength \mathcal{L} | 15.390598 | |
| Thickness Δ | $0.5877851 \approx \sin \frac{\pi}{5}$ | |
| MD5sums | a31a98545743150090221d7640ea28dc | k3_1_on_s3_generated.pkf |



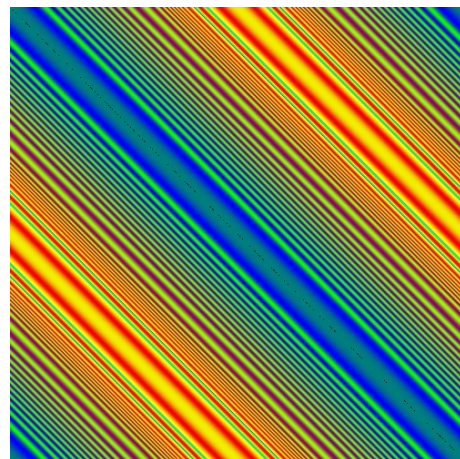
k3_1_on_s3_generated



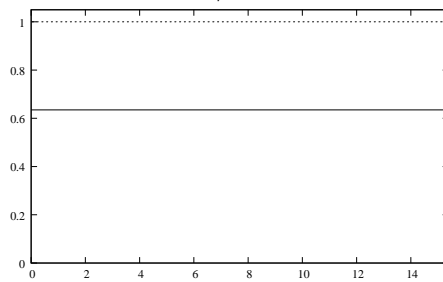
pp



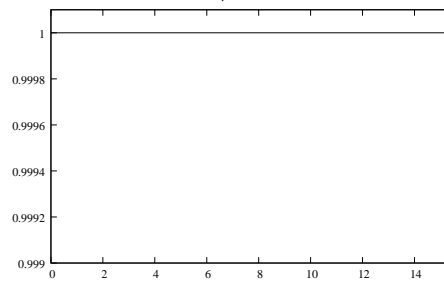
Δ/pt



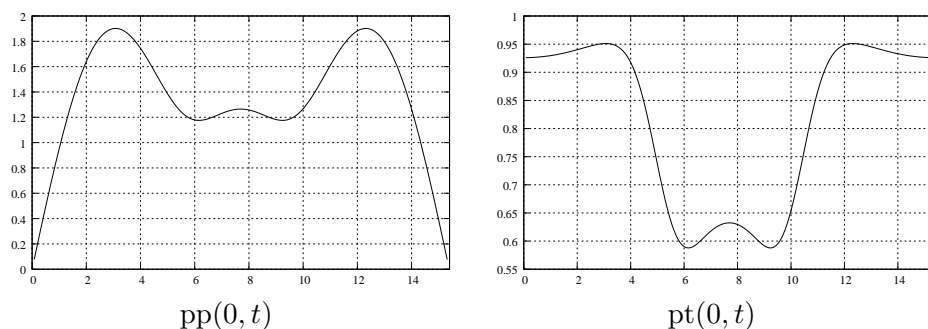
Δ/tt



$\Delta/(\text{radius of curvature})$



Δ/ρ_{pt}

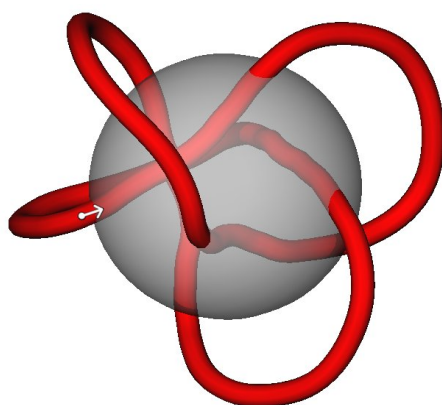


5.5.4 4_1 in \mathbb{S}^3

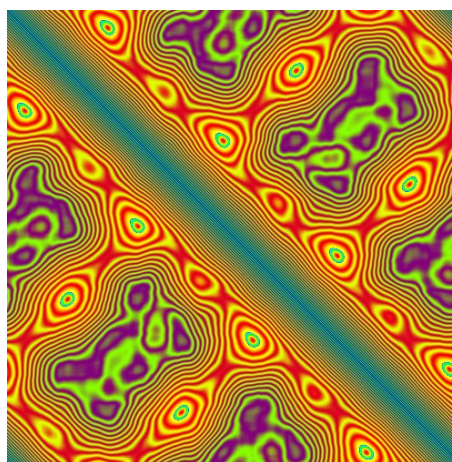
This simulation is considerably less well-converged. It seems to have similar symmetries to the \mathbb{R}^3 ideal 4_1 knot (see Conjecture 5.9) visible by the $1/4\mathcal{L}$ shift-symmetry along the diagonal (and the projection to \mathbb{R}^3). Unlike \mathbb{R}^3 there may also be a point symmetry at $(1/2\mathcal{L}, 1/2\mathcal{L})$ corresponding to a new 180 degree rotation. The curve's thickness is very close to $\sin(\pi/6)$, supporting Conjecture 4.18.

But there could be another explanation for the knot being so 'ugly'. If the ideal shape is not unique and the thickness is attained only in a few points (e.g. on a circle as in Conjecture 4.18) then other parts of the curve with $\rho_{pt} < \Delta$ could wander around freely.

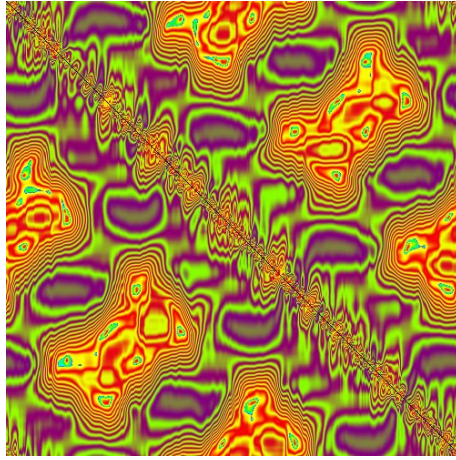
| | | |
|-------------------------|---|------------------|
| Name | k4_1_on_s3 | |
| Degrees of freedom | 534 | |
| Biarc nodes | 200 | |
| Arclength \mathcal{L} | 18.234058 | |
| Thickness Δ | $0.49999257 \approx \sin \frac{\pi}{6}$ | |
| MD5sums | 228162264519e0351c6f55713b21274a | k4_1_on_s3.coeff |
| | c3ebdf677ba7168a4f90afbfa6f7d5bd | k4_1_on_s3.pkf |



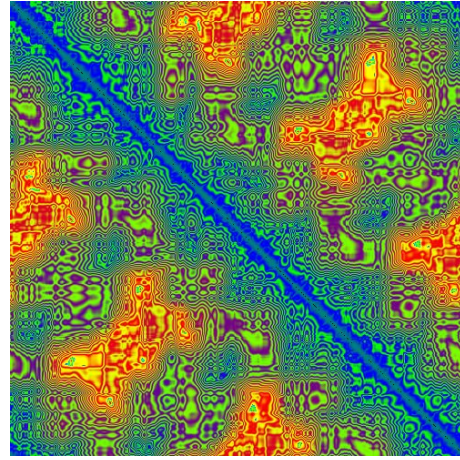
k4_1_on_s3



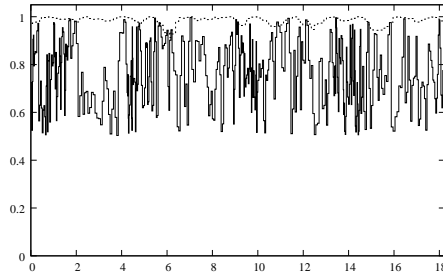
pp



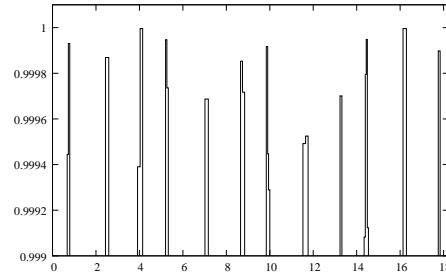
Δ/pt



Δ/tt



$\Delta/(\text{radius of curvature})$

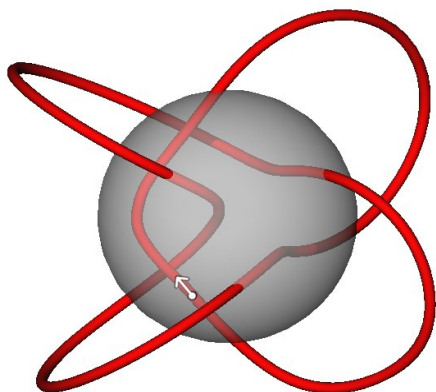


Δ/ρ_{pt}

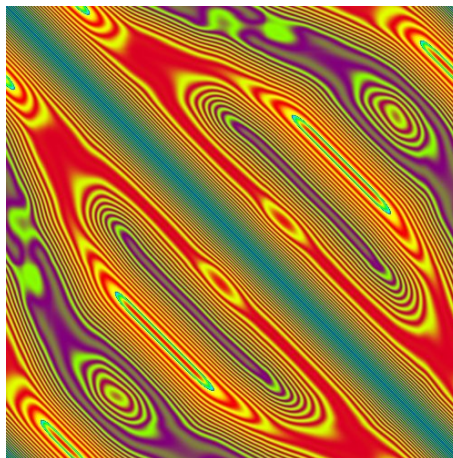
5.5.5 5_1 in \mathbb{S}^3

This knot seems to be reasonably converged. During the optimisation no symmetry was enforced, but the results show, as in \mathbb{R}^3 , a 180 degree rotational symmetry. Accordingly the plots show a point symmetry to a point close to $(1/2\mathcal{L}, 1/2\mathcal{L})$. The point is slightly shifted since the parametrisation of the curve does not start on the symmetry axis. The curve's thickness is close to $\sin(\pi/6)$, again supporting Conjecture 4.18. The ρ_{pt} function is close to Δ except around 1 which corresponds to the first “knee” in the projection to \mathbb{R}^3 . Considering that the knot looks well converged it may really not be in contact around this point. Something similar happened in the tight clasp [Sta03, CFKSW04] and the argument from [GM99] does not work in \mathbb{S}^3 since there are no dilations. Also note that this knot is thicker than the thickest $T_{2,5}$ Clifford torus knot described in Remark 4.16 that only has thickness $\sin \frac{\pi}{7} \approx 0.434$.

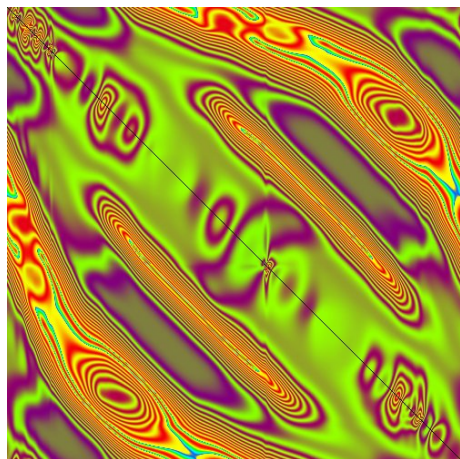
| | | |
|-------------------------|---|------------------|
| Name | k5_1_on_s3 | |
| Degrees of freedom | 210 | |
| Biarc nodes | 300 | |
| Arclength \mathcal{L} | 20.414732 | |
| Thickness Δ | 0.49993744 $\approx \sin \frac{\pi}{6}$ | |
| MD5sums | 0050085e41865d57a2408b0a7ed2c113 | k5.1_on_s3.coeff |
| | ec2eb6c8c49f83a1199f57ae0fe0ae2b | k5.1_on_s3.pkf |



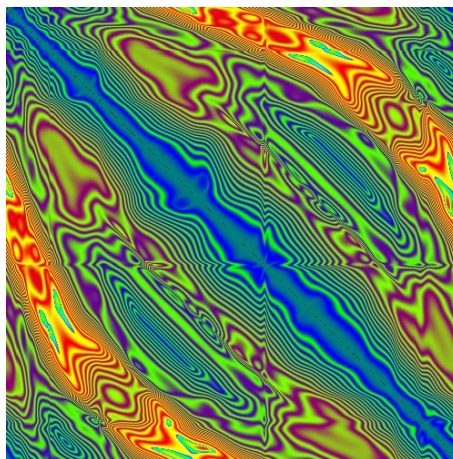
k5_1_on_s3



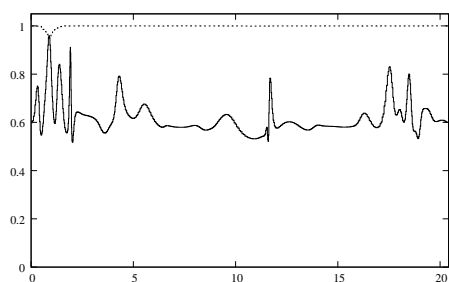
pp



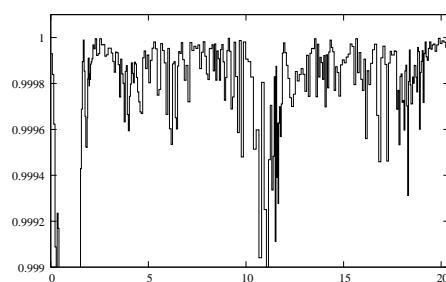
Δ/pt



Δ/tt



$\Delta/(\text{radius of curvature})$

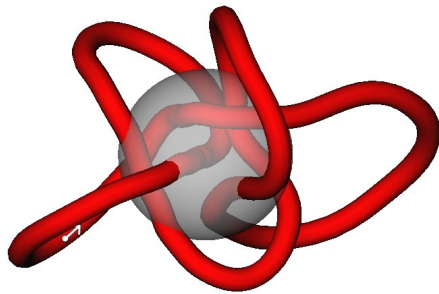


Δ/ρ_{pt}

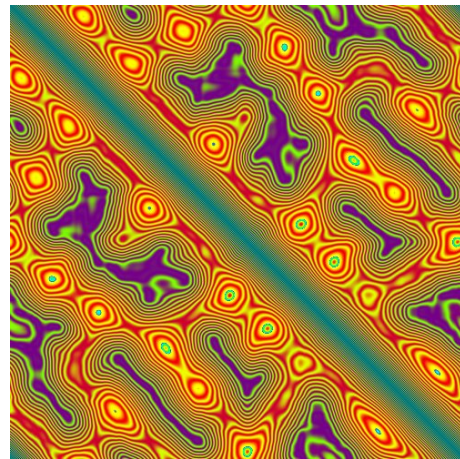
5.5.6 3.1p3.1 in \mathbb{S}^3

Again this knot is badly converged. Maybe there is a point symmetry. The ρ_{pt} function is comparatively close to Δ .

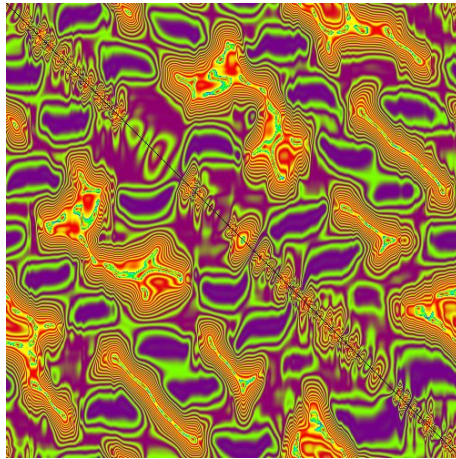
| | | |
|-------------------------|----------------------------------|---------------------|
| Name | kp31p31_on_s3 | |
| Degrees of freedom | 294 | |
| Biarc nodes | 300 | |
| Arclength \mathcal{L} | 24.04607 | |
| Thickness Δ | 0.45782474 | |
| MD5sums | 8f20ccec30d668e200840473ff2d1721 | kp31p31_on_s3.coeff |
| | 6f244dd0adce7cec5d011785e0c8cc7a | kp31p31_on_s3.pkf |



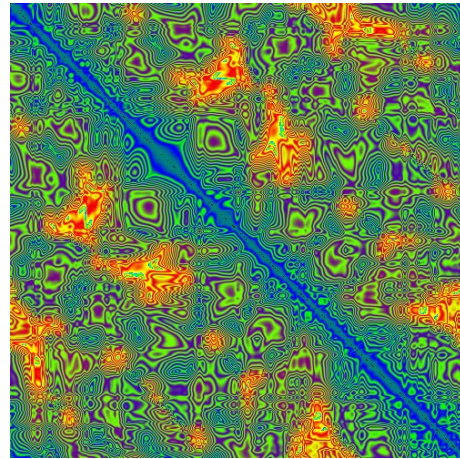
kp31p31_on_s3



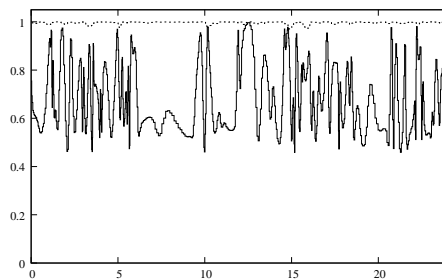
pp



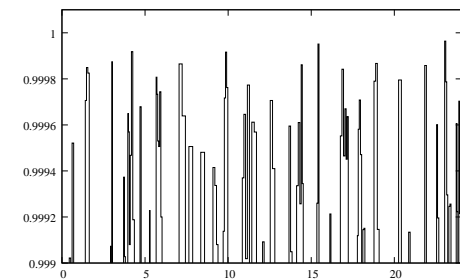
Δ/pt



Δ/tt



$\Delta/(\text{radius of curvature})$

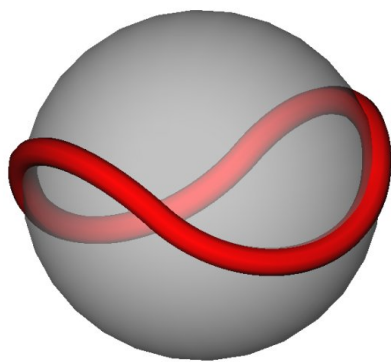


Δ/ρ_{pt}

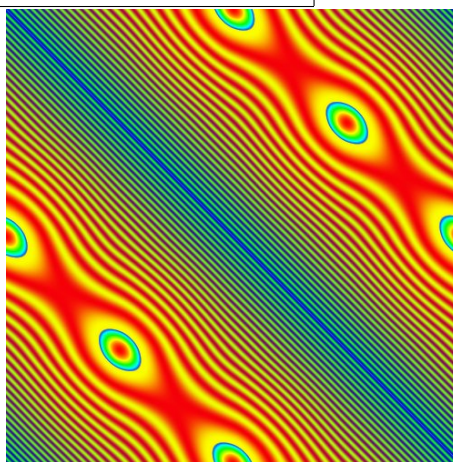
5.5.7 Competitor β_τ with $\alpha = 0.8$ on \mathbb{S}^2

For completeness and comparison we include a generated β_τ from Lemma 3.15 with $\alpha = 0.8$, i.e. $\tau \approx 0.86$.

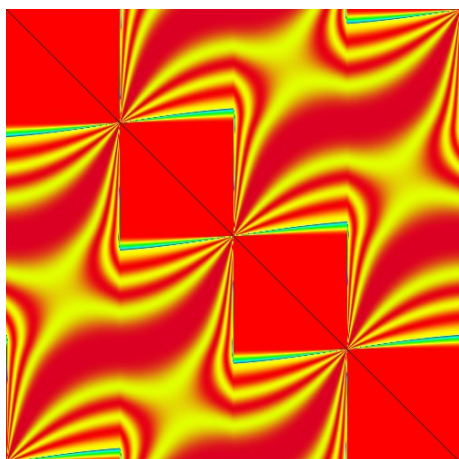
| | |
|-------------------------|---|
| Name | beta_tau_0_8 |
| Biarc nodes | 100 |
| Arclength \mathcal{L} | 6.6343751 |
| Thickness Δ | 0.8618005 |
| MD5sums | cdf199e0372f0da2425a6c6bb92a51f1 beta_tau_0_8.pkf |



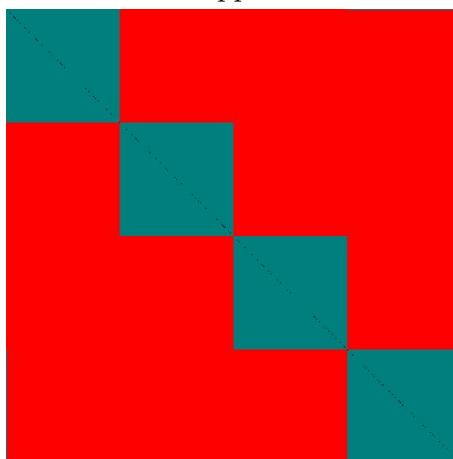
beta_tau_0_8



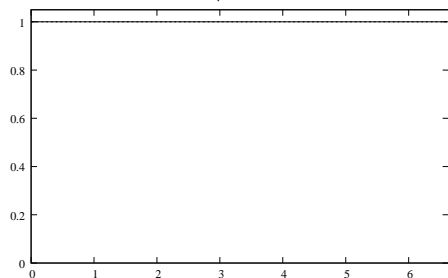
pp



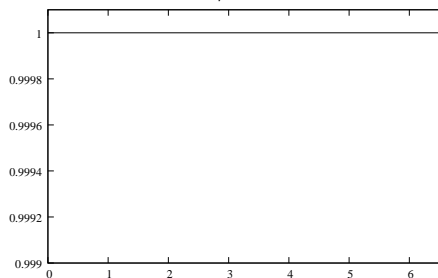
Δ/pt



Δ/tt



$\Delta/(\text{radius of curvature})$



Δ/ρ_{pt}

5.6 Ambient Isotopy of the Ideal Trefoil and its Contact Curve

The goal of this section is to explain why the contact curve of ‘the’ ideal trefoil, i.e. the set where the tubular neighbourhood touches itself, is also a trefoil.

Recall from Definition 2.15 that we call

$$c(s, t) := \gamma(t) - \gamma(s)$$

a contact chord of a curve γ if $|c(s, t)| = 2\Delta[\gamma]$ and $\gamma(s) - \gamma(t)$ is orthogonal to γ . We then say s and t are (globally) in contact.

For the rest of this section we fix $\gamma := k_{3_1} \in C^1(\mathbb{S}, \mathbb{R}^3)$ to be ‘the’ ideal trefoil with constant speed and arc length $|\gamma'| \equiv 1$. Numerical approximations of the ideal trefoil γ suggest [S04, CLMS05, ACPR05] that

Hypothesis 5.12.

(H1) *Every parameter r of the trefoil is globally in contact with precisely two distinct parameters that we denote by $\sigma(r)$ and $\tau(r)$, such that the contact chords $c(r, \sigma(r))$ and $c(r, \tau(r))$ are continuous functions in r .*

(H2) *There is some $s \in \mathbb{S}$, such that $\sigma(\sigma(s)) \neq s$,*

(H3) *The angle between the contact chords $\angle(c(r, \sigma(r)), c(r, \tau(r)))$ is bounded away from zero.*

Lemma 5.13. *Assuming Hypothesis 5.12, the functions $\sigma : \mathbb{S} \rightarrow \mathbb{S}$ and $\tau : \mathbb{S} \rightarrow \mathbb{S}$ defined above are*

- (a) *continuous,*
- (b) *(locally) strictly monotone⁷,*
- (c) *surjective,*
- (d) *fix-point free,*
- (e) *injective,*
- (f) *orientation preserving.*

Therefore σ and τ are homeomorphisms. Furthermore we have

- (g) $\sigma(s) \neq \sigma^{-1}(s) \quad \forall s \in \mathbb{S},$
- (h) $\tau = \sigma^{-1}.$

Proof. The proofs (a)-(f) are the same for τ and σ .

- (a) The curve γ is a homeomorphism on its image and (H1) implies that $\sigma(r) = \gamma^{-1}(c(r, \sigma(r)) + \gamma(r)) \in C^0$. Similarly for τ .

⁷We consider σ as a function from $[0, 1]$ to $[\sigma(0), \sigma(0) + 1]$.

- (b) If σ was locally constant, this would imply more than two contact chords contradicting (H1). Next we show, that it cannot have a local extremum and must therefore be strictly monotone.

Assume the contrary. By restriction to a small interval, we may treat σ as a continuous real function. W.l.o.g. σ has a local maximum in x . Then there exists an $\varepsilon \in (0, 1/8)$ and two sequences $a_i, b_i \in (x - \varepsilon, x + \varepsilon), a_i < x < b_i$, such that $\sigma(a_i) = \sigma(b_i) \rightarrow \sigma(x)$ for $i \rightarrow \infty$. This implies that the two different contact chords $c(a_i, \sigma(a_i), c(b_i, \sigma(b_i)))$ converge to the single $c(x, \sigma(x))$ contradicting (H3).

- (c) Assuming the contrary implies a local maximum contradicting (b).
- (d) A fix-point s contradicts the definition of a contact chord: $c(s, \sigma(s)) = c(s, s) = 0$.
- (e) With respect to (b), we have to rule out that σ covers \mathbb{S} multiple times. But this would imply a fixed point contradicting (d).
- (f) Assume σ was orientation reversing. We show that there exists a fixed point: Define $f(h) := \sigma(0 + h)$. Obviously $0 < f(0)$ by (d). The function f is monotone decreasing by assumption, while $0 + h$ is increasing. Therefore there exists h^* with $0 + h^* = f(h^*)$ and h^* is a fix-point of σ contradicting (d).
- (g) Define $S := \{s \in \mathbb{S} : \sigma(s) \neq \sigma^{-1}(s)\}$. Notice, that S is open and by (H2) non-empty. Let $s_i \in S$ be some sequence with $s_i \rightarrow s$ and consider the contact chords $c(s_i, \sigma(s_i))$ and $c(s_i, \sigma^{-1}(s_i))$. By (H3) we deduce $\sigma(s) \neq \sigma^{-1}(s)$, i.e. S is closed as well and therefore $S = \mathbb{S}$.
- (h) At any given $s \in \mathbb{S}$ consider the three potential contact chords $c(s, \sigma(s)), c(s, \tau(s))$ and $c(s, \sigma^{-1}(s))$, the first two are different by (H1), $c(s, \sigma(s)) = c(s, \sigma^{-1}(s))$ is impossible by (g). Thus $c(s, \sigma^{-1}(s)) = c(s, \tau(s))$, which resolves to $\tau = \sigma^{-1}$.

□

We may parametrise the union of all contact chords as the contact surface

$$\Sigma(s, h) := \gamma(s) + h \cdot c(s, \sigma(s)) = \gamma(s) + h(\gamma(\sigma(s)) - \gamma(s)),$$

for $s \in \mathbb{S}, h \in [0, 1]$. This defines a ruled surface with boundary $\gamma(\mathbb{S})$. Furthermore we define the contact curve

$$\gamma_{1/2}(s) := \Sigma(s, 1/2) = \frac{\gamma(s) + \gamma(\sigma(s))}{2},$$

where the tubular neighbourhood of γ touches itself.

Here, we have to make a stronger assumption on the smoothness of σ and on the angles between the tangents along a contact chord (see Figure 5.5) :

Hypothesis 5.14.

(H4) $\sigma \in C^1(\mathbb{S}, \mathbb{S}),$

(H5) $\gamma'(s) \cdot \gamma'(\sigma(s)) \geq 0 \quad \forall s \in \mathbb{S}.$

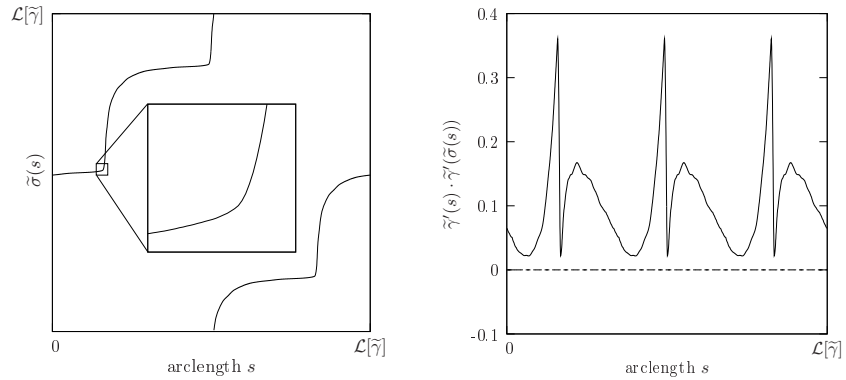


Figure 5.5: The left plot shows the periodic function $\tilde{\sigma}(s)$ for a numeric approximation of an ideal trefoil. It seems to be a C^1 -function. On the right we plot the dot product between the tangents at s and $\tilde{\sigma}(s)$ to verify that it is bounded away from zero.

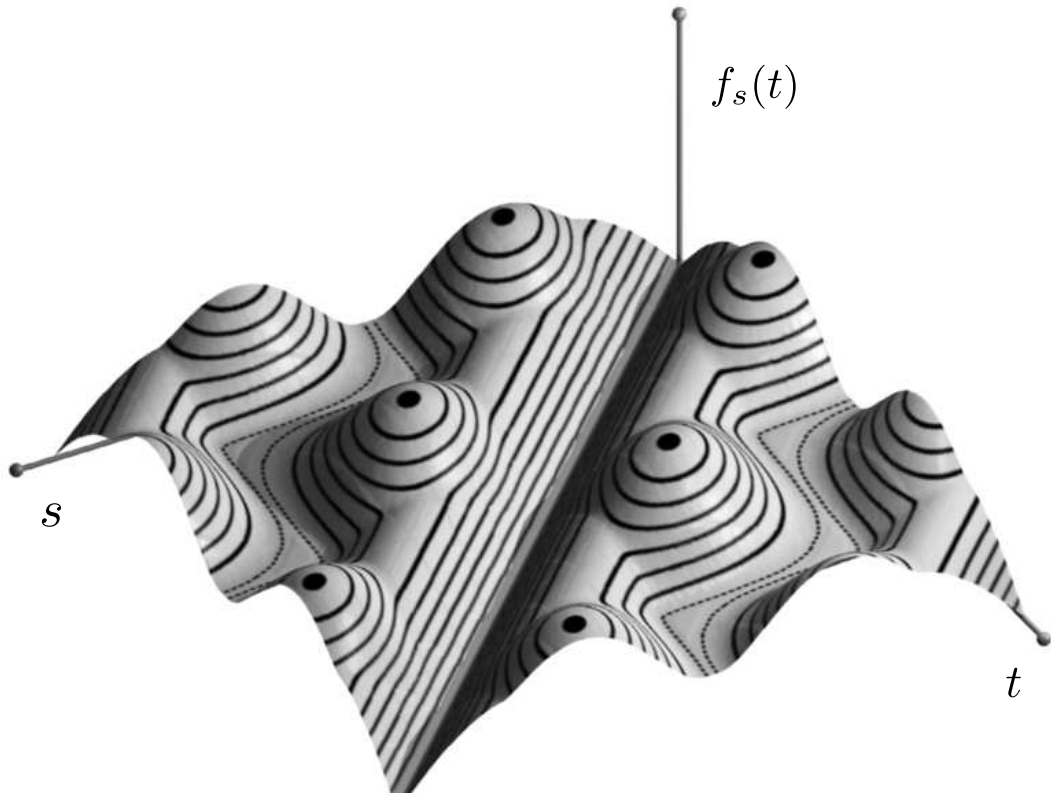


Figure 5.6: The distance function $f_s(t) := \text{pp}(s, t)$ for $s, t \in \mathbb{S}$. The dashed lines in the valleys indicate the two local minima, i.e. $\tilde{\sigma}(s)$ and $\tilde{\tau}(s)$.

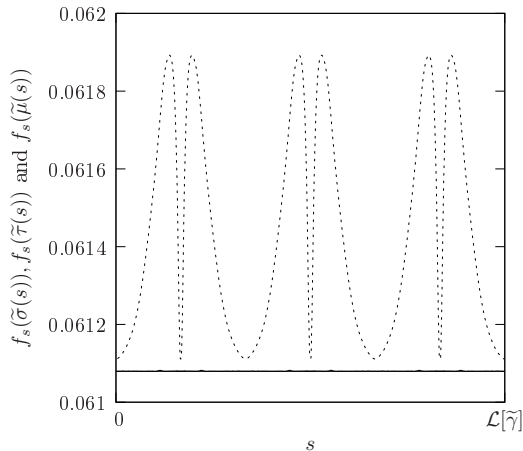


Figure 5.7: Graph of the local minima $f_s(\tilde{\sigma}(s))$ and $f_s(\tilde{\tau}(s))$ (solid lines at bottom), which are smaller than the local maximum $f_s(\tilde{\mu}(s))$ (dashed line) that separates them in the valley.

At this point we want to look at the numerical 'evidence':

Remark 5.15. *The curve $\tilde{\gamma}$ is the approximation of an ideal trefoil from Section 5.5.2. Since (H1) can only be approximately satisfied, and similar to [CLMS05, S04] we approximate σ by a function $\tilde{\sigma}$ computed as follows : fix $s = 0$ and consider $f_s(t) := \text{pp}(s, t) = |\tilde{\gamma}(s) - \tilde{\gamma}(t)|$. Numerics indicate that $f_s(t)$ has three local minima, especially $f_s(s) = 0$ (see Figure 5.6). Pick the local minimum of $f_s(t)$ closest to 2Δ and set $\tilde{\sigma}(s) = t$ for the corresponding t value. Sampling s up to $\mathcal{L}[\tilde{\gamma}]$ and restricting the minimisation to a small neighbourhood close to the previously found minimum yields $\tilde{\sigma}(s)$.*

If the numerical shape satisfies (H1)-(H5), then $\tilde{\sigma}(s) = \sigma(s)$. By picking the other minimum close to $2\Delta[\tilde{\gamma}]$ we can extract $\tilde{\tau}$ and compare it to $\tilde{\sigma}^{-1}$ using linear interpolation. They coincide up to an error of 10^{-3} . Further we have that for all s , the local minima $f_s(\tilde{\sigma}(s))$ and $f_s(\tilde{\tau}(s))$ in the valley are separated by a local maximum $f_s(\tilde{\mu}(s))$, which is always larger by at least $2 \cdot 10^{-5}$ than either of the local minima as depicted in Figure 5.7.

We take this as a hint that (H1)-(H5) are reasonable. In particular for (H1), $c(s, \tilde{\sigma}(s))$ deviates from 2Δ by less than $3 \cdot 10^{-6}$, the dot product between the contact chords and the tangents are less than $4 \cdot 10^{-5}$. Assumption (H4) and (H5) are suggested by Figure 5.5.

Fix $h \in [0, 1]$ and consider the curve

$$\gamma_h(s) := \Sigma(s, h).$$

Lemma 5.16. *Assuming Hypotheses 5.12 and 5.14 for $h \in [0, 1]$ the curve*

$$\gamma_h(s) = \gamma(s) + h(\gamma(\sigma(s)) - \gamma(s))$$

is

- (a) a regular C^1 -curve,

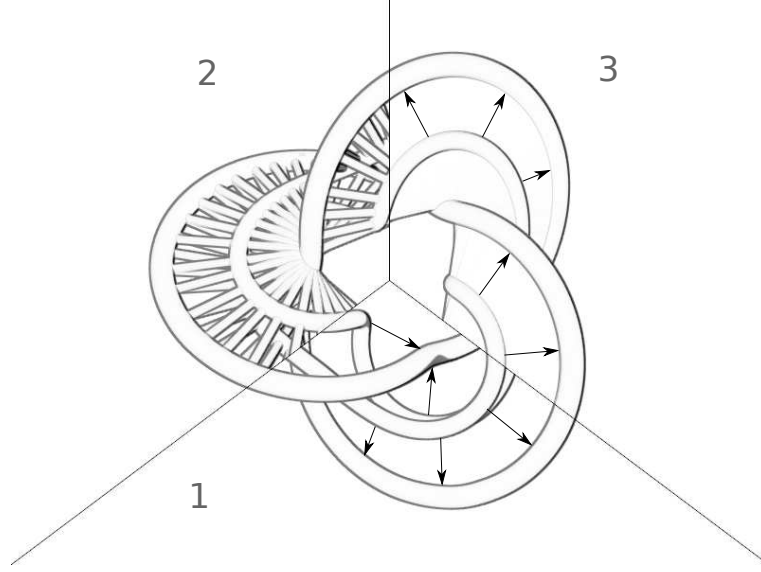


Figure 5.8: The trefoil homotopy visualised with the contact curve $\gamma_{1/2}$ (1-3), the chords $c(s, \sigma(s))$ (2) and the surface $\Sigma(s, h)$ (3). Note that the tube radius of the trefoil and the contact curve is smaller than Δ .

(b) *simple.*

(c) *There exists some constant $C < \infty$ such that $\|\gamma_h - \gamma_{h+\varepsilon}\|_{C^1(\mathbb{S}, \mathbb{R}^3)} < |\varepsilon|C$.*

Proof. (a) Since $\gamma \in C^1$ and $\sigma \in C^1$ by (H4) its composition γ_h is also C^1 . Further we compute

$$\begin{aligned} |\gamma'_h(s)|^2 &= \underbrace{\gamma'(s)^2}_{=1} + h \underbrace{\gamma'(s)\gamma'(\sigma(s))\sigma'(s)}_{\geq 0 \text{ by (H5)}} - h \underbrace{\gamma'(s)^2}_{=1} \\ &\quad + \underbrace{h^2(\gamma'(\sigma(s))\sigma'(s) - \gamma'(s))^2}_{\geq 0} \\ &> 0 \quad \text{for } h \in [0, 1). \end{aligned}$$

(b) We have to distinguish between the two cases $h \neq 1/2$ and $h = 1/2$. For the former, assume that there were distinct $s_1, s_2 \in \mathbb{S}$ with $\Sigma(s_1, h) = \Sigma(s_2, h)$, i.e. $\gamma(s_1) + hc(s_1, \sigma(s_1)) = \gamma(s_2) + hc(s_2, \sigma(s_2))$. This would imply that the normal disks of radius Δ around $\gamma(s_1)$ and $\gamma(s_2)$ (for $h < 1/2$) or $\gamma(\sigma(s_1))$ and $\gamma(\sigma(s_2))$ (for $h > 1/2$) would intersect contradicting the assumed thickness by Theorem 2.12.

For the latter, a double point of $\gamma_{1/2}$ would imply that the original γ touches a ball of radius Δ in four coplanar points from which we infer by Proposition 3.20 that it is a circle contradicting the fact that γ was assumed to be a trefoil.

(c) We compute $\gamma_h - \gamma_{h+\varepsilon}(s) = -\varepsilon(\gamma(\sigma(s)) - \gamma(s))$ and set $C := \|\gamma(\sigma(s)) - \gamma(s)\|_{C^1(\mathbb{S}, \mathbb{R}^3)}$ which yields the desired inequality. \square

We are about to prove that γ and $\gamma_{1/2}$ are ambient isotopic. To that end we need a corollary to Lemma 2.27:

Corollary 5.17. *Let $H : [0, 1] \times \mathbb{S} \rightarrow \mathbb{R}^3$ be a homotopy joining two simple, regular curves $\gamma : \mathbb{S} \rightarrow \mathbb{R}^3$ and $\eta : \mathbb{S} \rightarrow \mathbb{R}^3$, such that*

- (a) *each fibre $H(h, \cdot)$ is a simple, regular C^1 -curve ($h \in [0, 1]$) and*
- (b) *$\Phi : [0, 1] \rightarrow C^1(\mathbb{S}^1, \mathbb{R}^3)$, $\Phi(h) = H(h, \cdot)$ is a continuous map (in the $C^1(\mathbb{S}^1, \mathbb{R}^3)$ -topology).*

Then each fibre $H(h, \cdot)$ is ambient isotopic to all other fibres. In particular γ is ambient isotopic to η , i.e. they have the same knot type.

Proof. For each $h \in [0, 1]$ the curve $H(h, \cdot)$ satisfies the prerequisites of Lemma 2.27, therefore there exists an open environment $U_h \subset C^1(\mathbb{S}^1, \mathbb{R}^3)$ with $H(h, \cdot) \in U_h$. Then $B_h := \Phi^{-1}(U_h) \subset [0, 1]$ is an open neighbourhood of h . Now choose $\varepsilon_h > 0$ such that $C_h := (h - \varepsilon_h, h + \varepsilon_h) \cap [0, 1] \subset B_h$. Each environment C_h is connected and all curves $\Phi(C_h)$ are ambient isotopic by construction. The sets C_h ($h \in [0, 1]$) form an open cover of $[0, 1]$. By compactness a finite subset $\{C_{h_i}\}_i$ already covers $[0, 1]$. Since all curves $\Phi(C_{h_i})$ are ambient isotopic for each i and the sets C_{h_i} overlap using the transitivity of ambient isotopy yields that all curves in $\Phi([0, 1])$ are isotopic. \square

By Lemma 5.16 $\gamma_h = \Sigma(h, \cdot)$ satisfies the prerequisites of 5.17 for $h \in [0, 1]$ so we conclude the section with the following

Proposition 5.18. *Assuming Hypotheses 5.12 and 5.14 the curve*

$$\gamma_{1/2}(s) = \frac{\gamma(s) + \gamma(\sigma(s))}{2}$$

has the same knot type as γ . \square

A similar construction may work for other torus knots⁸ $T_{2,2n+1}$ as well since the ones we computed seem to fulfil Hypothesis 5.12 except for some additional isolated struts in the contact set (see Figure 5.9).

5.7 Closed Cycles

This section deals only with ‘the’ ideal trefoil k_{3_1} . While some ideas may carry over to 5_1 and other torus knots the available numerics are not sufficiently converged to be compelling. Recall from Section 5.6 that numerics suggests that every point on the ideal trefoil k_{3_1} is in contact with two other points (we assume Hypothesis 5.12 to hold for this section). Is there a finite tuple of points such that each parameter is in contact with its cyclic predecessor and successor? Inspired by Birkhoff’s *Dynamical Systems* [B27] we call a sequence of parameters, that are in contact with each predecessor, a billiard. If it closes, we call it cycle:

⁸ A $T_{p,q}$ torus knot is a knot on the surface of a torus winding p times around the hole of the torus and q times around the solid part of the torus. The 3_1 trefoil and 5_1 are torus knots.

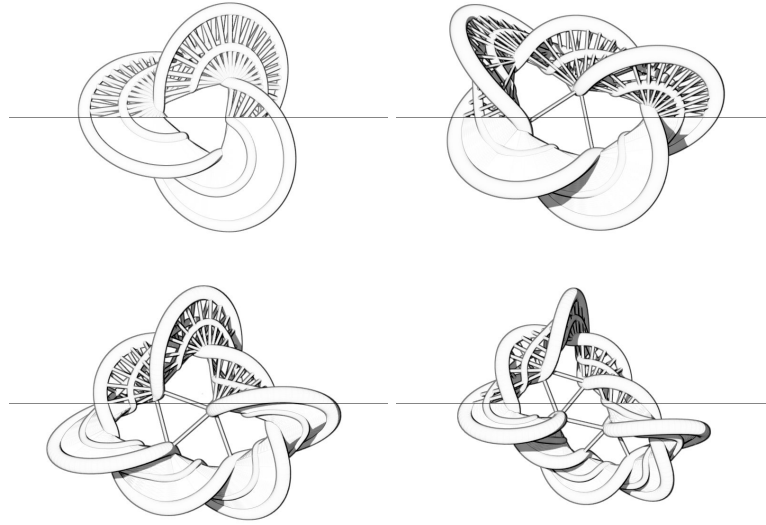


Figure 5.9: The contact surface and contact chords for the trefoil 3_1 , 5_1 , 7_1 and 9_1 (from upper left to lower right). Note the isolated contact chords for the higher knots.

Definition 5.19 (Cycle). For $n \in \mathbb{N}$ let $b := (t_1, \dots, t_n) \in \mathbb{S} \times \dots \times \mathbb{S}$ be an n -tuple. We call b an n -cycle iff $\sigma(t_i) = t_{i+1}$ for $i = 1, \dots, n - 1$ and $\sigma(t_n) = t_1$, where σ is defined as in Hypothesis 5.12. The cycle b is called minimal iff all t_i are pairwise distinct.

Each cyclic permutation of a cycle is of course again a cycle. Basing the definition of cycles on the continuous function σ makes it easier to find them numerically:

Lemma 5.20. The k_{3_1} has an n -cycle iff there exists some $t \in \mathbb{S}$ such that

$$\sigma^n(t) := \underbrace{\sigma \circ \dots \circ \sigma}_n(t) = t.$$

The cycle is then $b := (t, \sigma^1(t), \dots, \sigma^{n-1}(t))$. □

All parameters of a minimal n -cycle are pairwise distinct so each minimal n -cycle corresponds to n points in the set $\{t \in \mathbb{S} : \sigma^n(t) = t\}$. Since there are n cyclic permutations of an n -cycle and since minimal n -cycles that are not cyclic permutations must be point-wise distinct this leads to

Lemma 5.21 (Counting Cycles). Define the set of intersections of σ^n with the diagonal $I := \{t \in \mathbb{S} : \sigma^n(t) = t\}$. If there is a positive finite number of minimal n -cycles then

$$\begin{aligned} \#I &\geq (\text{Number of distinct minimal } n\text{-cycles}) \cdot n \\ &= (\text{Number of minimal } n\text{-cycles}). \end{aligned}$$

□

The symmetry conjectured in Section 5.2 easily implies:

Lemma 5.22 (Symmetry of σ, τ). *Assume Conjecture 5.9 about the symmetry of the constant speed parametrised trefoil $k_{3_1} : \mathbb{S} \rightarrow \mathbb{R}^3$ is true. Then the contact functions $\sigma, \tau : \mathbb{S} \rightarrow \mathbb{S}$ have the following properties:*

$$\sigma(s^* + t) \stackrel{\text{in } \mathbb{S}}{=} -\tau(s^* - t) \quad \forall t \in \mathbb{S} \quad (5.5)$$

$$\sigma(t + 1/3) \stackrel{\text{in } \mathbb{S}}{=} \sigma(t) + 1/3 \quad \forall t \in \mathbb{S} \quad (5.6)$$

$$\tau(s^* + t) \stackrel{\text{in } \mathbb{S}}{=} -\sigma(s^* - t) \quad \forall t \in \mathbb{S} \quad (5.7)$$

$$\tau(t + 1/3) \stackrel{\text{in } \mathbb{S}}{=} \tau(t) + 1/3 \quad \forall t \in \mathbb{S} \quad (5.8)$$

where $s^* \in \mathbb{S}$ is a parameter such that $k_{3_1}(s^*)$ is on a 180 degree rotation axis. \square

In Figure 5.10 we compiled small plots of σ^n for $n = 1, \dots, 34, 144$. The σ -function was computed as in Remark 5.15. For $n = 2$ the function σ^2 comes the first time close to the diagonal, but it can not touch in less than three points by Lemma 5.22. If it would touch it had to touch at least 6 times by Lemma 5.21. It does not seem that this is the case.

By similar arguments, we exclude the possibility of cycles for $n = 7, 11, 13, 16, 20, 25, 29$ and 34 . On the other hand the case $n = 9$ looks promising (see Figure 5.11). It seems to touch the diagonal precisely 9 times which suggests the existence of a single minimal cycle b_9 and its cyclic permutations. With our parametrisation the cycle b_9 happens to start at 0 and we compute a numerical error of only $\sigma^9(0) = 0.0007 \approx 0$. Consequently the cases $n = 18, 27$ would also touch the diagonal but the corresponding cycle would not be minimal. We studied the plots till $n = 100$ but did not find any other promising candidates (apart from $n = k \cdot 9$ for $k \in \mathbb{N}$). Keep in mind that the numerical error increases with n , but even for $n = 144$ the graphs look reasonable.

We believe that b_9 is indeed a cycle (see Figure 5.12):

Conjecture 5.23 (Existence of nine-cycle). *Let $k_{3_1} : \mathbb{S} \rightarrow \mathbb{R}^3$ be the ideal trefoil, parametrised with constant speed such that $k_{3_1}(0)$ is the outer point of the trefoil on a symmetry axis. Then $b_9 = (s_0, \dots, s_8)$ with $s_i := \sigma^i(0)$ is a nine-cycle. Numerics suggest that k_{3_1} passes from 0 to 1 through s_i in the sequence: $s_0, s_7, s_5, s_3, s_1, s_8, s_6, s_4, s_2$.*

For the rest of the chapter we assume the previous conjecture to be true.

Note that b_9 partitions the trefoil in 9 parts (see Figure 5.12): Three curves

$$\begin{aligned} \beta_1 &:= k_{3_1}|_{[s_0, s_7]}, \\ \beta_2 &:= k_{3_1}|_{[s_6, s_4]}, \\ \beta_3 &:= k_{3_1}|_{[s_3, s_1]}, \\ \text{or } \beta_i &:= k_{3_1}|_{[s_{6(i-1)}, s_{6(i-1)-2}]} \text{ with } s_k = s_{k+9}, \end{aligned}$$

which are congruent by 120 degree rotations around the z -axis. Three curves

$$\begin{aligned} \tilde{\beta}_1 &:= k_{3_1}|_{[s_2, s_0]}, \\ \tilde{\beta}_2 &:= k_{3_1}|_{[s_8, s_6]}, \\ \tilde{\beta}_3 &:= k_{3_1}|_{[s_5, s_3]}, \\ \text{or } \tilde{\beta}_i &:= k_{3_1}|_{[s_{6(i-1)+2}, s_{6(i-1)}]} \text{ with } s_k = s_{k+9}, \end{aligned}$$

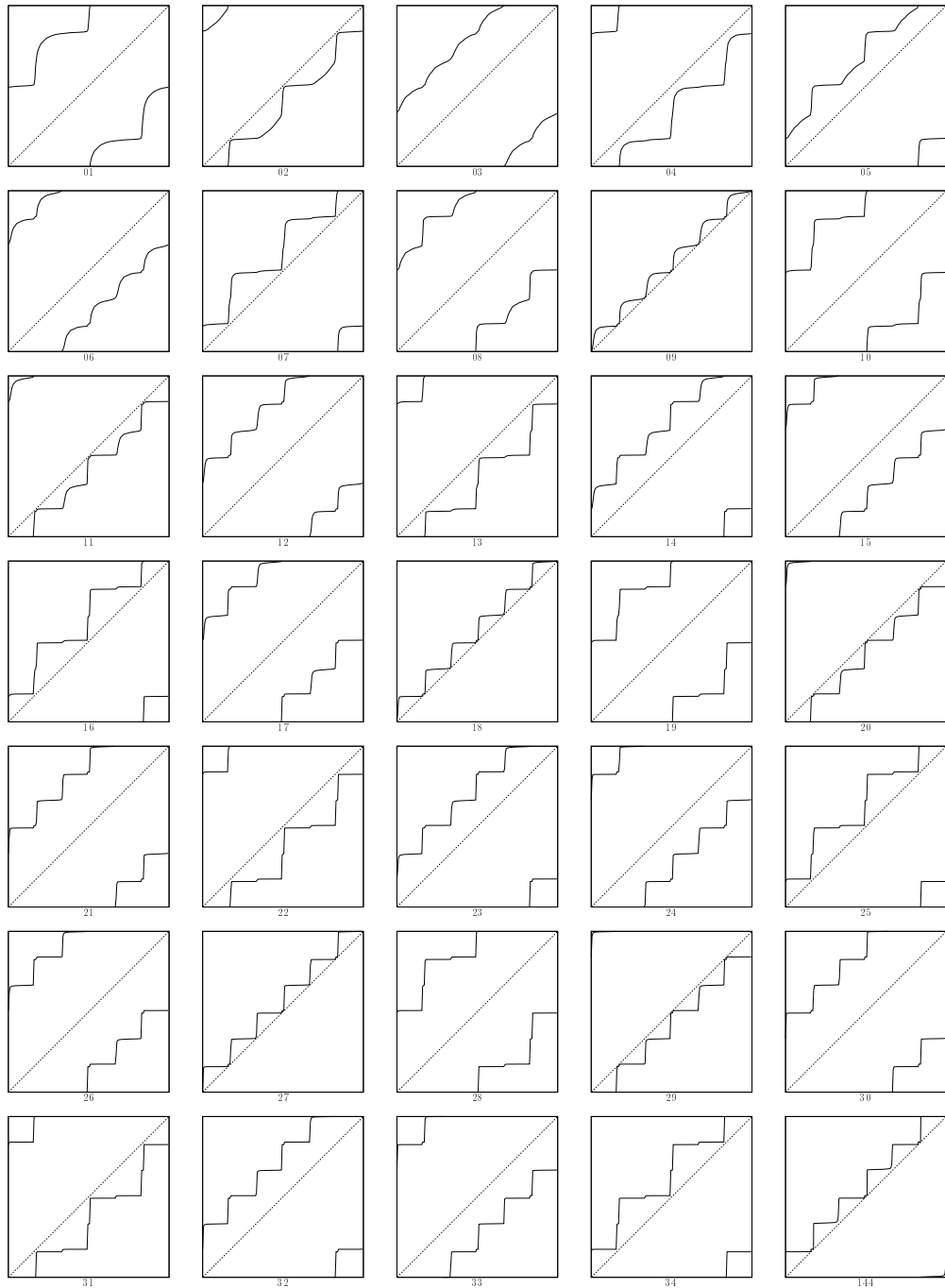
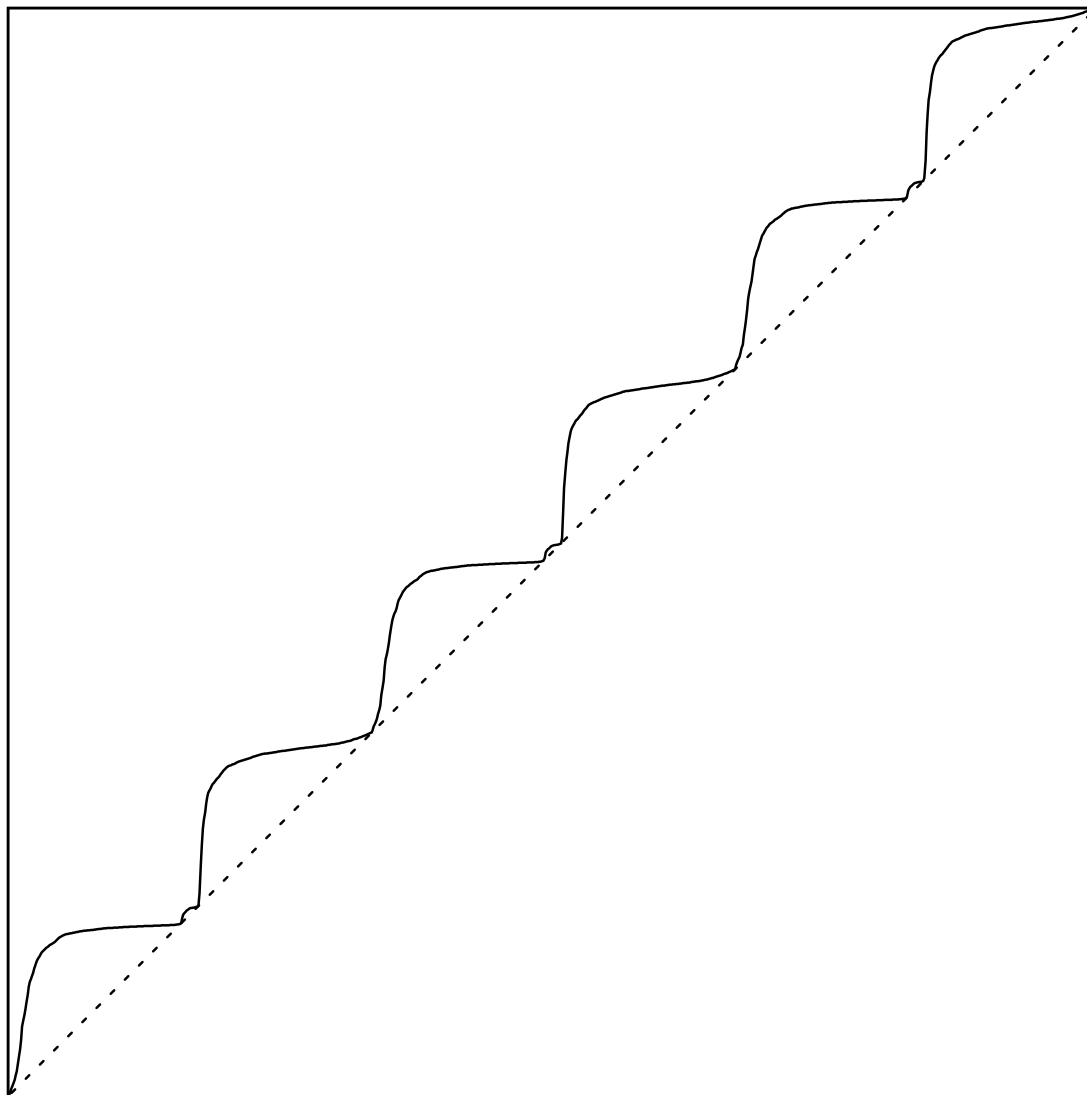


Figure 5.10: Plots of $\sigma^n : \mathbb{S} \rightarrow \mathbb{S}$. In plot 09 the function σ^9 seems to touch the diagonal (see also Figure 5.11 for an enlarged plot). Accordingly σ^i touches the diagonal in plot i for $i \in \{9, 18, 27, \dots\}$. Note that in plot 144 the numerical errors have added up so that σ^{144} no longer touches the diagonal.



09

Figure 5.11: The plot shows $\sigma^9 : \mathbb{S} \rightarrow \mathbb{S}$. It seems to touch the the diagonal 9 times in the points $0, 0.159, 0.175, 0.334 \approx 1/3, 0.492, 0.508, 0.667 \approx 2/3, 0.826, 0.841$. This indicates the existence of a nine-cycle $b_9 = (0, \sigma^1(0), \dots, \sigma^8(0))$.

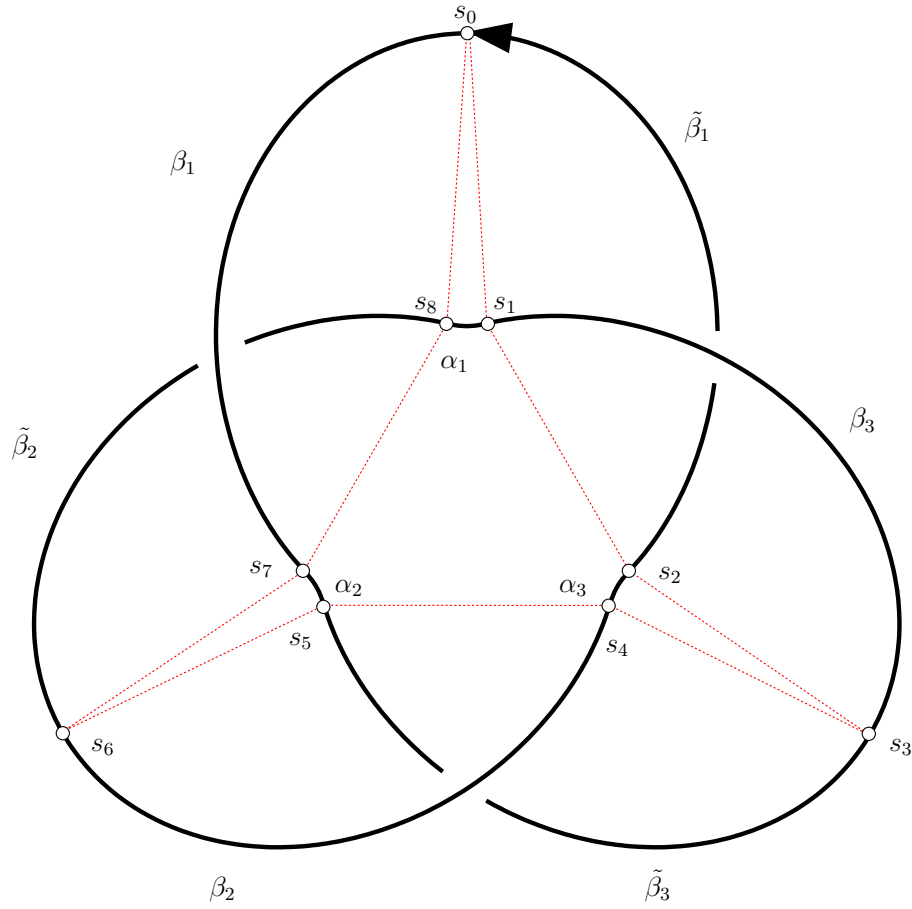


Figure 5.12: The parameters $s_i := \sigma^i(0)$ of the nine-cycle b_9 partition the trefoil in 9 curves: β_i and $\tilde{\beta}_i$ are all congruent as are α_i ($i = 1, 2, 3$). The contact function σ maps the parameter interval of each curve bijectively to the parameter interval of another curve (see Figure 5.13).

which are again congruent by 120 degree rotations and each $\tilde{\beta}_i$ is congruent to β_i by a 180 degree rotation. And finally three curves

$$\begin{aligned} \alpha_1 &:= k_{31} |_{[s_1, s_8]}, \\ \alpha_2 &:= k_{31} |_{[s_7, s_5]}, \\ \alpha_3 &:= k_{31} |_{[s_4, s_2]}, \\ \text{or } \alpha_i &:= k_{31} |_{[s_{6(i-1)+1}, s_{6(i-1)-1}]} \text{ with } s_k = s_{k+9}, \end{aligned}$$

which are congruent by rotations of 120 degrees and self congruent by a rotation of 180 degrees.

Because b_9 is a cycle, each piece of the curve gets mapped one-to-one to another piece of the curve.

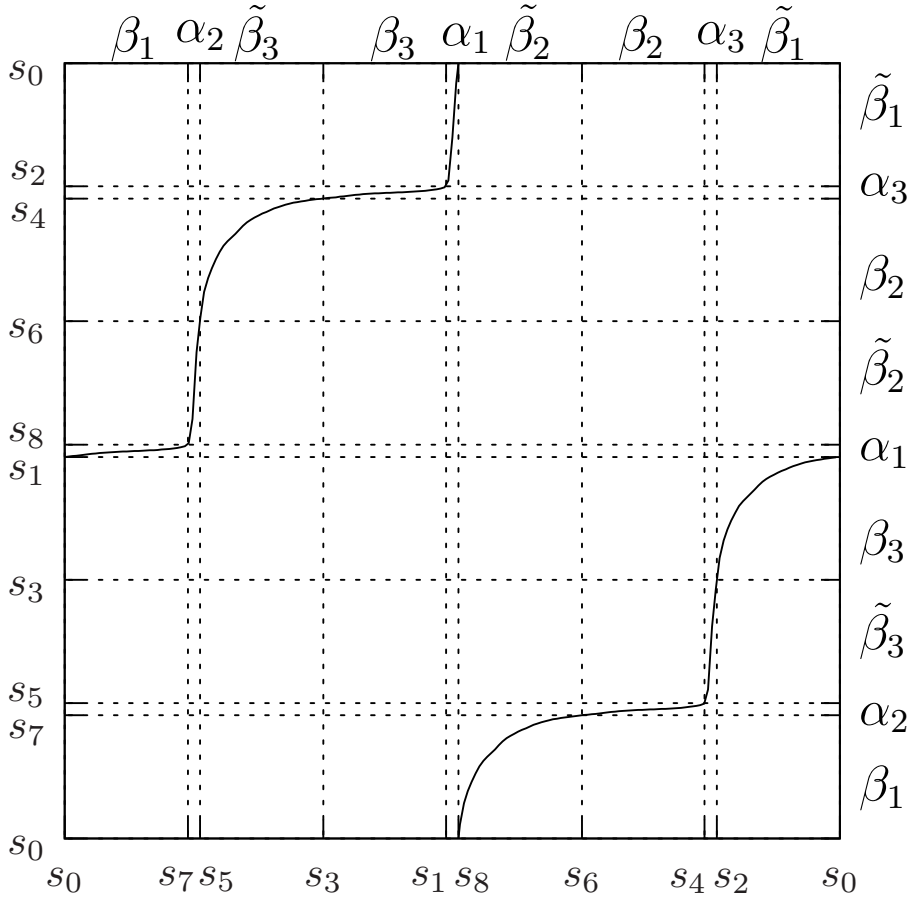


Figure 5.13: Plotting the σ function with a grid of the partition points s_i we can read off which piece of the curve is in contact (in the σ direction) with which other piece. For example starting at the top with α_1 we see that σ maps its parameter-interval to the parameter-interval of $\tilde{\beta}_1$ on the right, which itself gets mapped from top $\tilde{\beta}_1$ to β_3 on the right and so on (see Lemma 5.24).

Lemma 5.24 (Piece to piece). *Assume Hypothesis 5.12 about the nature of the contact function σ and Conjectures 5.9 about symmetry and 5.23 about the existence of a nine cycle $b_9 = (s_0, \dots, s_8)$ hold. Then σ maps each parameter interval $[s_i, s_j]$ to $[s_{i+1}, s_{j+1}]$. In particular: Following the contact in σ direction we get the sequence $\alpha_1 \rightarrow \tilde{\beta}_1 \rightarrow \beta_3 \rightarrow \alpha_3 \rightarrow \beta_3 \rightarrow \beta_2 \rightarrow \alpha_2 \rightarrow \tilde{\beta}_2 \rightarrow \beta_1 (\rightarrow \alpha_1)$. Each piece is in one-to-one contact with the next in the sequence (see also Figure 5.13).*

Proof. By definition s_i is mapped to s_{i+1} and by Lemma 5.13 σ is continuous, monotone and orientation preserving so the interval $[s_i, s_j]$ gets mapped to $[\sigma(s_i), \sigma(s_j)] = [s_{i+1}, s_{j+1}]$. \square

Taking a second look at Figure 5.10 it looks like σ^n is approaching a step function. What are the accumulation points of the sequence $\{\sigma^i(t)\}_i$ as a function of $t \in \mathbb{S}$? Looking at $(\sigma^i(t), \sigma^{i+1}(t), \dots, \sigma^{i+8}(t))$ for arbitrary $t \in \mathbb{S}$ it seems to converge to b_9 up to

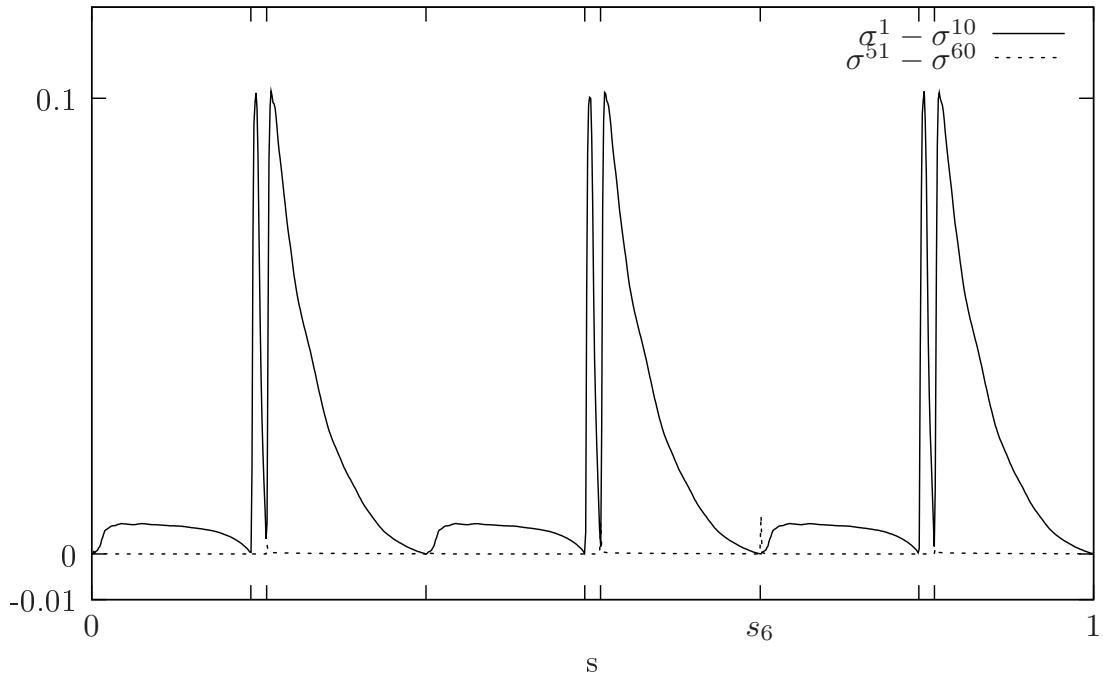


Figure 5.14: Since numerical experiments find $\sigma^{i+9} - \sigma^i$ converges pointwise to 0 for $i \rightarrow \infty$ we conjecture that the cycle b_9 acts as an attractor, i.e. $(\sigma^{9i}(s), \sigma^{9i+1}(s), \dots, \sigma^{9i+8}(s))$ converges to b_9 up to a cyclic permutation. Notice that the convergence is only point wise; with enough samples we would see spikes after each s_i as behind s_6 above.

a cyclic permutation for i large enough. This would imply that b_9 are the accumulation-points of the above sequence. Figure 5.14 shows some numeric values of $\sigma^{i+9} - \sigma^i$ which seems to converge pointwise to 0 for $i \rightarrow \infty$. The cycle b_9 seems to attract any infinite sequence.⁹ We conclude the paragraph with the

Conjecture 5.25 (Attractor). *For any $t \in \mathbb{S}$ and fixed $k \in \{0, \dots, 9\}$ the 9-tuple $(\sigma^i(t), \sigma^{i+1}(t), \dots, \sigma^{i+8}(t))$ converges to a cyclic permutation of b_9 for $j \rightarrow \infty$ with $i = 9j + k$.*

⁹We would like to thank Eugene Starostin for encouraging us to take a closer look at this issue.

Chapter 6

Conclusion and Discussion

Chapter 2 introduced necessary background material for the thesis, along with two new observations. First, we described how thickness in \mathbb{R}^N induces thickness in \mathbb{S}^N , and how it is related to the normal radius of injectivity. Second, two examples of curves converging in C^1 and in thickness, but not in $C^{1,1}$, were introduced. Consequently care must be taken when considering curvature graphs of approximations of ideal shapes.

In Chapter 3 we found simple solutions to the packing problem (P) on the sphere (as stated on page 25) and were even able to count their multiplicity, and to show their uniqueness, in the sense that there are no others for the respective thicknesses. Since the two-sphere is only two-dimensional, it is another essentially two-dimensional solution to an optimisation problem of tubes, similar to the tight clasp or the Borromean rings [Sta03, CFKSW04]. But unlike the latter, the solutions do not rely on any unproven – though natural – symmetry assumption. Nevertheless the solution of (P) is incomplete because explicit solutions are known only for a certain discrete series of thicknesses. Natural remaining questions for other optimal but non-sphere-filling curves are:

- Is the competitor β_τ from Lemma 3.15 really optimal?
- Are all solutions to Problem (P) arc curves, i.e. curves that piecewise consist of arcs of circles?
- Is there always a discrete number of solutions?
- What are the shapes of optimal solutions whose tubular neighbourhood does not fill the sphere?
- How are the solutions connected as thickness varies? For example, do they form continuous families? A complete answer to Problem (P) should include a branch diagram, which might look like Figure 6.1.

While these questions are for the moment unanswered they appear to be approachable.

In Chapter 4 we gave divers possible notions of ideal knots in \mathbb{S}^3 and showed their existence in $C^{1,1}$. Maximising the thickness of a knot seems to be the most natural notion. We connected solutions in \mathbb{S}^3 with the established notion of ideal knots in \mathbb{R}^3 via the problem of maximising thickness for shorter and shorter prescribed arc-length. Finally we gave an explicit competitor \mathfrak{g} for the thickness maximising trefoil in the three-sphere. Being located on a “flat” Clifford torus, this shape could be again considered as

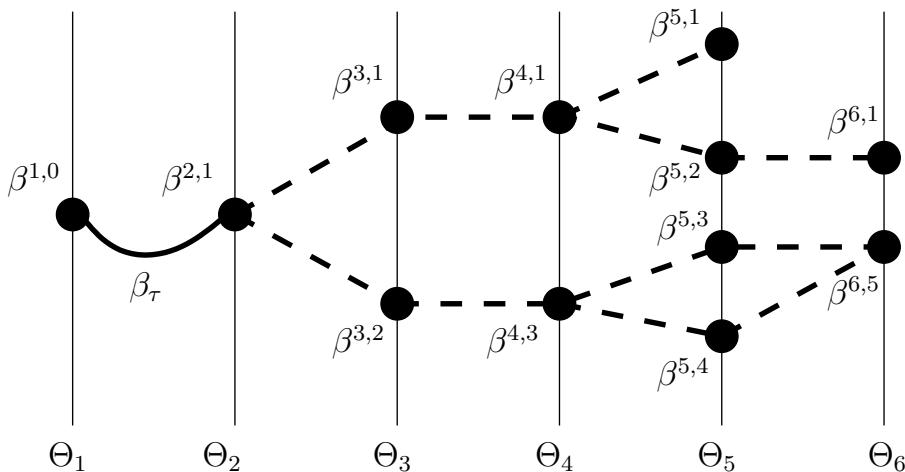


Figure 6.1: A complete solution of Problem (P) should answer how the solutions branch. For each Θ_n the number of solutions and their shapes are now known. There are perhaps branches of solutions linking the known ones for intermediate thicknesses. If β_τ from Lemma 3.15 is indeed optimal, it links the solutions of Θ_1 and Θ_2 . Since the number of solutions $\varphi(n)$ fluctuates, branches have to both appear, or split, and vanish or merge.

essentially two-dimensional. We showed that \mathbf{g} satisfies first order necessary conditions to be maximal. The rather special geometric properties of particular Clifford torus trefoil curve make it noteworthy, even if it turns out not to be thickness maximising. Remaining questions of this chapter are:

- How to prove maximality of \mathbf{g} ?
- Or, can a better competitor than \mathbf{g} be found numerically?

In another direction and assuming that \mathbf{g} is indeed the thickness maximising trefoil on the three-sphere, consider all thickness maximisers $\gamma_L : \mathbb{S} \rightarrow \mathbb{S}^3$ with prescribed length $\mathcal{L}[\gamma_L] = L$ for $L \in (0, \mathcal{L}[\mathbf{g}]]$. This family of curves (assuming a unique solution for each L) connects \mathbf{g} with the ideal trefoil in \mathbb{R}^3 .

- How do the symmetry-groups of γ_L evolve, starting from the infinite group of \mathbf{g} and ending at the rather small group G_{3_1} for the ideal \mathbb{R}^3 trefoil?
- Is there a closed formula for the family, such that the limit $L \rightarrow \mathcal{L}[\mathbf{g}]$ yields \mathbf{g} and the other end is the long sought ideal trefoil in \mathbb{R}^3 ?

In Chapter 5 we reintroduced Fourier knots and demonstrated the advantages of combining them with a biarc discretisation in simulated annealing. We showed how to exploit the (assumed) symmetry of knots to reduce the degrees of freedom in the Fourier representation. Next we examined the computed knot shapes and discussed various implications. In particular, we found that the thickness maximising 5_1 knot in \mathbb{S}^3 does not fit on a Clifford torus. Concerning the computations in \mathbb{S}^3 there certainly remains much room for improvement. For example:

-
- How can we apply initially more efficient algorithms like SONO or RidgeRunner in \mathbb{S}^3 ?
 - Might there be simple expressions for ideal knots other than 3_1 in \mathbb{S}^3 ? In particular do other ideal knots orthogonally intersect great circles realizing self distance $2 \sin \frac{\pi}{n}$ as suggested in Conjecture 4.18 and Sections 5.5.4 and 5.5.5?

This might mean giving up biarcs and going back to piecewise linear line segments (in \mathbb{R}^4) connecting points on \mathbb{S}^3 and later inscribing circular arcs (in \mathbb{S}^3) with some estimate that length and thickness only change slightly. [BPR05] might inspire how to do this.

In Section 5.6 we gave an intuitive ‘proof’ that the contact-curve of the ideal trefoil is a trefoil itself, based on some rather strong hypotheses that appear to be satisfied on numerical approximations. In Section 5.7 we saw that a closed contact cycle partitions the ideal trefoil in two basic curves α and β that are in contact with each other. Open questions in this direction include.

- Are there similar closed cycles in other ideal knots?
- Can the existence of such cycles be ‘proved’ by arguments based on hypotheses used in Section 5.6?
- Numerics suggest that the junction between α and β curves in the ideal trefoil is at points where local curvature is active in achieving thickness. Moreover the Frenet frame appears to be discontinuous at these matching points. Are these properties in fact true for the ideal trefoil? Are they typical features of other ideal knot shapes?

Index

- $\beta^{n,k}$, 26
- β_τ , 41
- B_r , 7
- \mathcal{B}_r , 7
- $C^{1,1}$, 6
- \mathcal{C}_Θ , 25
- Δ , 5
- diam, 5
- $\text{dist}_{\mathbb{R}^N}$, 7
- $\text{dist}_{\mathbb{S}^N}$, 7
- D_Θ , 8
- E , 8
- E_r , 8
- \mathfrak{g} , 71
- gcd, 27
- \mathcal{K} , 16
- \mathcal{L} , 16
- lcm, 32
- NIR, 8
- N^∞ , 13
- pp, 74, 86
- pt, 7
- $R(\cdot, \cdot, \cdot)$, 5
- \mathcal{R} , 16
- ρ_G , 5
- R_x , 80
- \mathbb{S} , 5
- σ , 97
- \mathbb{S}^N , 5
- S^0 , 13
- S_x , 80
- T_ϑ , 27
- Θ_n , 26
- ϑ_n , 26
- tt, 7
- $T_\Theta(\cdot)$, 8
- $\mathcal{V}(\cdot)$, 27
- ambient isotopy, 15
- arc curves, 86
- biarc, 78
- billiard, 102
- Clifford torus, 69
- conformal dilation, 64
- contact chord, 10
- curve
 - regular, 6
 - thick, 5
- cycle, 103
- Fourier knot, 79–86
- global radius of curvature, 5
- Hopf coordinates, 69
- Hotelling, 34
- ideal
 - knot in \mathbb{R}^3 , 16
 - knot in \mathbb{S}^3 , 63
 - trefoil, *see* trefoil knot
- knot, 15
- L -ideal, 63
- matching point, 78
- matching rule, 78
- non-self-overlapping, 33
- normal disk, 8
- normal injectivity radius, 8
- parameter reflection, 80
- parameter shift, 80
- point point function, 74, 86
- point tangent function, 6
- point-tangent pair, 77
- problem

- (P'), 57
- (P), 25
- proper
 - biarc, 78
 - point-tangent pairs, 77
- ropelength, 16, 85
- spherical torus property, 33
- stereographic projection, 13
- symmetry, 80–88, 104
- tame knot, 15
- tangent tangent function, 7
- theorems, corollaries, etc.
 - Actions on Fourier knots, 82
 - Adapted Ascoli, 17
 - Approx. of circle, 21
 - Approx. of stadium curve, 22
 - Approx. w. Fourier knots, 79
 - Assumed symmetries of $3_1, 4_1, 5_1$, 81
 - Big equivalence, 9
 - Char. of sphere filling curves, 49
 - Char. pat. of s. f. curves II, 53
 - Char. pat. of s. f. curves I, 51
 - Double touching ball, 48
 - Estimates on stereo. proj., 13
 - Exist. of sol. of (P), 25
 - Existence of ideal knots in \mathbb{S}^3 , 65
 - Explicit competitors β_τ , 41
 - Explicit sol. of (P), 27
 - Fourier coeff. of symmetric knots, 84
 - Great circles on spheres, 10
 - Hopf coordinates, 69
 - Hotelling, 34
 - Length and vol. of sol. of (P), 43
 - Lower vol. bound for sol. of (P), 46
 - NIR and Δ , 11
 - Not contained in hemisphere, 67
 - Piece to piece, 107
 - Properties of \mathfrak{g} , 72
 - Quantized thickness, 73
 - Shrinking into the tangent space, 67
 - Smooth approx. w. pos. thick. II, 37
 - Smooth approx. w. pos. thick. I, 19
 - Sol. of (P) attain thickness, 39
 - Speed limit II, 38
 - Speed limit I, 17
 - Sphere filling closed thick curves, 27
 - Sphere filling open thick curves, 60
 - Symmetry of σ, τ , 104
 - Uniqu. of sol. of (P) $\Theta = \Theta_n$, 27
- Θ -ideal, 63
- thickness, 5
- torus property, 8
- trefoil knot, 69–76, 88, 97, 102–109
- tubular neighbourhood
 - in \mathbb{R}^N , 8
 - on \mathbb{S}^2 , 27
- Villarceau circle, 72
- Weyl, 34

Bibliography

- [A91] M. Artin, *Algebra*, Prentice Hall (1991).
- [ACPR05] T. Ashton, J. Cantarella, M. Piatek, E.J. Rawdon, *Self-contact sets for 50 tightly knotted and linked tubes*, math.DG/0508248 *in prepatation* (2005).
<http://www.arxiv.org/abs/math.DG/0508248>
- [B01] T.F. Banchoff, *Osculating Tubes and Self-Linking for Curves on the Three-Sphere* in A. Gray, M. Fernández, J.A. Wolf (Eds.), *Global Differential Geometry: The Mathematical Legacy of Alfred Gray*: International Congress on Differential Geometry September 18-23, 2000, Bilbao, Spain, Contemporary Mathematics, vol. 288, American Mathematical Society (2000).
- [B27] G.D. Birkhoff, *Dynamical Systems*, American Mathematical Society (1927).
- [BaSh96] E. Bach, J. Shallit, *Algorithmic Number Theory*, MIT Press, Cambridge (1996).
- [Be87] M. Berger, *Geometry II*, Springer-Verlag, New York (1987).
- [BPR05] J. Baranska, P. Pieranski, and E.J. Rawdon, *Ropelength of tight polygonal knots*, in [CMRS05], 293–321.
- [BPP08] J. Baranska, S. Przybyl, and P. Pieranski, *Curvature and torsion of the tight closed trefoil knot*, Eur. Phys. J. B **66**, 547–556 (2008).
- [BS97] G. Buck, J. Simon, *Energy and length of knots*, in Lectures at Knots 96, ed. S. Suzuki, World Scientific, Singapore (1997).
- [BZ03] G. Burde, H. Zieschang, *Knots*, Walter de Gruyter & Co. Berlin, 2nd edition (2003).
- [dC92] M.P. do Carmo, *Riemannian Geometry*, Birkhäuser, Basel, (1992).
- [E98] L. C. Evans, *Partial differential equations*, Graduate Studies in Mathematics, 19, American Mathematical Society (1998).
- [C10] M. Carlen, *Computation and Visualization of Ideal Knot Shapes*, PhD thesis no. 4621, EPFL Lausanne (to appear 2010).
<http://library.epfl.ch/theses/?nr=4621>
- [CFKSW04] J. Cantarella, J.H.G. Fu, R.B. Kusner, J.M. Sullivan, N.C. Wrinkle, *Criticality for the Gehring link problem*, Geom. Topol. **10** (2006), 2055–2116.

BIBLIOGRAPHY

- [CG67] H.S.M. Coxeter, S.L. Greitzer, *Geometry Revisited*, The Mathematical Association of America, Washington (1967).
- [CKS02] J. Cantarella, R.B. Kusner, J.M. Sullivan, *On the minimum ropelength of knots and links*, *Inv. math.* **150** (2002), 257–286.
- [CMR02] J.A. Calvo, K.C. Millett, E.J. Rawdon (eds.), *Physical Knots: Knotting, Linking, and Folding Geometric Objects in \mathbb{R}^3* , Contemporary Mathematics, **304**, American Mathematical Society, Providence (2002).
- [CMRS05] J.A. Calvo, K.C. Millett, E.J. Rawdon, A. Stasiak (eds.) *Physical and Numerical Models in Knot Theory*, Ser. on Knots and Everything **36**, World Scientific, Singapore (2005).
- [CPR05] J. Cantarella, M. Piatek, E.J. Rawdon, *Visualizing the tightening of knots*. In: *VIS'05: Proc. of the 16th IEEE Visualization 2005*, 575–582, IEEE Computer Society, Washington DC (2005).
- [CLMS05] M. Carlen, B. Laurie, J.H. Maddocks, J. Smutny, *Biarcs, global radius of curvature, and the computation of ideal knot shapes* in [CMRS05], 75–108.
- [doC76] M.P. Do Carmo, *Differential Geometry of Curves and Surfaces*. Prentice Hall, New Jersey (1976).
- [D02] O.C. Durumeric, *Local Structure of Ideal Shapes of Knots*, *Top. Appl.* **154** (2007), 3070–3089.
- [Di03] Y. Diao, *The lower bounds of the lengths of thick knots*, *Journal of Knot Theory and Its Ramifications*, Vol. 12, Issue. 1 (2003), 1–16.
- [FHW94] M. Freedman, Z.-X. He, Z. Wang, *Möbius energies of knots and unknots*, *Ann. of Math.*, **139** (1994), 1–50.
- [Ge04] H. Gerlach, *Der Globale Krümmungsradius für offene und geschlossene Kurven im \mathbb{R}^N* , Diploma thesis at Bonn University (2004).
<http://www.littleimpact.de/permanent/math/2009/dipl/>
- [GdlL03] O. Gonzalez, R. de la Llave, *Existence of Ideal Knots*, *Journal of Knot Theory and Its Ramifications* **12**, No. 1 (2003) 123–133.
- [GM99] O. Gonzalez, J.H. Maddocks, *Global Curvature, Thickness and the Ideal Shapes of Knots*, *Proc. Natl. Acad. Sci. USA* **96** (1999), 4769–4773.
- [GMS02] O. Gonzalez, J.H. Maddocks, J. Smutny, *Curves, circles and spheres* in [CMR02], 195–215.
- [GMSvdM02] O. Gonzalez, J.H. Maddocks, F. Schuricht, H. von der Mosel, *Global curvature and self-contact of nonlinearly elastic curves and rods*, *Calc. Var.* **14** (2002), 29–68.
- [Gr90] A. Gray, *Tubes*. Sec.ed. Progress in Mathematics, 221, Birkhäuser Verlag, Basel (2004).

- [GevdM09] H. Gerlach, H. von der Mosel, *What are the longest ropes on the unit sphere?* Report Nr. 32, Institut für Mathematik, RWTH Aachen (2009).
- [H39] H. Hotelling, *Tubes and Spheres in n -Spaces*, Amer. J. Math. **61** (1939), 440–460.
- [K02] R.B. Kusner, *On Thickness and Packing Density for Knots and Links*, in [CMR02], 175–180.
- [K98] L.H. Kauffman, *Fourier Knots*, in [SKK98], 364–373.
- [KAB06] E. Katzav, M. Adda-Bedia, A. Boudaoud, *A statistical approach to close packing of elastic rods and to DNA packaging in viral capsids*, Proceedings of the National Academy of Sciences, USA, **103** (2006), 18900–18904.
- [KGV83] S. Kirkpatrick, C.D. Gelatt, M.P. Vecchi, *Optimization by Simulated Annealing*, Science, New Series 220 **4598** (1983), 671–680.
- [LSDR99] R.A. Litherland, J. Simon, O.C. Durumeric, E.J. Rawdon, *Thickness of Knots, Topology and its Applications* **91(3)** (1999), 233–244.
- [LM05] R. Langevin, G.-T. Moniot, *The Zone Modulus of a Link*, Journal of Knot Theory and Its Ramifications, Vol. 14, No. 6 (2005), 819–830.
- [M04] G.-T. Moniot, *Propriétés conformes des entrelacs et quelques autres conséquences de l'étude d'espaces de sphères*, PhD thesis, Université de Bourgogne (2004).
- [O'H91] J. O'Hara, *Energy of a Knot*, Topology, 30(2) (1991), 241–247.
- [O'H03] J. O'Hara, *Energy of Knots and Conformal Geometry*, Series on Knots and Everything Vol. 33, World Scientific, Singapore (2003).
- [P98] P. Pieranski, *In Search of Ideal Knots* in [SKK98], 20–41.
- [PP02] P. Pieranski, S. Przybyl, *In Search of the Ideal Trefoil Knot*, in [CMR02], 153–162.
- [Rt05] Ph. Reiter, *All curves in a C^1 -neighbourhood of a given embedded curve are isotopic* Preprint Nr. 4, Institut für Mathematik, RWTH Aachen (2005).
- [Rt09] Ph. Reiter, *Repulsive Knot Energies and Pseudodifferential Calculus* PhD thesis, RWTH Aachen (2009).
<http://darwin.bth.rwth-aachen.de/opus/volltexte/2009/2848/>
- [S04] J. Smutny, *Global radii of curvature and the biarc approximation of spaces curves: In pursuit of ideal knot shapes*, PhD thesis no. 2981, EPFL Lausanne (2004).
<http://library.epfl.ch/theses/?display=detail&nr=2981>
- [Sta03] E. Starostin *A constructive approach to modelling the tight shapes of some linked structures* Proc. Appl. Math. Mech. (2003) 3:1, 479–480.
- [Sa94] H. Sagan, *Space-Filling Curves*, Springer-Verlag, New York (1994).
- [Sh87] T.J. Sharrock, *Biarc in three dimensions*, in *The Mathematics of surfaces II*, Ed. R.R. Martin, Oxford Univ. Press, New York (1987), 395–411.

BIBLIOGRAPHY

- [SvdM03a] F. Schuricht, H. von der Mosel, *Global curvature for rectifiable loops*, Math. Z. **243** (2003), 37–77.
- [SvdM04] F. Schuricht, H. von der Mosel, *Characterization of ideal knots*, Calc. Var. Partial Differential Equations **19** (2004), 281–305.
- [SDKP98] A. Stasiak, J. Dubochet, V. Katritch, P. Pieranski, *Ideal knots and their relations to the physics of real knots* in [SKK98], 1–19.
- [StvdM04] P. Strzelecki, H. von der Mosel, *Global Curvature for Surfaces and Area Minimization Under a Thickness Constraint*, Calc. Var. **25** (2006), 431–467.
- [StvdM07] P. Strzelecki, H. von der Mosel, *On rectifiable curves with L^p -bounds on global curvature: Self-avoidance, regularity, and minimizing knots*. Math. Z. **257** (2007), 107–130.
- [SKK98] A. Stasiak, V. Katritch, L.H. Kauffman (Eds.), *Ideal Knots*, Series on Knots and Everything Vol. 19, World Scientific, Singapore (1998).
- [Tait] P.G. Tait *On Knots I, II, and III*. Scientific Papers, Vol. 1. Cambridge, England: University Press (1898), 273–347.
- [T98] A.K. Trautwein, *An introduction to harmonic knots*, in [SKK98], 353–363.
- [VAB99] C. Varea, J.L. Aragon, R.A. Barrio, *Turing patterns on a sphere*, Phys. Rev. E **60** (1999), 4588–4592.
- [W39] H. Weyl, *On the volume of tubes*, Amer.J. Math. **61** (1939), 461–472.
- [WT83] C.C. Wiggs, C.J.C. Taylor, *Bead puzzle*, US Patent D269629 (issued 1983).

Curriculum Vitae

I was born in Mannheim-Neckarau in 1977. After going to school in Mannheim I studied mathematics and computer science at the Rheinische Friedrich-Wilhelms-Universität Bonn from 1998 till 2005. From 2001 to 2002 I was granted a DAAD-stipend to visit Tel Aviv University. In 2005 I obtained my diploma in mathematics with Prof. Dr. Heiko von der Mosel.